

Dissertation zur Erlangung des Doktorgrades
der Fakultät für Chemie und Pharmazie
der Ludwig-Maximilians-Universität München

Recognition and silencing of new invading transposons in *Schizosaccharomyces pombe*



Luca Salvi
aus
Arezzo, Italien

2021

Erklärung

Diese Dissertation wurde im Sinne von § 7 der Promotionsordnung vom 28. November 2011 von Herrn Dr. Mario Halic betreut.

Eidesstattliche Versicherung

Diese Dissertation wurde eigenständig und ohne unerlaubte Hilfe erarbeitet.

München, 27/05/2021

.....
Luca Salvi

Dissertation eingereicht am 27/05/2021

1. Gutachter: Dr. Mario Halic

2. Gutachter: Prof. Dr. Klaus Förstemann

Mündliche Prüfung am 28/06/2021

TABLE OF CONTENTS

SUMMARY.....	1
1. INTRODUCTION.....	2
1.1 DNA organization in eukaryotic cells.....	2
1.1.1 Chromatin.....	2
1.2 Heterochromatin in <i>S. pombe</i>	4
1.2.1 Heterochromatin at centromeres.....	5
1.2.2 Heterochromatin at mating-type locus.....	9
1.2.3 Heterochromatin at telomeres.....	10
1.2.4 Facultative heterochromatin.....	10
1.3 Transposable Elements (TEs).....	12
1.3.1 TEs, a general overview.....	12
1.3.2 Transposon classification.....	13
1.3.3 Transposable Elements in <i>S. pombe</i>	16
1.3.4 Transposable Elements silencing in <i>S. pombe</i>	18
1.3.5 Transposable Elements silencing in other organisms.....	20
1.3.5.1 Transposon silencing in plants.....	20
1.3.5.2 Transposon silencing in <i>S. cerevisiae</i>	22
1.3.5.2 Transposon silencing in animals.....	23
2. AIM OF THIS STUDY.....	32
3. RESULTS.....	33
3.1 Introducing <i>tj1</i> , a TE from <i>Schizosaccharomyces japonicus</i> active in <i>S. pombe</i>	33
3.2 Setup of a plasmid system to induce a controlled propagation of Tj1 in <i>S. pombe</i> genome....	33
3.3 Generation of a readout system to identify <i>tj1</i> silencing cells and combination of donor and expression plasmids to induce a controlled Tj1 propagation.....	35
3.4 Multiple <i>tj1</i> copies are necessary to induce transposon silencing.....	37
3.5 Cells silence <i>tj1</i> via sRNA-mediated H3K9me2 deposition.....	39
3.6 Isolation of single <i>S. pombe</i> colonies with <i>de novo</i> transpositions.....	42
3.7 Transposition in the proximity of pericentromeric heterochromatin triggers <i>tj1</i> silencing.....	45
3.8 Sense and antisense transcription of <i>tj1</i> are necessary for efficient silencing of the element.	48
3.9 Low H3K9me2 is deposited already in cell populations of “2 <i>tj1</i> ” and “3 <i>tj1</i> ” strains.....	49
3.10 Silencing colonies strongly repress <i>tj1</i> via H3K9me2.....	51
3.11 <i>tj1</i> silencing is maintained more stably through generations when the element transposes close to pericentromeric heterochromatin.....	56
3.12 Locus independent <i>trans</i> -silencing of all endogenous <i>tj1</i> copies.....	59
3.13 H3K9me2 spreads to <i>tj1</i> neighboring regions.....	64
3.14 Establishment and maintenance of <i>tj1</i> silencing are RNAi-dependent.....	75
3.15 <i>tj1</i> silencing is Abp1-independent.....	77

3.16 <i>tj1</i> fitness effects.....	78
4. DISCUSSION.....	81
4.1 H3K9 methylation marks on silenced <i>tj1</i> elements.....	83
4.2 sRNA-dependent silencing of <i>tj1</i> in <i>S. pombe</i>	83
4.3 The importance of <i>tj1</i> transcription for the recognition of the TE.....	84
4.4 <i>Trans</i> silencing of dispersed genomic elements.....	85
4.5 Maintenance of <i>tj1</i> silencing is position-dependent.....	87
4.6 H3K9 methylation spreads from silenced <i>tj1</i> elements to flanking regions.....	89
4.7 Conclusions and future perspectives.....	95
5. MATERIALS AND METHODS.....	99
5.1 Materials.....	99
5.1.1 Strains used in this study (Table 5.1).....	99
5.1.2 Plasmids used in this study (Table 5.2).....	101
5.1.3 Strains + plasmids used in this study (Table 5.3).....	101
5.1.4 Oligonucleotides used in this study (Table 5.4).....	102
5.1.5 Media used in this study (Table 5.5).....	104
5.1.6 Antibodies used in this study (Table 5.6).....	105
5.1.7 Sequenced strains (Table 5.7).....	105
5.2 Methods.....	106
5.2.1 Strain and plasmid construction.....	106
5.2.2 Spot and silencing establishment assays.....	107
5.2.3 Transposition induction and isolation of colonies with transposed <i>tj1</i>	107
5.2.4 Silencing maintenance assay.....	108
5.2.5 Growth curve and competition assays.....	108
5.2.6 Chromatin Immunoprecipitation and sequencing (ChIP-seq).....	109
5.2.7 Ago1-bound sRNA sequencing.....	110
5.2.8 Genomic DNA purification.....	110
5.2.9 Total RNA purification, total RNA and RNA-polyA sequencings.....	111
5.2.10 Total RNA reverse transcription (RT).....	111
5.2.11 Quantitative Real-Time PCR (qPCR).....	111
5.2.12 Analysis of sequencing data.....	112
BIBLIOGRAPHY.....	113
ACKNOWLEDGMENTS.....	133

SUMMARY

Transposable Elements (TEs) are mobile DNA elements that can propagate extensively within the host genome that they colonize. TEs are divided in two major classes; Class I, represented by elements that propagate through an RNA-intermediate later retrotranscribed to cDNA and for this reason also known as retrotransposons, and Class II TEs, corresponding to transposons that mobilize via a DNA-intermediate. Uncontrolled transposition of both Classes of TEs represents a threat for the invaded organism, where these mobile elements can directly disrupt genes, impair their functions, induce detrimental genomic rearrangements and expand dramatically the genome size, conferring extra energetic costs to the cell during DNA replication. For these reasons, cells have evolved different strategies to control transposon activity, ranging from transcriptional silencing to post-transcriptional and post-translational repression.

Schizosaccharomyces pombe, also known as fission yeast, presents 13 copies of a retrotransposon named *tf2* and their repression is primarily maintained through the recruitment of specific DNA-binding proteins, which in turn induce local histone deacetylations and clustering of the dispersed *tf2* elements in nuclear foci called Tf bodies, preventing further transposon mobilizations. In addition, the exosome machinery is involved in degradation of the *tf2* RNA. H3K9 methylation, the heterochromatin hallmark, usually absent at *tf2* elements, is instead deposited in an RNAi-dependent manner when the exosome machinery is impaired, suggesting that fission yeast retains an alternative mechanism to silence *tf2* elements via the RNAi-mediated heterochromatin formation.

In this study, we simulated a foreign transposon invasion in *S. pombe* by the horizontal transfer of a retrotransposon (called *tj1*) from *Schizosaccharomyces japonicus*. Our results indicate that *S. pombe* retains the molecular tools to identify the exogenous element and that this recognition would eventually lead to the heterochromatinization of the retrotransposon, through an RNAi-dependent mechanism. We suggest that bidirectional transcription of *tj1* is important for the recognition of this element as a non-self DNA sequence and that transposition close to constitutive heterochromatin leads to an epigenetic stable silencing of the element. Furthermore, for the first time in wild-type fission yeast, we identify a sRNA-dependent mechanism responsible for the *trans* silencing of multiple homologous elements, corresponding to various *tj1* copies, dispersed within the genome. Finally, yet importantly, we show spreading of heterochromatin from the nucleation point (*tj1*) to the flanking genes, resulting in a negative fitness outcome. This finding suggests that the repression of the transposable element, in order to avoid further potentially lethal mobilizations, remains a priority in silencing cells.

1. INTRODUCTION

1.1 DNA organization in eukaryotic cells

In 1990, when the Human Genome Project (HGP) was just at the beginning, pediatrician and geneticist Jérôme Lejeune stated that “we have got 2 meters of so to speak magnetic tape in which everything is coded” (Louisiana Legislature, House Committee on the Administration of Criminal Justice, June 7, 1990). After 30 years, we can claim that that preliminary estimation was accurate (Piovesan et al. 2019; Clayton J, Dennis C. 2016), and therefore, the intriguing question is: how can 2 meters of DNA fit into a human cell nucleus, which size is typically $\sim 10\mu\text{m}$ (Sun, Shen, and Yokota 2000)? The answer is in the chromatin, the material that makes up chromosomes and that consists of DNA and proteins.

1.1.1 Chromatin

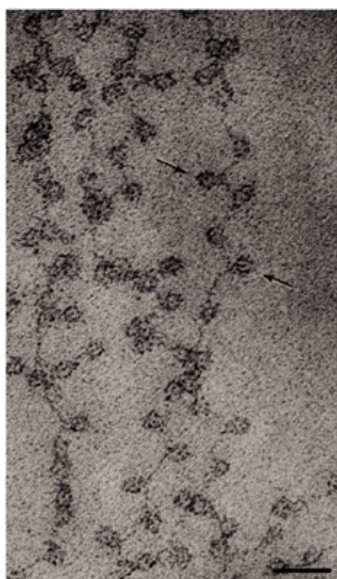


Figure 1.1: Electron micrograph of the "beads on a string".

From D. E. Olins and Olins 2003, black arrows indicate nucleosomes. Size marker: 30nm.

The term chromatin was introduced in 1879 by Walter Flemming, cytologist, referring to an easily stainable substance observed into nucleus of mitotic cells (Flemming, W. 1879). What Flemming identified were actually chromosomes, a term suggested a few years later by Wilhelm Waldeyer, anatomist (Waldeyer, H.W. 1888).

The basic structural and functional unit of chromatin is the nucleosome, consisting of four proteins called histones (H2A, H2B, H3 and H4), organized in an octamer of two copies of each histone, around which 146 bp of DNA is wrapped in 1.67 left-handed superhelical turns (Kornberg 1974; Luger et al. 1997). Under low salt conditions, consecutive nucleosomes establish the characteristic organization of nucleosomes as “beads on a string” (*10nm fiber*), where each histone octamer is a bead and the linker DNA is the string (A. L. Olins and Olins 1974; Woodcock, Safer, and Stanchfield 1976) (Figures 1.1 and 1.2). *In vitro*, the *10nm fiber* can aggregate further, forming the *30nm fiber* where the chromatin is coiled into a fiber with a diameter of 30nm (A. L. Olins and Olins 1974; Allan et al. 1981) (Figure 1.2). In the nucleus, however, consecutive nucleosomal units are dynamically spaced one to another, resulting in a globular compact structure, less organized than what observed *in vitro* under low salt conditions (reviewed in Baldi et al. 2020) (Figure 1.2).

A less conserved histone, H1 (absent in fission yeast *Schizosaccharomyces pombe*), binds the nucleosomal unit at the entry and exit site of the DNA to protect the linker DNA and to confer higher order organization to chromatin.

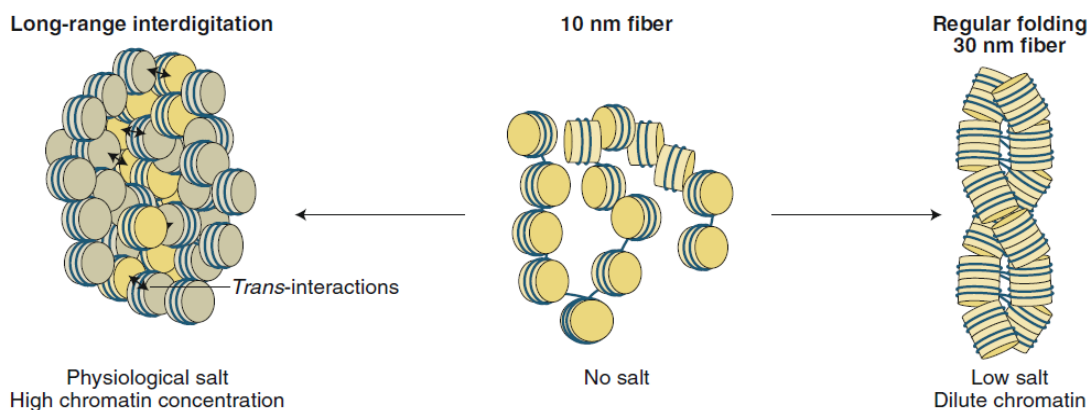


Figure 1.2: Folding of the 10 nm fiber under low and physiological salt conditions.

From Baldi et al. 2020, under low salt condition the 10 nm fiber folds into regular structures, such as the 30 nm fiber (right). On the other hand, at physiological conditions the 10 nm fiber forms less organized globular structures (left).

Despite some computational and biophysical evidences suggesting that the N- and C-termini of H3 and H4 may assume secondary structures *in vivo* (Banères, Martin, and Parello 1997; X. Wang et al. 2000; du Preez and Patterson 2013) and play a role in compacting the nucleosome (du Preez and Patterson 2013; W. Iwasaki et al. 2013; Bendandi et al. 2020), it is generally accepted that histones have less structured N-tails protruding from the nucleosome body (Luger et al. 1997; McGinty and Tan 2015) (Figure 1.3).

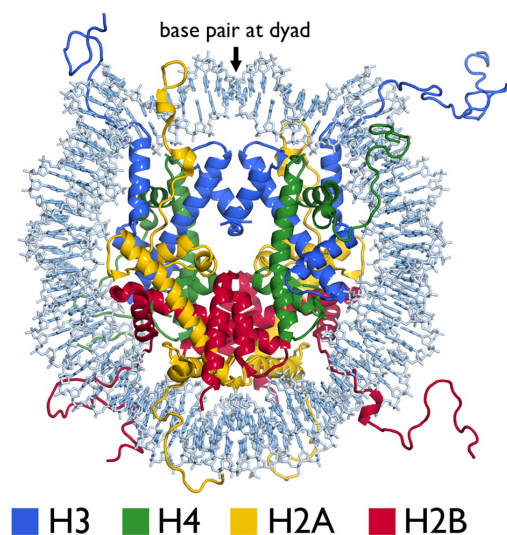


Figure 1.3: Nucleosome Structure.

From McGinty and Tan 2015, the structure of a nucleosome core particle is shown. Histone octamer and DNA are depicted in cartoon and sticks representation respectively. PDB ID 1KX5.

Histones are subjected to many post-translational modifications (PTMs) and most of them have been found at the histone tails (reviewed in (Kouzarides 2007)), although recent works proved that also histone cores are post-translationally modified (Ng et al. 2002; F. Xu, Zhang, and Grunstein 2005; Q. Li et al. 2008; Fenley et al. 2010). Histone writers, erasers and readers are the protein machinery that respectively add, erase and read these PTMs. In this dynamic process chromatin changes its properties and structure becoming, for example, more or less accessible. In fact, chromatin comes in two different forms, euchromatin and heterochromatin. While the first is less structured, highly transcribed and gene-rich, the second is more compact, silent and gene-poor. The discovery

of heterochromatin is attributed to Emil Heitz, botanist and geneticist, back in 1928, when he noticed that certain regions of mitotic chromosomes are more intensively stained and remain compact during the whole cell cycle, meanwhile other regions tend to be less stainable and disappear during telophase. Heitz defined the compact and the less stainable chromosome regions as heterochromatin and euchromatin, respectively (Heitz, E. 1928). Conserved histone PTMs are found in both hetero- and euchromatin, among them H3-mLys9, hypoacetylation and DNA-hypermethylation are common features of heterochromatin regions, while H3-mLys4, hyperacetylation and DNA-hypomethylation are normally found at euchromatin (Kouzarides 2007; Musselman et al. 2012). Importantly, *S. pombe* doesn't have DNA methyltransferase enzymes and therefore DNA methylations are not found in fission yeast. Another important feature of heterochromatin is the so called Position-Effect Variegation (PEV), observed by Muller in 1930, in which a normally expressed gene within an euchromatin environment, when positioned in proximity to heterochromatin (by chromosome rearrangement or transposition), acquires heterochromatin characteristics, becoming transcriptionally silent or less active (Muller 1930) (for PEV in *S. pombe* see Robin C. Allshire et al. 1994; R. C. Allshire et al. 1995; Locke and Martienssen 2009). The main function of heterochromatin is to preserve genome stability, ensuring proper chromosome segregation during cell division, and preventing transcription and recombination of repetitive elements (including transposable elements, TEs), chromosome fusion, and circularization (Robin C. Allshire and Madhani 2018).

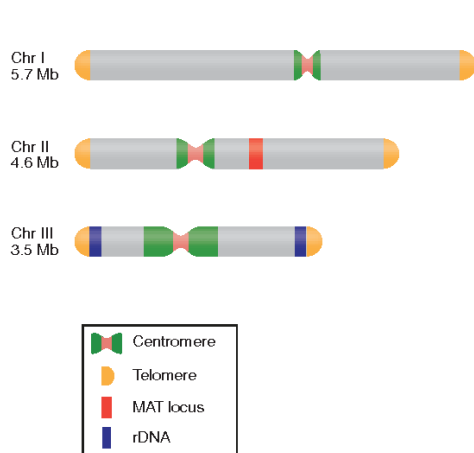


Figure 1.4: Constitutive heterochromatin regions in *S. pombe*.

From Allshire and Ekwall 2015, constitutive heterochromatin in the three chromosomes of *S. pombe* is represented.

1.2 Heterochromatin in *S. pombe*

Heterochromatin can be further divided in two categories, constitutive and facultative. The first is present at fixed chromosome regions and remains throughout the entire cell cycle. On the contrary, facultative heterochromatin is found only in specific phases of the cell cycle, representing a reversible silent chromatin state. In *S. pombe* constitutive heterochromatin is present in four regions: centromeres, telomeres, mating-type loci (MAT loci) and rDNA regions (Locke and Martienssen 2009) (Figure 1.4). Heterochromatin at centromeres and telomeres ensures proper chromosome segregation during cell division and avoids chromosome rearrangement (Bisht et al. 2008; Ellermeier et al. 2010; Nambiar and Smith 2018; Okita et al. 2019). At the MAT locus, heterochromatin regulates mating-type switching (Egel et al. 1984; Yamada-Inagawa, Klar, and Dalgaard 2007). Although the role of heterochromatin at the rDNA region hasn't been clearly elucidated yet, it may mirror the function that it has in the budding yeast *S. Cerevisiae*, where heterochromatin prevents recombination between rDNA repeats (Grunstein and Gasser 2013).

Recent studies have revealed a role for rDNA repeats in telomerase defective cells, where chromosomal rearrangement is prevented by translocation of rDNA repeats to all chromosome termini, where they recruit the machinery for heterochromatin formation and preserve chromosome linearity (D. Jain et al. 2010; Begnis et al. 2018).

1.2.1 Heterochromatin at centromeres



Figure 1.5: *S. pombe* centromere.

From Allshire and Ekwall 2015, schematic representation of centromere of fission yeast. *Cnt* represents a chromosome specific central sequence, flanked by innermost repeats (*imr*) and outermost repeats (*otr*). *Otr* are subdivided in repetitive elements called *dg* and *dh*. Orientation and number of *otr* change in the three chromosomes, with *cenI* having two, *cenII* three and *cenIII* ~13. Double arrow-heads represent t-RNA clusters, found in the *imr* and downstream the outermost repeats.

S. pombe has become a central model organism for studying heterochromatin, especially at centromeres. In fact, fission yeast presents a centromere organization that is similar to that of higher organisms, including mammals. Moreover, *S. pombe* has many of the heterochromatin proteins conserved in mammals, like Swi6 and Chp2, homologous to HP1 (Heterochromatin-Protein 1) and retains the RNA interference (RNAi) pathway components.

In fission yeast, centromeres consist of a central core, *cnt*, flanked by innermost repeats (*imr*) and outermost repeats (*otr*) (Robin C. Allshire and Ekwall 2015) (Figure 1.5). The central core represents the region where the kinetochore complex assembles during cell division and where in the mid to late G2 phase, canonical histone H3 is replaced by the H3 histone-like protein CENP-A (known as Cnp1), ensuring the correct kinetochore assembling (Takahashi, Chen, and Yanagida 2000; Roy et al. 2013). In a recent model, the replacement of H3 with Cnp1 at centromeres is enhanced by RNA-polymerase II (RNAPII, or RPII), which associates with the centromere central core in G2, simultaneously with H3 eviction (Shukla et al. 2018). Introduction of naked centromeric DNA guides the formation of functional centromeres, via CENP-A recruitment and kinetochore assembly, suggesting that CENP-A specifically recognizes centromeric DNA (Baum, Ngan, and Clarke 1994; Okada et al. 2007).

Even if all the three centromeres of *S. pombe* have a similar organization, they differ one to another for the number of *otr*. The centromere of chromosome I (*cenI*) has two, *cenII* has three and *cenIII* has ~13, making the length of centromeres 40, 65, and 110kb, respectively. *Otr* are subdivided in repetitive elements called *dg* (abbreviation for dogentai, japanese word for kinetochore) and *dh* (named so because discovered after *dg*).

Heterochromatin at centromeres, often referred to as pericentromeric heterochromatin, is found over the *otr*. Canonical heterochromatin marks are found here, like di- and tri-methylation of lysine 9 in H3 (H3K9me2 and H3K9me3) (Rea et al. 2000; Nakayama et al. 2001; Noma, Allis, and Grewal 2001), H3 deacetylation (especially at K14) (Kouzarides 2007) and HP1 homologs (Swi6 and Chp2)

(Fischer et al. 2009). Moreover, genes inserted within pericentromeric heterochromatin become silenced or less active, according to the PEV phenomenon previously mentioned (Robin C. Allshire et al. 1994; R. C. Allshire et al. 1995).

Crucial for the establishment and maintenance of pericentromeric heterochromatin is the RNA interference (RNAi) pathway (Volpe et al. 2002; Verdel et al. 2004). RNAi was first observed in plants, where the attempt to achieve overexpression of an endogenous gene by introducing a second copy of it, showed the opposite effect, resulting in co-suppression of both endogenous and exogenous genes (Napoli, Lemieux, and Jorgensen 1990). With the name of *quelling*, the same phenomenon was observed in the filamentous fungus *Neurospora crassa* (Romano and Macino 1992). Finally, in 1998, Fire and colleagues introduced the term RNA interference (RNAi) when they observed that exogenous dsRNA was the responsible for the gene silencing in *Caenorhabditis elegans* (Fire et al. 1998). Following studies showed that short RNAs of ~22 nucleotides, therefore called *small interfering RNAs* (siRNAs, or simply sRNAs), are produced by a member of the ribonucleases III family, *Dicer*. These siRNAs serve as guide sequences that direct the nuclease complex **R**NA-**I**nduced **S**ilencing **C**omplex (RISC), containing Argonaute (a piwi/sting/argonaute/zwillie/eIF2C family member), to the target mRNA for its **p**ost-**t**ranscriptional **g**ene **s**ilencing (PTGS) (Tabara et al. 1999; Hamilton and Baulcombe 1999; Bernstein et al. 2001; Martinez et al. 2002). RNAi as a PTGS mechanism has been proven to be a very powerful biological tool against virus infections in plants, fungi and invertebrates (Ding et al. 2004) and lately also in mammals, including humans (Y. Li et al. 2016; Ding et al. 2018). In 2018, the first therapeutic medical approach based on RNAi was globally introduced to treat a neurological disease called hereditary TTR-mediated amyloidosis (hATTR) (Hoy 2018). In this treatment, a double strand small interfering RNA is used (under the commercial name of Patisiran) to guide the RISC complex to degrade the endogenous mRNA of the mutated gene responsible for the disease (Coelho et al. 2013).

In *S. pombe*, the RNAi represents the central pathway for heterochromatin establishment and maintenance at pericentromeric repeats (Figure 1.6). To establish heterochromatin, generation of priRNAs (primal small RNAs), a distinct class of siRNAs, is necessary (Halic and Moazed 2010). Degradation products of bidirectional pericentromeric transcripts form the priRNA precursors. These slightly longer siRNAs are then bound by the Argonaute protein (Ago1) and processed to mature priRNAs by the trimming activity of the 3'-5' exonuclease Triman protein (Tri1) (Marasovic et al. 2013). Ago1 loaded with single strand siRNA is bound to the chromodomain containing protein Chp1 and the GW (glycine tryptophan) domain containing protein Tas3 to form the RITS (RNA-Induced Transcriptional Silencing) complex (Verdel et al. 2004). By base pairing interaction, the siRNA loaded on Ago1 guides the RITS complex to the complementary nascent pericentromeric antisense non-coding RNA, transcribed at low levels by RNA polymerase II (RPII) (Kato et al. 2005; Djupedal et al. 2005; Bühler, Verdel, and Moazed 2006). Once on chromatin RITS recruits the RDRC complex (RNA-Directed RNA polymerase Complex) and the CLRC complex (Clr4-Rik1-Cul4 complex) (Motamedi et al. 2004; Jia, Kobayashi, and Grewal 2005; K. Zhang et al. 2008). The

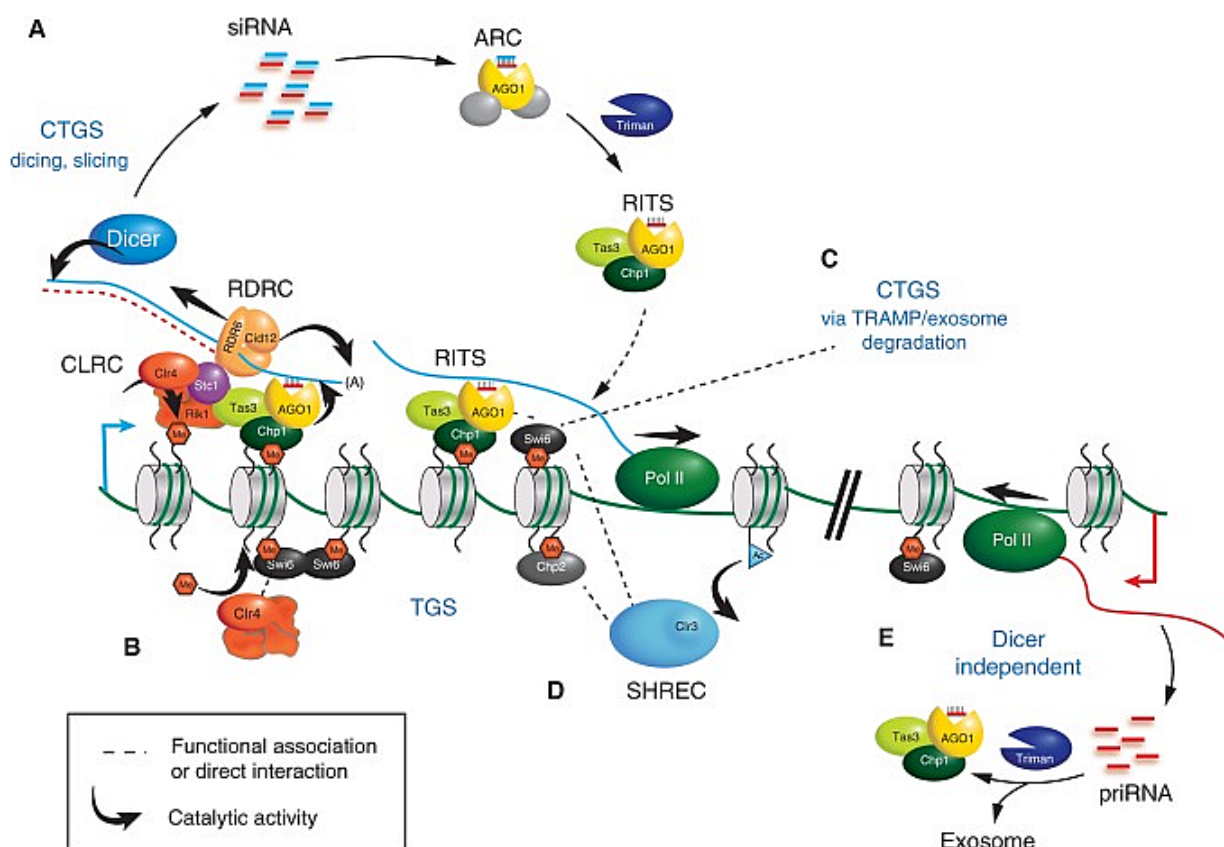


Figure 1.6: RNAi pathway and heterochromatin establishment at pericentromeric repeats in *S. pombe*.

From Martienssen and Moazed 2015, schematic representation of the concerted mechanisms responsible for heterochromatin establishment and maintenance at pericentromeric repeats. Heterochromatin preserves Transcriptional Gene Silencing (TGS). The slicing and dicing activities of Ago1 and Dicer respectively, together with exosome degradation, ensure Co-Transcriptional Gene Silencing (CTGS) of nascent non-coding RNA.

first contains the RNA-dependent RNA polymerase Rdp1 (together with the RNA helicase Hrr1 and the non-canonical poly-(A) polymerase Cid12) leading to the conversion of the target non-coding RNA into dsRNA, cleaved by Dicer into new double stranded siRNA precursors (Colmenares et al. 2007). siRNA duplex precursors are loaded onto Ago1 in the ARC complex (Argonaute Chaperone complex, also containing Arb1 and Arb2). There, the slicer activity of Ago1 leads to the loss of one of the two RNA strands (passenger strand) and following trimming by Triman results in a mature single stranded siRNA loaded onto the RITS complex to start the siRNA amplification loop again (Buker et al. 2007; Marasovic et al. 2013; R. Jain et al. 2016). As mentioned above, on chromatin RITS recruits also the CLRC complex, containing the Clr4 subunit. This recruitment is mediated by Stc1, a LIM domain protein that physically links Ago1 to Rik1 (Bayne et al. 2010; He et al. 2013). Clr4 is a methyltransferase specific for Lysine-9 of H3 (despite recent works suggesting that Clr4 may target also non-histone substrates (K. Zhang et al. 2011; Kusevic et al. 2017)), homologous to human Su(var)3-9 protein family, and the sole methyltransferase known in *S. pombe* (Lejeune and Allshire 2011). Clr4 is responsible for H3K9 di- and tri-methylations, the canonical marks for heterochromatin. Clr4 is not only a chromatin writer, but also a reader. In fact, it contains an N-terminal chromodomain that specifically binds H3K9 methylated tails (K. Zhang et al. 2008; Akoury et al. 2019). Also the Chp1 subunit of RITS complex contains a chromodomain which contributes to directing the complex to heterochromatin (Partridge et al. 2002; Zocco et al. 2016). These two mechanisms of protein complex recruitment represent a self-reinforcing loop for heterochromatin establishment and maintenance. A recent work showed that in addition to its methyltransferase activity, CLRC may also ubiquitylate H3K14, promoting H3K9 methylation, suggesting a further positive feedback loop to recruit CLRC on heterochromatin (Oya et al. 2019). Two other chromodomain containing proteins are subsequently recruited to methylated H3K9, Swi6 and Chp2 (Ekwall et al. 1995; Nakayama et al. 2001; Canzio et al. 2013) conferring a further compact state to the heterochromatin. Moreover, Swi6 promotes RDRC complex recruitment through a RNAi factor intermediate, Ers1, reinforcing the RNAi pathway (Hayashi et al. 2012; Rougemaille et al. 2012). Swi6 also retains nascent heterochromatin RNA, then dissociates from heterochromatin and mediates RNA degradation by the exosome machinery, preventing accumulation of non-coding RNA on chromatin, deleterious for the heterochromatin state (Keller et al. 2012a; Brönnner et al. 2017). Chp2, on the other hand, interacts with the histone deacetylase complex SHREC (Snf2/Hdac-containing repressor complex), which contains the Clr3 histone deacetylase (HDAC), promoting H3K14 deacetylation and contributing to transcriptional silencing of pericentromeric repeats (Motamedi et al. 2008; Fischer et al. 2009). The initial generation of Dicer-independent priRNAs by the concerted action of Ago1 and Triman is proposed to contribute to generate the low level of H3K9 methylation necessary to nucleate heterochromatin at pericentromeric repeats and intriguingly at bidirectionally transcribed elements, like exogenous transposons (Halic and Moazed 2010; Marasovic et al 2013).

The sequencing of the whole genome of *Schizosaccharomyces japonicus*, another member of the fission yeast clade, showed that this organism presents a completely different centromere organization, compared to *S. pombe* (Rhind et al. 2011). While the latter doesn't possess transposable elements at centromeres (Figure 1.5), the former presents numerous copies of a TE called Tj(1-10), located at the centromeric (and telomeric) heterochromatin (Rhind et al. 2011). Interestingly, *S. japonicus* retains the RNAi-machinery and the sequencing of siRNAs showed that the majority of these RNAs (94%) maps to Tj elements, underlying the central role of TEs in regulating heterochromatin formation in this organism (Rhind et al. 2011).

1.2.2 Heterochromatin at mating-type locus

In *S. pombe* the mating-type locus (MAT) consists of three distinct components, mat1, mat2-P and mat3-M (Figure 1.7). Only mat1 is transcribed, while mat2-P and mat3-M are silenced. The mating type of the cell depends on the information encoded by the mat1 component, where either P or M is present. Cells can switch type from M to P (and the other way around), swapping the component at mat1. In the wild, fission yeast populations are homotallic (called h90), meaning that half of the population is P and half is M, with cells continuously switching between the two types (Yamada-Inagawa et al. 2007). Cells with opposite mating-type, under stress conditions (like nitrogen starvation), can mate, generating a diploid cell and subsequently four haploid spores, more resistant to stress conditions. Laboratory strains are usually heterotallic, meaning that consist in only one of the two mating-types, either P (h+) or M (h-) and are kept in specific growing conditions to avoid mating-type switching, unless wanted.

The MAT locus is localized in the right arm of chromosome II and spans ~30kb. mat1 is ~15kb away from mat2-P, which is ~11kb away from mat3-M. The interval between mat1 and mat2-P is called the L-region, while that between mat2-P and mat3-M is the K-region (Grewal and Klar 1997). Located within the K-region is the *cenH* sequence, ~4.3kb long and ~96% homologous to the dg and dh repeats found on the outermost regions of centromeres (Grewal and Klar 1997) (Figure 1.7). The homology between *cenH* and pericentromeric regions suggests a common mechanism of heterochromatin formation guided by RNAi. However, RNAi is necessary only for *de novo* establishment of heterochromatin, while its subsequent maintenance and inheritance is RNAi independent (Hall et al. 2002). In parallel to RNAi dependent heterochromatin establishment, there is an RNA-independent nucleation and maintenance pathway involving the DNA binding proteins Atf1 and Pcr1 of the ATF/CREB transcription factor family (Jia et al. 2004). These two proteins bind a specific DNA sequence close to mat3-M, recruit Clr4, Swi6 and Clr3, and limit RPII access, silencing the MAT locus independently to RNAi (Jia et al. 2004; Yamada et al. 2005).

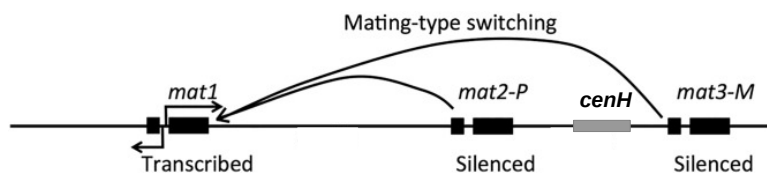


Figure 1.7: Mating-type locus in fission yeast (adapted version from Hoffman et al. 2015).

1.2.3 Heterochromatin at telomeres

Telomeres represent the ends of linear chromosomes in eukaryotic cells and possess species-specific tandem repeats. In fission yeast telomere repeats span for ~300 bp and present the consensus sequence TTAC(A)(C)G_{2,8} (Sugawara 1988). Adjacent to telomeres, there are the subtelomere regions, spanning for ~100kb. Subtelomeres contain sequences that differ to telomere repeats and share similarities with other subtelomeres. Heterochromatin is present within the first 50kb of subtelomeres, where the *tlh* (RecQ-type helicase) gene locus is. Recent studies discovered the presence of 4 different *tlh* genes (*tlh1-4*), each located in a different subtelomere of chrI and chrII (Kaji et al. 2020).

Similar to heterochromatin formation at the MAT locus, RNAi plays a role in heterochromatin establishment at subtelomere regions as well, where *cenH*-like sequences are found (Hansen et al. 2006). These sequences are able to nucleate heterochromatin formation at an ectopic locus (Hansen et al. 2006), like the *cenH* element from the MAT locus (Hall et al. 2002). However, RNAi mutants don't show heterochromatin defects or H3K9-methylation loss at subtelomeres, suggesting the existence of an RNAi-independent redundant pathway for heterochromatin formation (Kanoh et al. 2005). ~300bp of telomere repeats, together with Taz1 (a shelterin complex subunit), were identified as sufficient elements for recruiting Swi6 through Clr4 at subtelomeres, independently of the RNAi machinery and *cenH*-like sequences (Kanoh et al. 2005). The shelterin complex of fission yeast is similar to that of mammals and protects telomere ends, distinguishing them from "simple" DNA double strand breaks which would activate the cellular DNA damage response, leading to cell cycle arrest, chromosome end-to-end fusions and general genome instability, detrimental for cell viability (Bisht et al. 2008; Xue et al. 2017). Moreover, Taz1 and a second subunit of the shelterin complex, Ccq1, are involved in the recruitment of SHREC at telomeres, inducing further silencing through HDAC Clr3 and nucleosome re-positioning (thanks to the SHREC subunit Mit1, a SNF2 family of chromatin remodeling factor) to assemble higher order chromatin structures (Sugiyama et al. 2007).

1.2.4 Facultative heterochromatin

In addition to the large constitutive heterochromatin regions, in *S. pombe* heterochromatin is also present at the so-called facultative heterochromatin regions. These silent heterochromatin islands

correspond to genes silenced during vegetative growth and expressed during environmental stress growth conditions and/or meiosis induction (Zofall et al. 2012; Shah et al. 2014). Although H3K9me is found at these facultative loci, post-transcriptional silencing seems to be the main way for their silencing. Meiotic genes present a consensus sequence called DSR (Determinant of Selective Removal) (Harigaya et al. 2006) which is specifically recognized by an RNA-binding protein, Mmi1, leading to their degradation through a mechanism involving the zinc finger protein Red1, the poly(A) polymerase Pla1, and ultimately the exosome machinery (Yamanaka et al. 2010; Sugiyama and Sugioka-Sugiyama 2011). Red1, together with Mtr4-like protein 1, form a core module, called MTREC (Mtl1-Red1 core) (N. N. Lee et al. 2013). PTGS at facultative heterochromatin is coupled to H3K9me deposition thanks to Clr4 recruitment by Red1 (Zofall et al. 2012; Tashiro et al. 2013). Canonical RNAi members, such as Dcr1, Ago1 and chromodomain containing proteins Chp1 and Swi6 are also found at facultative heterochromatin (Woolcock et al. 2011; Tashiro et al. 2013). However, deletions of Ago1 and Dcr1 don't show important loss of H3k9me, indicating that RNAi plays a secondary role in heterochromatin formation at facultative heterochromatin loci (Tashiro et al. 2013). A recent work showed that HDAC Clr3 is recruited to a facultative heterochromatin gene, *pho1* (a gene involved in phosphate uptake and derepressed only under phosphate starvation), in a H3K9me-independent manner. According to this study, Clr3 is recruited through the concerted action of non-coding RNA and Set1/Set2 histone methyltransferases, conferring a further silencing state to the facultative heterochromatin loci (Watts et al. 2018).

Another type of facultative heterochromatin is found at HOODs (Heterochromatin Domains) where H3K9me is RNAi-dependent, differently to heterochromatin islands, where Clr4 is recruited also through Red1 (Zofall et al. 2012; Tashiro et al. 2013; Marasovic et al. 2013; Yamanaka et al. 2013). HOODs are established at diverse loci, including sexual differentiation genes, genes encoding transmembrane proteins, and retrotransposons that are also targeted by the exosome RNA degradation machinery (Marasovic et al. 2013; Yamanaka et al. 2013). Mutation of Rrp6, the catalytic subunit of the RNA exosome, and adverse growing conditions, result in the generation of siRNA clusters which trigger H3K9 methylation at normally exosome-targeted genes, through canonical RNAi machinery (Marasovic et al. 2013; Yamanaka et al. 2013). Interestingly, Clr4, RNAi and Rrp6 single mutants, don't show significant derepression of retrotransposons and sexual differentiation genes, suggesting that RNAi and exosome machinery act redundantly to silence these loci (Yamanaka et al. 2013). In a proposed model, HOODs are silenced by the exosome machinery and the RNAi. In this process, Red1, Pla1 and Pab2 (poly(A)-binding protein) interact with both the exosome machinery and RNAi pathway, promoting gene silencing (Yamanaka et al. 2013).

1.3 Transposable Elements (TEs)

1.3.1 TEs, a general overview

Transposable elements (TEs), also called “jumping genes” or simply “transposons”, are defined as DNA sequences that are able to move (transpose) from one location to another within the same genome, or to another. TEs were discovered more than 70 years ago by Barbara McClintock while studying *Zea mays* (maize) (McClintock 1950). Initially received with skepticism from scientific community, only ~35 years later TEs identification was eventually recognized with many awards, including a Nobel prize in Physiology or Medicine in 1983. Also referred to as selfish elements and “junk DNA” (Ohno 1972), TEs and elements deriving from them, represent a large percentage of prokaryotic and eukaryotic genomes. TEs constitute ~46% of human genome, 12% in *C. elegans*, over 80% in some plants and ~1.1% in *S. pombe* (SanMiguel et al. 1996; *C. elegans* Sequencing Consortium 1998; Lander et al. 2001; Bowen et al. 2003). However, the conception of transposable elements as pure genomic parasites has changed with time. Nowadays it is known that many organisms have co-evolved with their TEs in a process called domestication. For example, in jawed vertebrates, recombination of V(D)J is guided by the Recombination Activity Gene (RAG) proteins 1 and 2. Studies on RAG have discovered mechanistic and structural analogies to several transposons, indicating that the DNA cleavage activity of RAG1 and RAG2 represents an adaptation of the endonuclease activity of progenitor TEs (Y. Zhang et al. 2019a). In *Drosophila*, a telomerase gene is not present, nevertheless *Drosophila* telomeres resemble other eukaryotic repetitive telomere organization thanks to the presence of arrays of TEs. Their expression and nearby transposition extend telomere length, generally conferring the same telomeric repetitive aspect like other eukaryotes using telomerase (Mason et al. 2008). TEs co-evolved also together with prokaryotic organisms. An interesting example is the bacterial CRISPR–Cas systems, recognized as an adaptive immune defense against exogenous organisms. In this process, foreign DNA is processed and integrated in the Clustered Regularly Interspaced Short Palindromic Repeats (CRISPR). There, called “spacer”, it is transcribed together with other spacers in long precursors that are processed by Cas cassette members. Finally mature RNAs guide Cas proteins to foreign nucleic acids to eliminate them (Rath et al. 2015). Recent studies provide indications that the integrase member of Cas proteins, necessary to integrate spacers in CRISPR repeats, may derive from a TE family called “casposons” (Krupovic et al. 2017).

On the other end, transposable elements are also responsible for at least 100 heritable human diseases (Payer and Burns 2019) and their uncontrolled propagation can be detrimental for cell viability. For this reason, organisms have evolved strategies to silence them or reduce their negative effects (see sections 1.3.4 and 1.3.5).

1.3.2 Transposon classification

Transposable elements are generally divided in two large classes (Wicker et al. 2007) according to their propagation mechanism; Class I is represented by TEs that transpose through an RNA-intermediate that is later reverse-transcribed and integrated. For this reason, Class I TEs are also called retrotransposons. Retrotransposons can be subdivided into classes based on the presence or absence of LTRs (Long Terminal Repeats) at TE right and left borders. A further sub-classification is made according to their autonomy or not to synthesize all proteins necessary for transposition. Class II transposable elements propagate through a DNA-intermediate and consequently are also denominated DNA transposons (Wicker et al. 2007). Generally retrotransposons are replicative, meaning that they can increase their genome number at each propagation cycle, meanwhile DNA transposons are usually not-replicative, moving through a “cut and paste” mechanism that doesn’t increase their number. In humans, TEs represent more than 40% of the genome and both Classes of transposons are found (Figure 1.8) (Lander et al. 2001). Most human TEs represent fossil elements

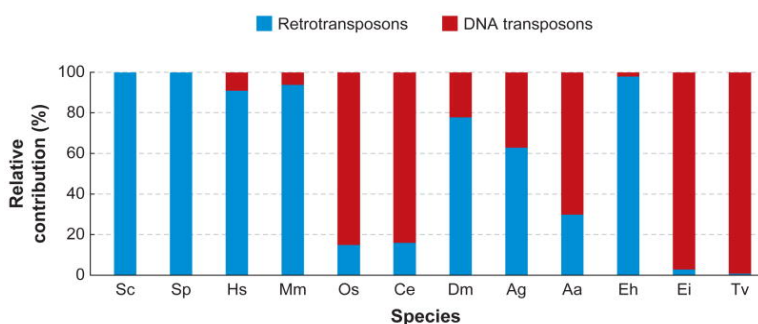


Figure 1.8: Relative amount of retrotransposons and DNA transposons in different eukaryotic organisms.

From Feschotte and Pritham 2007, representation of percentages of total genomes corresponding to retrotransposons (light blue) and DNA transposons (red). *Species abbreviations: Sc: Saccharomyces cerevisiae; Sp: Schizosaccharomyces pombe; Hs: Homo sapiens; Mm: Mus musculus; Os: Oryza sativa; Ce: Caenorhabditis elegans; Dm: Drosophila melanogaster; Ag: Anopheles gambiae, malaria mosquito; Aa: Aedes aegypti, yellow fever mosquito; Eh: Entamoeba histolytica; Ei: Entamoeba invadens; Tv: Trichomonas vaginalis.*

genome, due to its bigger size (~6kbp) (Lander et al. 2001). In *S. pombe* only two autonomous LTR-retrotransposons families are present, Tf1 and Tf2 (Transposon of fission yeast 1 and 2) (Figure 1.8) (Bowen et al. 2003). In wild fission yeast both Tf1 and Tf2 coexist, while in commonly used laboratory Leupold strain, only the Tf2 full-sequence is found. However, evidence of the previous presence of Tf1 in the laboratory strain is left in the form of numerous solo Tf1 LTRs (Bowen et al. 2003).

because they are not able to move anymore, but some can still propagate. The only active elements identified in humans are the non-LTR TEs autonomous LINE1, or L1 (of the Long INterspersed Elements TE group) and non-autonomous Alu genes of SINEs group (Short INterspersed Elements). As the group name suggests, Alu elements are relatively small (~300bp) and over 1 million copies are dispersed throughout the human genome (Lander et al. 2001). Despite its lower number in the genome, L1 represents around 15-18% of human

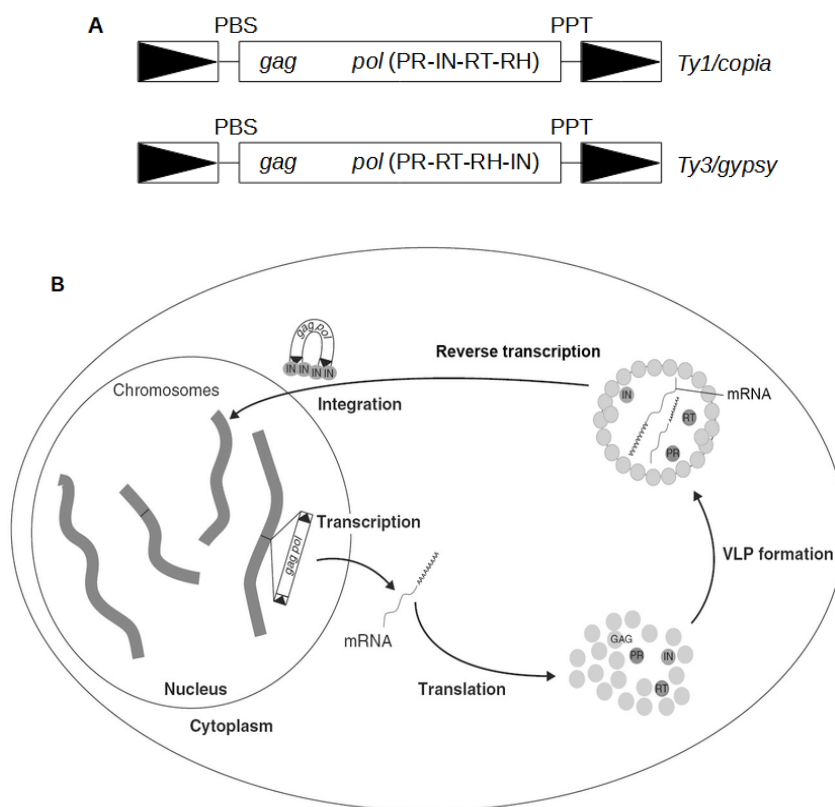


Figure 1.9: *Ty1/copia* and *Ty3/gypsy* retrotransposons scheme and retrotransposon cell cycle.

(A) Representation of *Ty1/copia* and *Ty3/gypsy* TE superfamilies. In *copia-like* elements, IN subunit is found between PR and RT, while in *gypsy-like* transposons IN is the last subunit of *pol* ORF. Boxes with black triangles define LTRs. Primer-binding sites (PBS) and polypurine tracks (PPT) are represented after 5' LTRs and before 3' LTRs respectively. PR, protease; IN, integrase; RT, reverse-transcriptase; RH, ribonuclease H (RNase H). (B) From Kovalchuk 2005, retrotransposon cell cycle, from nuclear transcription to integration of a new transposon copy in the host genome.

As mentioned, Class I transposons move through an RNA-intermediate that is retrotranscribed to cDNA. In Figure 1.9A a general scheme of two autonomous LTR-retrotransposon superfamilies (*Ty1/copia* and *Ty3/gypsy*) is represented. Between the two LTRs there are two Open Reading Frames (ORFs), *gag* and *pol*. The first encodes a structural protein that builds up a virus like particle (VLP). The *pol* ORF, where *pol* stands for poliprotein, encodes the catalytic subunits necessary for reverse transcription and integration: protease (PR), integrase (IN) and reverse-transcriptase (RT) with an RNase H domain (RH). A canonical retrotransposon cell cycle consists of transcription of the element, cytosol export of the mRNA and translation into Gag and Pol. Pol is cleaved by its PR into PR, IN and RT subunits that together with the mRNA are packed into the VLP formed by Gag polymerization. At this point the mRNA inside the VLP is retro-transcribed to form double stranded cDNA which enters back into the nucleus associated to IN subunits. Once in the nucleus, INs guide the cDNA to the host genome to promote a new insertion (Figure 1.9B). Important for successful

transposition is the ratio between Gag and Pol, with the first more abundant than Pol in order to assemble functional VLPs. To do so, different strategies are used by retrotransposons. The most common mechanism consists of ribosomal frameshifting and resembles that of many retroviruses, including HIV (Jacks et al. 1988). In this process pol is usually frameshifted +1 or -1 with respect to gag and overlaps the gag 3' end. Standard translation results in predominantly Gag synthesis, however, a fraction of ribosomes shifts to the ± 1 frame at the end of gag producing fused Gag-Pol protein, later cleaved in Gag and Pol subunits. +1 ribosomal frameshifting is utilized by *S.cerevisiae* retrotransposons Ty1 and Ty3 (Belcourt and Farabaugh 1990). Another mechanism is present in *S. pombe* where Tf1 and Tf2 contain a single ORF for gag and pol. Gag-Pol protein is afterwards cleaved into subunits and through an unknown activity, RT and IN are degraded to maintain Gag at higher levels (Atwood et al.1996). Some other retrotransposons have gag and pol in frame, but utilize a stop codon readthrough strategy. A “stop” is placed between gag and pol, therefore, the first is produced at higher concentration than the second. Occasionally ribosomes read the “stop” as an amino acid codon, synthesizing Gag-Pol. In *Drosophila melanogaster*, copia retrotransposon utilizes alternative splicing to remove pol from gag-pol mRNA, thereby allowing Gag to be at higher levels than Pol (Brierley and Flavell 1990).

To understand how retrotransposons retro-transcribe their RNA, it is necessary to have a close-up of the LTR structure (Figure 1.10A). Each Long Terminal Repeat works as a transcription promoter and terminator, and is divided in three regions, U3, R and U5. U3 contains the promoter and a transcript goes from R in the 5' LTR to R in the 3' LTR. Once incorporated in a VLP, the transcript is bound by a retro-transcription primer in correspondence to the PBS sequence. Generally a host t-RNA functions as primer (Figure 1.10B_1). In other cases, like in fission yeast TEs, the transcript itself forms a 5' stem-loop, later cleaved in correspondence to the PBS sequence, in a self-priming host-independent mechanism (J. H. Lin and Levin 1997). RT reverse-transcribes up to R in the 5' LTR (2). The single-stranded DNA R region pairs with the 3' terminus in the “first jump”(3). Retro-transcription proceeds up to R in 5' LTR copying it a second time (4). The initial primer and remnant RNA are degraded by RNaseH, except a sequence in corresponding to PPT (5), which works as primer for the second strand DNA synthesis up to U5 in 3' LTR (6). Newly synthesized DNA switches to R in 5'LTR (“second jump”) and double stranded cDNA synthesis ends (7 and 8). At this point IN guides transposition of the new retrotransposon copy into the host genome (9).

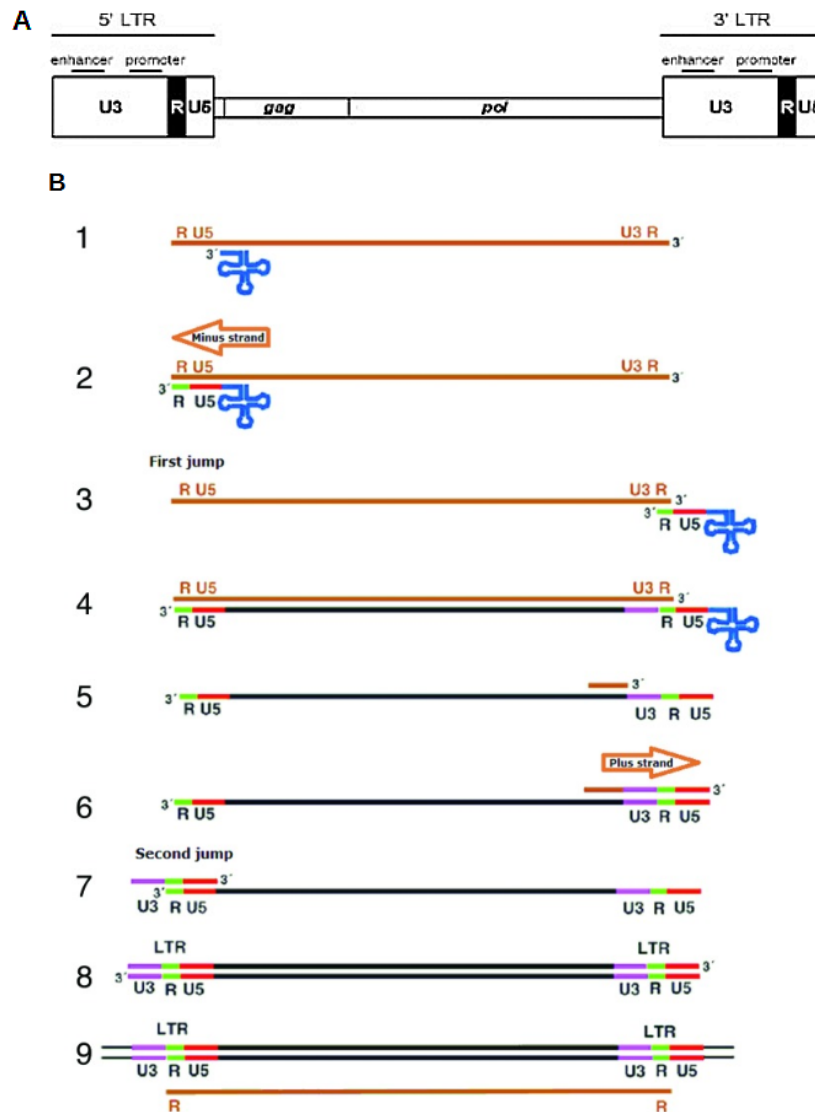


Figure 1.10: LTR close-up and retrotransposon reverse-transcription mechanism.

(A) Adapted from Zhang et al. 2014 ,LTR-retrotransposon with LTR details. (B) Adapted from Zhang et al. 2014, mechanism for retrotransposon reverse-transcription (see text for explanations).

1.3.3 Transposable Elements in *S. pombe*

As mentioned above, the only TEs present in *S. pombe* are full-length autonomous LTR-retrotransposons (Figure 1.8), called Tf1 and Tf2, and their associated elements (Table 1.1) (Bowen et al. 2003). In the Leupold strain, 13 full-length Tf2 copies are found dispersed throughout the three chromosomes, together with sequences related to both Tf2 and the extinct Tf1, present only in wild fission yeast (Levin et al. 1990; Bowen et al. 2003). In total, TEs constitute 1.1% of the *S. pombe* genome (Bowen et al. 2003). Tf1 and Tf2 belong to the Ty3/gypsy family, where RT precedes IN in

pol (Figure 1.11). Sequence analysis of Tf1 and Tf2 shows that they differ significantly at gag and in a segment of the LTRs, while pol is virtually identical (Figure 1.11) (Weaver et al. 1993). Differently to most LTR TEs that use host t-RNAs to prime retro-transcription, Tf1 and Tf2 use a self-priming system that relies on the first 11 bp of the 5' mRNA. The transcript forms a complex stem-loop structure annealing its 5' end to the PBS sequence. Afterwards, the RNaseH domain of RT cleaves the mRNA duplex between nucleotide 11 and 12, and RT can start reverse-transcription of the minus strand cDNA (Figure 1.10B_2) (Levin 1996; Hizi 2008).

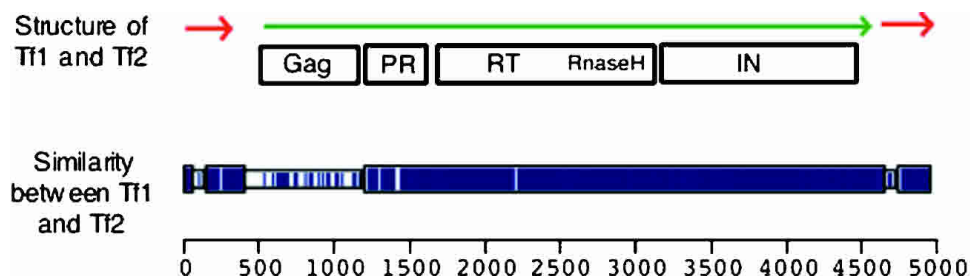


Figure 1.11: Tf1 and Tf2 diagram and homology between them.

From Bowen et al. 2003, on top, diagram of Tf1 and Tf2. Red arrows represent LTRs, green arrow represents the retrotransposon protein coding region. Gag and Pol subunits are indicated into white boxes. RT precedes IN, making Tf1 and Tf2 *Ty3/gypsy*-like elements. The block diagram on the middle shows sequence homology between Tf1 and Tf2. High and low homology are represented by taller blue rectangles and white rectangles respectively. On the bottom, a bp scale.

Tf1 and Tf2 associated elements (Table 1.1) represent a footprint of former transpositions. A genome-wise analysis of these elements showed that both transposons were preferentially located in intergenic regions with a strong preference for promoters of RPII transcribed genes (Bowen et al. 2003). A closer analysis of the TEs indicate a preferential integration window between 100 and 400 bp to the 5'ORF of the next RPII transcribed gene (Bowen et al. 2003). This preferential pattern may

Repeat	Copy number
Full-length Tf2 elements	13
Solo Tf2 LTRs (>200 bp)	35
Full-length Tf1 element	0
Solo Tf1 LTRs (>200 bp)	28
Related LTRs (>200 bp)	111
Related LTR fragments (<200 bp)	75
Totals	
Total base pairs	132,790
Percent of genome	1.1%

Table 1.1: Transposon content of fission yeast genome (from Bowen et al. 2003).

simply reflect the result of selective pressure that favors these transpositions, or can be the consequence of an active selective mechanism of Tf1 and Tf2 transposition at RPII transcribed genes. The first studies of *de novo* Tf1 transposition from a plasmid showed 78 new insertions, 77 of which were in intergenic regions in close proximity of RPII transcribed genes and only one was in a gene ORF (Behrens et al. 2000; Singleton and Levin 2002). These behavioral similarities with the endogenous TE element positions, strongly argue that Tf1 and Tf2 have a biochemical preference for RPII transcribed genes, rather than being the result of selective pressure (Bowen et al. 2003). With the

advent of deep-sequencing technologies, up to ~1 million *de novo* Tf1 transpositions were mapped, confirming again the strong preference for promoters of RPII transcribed genes, with only ~3% of transpositions occurring in ORFs (Guo and Levin 2010; Chatterjee et al. 2014). A further analysis of Tf1 RPII-transcribed target genes, showed that this element preferentially transposes in the proximity of stress-response genes, suggesting a connection between the transcription factors responsible for the stress-response and Tf1 site selection (Guo and Levin 2010). Together with the possibility that Tf1 elements may affect expression of neighboring genes (Leem et al. 2008), this stress-response gene target selection, suggests the intriguing possibility of a beneficial coexistence between Tf1 and the host. In this model, Tf1 would modulate the expression of the stress-response gene in the attempt to overcome the stress conditions that cells are facing. In *S. cerevisiae*, the retrotransposon Ty5 targets specifically heterochromatin, thanks to the interaction between its IN and the heterochromatin factor Sir4 (Xie et al. 2001). However, this interaction needs IN phosphorylation and if cells grow under nutrient starvation, IN phosphorylation diminishes, disrupting IN-Sir4p interaction. This leads to loss of heterochromatin Ty5 targeting, with the element transposing in gene-rich regions instead and, therefore, actively reshaping the genome (Dai et al. 2007). In recent works, a connection between beneficial Tf1 site selection and growth under stress conditions was found (Feng et al. 2013; Esnault et al. 2019). When fission yeast was grown in the presence of heavy metal (CoCl₂), Tf1 showed increases in transcription and transposition, indicating an active cellular response to the stress (Esnault et al. 2019). Finally, cells containing Tf1 transpositions near genes involved in CoCl₂ resistance, overtake wt cells when grown in the presence of CoCl₂, either stimulating expression of genes involved in CoCl₂ elimination, or down-regulating genes involved in CoCl₂ uptake (Esnault et al. 2019). However, little is known about the factors that direct Tf1 integration in promoters of RPII transcribed genes. Sap1 (Switch-activating protein 1), a DNA binding protein involved in different cellular processes, including mating-type switching (Arcangioli and Klar 1991), directly promotes Tf1 transposition and its target-specificity (Hickey et al. 2015). Sap1 DNA localization strongly correlates with *de novo* Tf1 transpositions (Zaratiegui et al. 2011), and Sap1 mutants show a ~10-fold reduction in Tf1 mobilization, suggesting that Sap1 guides Tf1 to the target DNA (Hickey et al. 2015).

Despite potential beneficial effects of TEs in hosts facing stress conditions, cells have evolved active mechanisms to minimize detrimental genome transpositions.

1.3.4 Transposable Elements silencing in *S. pombe*

Uncontrolled proliferation of TEs, even if directed in gene-poor regions, is harmful for cell viability and its competition with other organisms. Transpositions can dramatically increase the host genome size, adding extra work to the DNA replication machinery and decreasing genome stability. In wt (wild type) fission yeast cells grown in non-stress conditions, endogenous Tf2 elements are silenced. However, no heterochromatin marks, such as H3K9 methylations and Swi6, are deposited at Tf2 copies (Cam et al. 2005). Furthermore, neither RNAi-mutants nor Clr4 deleted strains show an

increase of Tf2 transcription, indicating a marginal role of heterochromatin in Tf2 silencing (Hansen et al. 2005). On the other hand, Tf2 expression is highly enriched in Clr6 and Clr3 double mutant, indicating that HDACs play a central role in Tf2 silencing (Hansen et al. 2005). The term “transposon domestication” refers to a process of co-evolution of the TE with its host organism (some examples in section 1.3.1). Another case of transposon domestication is found in humans, where the CENP-B protein, involved in correct centromere formation, derives from the transposase of Class II TE pogo. CENP-B is highly conserved among organisms and *S. pombe* possesses three CENP-B homologous, Abp1 (also called Cbp1), Cbh1 and Cbh2 (Casola et al. 2008). They play a role in heterochromatin silencing at pericentromeric repeats promoting Swi6 recruitment (Nakagawa et al. 2002). Moreover, CENP-B homologous, especially Abp1, are involved in Tf2 repression through direct recruitment of HDACs Clr6 and Clr3 (Cam et al. 2008). In addition, CENP-B homologous and HDACs (including Sirtuins homologous Hst2 and Hst4, NAD⁺ dependent) organize Tf2 elements in one to three subnuclear foci, called Tf bodies. Although their function is not clear, Tf bodies may have a direct role in Tf2 silencing, since under stress conditions Tf bodies are dispersed and exogenous Tf1, once introduced in cell, is also recruited in Tf bodies (Cam et al. 2008; Lorenz et al. 2012).

A distinct Tf2 silencing pathway involves HIRA histone chaperone proteins (Greenall et al. 2006). Deletion of each of the four components of HIRA complex, Hip1, Hip3, Slm9 and Hip4, de-represses *tf2* silencing in all 13 endogenous copies, several solo LTRs from Tf2 and Tf1, and a Tf2 element integrated in an ectopic locus (Greenall et al. 2006; Anderson et al. 2009; 2010). Interestingly, despite increased Tf2 expression, HIRA mutants don't show an increase in Tf2 mobilization, in fact in these mutants Tf bodies are maintained, suggesting a role for Tf bodies in preventing ectopic mobilization of Tf elements (Murton et al. 2016).

Surprisingly, Set1 also has a role in silencing Tf2 elements, despite H3K4 methylation being a hallmark for transcribed regions, found also at *tf2* (Lorenz et al. 2012). In this case, however, Set1 function is independent of H3K4 methylation of Tf2 chromatin, uncovering a diverse role for this enzyme in shaping chromatin status (Lorenz et al. 2012). Furthermore, Set1 promotes clustering of Tf2 elements in Tf bodies like CENP-B homologous and HDACs (Cam et al. 2008; Lorenz et al. 2012). These results suggest that Set1 is recruited to *tf2* chromatin by- or together with- CENP-B homologues to silence Tf2 by HDAC recruitment and Tf body organization (Cam et al. 2008; Lorenz et al. 2012).

Exosome mutants show RNAi-dependent heterochromatin formation at HOODs, including Tf2 (Marasovic et al. 2013; Yamanaka et al. 2013). These results suggest that the exosome machinery and the RNAi pathway compete for Tf2-mRNA and if exosome function is impaired, Tf2 silencing is maintained through RNAi-dependent heterochromatin formation.

In conclusion, *tf2* silencing in fission yeast can be seen like a two-level silencing mechanism, one performed through Tf2 RNA (exosome and RNAi) and one through DNA binding proteins (CENP-B homologous).

1.3.5 Transposable Elements silencing in other organisms

1.3.5.1 Transposon silencing in plants

In plants, like in many other eukaryotes, transposable elements and associated sequences represent a high percentage of the genome composition. In *Arabidopsis thaliana*, for example, ~18% of the genome consists in TEs, while in *Zea mays* this representation reaches the ~85%. Despite being abundant, most TEs are stably silenced in plants, mainly transcriptionally through DNA and H3K9 methylations. Heterochromatin TEs maintain their silenced state via a RNA-dependent pathway that leads to DNA methylation, hence called RNA-directed DNA methylation (RdDM) (Figure 1.12). First, RNA polymerase IV (RPIV) is recruited to TEs through H3K9me2 (Law et al. 2013), there it transcribes the transposable element in a non-coding RNA. RDR2 (RNA-dependent RNA polymerase 2) converts the single stranded TE RNA into double stranded, which is subsequently cleaved in 24bp long siRNAs via Dicer-like 3 (DCL3). These siRNAs are loaded onto AGO4 and AGO6 to target TE non-coding RNA transcribed by a second RNA polymerase recruited via DNA methylations, called RNA polymerase V (RPV) (Johnson et al. 2014). AGO4/6 interacting with RPV transcripts recruits DNA methyltransferases DRM1 and DRM2 which, in turn, methylate the TE DNA sequence (Cao and Jacobsen 2002). At this step, H3K9 methyltransferase KYP (KRYPTONITE) interacts with methylated DNA and methylates H3K9 of the target TE (Johnson et al. 2007). The heterochromatin state of silenced TEs is maintained through cell division via MET1, CMT2 and CMT3, DNA methyltransferase enzymes that restore the DNA methylations present on the parental DNA. Afterward, *de novo* methylated DNA recruits KYP and also H3K9 methylations are reestablished after DNA duplication (Figure 1.12). If an exogenous TE invades a plant genome, *de novo* silencing of the element eventually occurs. If there are sequence-homologies between the invading TE and silenced endogenous TEs, AGO4/6 loaded with 24bp-long siRNAs from the latter, can work in *trans* to direct homology-dependent silencing of the exogenous element (Fultz et al. 2015). However, how RPV (necessary to synthesize the non-coding RNA target of AGO4/6) is recruited to the invading TE, rather than canonical RPII, is not known. Moreover, plants have also a RNAi-mediated mechanism to silence new TEs that don't have sequence homologies with endogenous heterochromatic transposons. The critical point in targeting these elements consists in how AGO members target nascent TE RNA to induce their silencing. Initially, the exogenous TE is post-transcriptionally silenced through mRNA degradation triggered by AGO1 loaded with TE antisense 21-22bp siRNAs. Once bound to nascent RPII-transcribed TE mRNA, AGO1 directly cleaves it and induce dsRNA generation via RDR6. DCL4 and DCL2 cut these dsRNAs producing

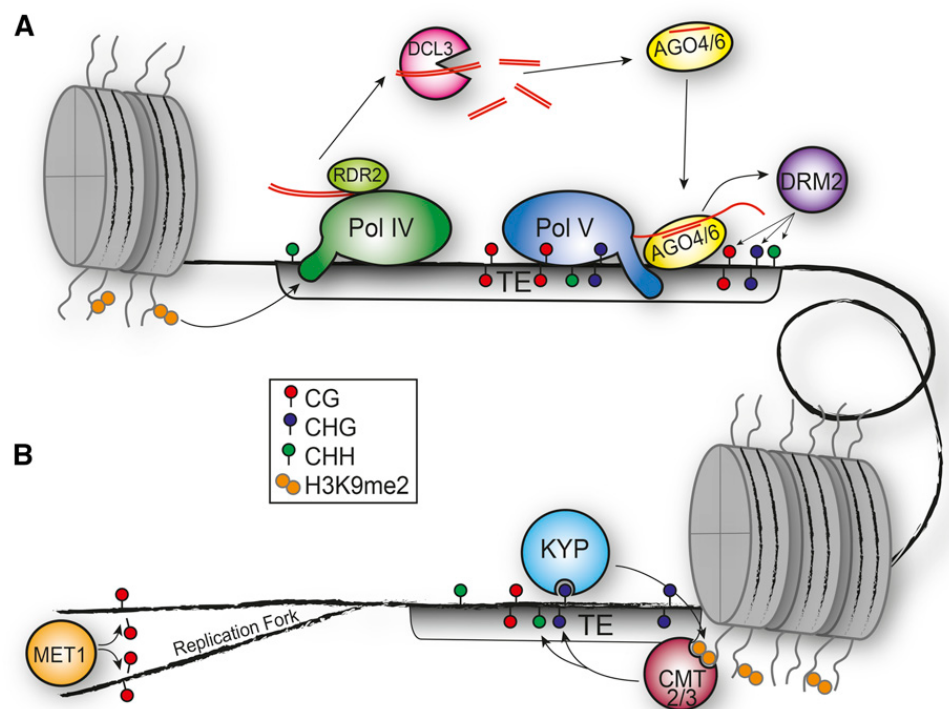


Figure 1.12: RdDM and heterochromatin maintenance at TEs in plants.

From Sigman and Slotkin 2016, **(A)** RNA-directed DNA methylation (RdDM) pathway at TEs in plants; RPIV is recruited to TEs chromatin through H3K9 methylated histones. There the enzyme synthesizes non-coding RNAs, converted to dsRNAs via RDR2. dsRNAs are cleaved in 24bp-long siRNAs by DCL3 and loaded onto AGO4/6. Through base-pairing, AGO4/6 target nascent non-coding TE RNA synthesized by RPIV, recruited in chromatin via pre-existing DNA-methylations. AGO4/6 interact with DNA methyltransferases DRM1 and DRM2 which methylate TE DNA. Methyltransferase KYP, is recruited to TEs chromatin via DNA methylations, where methylates H3K9. **(B)** Maintenance of heterochromatin at TEs after DNA duplication; DNA methylations are restored through MET1, CMT2 and CMT3. KYP interacts with DNA-methylations and reestablishes H3K9 methylations.

secondary siRNAs of 21 and 22bp, respectively. AGO1 is loaded again with these siRNAs, feeding the RNAi mechanism and, therefore, the exogenous mRNA decay (Fultz et al. 2015). Different possibilities have been proposed to explain how AGO1 is loaded with antisense siRNAs in the first place. One hypothesis is that endogenous microRNAs, a class of siRNA produced from a short stem-loop mRNA cleaved by DCL1, are synthesized in the cell and loaded onto AGO1 in a process of genome surveillance (Creasey et al. 2014). This process, however, can trigger uncontrolled silencing throughout the genome, and was shown to be regulated in *S. pombe* by siRNA degradation (Pisacane and Halic 2017). Another mechanism explaining the initial generation of AGO1-siRNA complex, consists of antisense transcription of the invading TE feeding the RNAi pathway. Initial PTGS of non-homologous TEs, eventually switches to TGS by DNA and H3K9 methylations. Different models have been proposed to explain this silencing switch. One suggests that although AGO1 mediated post-transcriptional silencing is the first mechanism defending the host from the invading TE, when a

certain number of transpositions happen, the dsRNAs produced by RDR6 overwhelm DCL4 and DCL2, resulting in DCL3 recruitment and switching from 21-22bp siRNAs to 24bp siRNAs (Marí-Ordóñez et al. 2013). Once 24bp-long siRNAs are produced, they are loaded onto AGO4/6 which would trigger heterochromatin establishment, similarly to the previously described RdDM pathway (Marí-Ordóñez et al. 2013). According to this model, plants can sense the transcription of the new transposon, switching to TGS if the element is too active (i.e. transcribed). A second model for heterochromatin establishment suggests that the 21-22bp siRNAs, respectively produced by DCL4 and DCL2, can be loaded onto AGO6 instead of AGO1, bypassing the AGO6 requirement of 24bp-long siRNAs. In this way, also 21-22bp siRNAs can trigger AGO6 mediated heterochromatin establishment, in a process called RDR6-RdDM, to distinguish it from the previously described RdDM RDR2-mediated mechanism (Nuthikattu et al. 2013; McCue et al. 2015).

1.3.5.2 Transposon silencing in *S. cerevisiae*

In *S. cerevisiae*, or budding yeast, only LTR-retrotransposons and associated sequences are present (Figure 1.8) (Engel et al. 2014). 5 full-length TE families are found, consisting of Ty1-5. All belong to the *copla-like* retrotransposons group, with the only exclusion being Ty3, from the *gypsy-like* group. Ty1-4 elements are preferentially integrated in proximity to RNA-polymerase III (RPIII) transcribed genes, while Ty5 transposons are integrated in heterochromatic regions (Zou et al. 1995; Kim et al. 1998). Ty1 represents the most abundant and active retrotransposon in budding yeast, where 31 copies of the element are found and its RNA consists in 5-10% of the total polyA-RNA (Elder et al. 1981; Carr et al. 2012).

Budding yeast doesn't have AGO, Dicer and RDP homologues and, therefore, the RNAi pathway is absent in this organism (Drimmenberg et al. 2009a). However, if budding yeast is genetically engineered and *ago1* and *dcr1* from *S. castelii* are introduced, cells acquire RNAi. Interestingly, the genetically modified yeast produces siRNAs that target and silence endogenous Ty1 (Drimmenberg et al. 2009a).

Despite the lack of RNAi, budding yeast has evolved other strategies to silence active Ty elements. Recently, a post-translational model for Ty1 regulation has been proposed (Salinero et al. 2018). Ty1 has two promoters, the first is within the 5' LTR, like other LTR-retrotransposons, the second is internal, around 760bp from Ty1 transcription start site. Transcription from the regular LTR promoter results in the synthesis of Gag and Pol, while transcription from the internal promoter produces a shorter mRNA, called Ty1i RNA, subsequently translated into a truncated version of Gag, called p22 (Saha et al. 2015). When p22 is incorporated into Ty1 VLPs, it destabilizes these virus-like structures, resulting in impaired packaging of Ty1 RNA into VLPs and, consequently, Ty1 transposition (Pachulska-Wieczorek et al. 2016). A fine regulation of Ty1 transcription from the two promoters results in differential Ty transposition activity, via a post-translational auto-tuned controlling system. Transcription from both promoters is mediated by a positive transcriptional

factor, Mediator (Salinero et al. 2018). The relative Mediator occupancy at the two promoters regulates the ratio between full-length Ty1 RNA and Ty1i RNA and, therefore, controls Ty1 transposition. From this perspective, a model is proposed, where cells can detect environmental stress, internal changes and increased Ty1 copies and consequently modulate Mediator occupancy at the two promoters. Stimulation of transposition under stress conditions is an active response observed also in fission yeast, in an attempt to reshape the genome to survive the stress (Esnault et al. 2019). On the other hand, uncontrolled transpositions may be detrimental for the host and, therefore, when too many copies of the element are present, Ty1i RNA transcription is activated, reducing Ty mobilization, in a process called “Copy Number Control” (CNC) where increasing Ty1 copies result in decreasing levels of transpositions (Salinero et al. 2018). Another CNC mechanism post-transcriptionally regulating Ty1 transposition involves antisense transcription of the element (Berretta et al. 2008). Short antisense RNAs, called Ty1AS, are synthesized from the 5' end of *gag* and their increased levels, correlating with Ty1 proliferation, result in association of the Ty1AS with the cytoplasmic VLPs (Matsuda and Garfinkel 2009). Once inside the VLPs, Ty1AS is proposed to inhibit Ty1 mRNA retrotranscription, interfering with the correct processing of Pol into the functional subunits, destabilizing directly RT or competing with t-RNA retrotranscription primers for Ty1 mRNA binding, all events resulting in decreased Ty1 transpositions (Matsuda and Garfinkel 2009).

Budding yeast is found in three cell types, *a* and α (haploids) and *a*/ α (diploid). During mating, opposite cell type pheromones bind to receptors of haploid cells, triggering a cascade of events ending with the activation of pheromone regulated genes. Ty1, Ty3 and Ty5 are also regulated in response to pheromones. Ty5, generally repressed by heterochromatin, is surprisingly activated in haploid cells in response to pheromones (Ke et al. 1997). Ty3 is also upregulated in response to pheromones (Bilanchone et al. 1993). Ty1, on the contrary, is transcriptionally and post-translationally downregulated during mating (Xu and Boeke 1991).

Ty1 is also regulated in response to stress conditions. During nitrogen starvation diploid cells form filaments, allowing them to search for nutrients far away from the colonization site (Gimeno et al. 1992). During the filamentous growth, Ty1 is upregulated, supporting a model where Ty1 *de novo* transpositions represent an active response to the stress, aimed to induce genomic rearrangements which might confer selective advantages to the cells (Morillon et al. 2000).

1.3.5.2 Transposon silencing in animals

In order to understand transposon silencing in animals, it is necessary to reintroduce the Argonaute proteins; these proteins are divided into two subfamilies, Argonaute (AGO) and PIWI (P-element-induced wimpy testes) (Peters and Meister 2007). AGO subfamily proteins are ubiquitously present and are loaded with miRNAs or siRNAs usually generated by Dicer activity. On the other hand, PIWI proteins are expressed mainly in the gonads and loaded with a specific small RNA population, called PIWI-interacting RNAs (piRNAs). PIWI proteins with their associated piRNAs form specific

RISC complexes, known as piRISCs. piRNAs are generated in a Dicer-independent manner, from intergenic regions called piRNA clusters. piRNAs possess 2'-O-methyl modification at their 3' terminus and are generally longer (24-31 nt) than miRNAs and siRNAs (Vagin et al. 2006; Siomi et al. 2011). piRNA clusters contain a large number of different types of transposon related sequences (Schreiner and Atkinson 2017). Therefore, the resulting piRNAs, once loaded onto PIWI, guide the piRISC complex to transposon RNA, inducing their transcriptional and post-transcriptional silencing (Kalmykova et al. 2005; Girard et al. 2006; Saito et al. 2006; Vagin et al. 2006; Brennecke et al. 2007).

As mentioned above, PIWI proteins are expressed mainly in metazoan gonads, where proper transposon silencing is necessary to maintain genome stability and ensure proper gametogenesis and reproduction.

In *Drosophila melanogaster*, three PIWI genes are present; ago3, aub (aubergine) and piwi. PIWI proteins are essential for female and male fertility (H. Lin and Spradling 1997; Harris and Macdonald 2001; C. Li et al. 2009). The first piRNAs in *D. melanogaster* were found in males gonads, associated with the Suppressor of Stellate (Su(Ste)) locus on Chromosome Y. Suppressor of Stellate derived piRNAs post-transcriptionally repress the Ste gene on chromosome X through the concerted action of Aub and Ago3 (Malone et al. 2015). In males, regulation of Ste protein accumulation is crucial to ensure proper spermatogenesis and a completely fertile phenotype (Meyer et al.; Palumbo et al. 1994).

Most of the piRNA studies on *Drosophila* have been done on ovaries, where mutations of PIWI genes result in TE derepression (Sarot et al. 2004; Savitsky et al. 2006). AGO3 and Aub act post-transcriptionally in the cytoplasm cleaving TE mRNAs, whereas Piwi protein silences TEs at transcriptional level (Vagin et al. 2004; Kalmykova et al. 2005; C. Li et al. 2009). In the ovaries, Piwi is expressed in both germline and surrounding somatic cells and localizes predominantly into the nucleus (Cox et al. 2000; Brennecke et al. 2007). On the other hand, Aub and Ago3 are principally found in the germline where they localize mostly in an electron-dense perinuclear structure called nuage (Brennecke et al. 2007). In *D. melanogaster*, piRNAs are generated in the cytoplasm via two mechanisms; the primary pathway and the ping-pong cycle that produces secondary piRNAs (Figure 1.13). Primary piRNAs are generated from long piRNA precursors, harbor a strong preference for uridine at their 5' terminus and bind specifically to Aub and Piwi proteins. Furthermore, primary piRNAs are mainly antisense orientated with respect target to transposons. Secondary piRNAs, on the other hand, possess a sense bias and most interestingly they are complementary to primary piRNAs for their first 10nt from the 5' terminus, with adenosine as the tenth nucleotide. This complementarity suggested a model where primary piRNAs loaded (mainly) in Aub, recognize and cleave TE mRNA, producing short transcripts subsequently processed to sense secondary piRNAs and loaded onto cytoplasmic Ago3. Ago3 is then guided to piRNA precursors where it cleaves its target generating the original antisense piRNAs, further loaded on Aub, starting the ping pong mechanism of both piRNA

amplification and TE post-transcriptional silencing via Aub activity (Gunawardane et al. 2007; Brennecke et al. 2007).

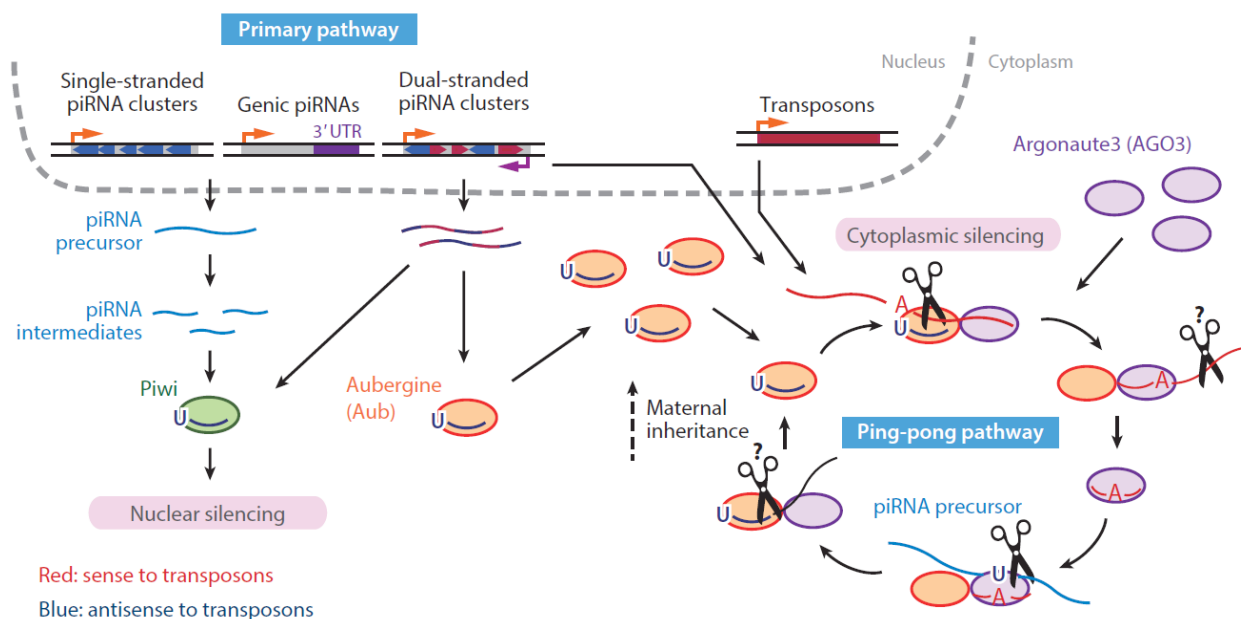


Figure 1.13: piRNA biogenesis pathways in *Drosophila melanogaster*.

From Y. W. Iwasaki et al. 2015, primary and ping-pong pathways for piRNA biogenesis in *Drosophila*. piRNA precursors are synthesized from genomic regions known as piRNA clusters, processed to mature piRNAs and loaded onto Piwi and Aub. Primary piRNAs are amplified by the ping-pong cycle where piRNAs loaded onto Aub guide the enzyme to TE mRNAs directing their cleavage. Ago3 binds the cleavage products (secondary piRNAs) and targets back the piRNA precursors, generating the original antisense piRNAs, feeding the ping-pong cycle and TE post-transcriptional silencing.

As mentioned before, piRNAs are generated in a Dicer-independent manner from piRNA clusters. In *Drosophila*, the *flamenco* (*flam*) locus represents one of the principal sources of piRNAs (Zanni et al. 2013; Goriaux et al. 2014). *flam* extends over 180kb on chromosome X and harbors a vast number of truncated antisense oriented TE sequences. RPII transcribes unidirectionally *flam* and alternative splicing generates piRNA precursors, subsequently exported to the cytoplasm. Although the subsequent mechanisms responsible for piRNA precursor processing to produce mature piRNAs are not well understood, Zucchini endonuclease (Zuc), located on the mitochondria surface, participates in this maturation process (Nishimasu et al. 2012; Ipsaro et al. 2012). Consecutive piRNA processing occurs within perinuclear granules called Yb bodies, also formed on the mitochondria surface. Different factors are involved in piRNA maturation, among them the DmHen1/Pimet methyltransferase which 2'-O-methylates the piRNAs in their 3' terminus (Saito et al. 2007; Horwich et al. 2007). Finally, mature piRNAs are loaded onto Piwi or Aub to form the piRISC complexes and to enter the ping-pong cycle, respectively. piRISC complexes are imported into the nucleus where they direct transcriptional silencing of TEs. Another type of piRNA clusters, called dual-stranded

piRNA clusters, consist of bidirectionally transcribed regions where transposon sequences are randomly sorted into sense and antisense orientations (Figure 1.13) (Brennecke et al. 2007).

A representative dual-stranded piRNA cluster is *42AB*, which spans ~240kb in proximity to the pericentromeric heterochromatin boundary of chromosome 2R. It is not clear yet how antisense bias is conserved from double-stranded piRNA clusters, an hypothesis is that Aub binds both sense and antisense piRNAs, but if there is an actively transcribed TE, Aub-antisense is “selected” and amplified in the ping-pong loop. However this model doesn’t explain antisense bias observed also in piRNAs generated from *42AB* and loaded onto Piwi. In fact, piRNA loaded Piwi forms the piRISC complex which is imported into the nucleus and, therefore, it is unlikely that Piwi participates in the ping-pong pathway (Y. W. Iwasaki et al. 2015). In Figure 1.13 also a third class of piRNA source is represented, consisting of the 3’UTR of protein coding genes, thus called genic piRNAs (Robine et al. 2009). These piRNAs are not involved in transposon silencing, but they regulate expression of endogenous coding genes (Saito et al. 2009).

In *D. melanogaster*, transcription of single stranded and dual-stranded piRNA clusters is regulated differently, although both cluster-types are usually heterochromatic. *flamenco* is unidirectionally transcribed via RPII, recruited to the cluster promoter by the transcription factor Ci (Cubitus interruptus) (Goriaux et al. 2014). RNA transcripts from *flam* are subsequently differently spliced, generating a vast variety of TE antisense sequences. Afterwards, priRNA precursors are exported to the cytoplasm and directed to the Yb bodies where they are processed to mature piRNAs. Unlike *flam*, where the transcriptionally active mark H3K4me3 is found, dual-stranded piRNA clusters (such as *42AB*) present only the repressive H3K9me3 mark (Ozata et al. 2019). Transcription of these elements is facilitated by the germline-specific H3K9me3-binding protein Rhino, a variant of HP1 (Klattenhoff et al. 2009). Together with Deadlock (Del) and Cutoff (Cuff), Rhino induces RPII transcription, bypassing the need for promoter sequences. Transcription mediated by Del-Cuff-Rhino is initiated at different sites on both DNA strands and ignores splicing, termination and poly-A signals (Figure 1.14) (Mohn et al. 2014; Z. Zhang et al. 2014; Andersen et al. 2017). Thereafter, piRNA precursors generated from dual-stranded piRNA clusters, are also exported to the cytoplasm for their maturation.

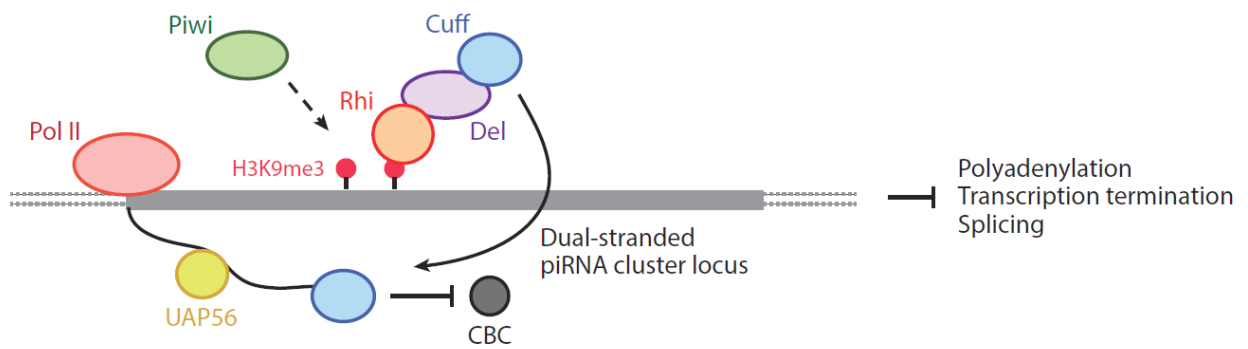


Figure 1.14: Non-canonical transcription of heterochromatic dual-stranded piRNA cluster in *D. melanogaster*.

From Y. W. Iwasaki et al. 2015, Pol II bidirectionally transcribes dual-stranded piRNA clusters in a promoter independent manner, thanks to its recruitment via Rhi-Ded-Cuff complex bypassing splicing, poly-A and termination signals. Rhi is recruited via H3K9me3, deposited through the concerted action of Piwi-piRNA complex and histone-methyl transferase. Cuff binds 5' of the nascent piRNA precursor, competing with CBC. With the help of UAP56, later the piRNA precursor is exported to the cytoplasm where it is processed to form mature piRNAs.

As mentioned before, Piwi protein silences transposons transcriptionally. Once loaded with piRNAs, Piwi is imported into the nucleus where it scans the genome to detect complementary nascent transposon RNAs. Then, by the Piwi-interacting mediator proteins Asterix and Panoramax, Piwi promotes H3K9 methylation of the target transposon via recruitment of the histone-methyl transferase Eggless, followed by further chromatin compaction through HP1a deposition (S. H. Wang and Elgin 2011; Rangan et al. 2011; Le Thomas et al. 2013; Ohtani et al. 2013; Yu et al. 2015). Additionally, Piwi on chromatin recruits the Lysine-specific demethylase 1 (Lsd1) which removes active histone 3 lysine 4 dimethylation marks from the target transposon, leading to efficient transcriptional silencing of the element (Lepesant et al. 2020). In this genome survey mechanism, Piwi protein directs transcriptional silencing of transposons independently of its slicing activity (Darricarrère et al. 2013). Once H3K9 methylated, the transposon elements are recognized by Rhino, promoting the non-canonical transcription described above; thus, heterochromatic TEs are still transcribed, but unspliced, not properly terminated and from both DNA strands, generating non-coding TE RNA and piRNA precursors that keep the transposons repressed (Rangan et al. 2011; Andersen et al. 2017; Z. Zhang et al. 2014).

Also in mouse three PIWI proteins are present; MIWI, MIWI2 and MILI. These proteins are mostly expressed in male gonads, while almost absent in female oocytes (S. Kuramochi-Miyagawa et al. 2001). Piwi proteins in testis are found at different stages of spermatogenesis and the deletion of each of them leads to transposon activation and impaired sperm production (Deng and Lin 2002; Carmell et al. 2007; Aravin et al. 2007). MIWI2 and MILI are expressed during the initial phase of spermatogenesis, called the pre-pachytene stage. On the other hand, MIWI, together with MILI, is expressed in the final part of spermatogenesis, known as pachytene stage. piRNAs produced during the pre-pachytene stage are called pre-pachytene piRNAs, while piRNAs from the pachytene phase

are called pachytene piRNAs (Figure 1.15) (S. Kuramochi-Miyagawa et al. 2001; Deng and Lin 2002; Aravin et al. 2008). Primary piRNA biogenesis in mouse is different to that described for *Drosophila*, where piRNAs are mostly produced from precursor transcribed at piRNA clusters. In mouse, mRNA from TEs are processed to mature sense primary piRNAs, and loaded onto MILI to feed the primary piRNA generation (Aravin et al. 2008; Gan et al. 2011). MILI, guided by its piRNAs, interacts with antisense piRNA precursor RNAs generated from piRNA clusters. Subsequently, MILI cleaves the piRNA precursors producing secondary piRNAs, antisense oriented. Secondary piRNAs are loaded either onto MILI or MIWI2, MILI-piRNA complexes participate now in the so called homotypic MILI:MILI ping-pong cycle, where they target and cleave sense TE mRNAs, generating more sense oriented piRNAs (Figure 1.15) (Aravin et al. 2008). Although initially hypothesized, MIWI2 doesn't participate in this mechanism, in fact its activity is dispensable for the ping-pong cycle (De Fazio et al. 2011). On the other hand, MIWI2-piRNA complexes are imported into the nucleus where their antisense piRNA guides them to nascent TE mRNAs, inducing transposon transcriptional silencing. MIWI2 directs transposon TGS through induction of DNA methylation and H3K9me3 deposition (Aravin et al. 2008; Satomi Kuramochi-Miyagawa et al. 2008; Pezic et al. 2014). Although not completely clear how MIWI2 guides DNA methylation, a study showed that the DNA methyltransferase MORC1 can be directly involved in the silencing of TEs (Pastor et al. 2014). Furthermore, it was initially thought that MILI doesn't participate directly in DNA methylations, but only indirectly, via the generation of secondary piRNAs then loaded onto MIWI2 and via its role in guiding MIWI2-piRNA complexes to the nucleus (De Fazio et al. 2011). However, Manakov and colleagues showed that also MILI may participate directly in the *de novo* DNA methylation of transposable elements (Manakov et al. 2015).

During the pachytene phase of mouse spermatogenesis, piRNAs are loaded onto both MILI and MIWI. Unlike pre-pachytene piRNAs, the majority of pachytene piRNAs don't originate from TEs, but from intergenic regions. MIWI guided by pachytene piRNAs participates in a broad mRNA elimination program, via the cooperation with CAF1 deadenylase (Gou et al. 2014). Nevertheless, MILI- and MIWI-piRNA complexes are necessary to post transcriptionally silence L1 transposons during late spermatogenesis stages (Reuter et al. 2011; De Fazio et al. 2011). Altogether, Piwi proteins in mouse testis guide transposon repression through initial post-transcriptional silencing via MILI activity and transcriptional silencing through *de novo* DNA methylation via MIWI2, followed by a post-transcriptional silencing reinforcement performed through MILI and MIWI (Figure 1.15).

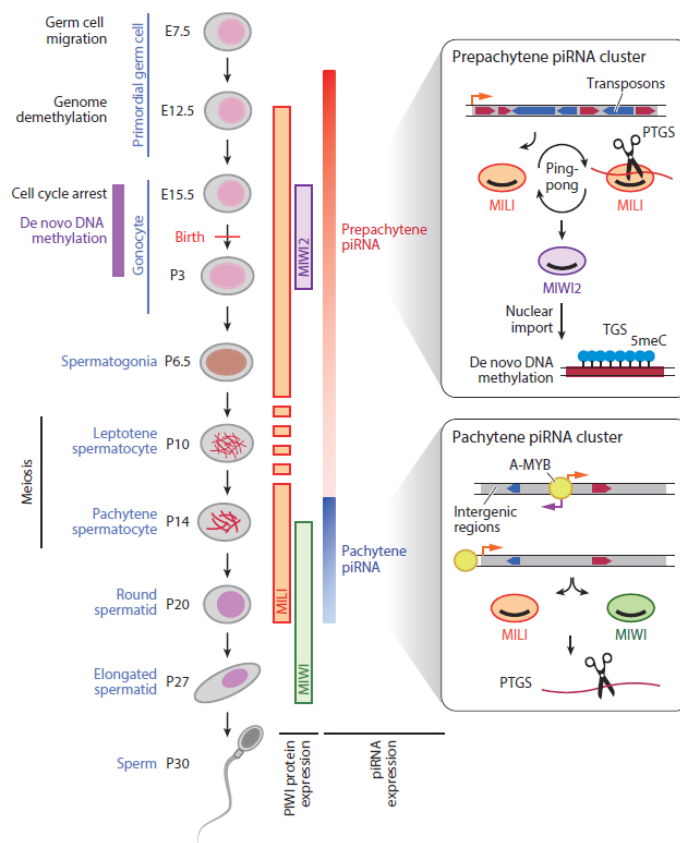


Figure 1.15: Prepachytene and pachytene distribution of PIWI proteins and piRNAs during mouse spermatogenesis (from Y. W. Iwasaki et al. 2015).

During earlier mouse spermatogenesis stages TEs are silenced post-transcriptionally through MILI and transcriptionally via MIWI2-mediated DNA methylation. Later, pachytene piRNAs direct PTGS of TE and non-TE genes.

piRNA-dependent silencing of TEs is not the only repressive mechanism observed in mouse (and human). In mammals, it has been shown that specific DNA binding proteins localize on transposon DNA during embryonic development and in adult somatic cells, directing TE silencing (Ecco et al. 2016; Imbeault et al. 2017). A large family of transcription factors, called KRAB-containing zinc finger proteins (KRAB-ZFPs), are involved in this process. KRAB-ZFPs bind to specific DNA sequences through an array of zinc fingers and recruit their cofactor KAP1 (KRAB-Associated Protein 1), which constitutes the scaffold for heterochromatin nucleation through the recruitment of the histone methyltransferase SETDB1, HDACs and DNA methyltransferases, although the exact mechanism is not known yet (Quenneville et al. 2012; Rowe et al. 2013; Ecco et al. 2016; Imbeault et al. 2017).

C. elegans presents both class I and class II transposons (Figure 1.8), with DNA transposons Tc1 and Tc3 representing the most populated and active elements (*C. elegans* Sequencing Consortium 1998). piRNAs have been identified in *C. elegans*, however their function in transposon silencing seems to be restricted to Tc3 elements in male and female germline cells (Das et al. 2008). piRNAs in worm are known as 21U-RNAs due to their 5'-U bias and length. Around 15000 21U-RNAs are produced in *C. elegans* from two large clusters on chromosome IV, with each piRNA transcribed from a specific mini-gene (Ruby et al. 2006). 21U-RNA precursors are loaded and processed to mature piRNAs on PRG-1, the piwi protein homologue in *C. elegans* (Das et al. 2008). 21U-PRG-1 complexes scan the transcriptome in order to find non-self RNAs, like transposon mRNAs. When they base-pair with non-self RNAs, PRG-1 proteins recruit a RNA-dependent RNA-polymerase (RdRP) which leads to generation of dsRNAs subsequently processed to 22G-RNAs, a subclass of small interfering RNAs. 22G-RNAs are then loaded onto specific Argonaute proteins, collectively known as WAGOs. WAGO-1, WAGO-2 and WAGO-3 direct cytoplasmic post-transcriptional silencing of non-self RNAs via their endonuclease activity (Luteijn et al. 2012), while WAGO-9 is imported into the nucleus where it binds nascent non-self RNA directing transcriptional silencing through recruitment of histone-methyl transferases (HMTs) and HP1 chromodomain protein homologue HPL2 (Das et al. 2008; H.-C. Lee et al. 2012; Ashe et al. 2012). Collectively, this epigenetic silencing is also known as RNAe (RNA-induced epigenetic silencing). Furthermore, *C. elegans* is capable of distinguishing between non-self and self RNAs during PRG-1 transcriptome surveillance. In a current model, the Argonaute protein CSR-1 binds self 22G-RNAs and base-pairs with self cytoplasmic RNA, protecting it from cleavage by WAGO proteins. Moreover, CSR-1-22G-RNA complexes localize into the nucleus, suggesting that CSR-1 recognizes self nascent transcripts competing with WAGO-9 to inhibit self heterochromatin gene silencing (Figure 1.16) (Seth et al. 2013).

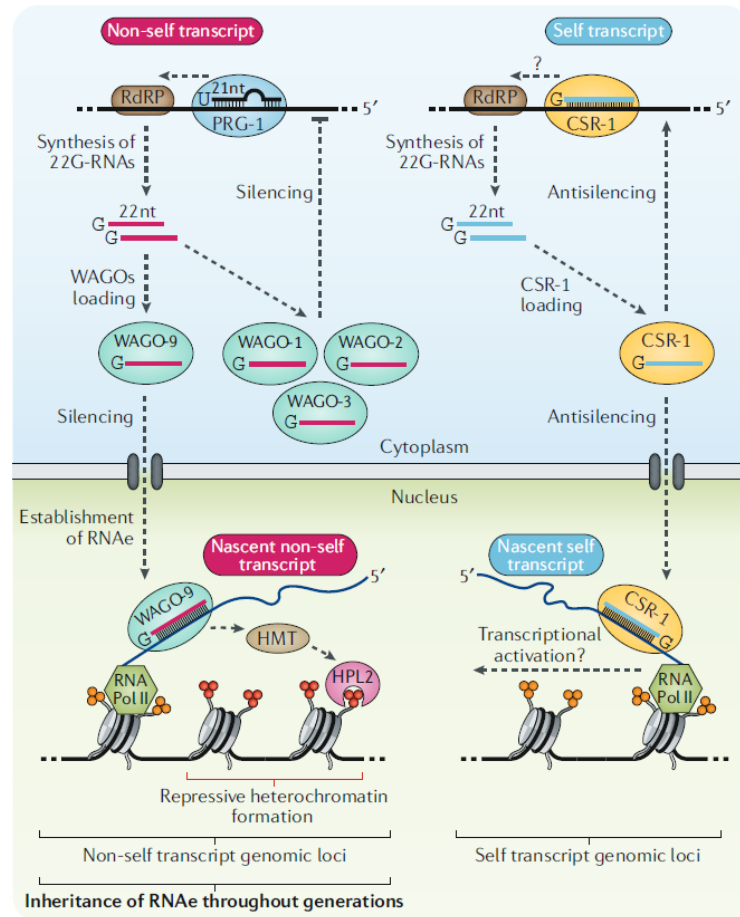


Figure 1.16: Self and non-self recognition in piRNA-mediated silencing in *C. elegans* (from Ozata et al. 2019).

2. AIM OF THIS STUDY

Uncontrolled propagation of transposable elements can be detrimental for the host they inhabit where they can lead to gene disruptions, gene mutations and genome rearrangements. Currently, more than 100 human genetic diseases are associated with transposon activities, from haemophilia to neurological disorders and different types of cancer (Payer and Burns 2019). In unicellular organisms, transposon mobilization might be lethal for the host and, therefore, cells have developed different strategies to suppress extensive transposon activity. *S. pombe* contains 13 copies of an LTR-retrotransposon called *tt2* and their silent state is tightly regulated through diverse mechanisms, involving histone deacetylations, RNA degradation and clustering in nuclear loci called Tf bodies (Cam et al. 2008; Lorenz et al. 2012). Canonical heterochromatin marks are normally not found at *tt2* in wild-type cells and the RNAi pathway leads to heterochromatinization of the elements only when cells are grown under stress conditions or if the exosome machinery is impaired (Cam et al. 2005; Hansen et al. 2005; Marasovic et al. 2013; Yamanaka et al. 2013).

In this balanced scenario, we wondered what would happen in fission yeast if the organism faces the invasion of an unknown exogenous transposon. Does *S. pombe* possess an innate tool to recognize and block potentially harmful invading transposons? If so, what are the features that the foreign transposon has and that the cell utilizes to identify it as a non-self genetic element?

To answer these questions, we horizontally transferred *tj1* into the *S. pombe* genome. *Tj1* is an LTR-retrotransposon from *Schizosaccharomyces japonicus*, previously described as active in *S. pombe* (Guo et al. 2015).

The aim of the study described in this thesis was the investigation of the capacity of this organism to recognize the foreign retrotransposon as a non-self genetic element and, therefore, the ability of fission yeast to block its propagation.

3. RESULTS

3.1 Introducing *tj1*, a TE from *Schizosaccharomyces japonicus* active in *S. pombe*

In order to simulate a transposon invasion in *S. pombe*, an exogenous element active in fission yeast was necessary. Tj1, an LTR-retrotransposon from *Schizosaccharomyces japonicus* has been identified as active when introduced in *S. pombe* (Guo et al. 2015) and, therefore, it was used in this study. Tj1 is a *Ty3/gypsy* like element of 5003bp in length with two identical LTRs of 244bp (Figure 3.1) (Rhind et al. 2011; Guo et al. 2015). *tj1* contains a 5' sequence complementary to its PBS sequence, suggesting that retro-transcription of this element is initiated by a self-priming mechanism, similarly to *tf* in *S. pombe* (J. H. Lin and Levin 1997; Rhind et al. 2011). As mention in section 1.3.2, in order to transpose efficiently, LTR-retrotransposons synthesize Gag protein at a higher level than Pol-subunits. To achieve this goal, retroelements use different strategies; in the case of Tj1, a stop codon is placed between Gag and Pol ORFs and Pol ORF lacks a start codon, ensuring higher amount of Gag over Pol, with the second produced only occasionally via ribosomal readthrough of the stop codon. In fact, point mutation of the TGA stop codon to GGA (TGAX-tj1) results in decreased Tj1 transposition efficiency, possibly because of the impairment of the Gag/Pol ratio (Guo et al. 2015). Finally, Tj1 preferentially transposes at RPIII transcribed genes, similarly to Ty3 in *S. cerevisiae* (Chalker and Sandmeyer 1992; L. Yieh et al. 2000; Lynn Yieh et al. 2002; Guo et al. 2015).

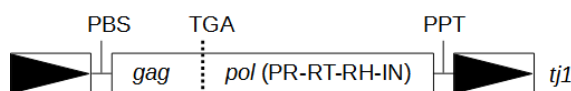


Figure 3.1: *tj1* structure.

tj1 structure is shown, boxes with black triangles define LTRs. Pimer-binding sites (PBS) and polypurine tracks (PPT) are represented after 5' LTRs and before 3' LTRs respectively. TGA codon between *gag* and *pol* ORFs is indicated with dashed line.

3.2 Setup of a plasmid system to induce a controlled propagation of Tj1 in *S. pombe* genome

For this study, a system to induce controlled Tj1 transposition was necessary. For this purpose, the mutated TGAX-tj1 element (Guo et al. 2015) was cloned in a plasmid, called donor plasmid (Figure 3.2A). TGAX-tj1 alone is unable to transpose unless coupled with *tj1* Gag and Pol ORFs, where the stop codon between Gag and Pol is present and, therefore, higher amount of Gag over Pol is reestablished, ensuring the correct formation of VLPs (where TGAX-tj1cDNA is incorporated) and eventually TGAX-tj1 transposition. Tj1 ORFs were cloned in a second plasmid, named expression plasmid (Figure 3.2B). Due to the lack of LTRs, Tj1 in the expression plasmid is unable to transpose and its sole function is to permit transposition of TGAX-tj1 from the donor plasmid. Once *S. pombe*

efficiently recognizes and silences TGAX-tj1, the two plasmids can be removed from cells, in order to avoid further propagation of TGAX-tj1 and subsequent genome changes.

In addition, aiming to select cells with *de novo* transpositions, an antibiotic resistance cassette (*neo* and *hph*) was inserted between the Pol ORF and 3'LTR, in the opposite direction of *tj1*. Furthermore, a 36bp long artificial intron (AI) was integrated into the cassette in the same transcriptional direction as that of *tj1*, but opposite to that of the antibiotic resistance gene (Figure 3.2C-D), therefore a functional cassette is generated only when *tj1* is transcribed, the AI is spliced-out, the RNA is retro-transcribed and the AI-free cassette Tj1 cDNA is integrated into the *S. pombe* genome (Figure 3.2E) (Heidmann et al. 1988; Levin 1995; Dang et al. 1999).

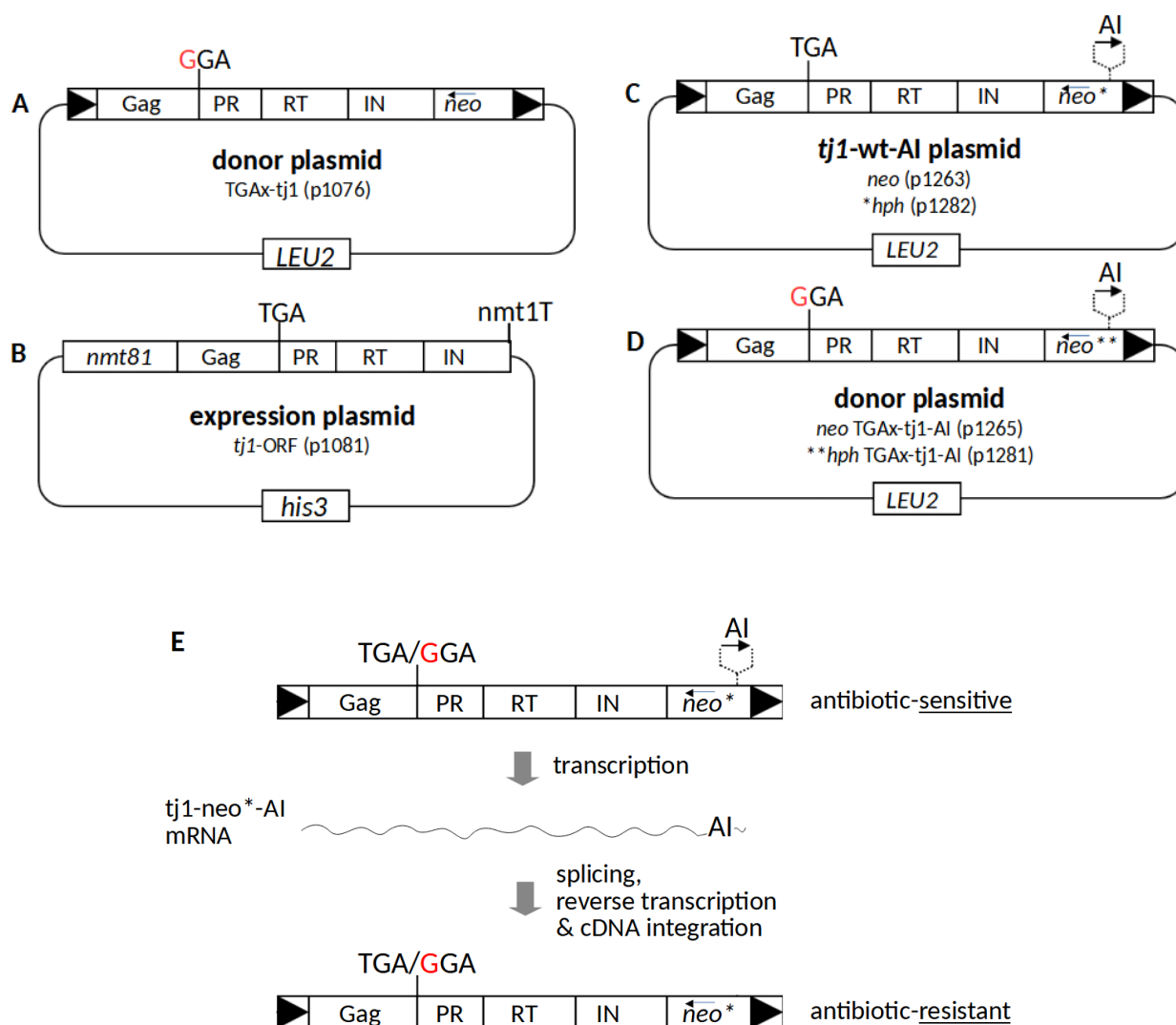


Figure 3.2: Plasmids generated for this study and artificial intron strategy to select cells with transpositions.

(A) Donor plasmid with *neo* cassette, without artificial intron (AI). The stop codon between Gag and Pol is mutated to GGA. *LEU2* gene, from *S.cerevisiae*, is fission yeast *leu1* ortholog. (B) Expression plasmid containing *tj1* ORFs under control of *nmt81* promoter and *nmt1* terminator (*nmt1T*). *his3* gene is from *S.pombe*. (C) *wt-tj1* plasmid with AI integrated into the antibiotic resistance cassette (*neo* or *hph*). (D) Donor plasmid with AI into *neo* or *hph*. (E) Scheme of the AI strategy to select cells with transpositions (either *wt-tj1* or TGAX-*tj1*); AI disrupts the antibiotic resistance ORF in the plasmids, therefore cells are antibiotic-sensitive. However, when *tj1* is transcribed, if the AI is spliced-out, the mRNA is retrotranscribed and the AI-free cDNA is integrated in the host genome, the cassette becomes functional and cells are antibiotic-resistant. (A-D) Plasmid names are indicated in brackets.

3.3 Generation of a readout system to identify *tj1* silencing cells and combination of donor and expression plasmids to induce a controlled Tj1 propagation

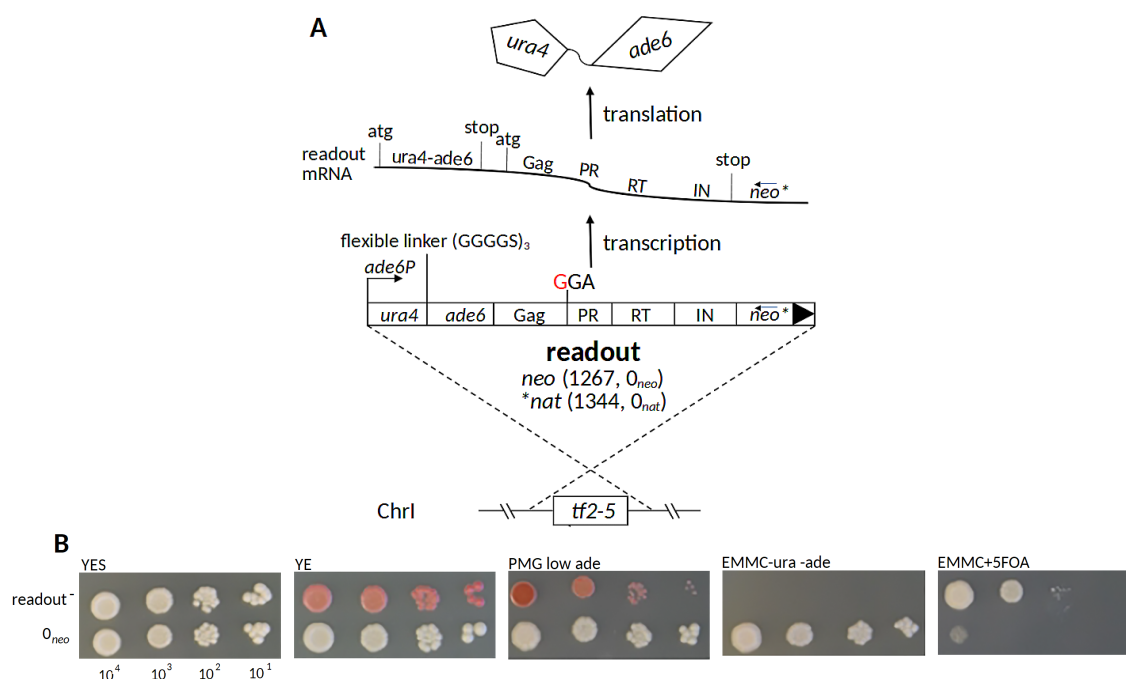
To identify *S. pombe* cells actively recognizing and silencing the exogenous *tj1* element, a readout system was generated in this study (Figure 3.3A). A TGAX-*tj1* copy is fused at its 5' to a sequence consisting of *ura4* and *ade6* fused genes (coding for orotidine 5'-phosphate decarboxylase and phosphoribosylaminoimidazole carboxylase, respectively). The *ura4-ade6*-TGAX-*tj1* polycistronic sequence is transcribed from the *ade6* promoter (*ade6P*) and its transcription terminates at the Tj1 3' LTR. *ade6P* at the 5' end was preferred to Tj1 LTR in order to reduce the probability of genetic homologous recombination between transposing Tj1 copies and the readout construct, leading to *ura4-ade6* elimination. A flexible linker of 15 amino acids (GGGGS)₃ is inserted between Ura4 and Ade6 of the chimeric protein (Chen et al. 2013). At the 3' of TGAX-*tj1*, and before the 3'LTR, an antibiotic resistance cassette (*neo* or *nat*) is inserted for selection during readout cloning. Conventionally, the readout strains with *neo* and *nat* cassettes are called 0_{neo} and 0_{nat}, respectively.

Ade6 takes part in the synthesis of adenine, however, the *S. pombe* strains used in this study have a mutated copy of the endogenous *ade6* gene, called *ade6M210*. With this mutation, Ade6 is not functional and interrupts the adenine synthesis pathway, with the accumulation of an intermediate red compound (phosphoribosylaminoimidazole, AIR) (Smirnov et al. 1967). AIR accumulates only if cells are grown in an adenine-limiting medium since the adenine synthesis pathway is repressed during growth in an adenine-rich medium. Ade6 in the chimeric protein of the readout used in this study, complements the *ade6M210* mutation and therefore the red compound doesn't accumulate. However, if the readout is silenced and Ura4-Ade6 is not synthesized, in an adenine-limiting medium, cells would appear red. On the other hand, Ura4 normally participates in the biosynthesis of UMP (uridine monophosphate), yet if the growth medium contains 5-Fluoroorotic acid (5FOA), Ura4 converts it to fluorodeoxyuridine, a cell toxic compound (Grimm et al. 1988). *S. pombe* strains used in this study have their endogenous *ura4* gene deleted (*ura4D18*). Nonetheless, if the readout is not silenced, in presence of 5FOA, cells would die due to the catalytic activity of the chimeric Ura4, while

they would survive if the readout is silenced. The readout construct is integrated replacing the *tf2-5* element, to introduce as few changes as possible in the *S. pombe* genome, in terms of size and locus function (Figure 3.3A).

To verify the functionality of the readout construct, a series of spot assays were performed, where the 0_{neo} strain was compared to a readout-negative (readout⁻) control strain (Figure 3.3B). Growth in YES shows that the readout construct doesn't affect the overall fitness of 0_{neo} . In low adenine medium YE and PMG low ade, the control strain appears red, while 0_{neo} shows no pigmentation, indicating that Ade6 of the chimera efficiently participates in the adenine biosynthesis pathway. Readout⁻ in PMG low ade presents a more intense red pigmentation than in YE, due to the lower adenine concentration in the first medium. The growth of 0_{neo} in EMMC-ura-ade minimal medium indicates the activity of the Ura4-Ade6 chimera. Moreover, Ura4 activity is confirmed in EMMC+5FOA medium, where 0_{neo} grows at least 100 times less than the control strain. A limited number of 0_{neo} colonies, however, grows in EMMC+5FOA, likely a result of the high mutagenic pressure that 5FOA exerts over *ura4*, leading to 5FOA-resistant cells into the culture. Altogether, these results show the functionality of the readout construct generated in this study (Figure 3.3B).

Finally, the 0_{nat} strain was transformed with p1263 and with the donor plus the expression plasmids (p1265 and p1081 respectively), to verify the TGAX-tj1 activity mutant and its transposition rescuing in the presence of the expression plasmid (Figure 3.3C). A spot assay shows that TGAX-tj1 transposes ~10 times less efficiently than wt Tj1 and that the expression plasmid efficiently rescues the TGAX-tj1 activity mutant. Although the transposition efficiency difference between wt Tj1 and TGAX-tj1 is less than expected (Guo et al. 2015), this result confirms that the use of the two plasmids system would reduce the risk of further TGAX-tj1 transpositions in cells where the element has transposed and the plasmids are eliminated, avoiding subsequent undesired genomic variation.



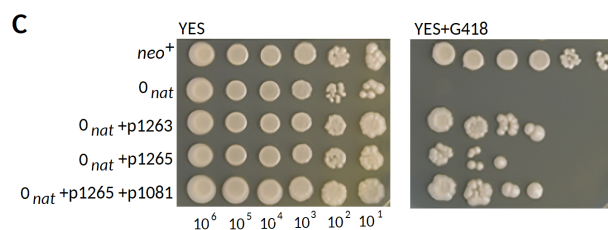


Figure 3.3: Readout generated for this study, activity of its Ura4-Ade6 chimera and TGAX-tj1 transposition efficiency.

(A) Readout structure; TGAX-tj1 copy is fused at 5' to the chimera *ura4-ade6*. *ade6* promoter (*ade6P*) and *tj1* LTR regulate the readout transcription. A flexible linker of 15 amino acids ($(GGGS)_3$) is inserted between Ura4 and Ade6. Transcription and translation of the readout result in Ura4-Ade6 chimera. In brackets the laboratory names for the readout strains are indicated, 1267 or 1344, depending on the presence of *neo* or *nat* cassette respectively. In the continuation of this study, *neo* strain is conventionally called 0_{neo} , while *nat* readout strain is indicated as 0_{nat} . **(B)** Spot assays of readout-negative (readout⁻) and 0_{neo} strains in YES, YE, PMG low ade, EMMC-ura⁻ade and EMMC+5FOA media. The same number of cells is plated in each media and is indicated under YES plate. **(C)** Spot assay showing that TGAX-tj1 (in p1265) transposes less efficiently than wt Tj1 (in p1263) and that the expression plasmid (p1081) efficiently rescues TGAX-tj1 activity mutant. G418 indicates the Gibco Geneticin antibiotic and *neo*⁺ represents a control strain carrying G418 resistance cassette. The number of cells plated is indicated under YES plate.

3.4 Multiple *tj1* copies are necessary to induce transposon silencing

In order to study whether *S. pombe* is capable of recognizing and silencing the exogenous *tj1* element, an experiment to investigate the establishment of transposon silencing was performed. In this experiment, 0_{neo} and 0_{nat} strains were transformed with different plasmid combinations, and afterward, cells with plasmids were kept in exponential growth up to 10 continuous days. ~30.000 cells were plated in PMG low ade plates at day 1, 3, 5, 7 and 10 of the continuous cultures and the number of red colonies growing on the plates was counted (Figure 3.4A). As shown in Figure 3.4B, silencing colonies in low ade plates were present only when cells contained *tj1* plasmids, indicating that they can recognize the retrotransposon if present in more than the single copy at the readout construct.

Although red colonies reflect silencing of the readout rather than direct silencing of exogenous *tj1*, the absence of silencing in 0_{neo} and 0_{nat} strains without plasmids, suggests that silencing is triggered by *tj1* on the plasmids, with subsequent trans-silencing of the readout locus.

Moreover, this experiment shows that different plasmid combinations with 0_{neo} and 0_{nat} result in similar silencing outcomes, suggesting that recognition of *tj1* is not affected by either the cassettes used or the wt *tj1* or TGAX-tj1 present in the plasmids, therefore indicating that silencing is triggered directly by *tj1* sequence, independently to its transposition efficiency.

Finally, a higher number of *tj1* copies doesn't increase the number of silencing colonies directly (Figure 3.4B), suggesting that there is no directly proportional correlation between the element copy number and its recognition, but rather that cells recognize the retrotransposon simply when present in more than the single copy at the readout construct. Supporting this hypothesis, 0_{neo} +p1076+p1081 silencing and not silencing cells (selected in PMG low ade -leu-his plates), contain the same total

number of *tj1* copies (Figure 3.4C), indicating that it is not a higher number of copies that leads to more efficient *tj1* recognition and silencing.

Unfortunately, due to the high mutation frequency of *ura4* under 5FOA selection and consequent high number of false-positive, the use of this compound to select cells actively silencing *ura4* in the readout was impossible. A functional Ura4-5FOA based system would have increased the potential number of cells screened at each plating to hundreds of thousands, while the red/white screening in PMG low ade limited the analysis to ~30,000 cells per plating, corresponding to the maximum number of distinguishable colonies grown on the plate (see Figure 3.4A for an example of plating).

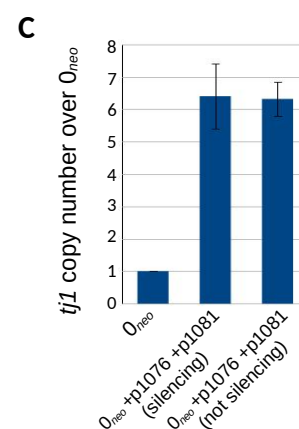
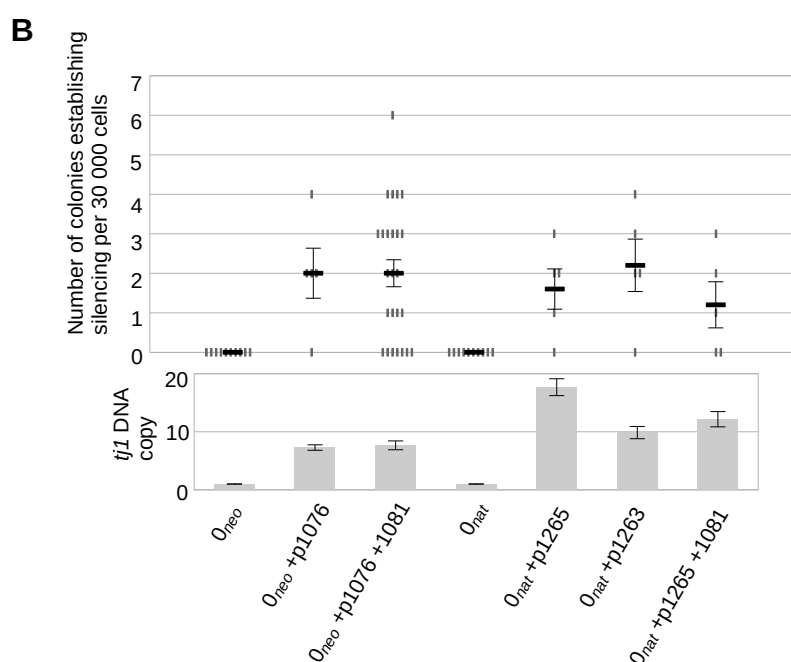
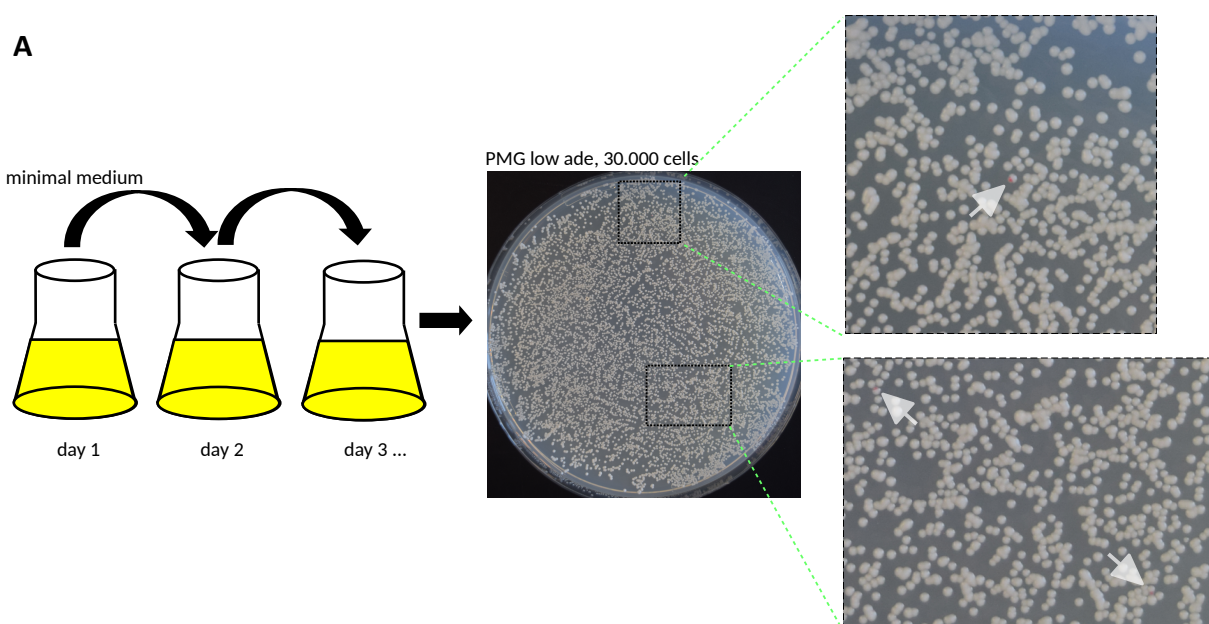


Figure 3.4: Procedure adopted to count the number of silencing colonies and silencing establishment assay in different cellular setups.

(A) In order to study if *tj1* is silenced, 0_{neo} and 0_{nat} strains with and without plasmids were analyzed. Cells were kept in exponential growth and after 1, 3, 5, 7 and 10 days 30.000 cells were plated in PMG low ade plates. The number of red colonies was counted, corresponding to the number of silencing colonies per 30.000 cells. The minimal medium used for the continuous exponential growth depended on the strain analyzed; PMG for 0_{neo} and 0_{nat} , PMG -leu for 0_{neo} +p1076, 0_{nat} +p1265 and 0_{nat} +p1263, PMG -leu -his for 0_{neo} +p1076 +p1081 and 0_{nat} +p1065 +p1081. Transparent-white arrows indicate some red colonies on a PMG low adenine plate. (B) Single gray points on the upper graph represent the number of red colonies spotted at each PMG low adenine plating. Black horizontal lines indicate the average of silencing colonies per 30.000 cells. Error bars indicate s.e.m. of five independent plating. The lower graph shows the total copy number of *tj1* in the corresponding strains (normalized to *act1* copy number). Error bars indicate s.e.m. for at least a technical triplicate of one independent experiment. (C) Total *tj1* copy number in silencing and not silencing cells, normalized to *act1*. Error bars indicate s.e.m. of three independent experiments.

3.5 Cells silence *tj1* via sRNA-mediated H3K9me2 deposition

In order to determine the mechanism responsible for *tj1* silencing, red colonies from 0_{neo} +plasmids (p1076 and p1081) were isolated. The first silencing mechanism hypothesized to participate in *tj1* repression was H3K9 methylation guided by the RNAi pathway. To verify this hypothesis, H3K9me2-ChIP (Chromatin Immunoprecipitation) was performed and precipitated DNA was analyzed by NGS (Next-generation-sequencing). Although the color selection is performed on PMG low ade medium and therefore red colonies may have already lost the plasmids necessary for the liquid growth, red colonies were kept in exponential growth in liquid YES for three days, inducing plasmid loss. Only at that point cells that maintained red pigmentation were selected again and replicated in EMMC-leu and EMM-his plates to confirm that the plasmids were lost. Using this approach, as mentioned already, further *tj1* transpositions were less likely to happen, permitting the analysis of genomically stable cells. In addition, the absence of plasmids permitted an easier NGS-reads assignment due to the absence of identical *tj1* sequences.

Red colonies showed epigenetic silencing instability, reflected in pigment variegation of silencing cells spread in PMG low ade plates, with generation of white colonies. These white colonies obtained from re-streaking of red colonies were isolated (from now on referred as “not silencing” colonies). H3K9me2-ChIP of these not silencing colonies was performed. The analysis clearly show H3K9 dimethylation of red cells over the readout locus, is completely lost in not silencing cells (Figure 3.5A). This result indicates that H3K9me2 of *tj1* is involved in the silencing of the exogenous transposable element.

To investigate if sRNAs participate in the H3K9me2 deposition, Ago1-bound sRNAs of silencing and not silencing cells were analyzed. As shown in figure 3.5A, sRNAs were detected at the readout locus in silencing cells, with their drastic reduction in not silencing cells. This result indicates that H3K9me2 deposition is a process regulated by sRNAs, likely produced via the RNAi pathway. It is

possible that the residual sRNAs observed in not silencing cells are not enough to maintain H3K9me2 at the readout locus.

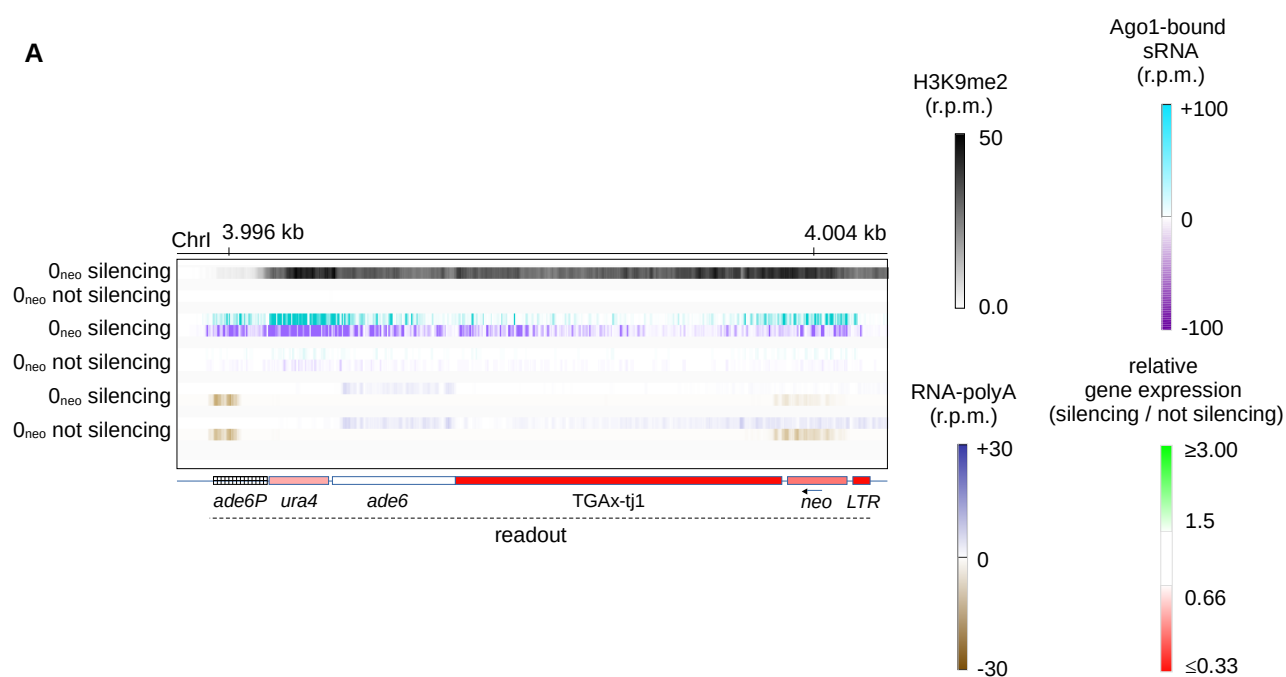
Finally, RNA sequencing was performed to investigate if H3K9me2 had a transcriptional gene silencing effect on *tj1*. Compared to not silencing cells, red cells show an evident reduction of readout transcription. As represented by the colors of the gene boxes, quantification of RNA showed that in red cells *tj1* was repressed at least three fold, when compared to white cells (Figure 3.5A). Due to the presence of the endogenous copy of *ade6M210*, which differs to *ade6* at the readout only for a SNP, it is impossible to assign correctly NGS-reads from this sequence. *ura4*, however, like TGAX-*tj1* and *neo*, represents a unique gene and therefore NGS specifically indicates reads generated at the readout locus.

Clearly, these results indicate that the exogenous copy of *tj1* is recognized when introduced in *S. pombe* and eventually silenced, although unstably, via sRNA-mediated H3K9me2 deposition (Figure 3.5A).

As H3K9me2-ChIP and Ago1-bound sRNA controls, in Figure 3.5B, centromeric dh and dg repeats of chromosome I are shown.

Interestingly, in silencing cells, H3K9me2 and sRNAs are observed at flanking regions of the endogenous *ade6M210*, indicating a trans-acting mechanism guided by the sRNAs generated at *ade6* of the readout (Figure 3.5C). However, no transcriptional silencing of flanking genes is detected.

In figures 3.5D,E Ago1-bound sRNAs features are represented, compared to those of Ago1-bound sRNA sequencing from a wt *S. pombe* strain. Typical 5' end uridine bias and usual sRNA lengths are present in both silencing and not silencing cells (Figure 3.5D and Figure 3.5E, respectively) (Halic and Moazed 2010; Marasovic et al. 2013; Pisacane 2017).



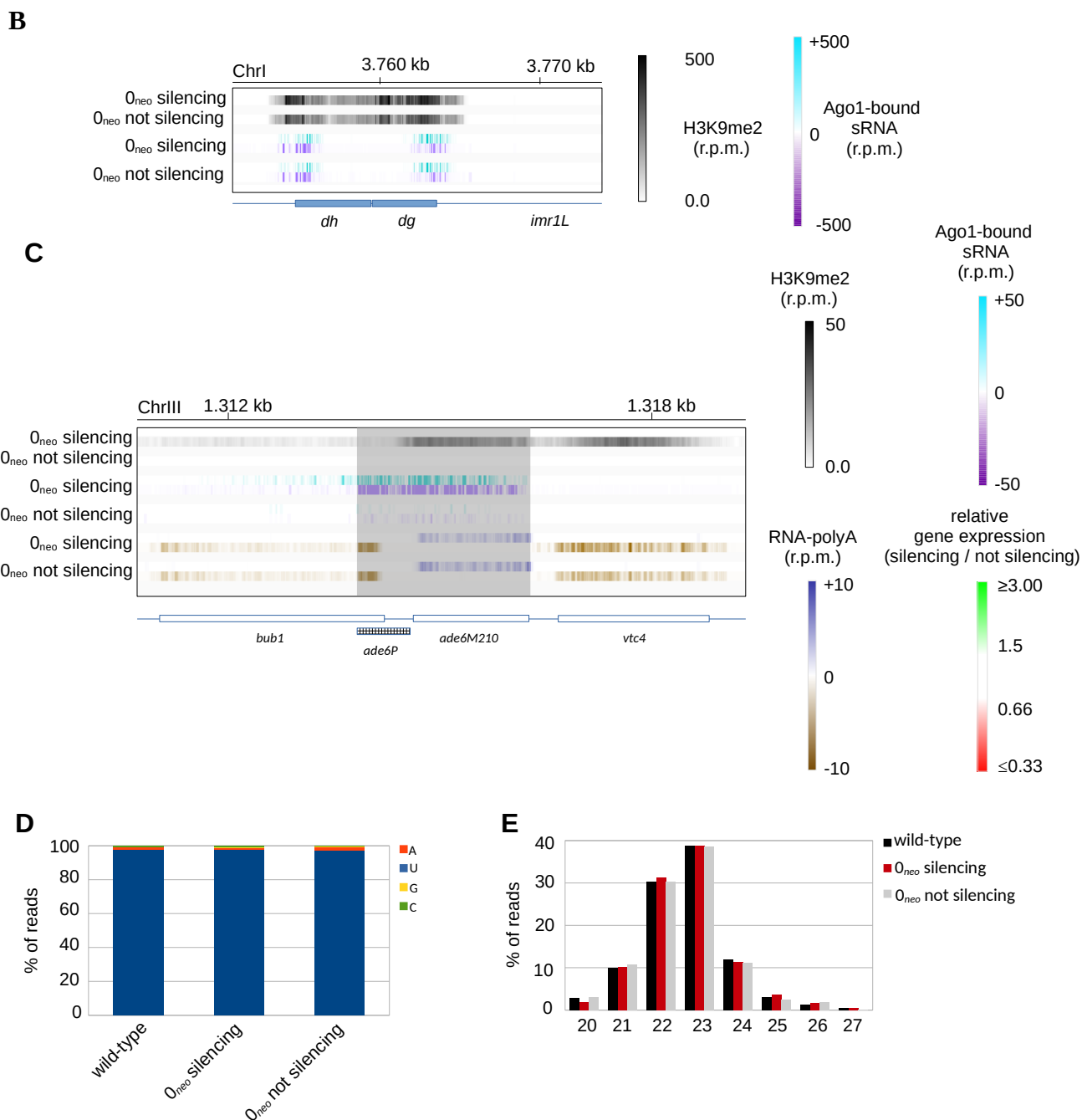
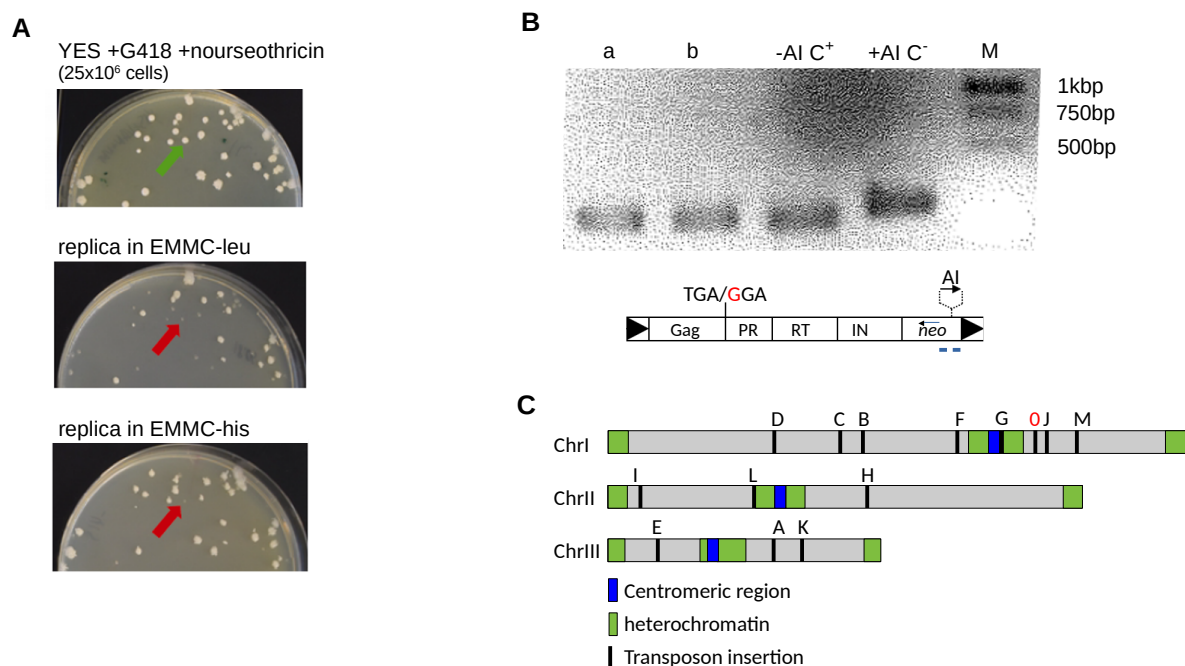


Figure 3.5: Silencing cells show H3K9me2 and sRNAs at the readout locus.

(A) Silencing cells present H3K9me2 at the readout locus, lost in not silencing cells. Ago1-bound sRNAs are enriched at the readout of silencing with only some residual sRNAs in not silencing cells. H3K9me2 is associated with transcriptional repression in the silencing cells. (B) H3K9me2 and Ago1-bound sRNAs at centromeric *dh* and *dg* repeats of silencing and not silencing cells. (C) Trans-acting mechanism is observed at the endogenous *ade6M210* locus. The transparent light-gray area indicates the region present in the readout construct and therefore not unique in the genome. (A-C) On black gradation scale H3K9me2 is represented, normalized per one million reads (r.p.m.). Positive and negative Ago1-bound sRNAs strands are normalized per one million reads and depicted in light-blue and purple gradations, respectively. (A, C) RNA-polyA + and – strands are normalized to coding sequences (cds) and represented in dark-blue and brown gradations, respectively. The relative gene expression is indicated with red to green gradation and calculated as ratio between cds normalized RNA-polyA reads of silencing and not silencing cells. Ade6P is represented as hatched box. (D) 5' end nucleotide preference of Ago1-bound sRNAs in indicated strains. (E) Length distribution of Ago1-bound sRNAs in indicated cells.

3.6 Isolation of single *S. pombe* colonies with *de novo* transpositions

Although with the previous results we could prove that fission yeast can recognize and silence the exogenous *tj1* element when introduced into the cells via plasmids, we wondered how cells would respond in the case of *de novo* *tj1* transpositions into the *S. pombe* genome. With the aim of inducing *tj1* retrotransposition, the 0_{nat} strain was transformed either with p1063, carrying a wt *tj1* copy, or with the combination of donor and expression plasmids p1065 and p1081, respectively. In both cellular setups, the artificial intron (AI) was present in the *neo* cassette, permitting the G418 selection of cells where a complete retrotransposition cycle was completed. However, G418 resistant cells were not necessarily cells where *tj1* cDNA was integrated into the genome, in fact, cDNA could recombine with *tj1* in the plasmid conferring G418 resistance without an actual genomic transposition. To distinguish *de novo* genomic transpositions to plasmid recombinations, cells with plasmids were initially grown in minimal media to induce transposition and subsequently in YES rich-medium to permit plasmid loss. Only at this point, 25×10^6 cells were plated in G418 (+nourseothricin) plates and resistant cells were replica plated in EMMC-leu and EMMC-his to identify transposed colonies in the original G418 (+nourseothricin) plate that lost the plasmids (Figure 3.6A). To confirm the isolation of *de novo* transposition cells without AI and plasmids, rather than plasmid recombinants, genomic DNA PCRs of G418 (and nourseothricin) resistant and plasmid negative colonies were finally performed (using PCR primers external to the AI sequence, into *LEU2* and *his3*) (Figure 3.6B, negative PCRs for *LEU2* and *his3* detection are not shown).



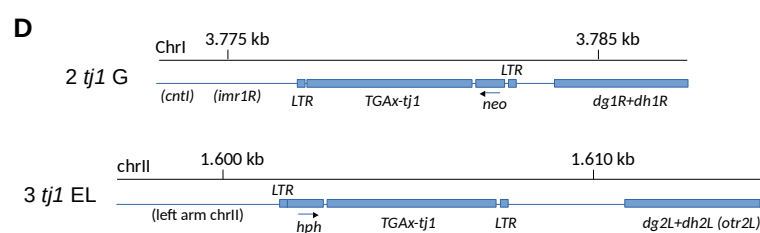


Figure 3.6: Selection of *de novo* genomic transpositions.

(A) After transposition induction and YES growth, 25×10^6 cells are plated in +G418 +nourseothricin selective medium. Resistant colonies are replicated in EMMC-leu and EMMC-his. The green arrow indicates a resistant colony which lost plasmids, as shown with red arrows on replica plates. (B) 3% agarose gel showing two -AI colonies (a and b), compared to a positive control (-AI) and a negative control (+AI). On the right, the sizes of the marker bands are indicated. In the lower scheme, positions of PCR primers for AI detection are depicted with blue lines (not in scale). Negative PCRs for *LEU2* and *his3* detection are not shown. (C) Scheme of all *de novo* transposition loci in the three *S. pombe* chromosomes. Each locus is represented with a letter (see also Table 3.1). 0 in red represent the position of the readout construct. Blue boxes indicate centromeres, green boxes indicate constitutive heterochromatin at telomeres and pericentromeric regions. (D) Close up of *tj1* transposition loci in strains “2 *tj1* G” (upper scheme) and “3 *tj1* EL” (second transposition locus, lower scheme) (respectively locus G and L in Figure 3.6C).

Different colonies with single *de novo tj1* transpositions were isolated with this approach. In Table 3.1 all *tj1* transpositions are represented. Via NGS and/or nanopore-sequencing all transpositions were confirmed and mapped on the *S. pombe* genome. Each transposition locus is indicated with a letter, whether the transposition was obtained from wt *tj1* or TGAX-*tj1* (coupled with p1081 expression plasmid), as well as the strain name used from now on in this Thesis, is also written. All *de novo* transpositions are in close proximity to and in forward orientation with an RPIII transcribed gene, a *tj1* bias already shown by Guo and colleagues (Guo et al. 2015). Target site duplication (TSD) and the exact transposition coordinates (as position of the first 5’LTR nt) are also indicated in Table 3.1. “2 *tj1* A” to “2 *tj1* G” strains were transformed again with the donor p1281 and p1081 expression plasmids, in order to isolate colonies with a second *de novo* transposition, again by the AI strategy, but this time selecting colonies resistant to hygromycin B (+G418 and +nourseothricin) due to the *hph* cassette present in p1281. A second Tj1 transposition was obtained from the parental strains “2 *tj1* E” and “2 *tj1* F”, generating two new strains, named “3 *tj1* EL” and “3 *tj1* FM”, respectively (Table 3.1). Figure 3.6C shows all the transposition loci in *S. pombe* chromosomes, interestingly, the transposition of strain “2 *tj1* G” and the second transposition (locus L) of strain “3 *tj1* EL”, are inserted close to pericentromeric heterochromatin (Figure 3.6D for a close up of these two loci).

transposition locus and Tj1 type	strain name (lab)	strain name (this study)	gene target type	gene name	orientation	TSD	position first 5'LTR nt
0 -	1267	0 _{neo}	-	-	-	-	*ChrI 3.995.823
0 -	1344	0 _{nat}	-	-	-	-	*ChrI 3.995.823
A <i>tj1</i>	1352	2 <i>tj1</i> A	tRNA	SPCTRNAHIS.04	forward	A	ChrIII 1.842.871
B <i>tj1</i>	1363	2 <i>tj1</i> B	tRNA	SPATRNALYS.03	forward	TGTCA	ChrI 2.441.957
C <i>tj1</i>	1365	2 <i>tj1</i> C	tRNA	SPATRNAVAL.03	forward	TTGAT	ChrI 2.215.066
D TGAX- <i>tj1</i>	1386	2 <i>tj1</i> D	tRNA	SPATRNATHR.01	forward	TGGTT	ChrI 1.609.113
E TGAX- <i>tj1</i>	1416	2 <i>tj1</i> E	5S rRNA	SPRRNA.24	forward	GATTG	ChrIII 521.555
F TGAX- <i>tj1</i>	1417	2 <i>tj1</i> F	5S rRNA	SPRRNA.16	forward	TTAAT	ChrI 3.634.371
G TGAX- <i>tj1</i>	1376	2 <i>tj1</i> G	tRNA	SPATRNAGLU.04	forward	AACTA	ChrI 3.776.764
H <i>tj1</i>	1374	-	tRNA	SPBTRNAMET.06	forward	-	ChrII 2.434.303
I <i>tj1</i>	1375	-	tRNA	SPBTRNAGLN.03	forward	CGTTT	ChrII 258.848
J TGAX- <i>tj1</i>	1366	-	5S rRNA	SPRRNA.20	forward	AAA	ChrI 4.240.850
K TGAX- <i>tj1</i>	1419	-	tRNA	SPCTRNASER.13	forward	AATGC	ChrIII 2.072.080
L TGAX- <i>tj1</i>	1428**	3 <i>tj1</i> EL	tRNA	SPATRNAGLU.06	forward	GACTT	ChrII 1.607.760
M TGAX- <i>tj1</i>	1427***	3 <i>tj1</i> FM	5S rRNA	SPRRNA.19	forward	CATTT	ChrI 4.194.174

* first ade6P nt

** 1416 background strain

*** 1417 background strain

Table 3.1: Table of all *de novo* transpositions obtained in this study.

All transposition loci are indicated with a letter. If transposition originates from wt *tj1* or TGAX-*tj1* is written. Names used to refer to each strain from now on in this study are indicated as well. Tj1 target gene types, specific names and Tj1-relative orientation are shown. Target site duplication (TSD) and precise transposition coordinates are represented.

A closer analysis of transposition features, shows a preference for *tj1* transpositions at 5S rRNAs with respect to tRNAs of 2.11 fold (Table 3.2). However, this bias can be caused by a slight preference for Tj1 transpositions at euchromatin compared to heterochromatin (Table 3.3) and the absence of 5S rRNAs at heterochromatin. Therefore, it is difficult to argue that Tj1 transposes preferentially at 5s rRNAs. However, considering the recombination repression of heterochromatic regions (Ellermeier et al. 2010; Okita et al. 2019), we can speculate that Tj1 integration at euchromatic loci is slightly favored over heterochromatic loci (Table 3.3), although this analysis is performed with a total of only 13 transpositions (Table 3.1).

% <i>S.pombe</i> tRNA*	% <i>S.pombe</i> 5S rRNA*	<i>S.pombe</i> tRNA/5S rRNA	% transpositions at tRNA	% transpositions at 5S rRNA	transposition tRNA/5S rRNA	transposition preference for 5S rRNAs over tRNA
82.6	17.4	4.75	69.2	30.8	2.25	2.11

*of RPIII transcribed genes

Table 3.2

% <i>S.pombe</i> RPIII transcribed genes at euchromatin	% <i>S.pombe</i> RPIII transcribed genes at heterochromatin	<i>S.pombe</i> RPIII genes euchromatin/heterochromatin	% transpositions at euchromatin	% transpositions at heterochromatin	transposition euchromatin/heterochromatin	transposition preference for euchromatin over heterochromatin
79.9	20.1	3.98	84.6	15.4	5.5	1.38

Table 3.3

Finally, Tj1 shows the propensity to transpose at RPIII transcribed genes where the first cds at 5' has a parallel orientation to the tRNA/5S rRNA genes, with a preference of 2.18 fold with respect to the divergent orientation (Table 3.4 and Table 3.5).

locus	A	B	C	D	E	F	G	H	I	J	K	L	M
5'cds gene orientation	 (tj1>)	 (tj1>)	 (tj1>)	 (tj1>)	 (tj1>)	 (tj1>)	-	 (tj1>)	 (tj1>)	 (tj1>)	 (tj1>)	-	 (tj1>)

Table 3.4.

Gene orientation of the first cds gene at 5' of *tj1* LTR in each transposition locus obtained in this study. Divergent and parallel orientations highlighted in red and green, respectively.

% <i>S.pombe</i> parallel orientation of first cds at 5' of RPIII transcribed genes	% <i>S.pombe</i> divergent orientation of first cds at 5' of RPIII transcribed genes	<i>S.pombe</i> parallel/divergent orientation of first cds at 5' of RPIII transcribed genes	% parallel orientation of first cds at 5' of transpositions	% divergent orientation of first cds at 5' of transpositions	parallel/divergent orientation of first cds at 5' of transpositions	transposition preference for parallel orientation of first cds at 5'
35.48	64.52	0.55	54.5	45.5	1.2	2.18

Table 3.5

3.7 Transposition in the proximity of pericentromeric heterochromatin triggers *tj1* silencing

The assay described in section 3.4, performed with the aim of investigating *tj1* silencing establishment in cells with one *tj1* copy at the readout and in cells with multiple copies on plasmids, showed that the single *tj1* endogenous copy at the readout is not capable of triggering silencing and that more *tj1* copies (on plasmids) are necessary to establish silencing (Figure 3.4B). At this point, with the new strains generated, we wondered whether a second endogenous *tj1* copy would trigger silencing of the transposable element. To answer this question, the same establishment experiment was performed

with strains from “2 *tj1* A” to “2 *tj1* G” (together with 0_{nat} as not silencing control) without and with plasmids (p1281 donor or p1282 in “2 *tj1*” strains, p1263 or p1265 in 0_{nat}). The average establishment of all “2 *tj1*” strains without plasmids shows that two endogenous *tj1* copies can trigger silencing (Figure 3.7A) and that the presence of multiple *tj1* copies on plasmids increases the number of cells capable of *tj1* recognition and silencing (Figure 3.7C). To investigate how a third endogenous *tj1* copy would modulate its silencing, the establishment assay was performed with “3 *tj1* EL” and “3 *tj1* FM” strains, without and with plasmids (p1281 donor), compared to their parental strains (“2 *tj1* E” and “2 *tj1* F”, respectively). The average establishment of “3 *tj1* EL” and “3 *tj1* FM” shows that a third copy of *tj1* increases the number of silencing cells, compared to the average of the parental strains (Figure 3.7B). Alike the case of “2 *tj1*” strains, the introduction of multiple *tj1* copies with plasmids in both “3 *tj1* EL” and “3 *tj1* FM”, heightens the number of silencing colonies (Figure 3.7D).

These results indicate that as few as two (or three) endogenous *tj1* copies can trigger the silencing of the TE.

In the presence of multiple *tj1* copies on plasmids, the average of silencing colonies increases in both “2 *tj1*” and “3 *tj1*” strains, when compared to their control (0_{nat} and “2 *tj1* parental to 3 *tj1* EL and 3 *tj1* FM”, respectively), overall indicating that a +1 endogenous *tj1* copy heightens the possibility to trigger silencing (Figure 3.7C,D). In fact, although the average total number of *tj1* copies in “3 *tj1*” with plasmids is similar to that of their parental strains, silencing on average is higher in “3 *tj1*” strains (Figure 3.7D). Similarly, “2 *tj1*” strains with plasmids show on average even less *tj1* copy than 0_{nat} control, yet they silence more frequently than 0_{nat} (Figure 3.7C).

A closer look at the single establishment experiments performed with all “2 *tj1*” and “3 *tj1*” strains without plasmids, however, indicates that silencing was triggered specifically in “2 *tj1* G” and “3 *tj1* EL”. Importantly, these two strains present, respectively, their second and third endogenous *tj1* copy transposed in close proximity to pericentromeric heterochromatin (Figure 3.7 E,F). Therefore, neither two nor three endogenous *tj1* copies can trigger the silencing of the element, unless *tj1* transposes near constitutive (pericentromeric) heterochromatin (Figure 3.7 E,F).

Finally, a closer analysis of single establishment experiments of all “2 *tj1*” and “3 *tj1*” strains with plasmids, shows that when multiple *tj1* copies were introduced into cells by the use of plasmids, all “2 *tj1*” and “3 *tj1*” strains (and not only “2 *tj1* G” and “3 *tj1* EL”) established silencing, indicating that multiple copies of the element are necessary for its recognition, unless *tj1* transposes close to heterochromatin (Figures 3.7G,H and as seen in Figure 3.4B). Specifically, more than three endogenous (euchromatic) copies are needed, as proved by the absence of silencing in the “3 *tj1* FM” strain without plasmids. However, it was impossible to define the precise *tj1* copy number needed to trigger silencing, considering that also in “2 *tj1*” and “3 *tj1*” +plasmids strains, there is no direct proportionality between the number of *tj1* element and number of silencing colonies (Figures 3.7G,H and 3.4B).

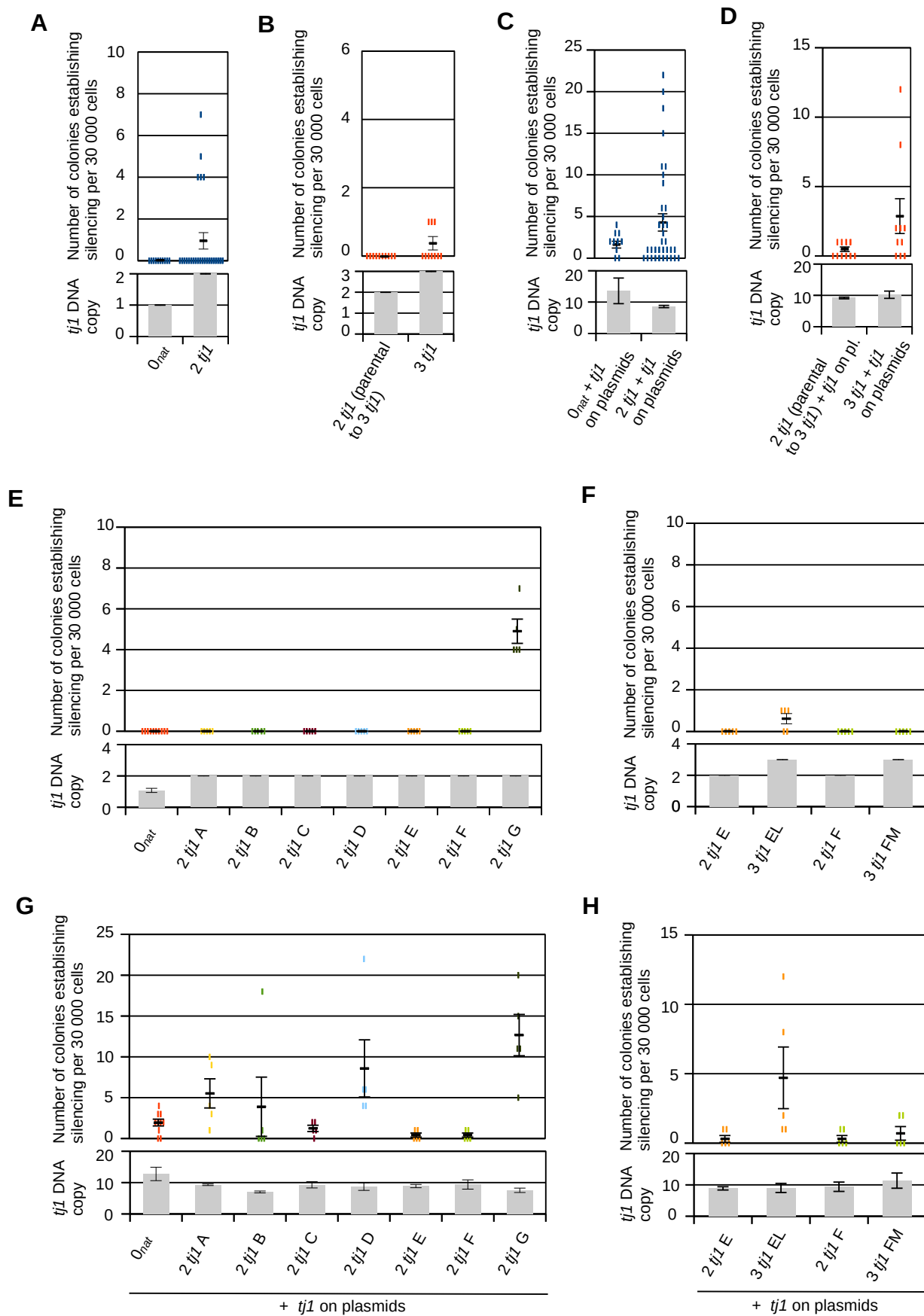


Figure 3.7: *S.pombe* establishes silencing when *tj1* transposes in close proximity to pericentromeric heterochromatin.

(A) Silencing establishment average in all endogenous “2 *tj1*” strains without plasmids (0_{nat} as not silencing control). (B) Silencing establishment average in “3 *tj1* EL” and “3 *tj1* FM” strains without plasmids, compared to their paternal strains, “2 *tj1* E” and “2 *tj1* F”, respectively. (C) Silencing establishment average in all endogenous “2 *tj1*” strains + plasmids (p1281 donor or p1282). 0_{nat} + plasmids (either p1263 or p1265) as control. (D) Silencing establishment average in “3 *tj1* EL” and “3 *tj1* FM” strains with plasmids (p1281 donor), compared to their parental strains. (E) Silencing establishment in all endogenous “2 *tj1*” strains, 0_{nat} as not silencing control. Silencing is present only in centromeric transposition strain “2 *tj1* G”. (F) Silencing establishment in “3 *tj1* EL” and “3 *tj1* FM” strains compared to their paternal strains, “2 *tj1* E” and “2 *tj1* F”, respectively. Silencing is established only in “3 *tj1* EL” strain, where *tj1* transposed close to centromeric heterochromatin. (G,H) Multiple copies of *tj1* on plasmids, trigger silencing. (A-H) In the upper graph, single colored vertical lines indicate the number of red colonies per 30.000 cells and the black horizontal lines represent the average of silencing colonies per 30.000 cells. Error bars indicate s.e.m. of at least five independent plating. The lower graph shows the total copy number of *tj1* in the corresponding strains (normalized to *act1* copy number). Error bars indicate s.e.m. for at least a technical triplicate of one independent experiment.

3.8 Sense and antisense transcription of *tj1* are necessary for efficient silencing of the element

Excluding centromeric transposition strains “2 *tj1* G” and “3 *tj1* EL”, establishment assays with plasmids show that strains “2 *tj1* A” and “2 *tj1* D” on average silence more efficiently among all strains analyzed (Figure 3.7G,H). However, no direct proportionality between *tj1* copy number and silencing was observed (Figures 3.4B and 3.7G,H), therefore, we wondered whether the sense and antisense transcription of the element is important for its recognition and silencing, independently of *tj1* copy number. In order to answer this question, the strains with plasmids were divided into three groups: (i) efficient in silencing (euchromatic insertions, “2 *tj1* A” and “2 *tj1* D”), (ii) efficient in silencing (heterochromatic insertions, “2 *tj1* G” and “3 *tj1* EL”) and (iii) not efficient in silencing (0_{nat} , “2 *tj1* B”, “2 *tj1* C”, “2 *tj1* E”, “2 *tj1* F” and “3 *tj1* FM”). Although efficient in silencing, the strains with heterochromatic insertions (“2 *tj1* G” and “3 *tj1* EL”) formed a specific and separated group because they likely have a different silencing establishment mechanism, due to their positions close to heterochromatin. Total RNA was extracted from all strains with plasmids and from 0_{nat} , sense and antisense *tj1* RNAs were analyzed via RT-qPCR, compared to 0_{nat} . The results show that total *tj1* sense transcription doesn’t change clearly between groups of “efficient” and “not efficient” in silencing (Figure 3.8A), however, total *tj1* antisense RNA appears higher in strains “efficient” in silencing (Figure 3.8B). These results indicate that antisense transcription of *tj1* is important for establishing the silencing of the transposable element and suggest that a certain “threshold” amount of antisense RNA needs to be reached to trigger *tj1* silencing.

To investigate more extensively the role of *tj1* sense transcription in silencing the transposable element, a promoter deficient *tj1* sequence was generated and cloned into a plasmid (p1290). More specifically, 5’LTR of the element was completely removed from *tj1*, to repress sense transcription of

the element, 5'LTR dependent. Then, 0_{nat} strain was transformed with the new plasmid p1290 and total RNA was extracted, included from 0_{nat} +p1263, used as control. Sense (and antisense) *tj1* transcription were analyzed by RT-qPCR and compared to sense transcription of 0_{nat} +p1263 (Figure 3.8C). Finally, a canonical silencing establishment assay was performed to determine the number of silencing colonies when *tj1* sense transcription is impaired (figure 3.8D). RT-qPCR shows that the deletion of 5'LTR from *tj1* decreases sense RNA transcription from each *tj1* copy of more than two fold, while antisense transcription is weakly affected (Figure 3.8C). This result, together with the clear reduction of silencing colonies when 5'LTR is removed (Figure 3.8D), suggests that a threshold RNA value for sense *tj1* is also necessary to trigger silencing of the transposable element (although antisense transcription is not impaired).

In consideration of these results, it is possible to argue that sense and antisense transcription of *tj1*, over a certain threshold level, is necessary for the cells to initially recognize and trigger silencing (independently to the number of *tj1* copies).

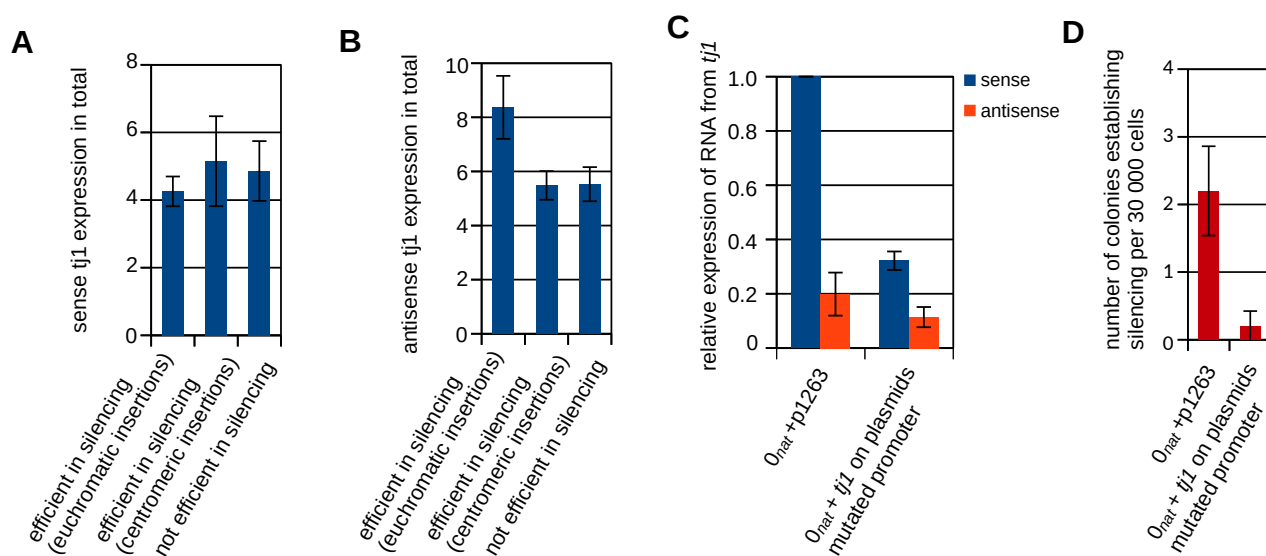


Figure 3.8: Sense and antisense *tj1* transcription are necessary for efficient silencing of the element.

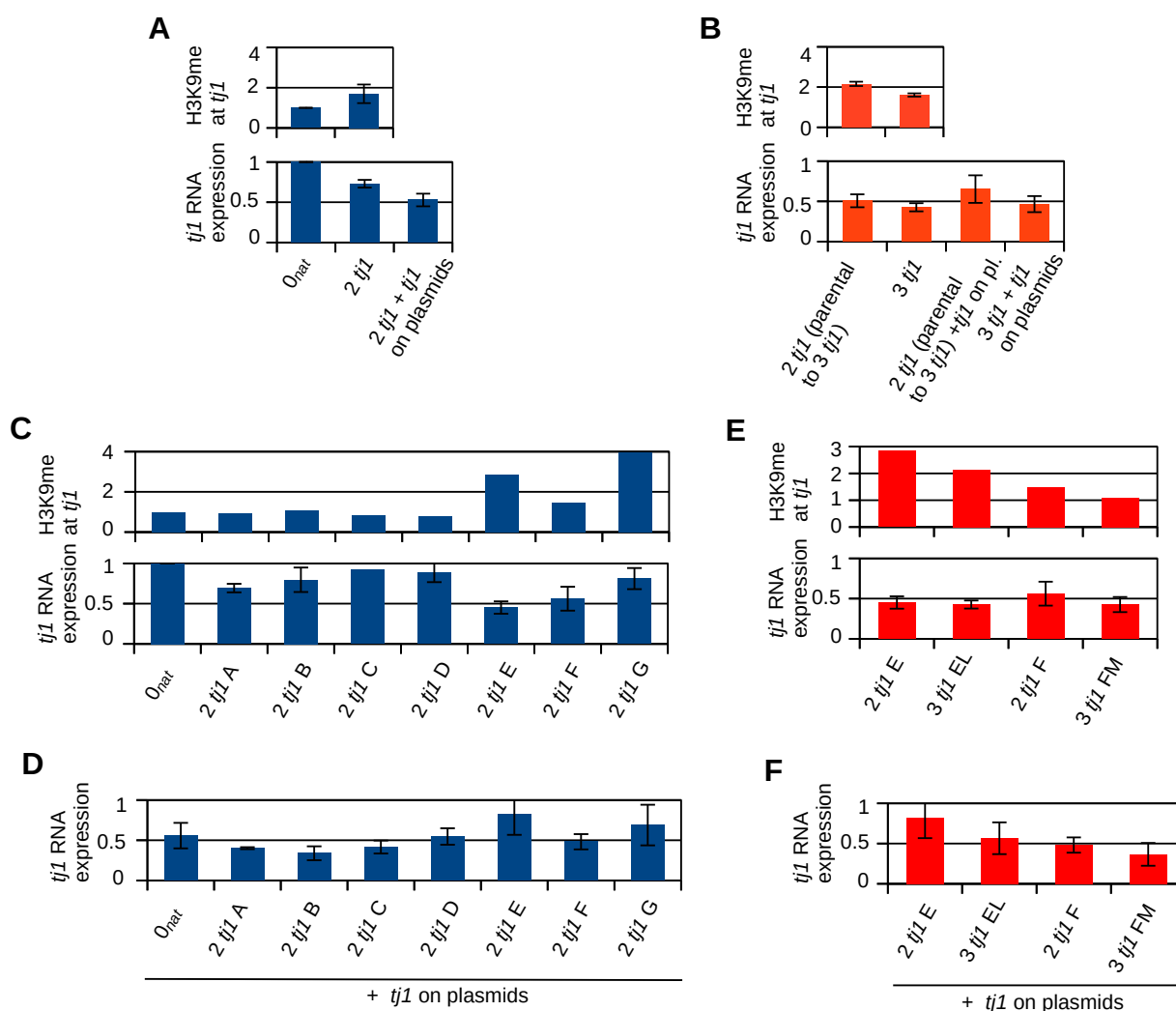
(A) Total *tj1* sense RNA in indicated strain groups, over total *tj1* sense RNA of 0_{nat} . (B) Total *tj1* antisense RNA in indicated strain groups, over total *tj1* sense RNA of 0_{nat} . (C) Sense and antisense *tj1* RNA per *tj1* copy in indicated strains, over 0_{nat} +p1263 *tj1* sense RNA. (D) Average silencing establishment in indicated strains. Error bars indicate s.e.m. of at least five independent plating. (A-C) RT-qPCR data, normalized to *act1* RNA. (A,B) Error bars indicate s.e.m. of at least 2 independent experiments. (C) Error bars indicate s.e.m. of at least 3 technical replicates.

3.9 Low H3K9me2 is deposited already in cell populations of “2 *tj1*” and “3 *tj1*” strains

Unless *tj1* transposed close to pericentromeric heterochromatin, none of the “2 *tj1*” nor “3 *tj1* FM” without plasmids show red colonies (Figure 3.7E,F), however, we wondered whether cells could recognize *tj1*, yet not efficiently silencing it. H3K9me2-ChIP and *tj1* transcriptional analysis of all “2

tj1" and "3 *tj1*" without (and with) plasmids were performed. Surprisingly, when compared to 0_{nat} on average all "2 *tj1*" and "3 *tj1*" without plasmids show low H3K9me2 enrichment at each *tj1*, together with a reduction of RNA transcription (Figure 3.9A,B). A closer look at the single strains shows that H3K9me2 at *tj1* are not exclusively enriched on pericentromeric transposition "2 *tj1* G" and "3 *tj1* EL" strains, as expected, but also on some euchromatic transposition strains, i.e. "2 *tj1* B", "2 *tj1* E" and "2 *tj1* F" (Figure 3.9C,E). *tj1* RNA instead decreases in all "2 *tj1*" and "3 *tj1*" (Figure 3.9C,E), suggesting that all strains recognize the second (and third) *tj1* copy, although not efficiently enough to silence it.

When multiple copies of the TE are present on plasmids, on average "2 *tj1*" show a slight additional reduction of *tj1* RNA per copy (Figure 3.9A), as well as "3 *tj1*" with plasmids, compared to their parental "2 *tj1*" strains (Figure 3.9B), suggesting again that multiple copies of the element are necessary to heighten *tj1* silencing. Figure 3.9D,F shows *tj1* RNA of all "2 *tj1*" and "3 *tj1*" strains with plasmids. In Figure 3.9G, Integrative Genomics Viewer (IGV) H3K9me2 tracks of some strains without plasmids are represented. Figure 3.9H shows the average of H3K9me2 of all "2 *tj1*" strains.



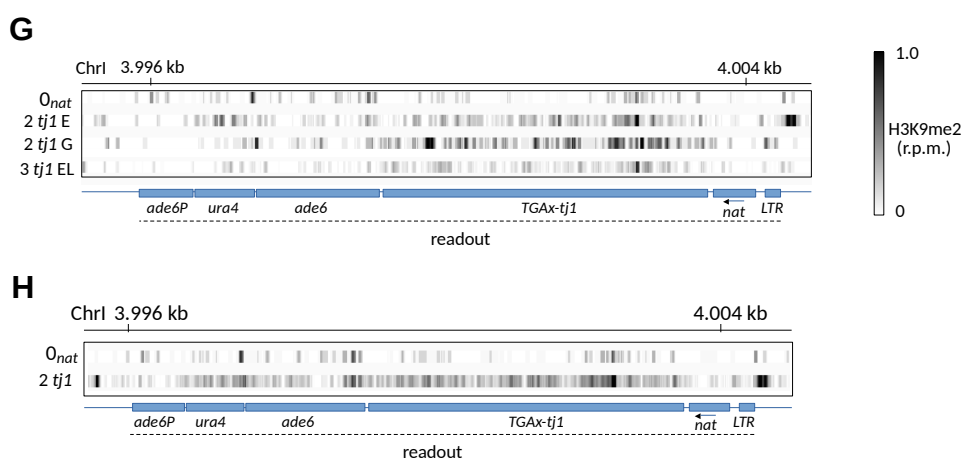


Figure 3.9: Low H3K9me2 is deposited already in cell populations of “2 *tj1*” and “3 *tj1*” strains.

(A,B,C,E) H3K9me2 and *tj1* RNA expression in indicated strains. (D,F) *tj1* RNA expression in indicated strains. (G,H) H3K9me2 IGV tracks of indicated strains, normalized to background. Reads per one million reads (r.p.m.) H3K9me2 scale is represented on black gradation. (A-F) H3K9me2 quantified by H3K9me2-ChIP sequencing (normalized to background), over strain 0_{nat} . Error bars indicate s.e.m of at least 2 independent experiments. *tj1* RNA expression calculated as average of RNA-polyA and total RNA sequencing (normalized to cds), over strain 0_{nat} . Error bars indicate s.e.m of at least 2 independent experiments.

3.10 Silencing colonies strongly repress *tj1* via H3K9me2

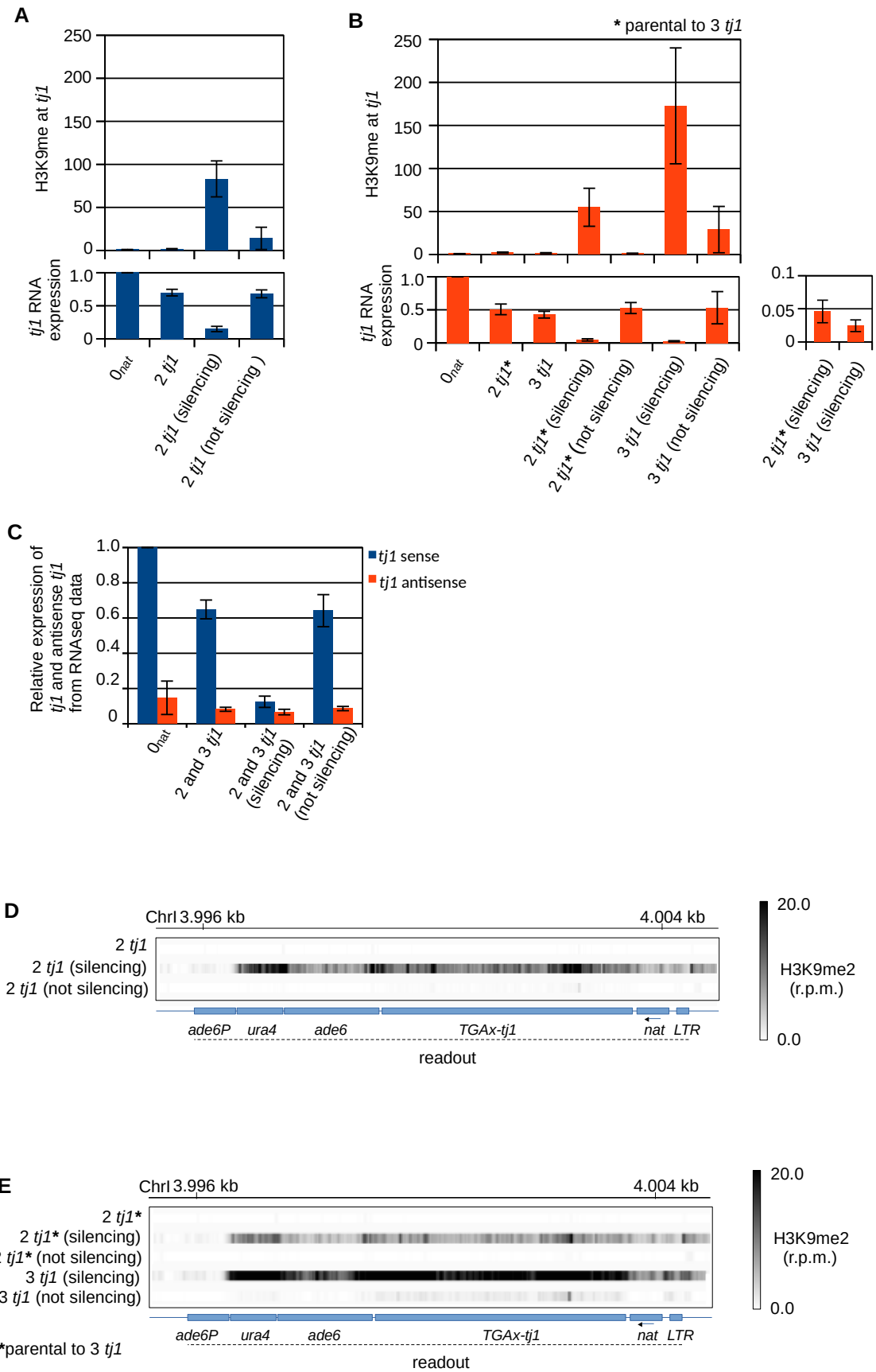
In order to deeply investigate the mechanisms and dynamics of *tj1* silencing, red colonies of all “2 *tj1*” and “3 *tj1*” strains were isolated. As briefly described in section 3.5, red colonies were forced to lose their plasmids and from these colonies, the correspondent white colonies were isolated, therefore constituting the “silencing” and the “not silencing” colonies of each strain, respectively. Each “silencing” and “not silencing” colony of all “2 *tj1*” and “3 *tj1*” strains was analyzed via H3K9me2-ChIP and RNA sequencings. On average, “2 *tj1*” silencing strains show an enrichment of H3K9me2 at *tj1* of -80 fold over 0_{nat} control, together with more than 6 fold decrease in *tj1* transcription (Figure 3.10A). When 3 *tj1* copies are present, silencing colonies on average increase H3K9me2 at *tj1* up to more than -150 fold, compared to 0_{nat} control, -3 fold more than the average of their “2 *tj1*” parental silencing strains (Figure 3.10B). Regarding *tj1* RNA, when a third copy of the element is present, on average silencing strains repress *tj1* transcription more than 40 fold if compared to 0_{nat} control RNA (Figure 3.10B) and -2 fold when compared to the average of their parental silencing strains (Figure 3.10B, adjacent small figure box). These results indicate that when *tj1* is silenced, high levels of H3K9me are deposited throughout the element, accompanied by considerable repression of RNA transcription. Moreover, when 3 copies of *tj1* are present, on average H3K9me deposition and *tj1* repression increase compared to “2 *tj1*” parental silencing strains, suggesting a stronger silencing in colonies with a +1 *tj1* copy.

A transcriptional analysis of *tj1* sense and antisense, averaging the colonies according to their silencing state (red, white from red, and as cell populations), was performed and compared to 0_{nat} (Figure 3.10C). The results show that in 0_{nat} antisense *tj1* is ~5 fold less transcribed than sense *tj1* and that, more interestingly, antisense transcription doesn't decrease in silencing colonies, compared to cell population (and not silencing colonies). This observation shows the importance of antisense RNA, weakly maintained transcribed also in silencing colonies.

Figures 3.10D and 3.10E show IGV tracks of H3K9me2 averages of silencing and not silencing “2 *tj1*” and “3 *tj1*” strains, respectively.

Interestingly, not silencing “2 *tj1*” and “3 *tj1*” strains on average show residual H3K9me2 at *tj1* element (Figures 3.10A,B and D,E), however a closer look at the single silencing and not silencing colonies indicates that H3K9me2 in not silencing colonies is strongly present only in “2 *tj1* G” and “3 *tj1* EL”, the strains with transpositions close to pericentromeric heterochromatin (Figure 3.10F,G). This result indicates that when *tj1* transposes close to constitutive heterochromatin, its silencing is strongly maintained also in not silencing (white) colonies, suggesting that white colonies lost silencing specifically at the readout locus, but not at the transposed pericentromeric *tj1* copy. Moreover, although silencing appears stronger when *tj1* copies are 3 than when they are 2 (as visible in “3 *tj1* FM” silencing colony) (Figure 3.10A,B,F,G), the maintenance of silencing doesn't depend on the number of *tj1* elements, as indicated by “3 *tj1* FM” not silencing colony which loses completely H3K9me2 (Figure 3.10G), but rather maintenance depends on *tj1* transposition environment. In conclusion, regardless of whether the number of *tj1* copies is 2 or 3, silencing of the element(s) is maintained in white colonies only when *tj1* is integrated close to heterochromatin.

Thanks to the unique *ura4* and *nat* sequences present in the readout, *neo* in the second *tj1* element and *hph* in the third *tj1* copy, it was possible to deeply characterize the silencing of each region. If it is true how hypothesized, that white colonies from silencing strains with transpositions close to pericentromeric heterochromatin (“2 *tj1* G” and “3 *tj1* EL”), specifically lost silencing at the readout locus, but not at the pericentromeric copy (Figure 3.10F,G), *nat* RNA, but not *tj1* RNA of pericentromeric elements, should be specifically derepressed in pericentromeric not silencing colonies. Readout, euchromatic and heterochromatic specific RNA levels were therefore studied.



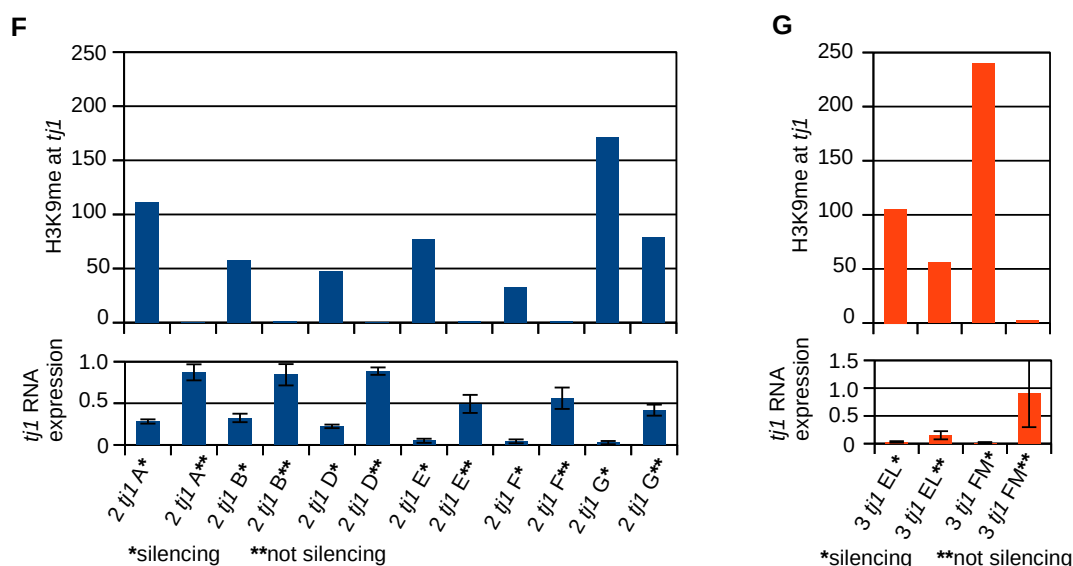
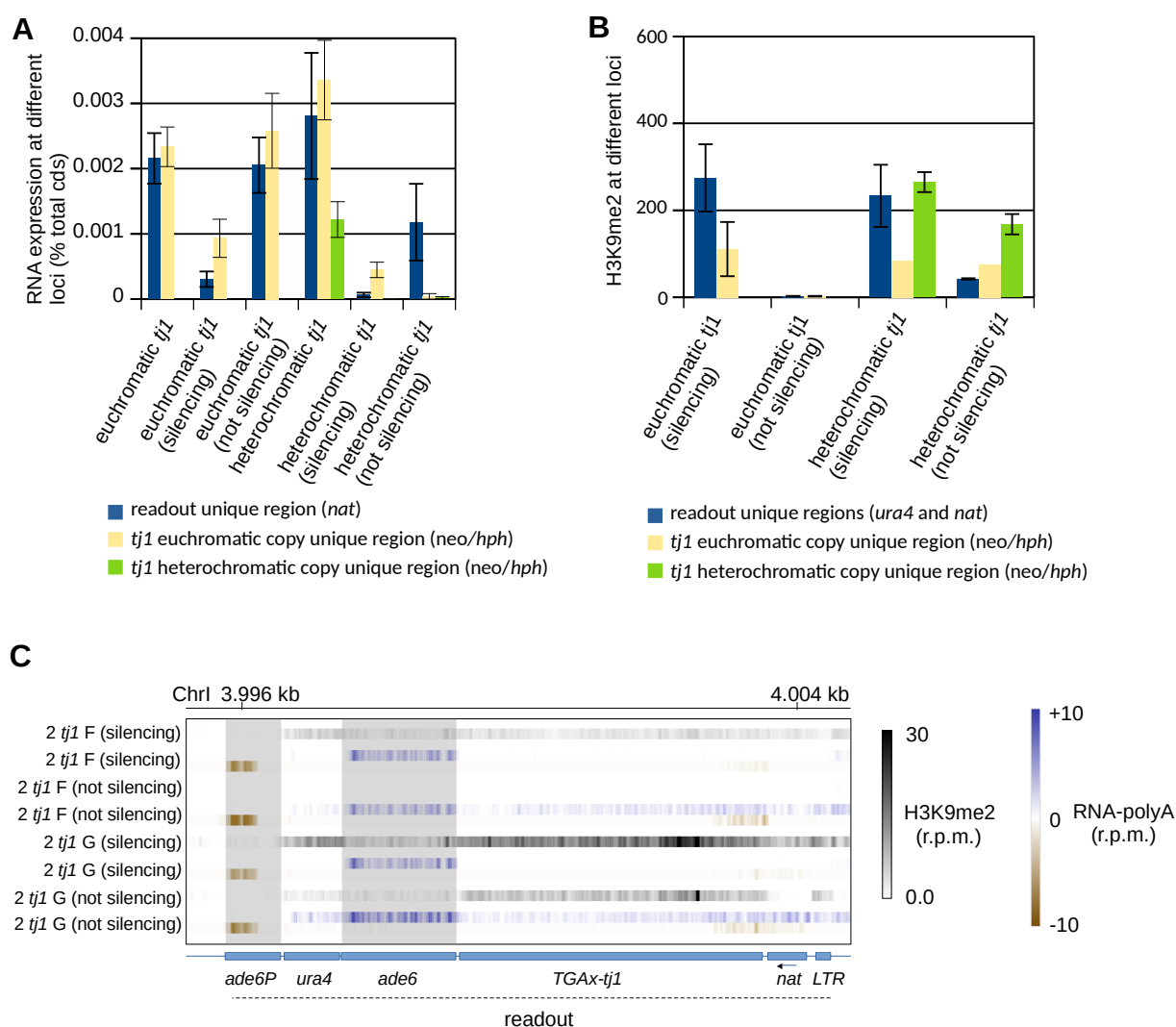


Figure 3.10: Silencing colonies strongly repress *tj1*.

(A,B) H3K9me2 and *tj1* RNA expression in indicated strains. The small graph adjacent to Figure B shows a close up of *tj1* RNA average expression of “3 *tj1*” strains and their “2 *tj1*” parental strains. H3K9me2 quantified by H3K9me2-ChIP sequencing (normalized to background), over strain 0_{nat} . Error bars indicate s.e.m of at least 2 independent experiments. *tj1* RNA expression calculated as average of RNA-polyA and total RNA sequencing (normalized to cds), over strain 0_{nat} . Error bars indicate s.e.m of at least 2 independent experiments. (C) Sense and antisense *tj1* RNA transcription in indicated strain groups, compared to sense *tj1* of 0_{nat} . Error bars indicate s.e.m of at least 2 independent RNA-polyA and total RNA sequencing experiments (normalized to cds). (D,E) IGV H3K9me2 average tracks of indicated strains, normalized to background. Reads per one million reads (r.p.m.) H3K9me2 scale is represented on black gradation. (F,G) H3K9me2-ChIP sequencing and *tj1* RNA sequencing quantification in indicated strains, over strain 0_{nat} . Error bars indicate s.e.m of 2 independent RNA-polyA and total RNA sequencing experiments (normalized to cds).

All the colonies were grouped according to their transposition loci, euchromatic or heterochromatic and either *neo* or *hph* RNA was accordingly analyzed, together with readout specific *nat* RNA. More precisely, *neo/hph/nat* antisense strands were studied, as part of the 3' sense *tj1* transcripts (Figures 3.2 and 3.3) and therefore representing a good estimation of *tj1* transcription at each locus. The results in Figure 3.11A show that in not silencing strains with transpositions at euchromatin, both *nat* and *tj1* transcriptions are derepressed, on the other hand, in not silencing strains with pericentromeric transpositions, only *nat* transcription is derepressed, while *tj1* elements are maintained repressed. With the same approach, H3K9me was analyzed as well, including *ura4* in the readout specific regions (Figure 3.11B). The results reflect what was observed in the RNA analysis; in not silencing colonies with pericentromeric transposition, H3K9me is mostly lost at the readout locus (*ura4* and *nat*), while heterochromatin is maintained at *tj1* elements, in particular at the pericentromeric copies. As examples, H3K9me2 and RNA-polyA IGV tracks at readout locus of a euchromatic transposition strain (“2 *tj1* F”) and a heterochromatic strain (“2 *tj1* G”) are shown in Figures 3.11C and 3.11D. *ura4*

and *nat* represent readout unique regions, and their observation indicates that “2 *tj1 G*” not silencing colony lost most of the silencing specifically at the readout locus due to selection of white colonies. In fact, H3K9me2 is completely absent at *nat* in “2 *tj1 G*” not silencing colony, while residual methylations are maintained only at *ura4*, yet not strong enough to silence the locus, as indicated by *ura4* (and *nat*) RNA levels, comparable to “2 *tj1 F*” not silencing colony (Figure 3.11C). On the other hand, silencing in “2 *tj1 G*” not silencing colony is mostly maintained at the pericentromeric *tj1* copy, as indicated by strong H3K9me2 and extremely poor RNA levels at *neo* region (Figure 3.11D). Instead, euchromatic transposition “2 *tj1 F*” not silencing colony shows complete loss of silencing at the transposed *tj1* element, as shown by the total absence of methylations and high *neo* RNA levels (Figure 3.11D). Figure 3.11E shows the RNA quantification of “2 *tj1 F*” and “2 *tj1 G*” silencing and not silencing colonies, at readout (*nat*) and transposed *tj1* (*neo*). “2 *tj1 G*” not silencing colony maintains repression of pericentromeric *tj1*, while the readout silencing is selectively lost, as observed in IGV tracks (Figures 3.11C,D).



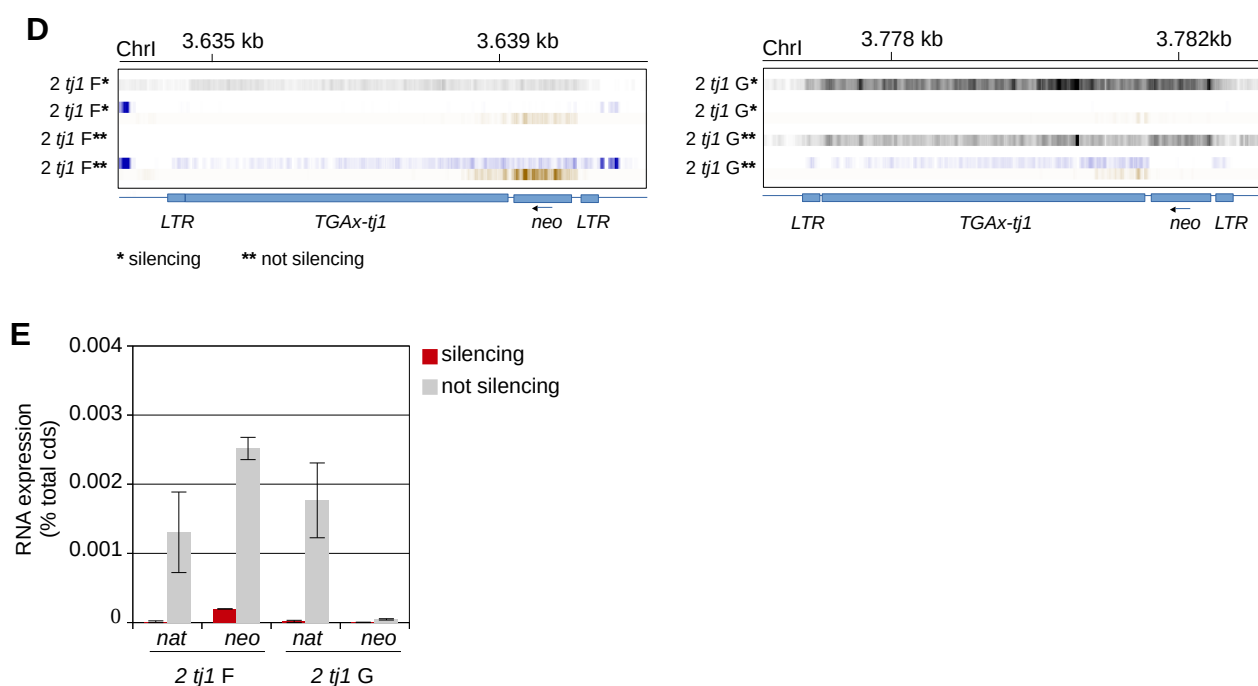


Figure 3.11: *tj1* copies close to pericentromeric heterochromatin are strongly repressed and maintained silenced independently to the readout repression state.

(A) RNA expression at unique readout, euchromatic *tj1* and heterochromatic *tj1* regions, in indicated strain groups. In heterochromatic *tj1* not silencing colonies, transcription is specifically derepressed at readout locus, but maintained repressed at pericentromeric (and euchromatic) *tj1*. Quantification from average of RNA-polyA and total RNA sequencings (% of total cds). Error bars represent s.e.m. of at least four independent experiments. (B) H3K9me2 at unique regions in indicated strain groups. Quantification from H3K9me2-ChIP sequencing (over background, normalized to sequence length). Error bars represent s.e.m. of at least three independent experiments. (C) H3K9me2 and RNA-polyA IGV tracks in indicated colonies, at readout locus. The transparent light-gray area indicates not unique regions, identical to endogenous *ade6* locus. H3K9me2 is represented on black gradation scale, normalized to background and per one million reads (r.p.m.). RNA-polyA + and – strands are normalized to coding sequences (cds) and represented in dark-blue and brown gradations (scale on the right), respectively. (D) H3K9me2 and RNA-polyA IGV tracks in indicated colonies, at transposition specific loci. Scales as in C. (E) RNA expression at readout (*nat*) and transposed element (*neo*), in indicated strains, silencing (red) and not silencing (gray). Quantification and normalization as in A. Error bars represent s.e.m. of two independent experiments.

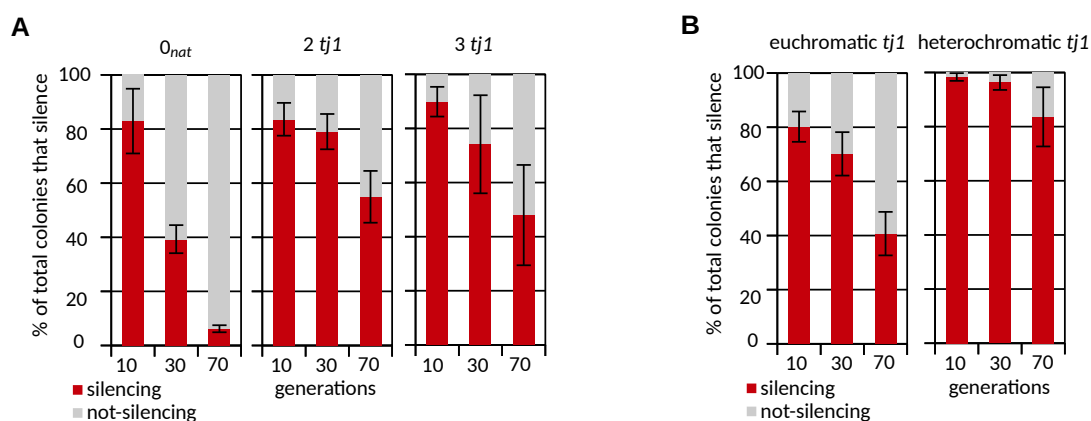
3.11 *tj1* silencing is maintained more stably through generations when the element transposes close to pericentromeric heterochromatin

The observation that pericentromeric white colonies from silencing colonies maintained *tj1* repression at the transposed copies (Figures 3.11A,B), made us wonder how silencing would be inherited through generations in silencing colonies of both heterochromatic and euchromatic *tj1* transposition loci strains, when white selection is avoided. Furthermore, we wondered if increasing the number of endogenous *tj1* copies would lead to a more stable silencing through cell divisions. To answer these questions, a silencing maintenance assay was performed; red colonies without plasmids

were selected and propagated via several plating in low adhesion plates, until stably silencing colonies were obtained (considered stable when at least 75% of the colonies on low adhesion plate was red). Then, stable silencing colonies were exponentially grown in liquid rich media (YES) and ~1000 cells were plated on PMG low adhesion plates after 10, 30 and 70 generations. Finally, the % of red colonies in each plate was calculated. As shown in Figure 3.12A, *tj1* silencing is more stably maintained through generations when either 2 or 3 copies of the element are present, compared to 0_{nat} . However, no substantial differences are observed between “2 *tj1*” and “3 *tj1*” (Figure 3.12A). When the results are observed according to *tj1* transposition loci, euchromatic or heterochromatic, the assay shows a clear increase in silencing maintenance through generations in strains where the element integrated close to heterochromatin (Figure 3.12B). Finally, also the previous data of basal H3K9me2 deposition in cell populations (before red selection, without plasmids) (Figure 3.9) were grouped according to the transposition loci, either euchromatic or pericentromeric. The results show that, on average, strains with pericentromeric *tj1* have higher basal H3K9me2 levels, than strains with euchromatic *tj1* (Figure 3.12C), leading to the establishment of silencing observed exclusively in pericentromeric “2 *tj1* G” and “3 *tj1* EL” strains in the absence of multiple *tj1* copies (on plasmids) (Figure 3.7E,F and on average in Figure 3.12D).

Altogether, these results suggest that *tj1* transpositions close to heterochromatic regions, increase considerably the maintenance of silencing of the element through cellular generations, indicating that, like for silencing establishment, its maintenance depends on the transposition environment, rather than the presence of 2 or 3 *tj1* copies (Figures 3.12A-D and 3.7E,F).

Three examples of PMG low adhesion plates for the maintenance assay are shown in Figure 3.12E.



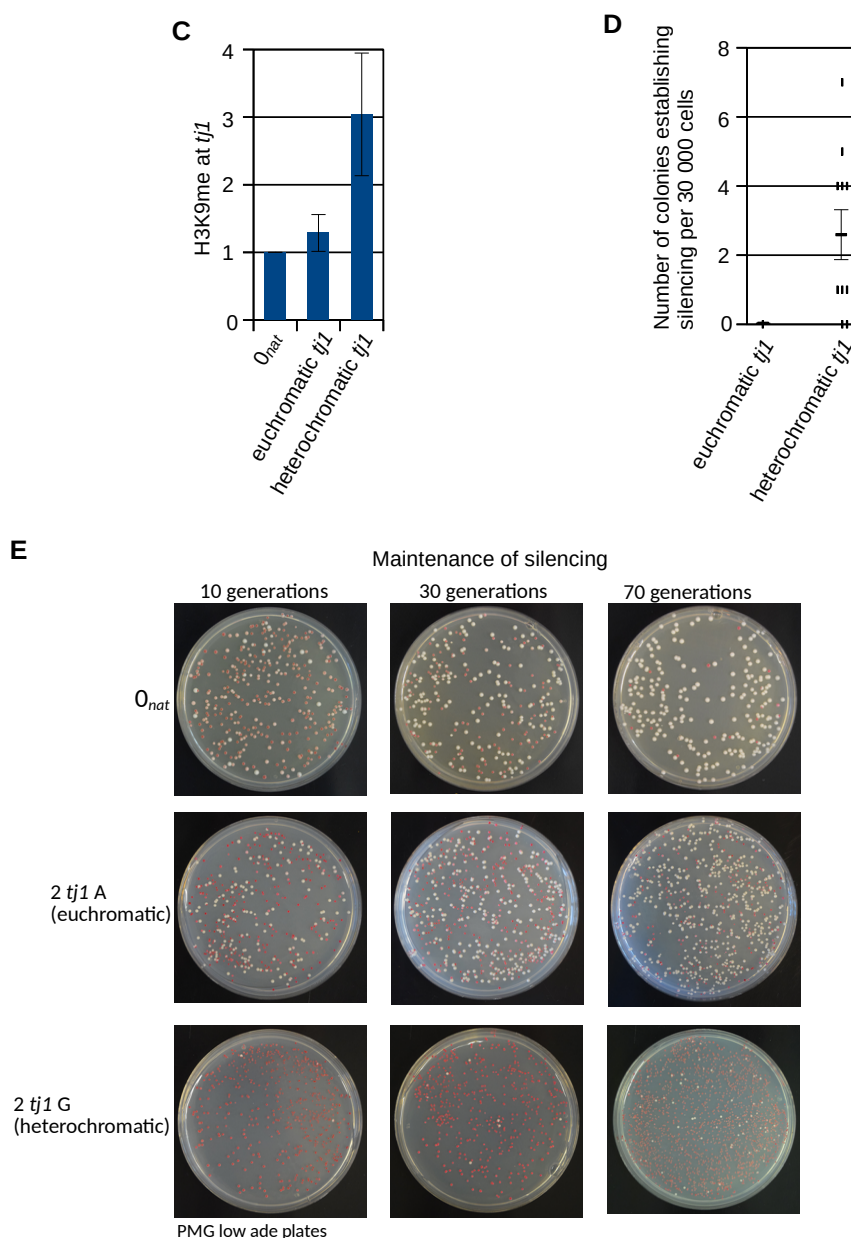


Figure 3.12: Cells maintain *tj1* silencing through generations more efficiently when the element transposes close to heterochromatin.

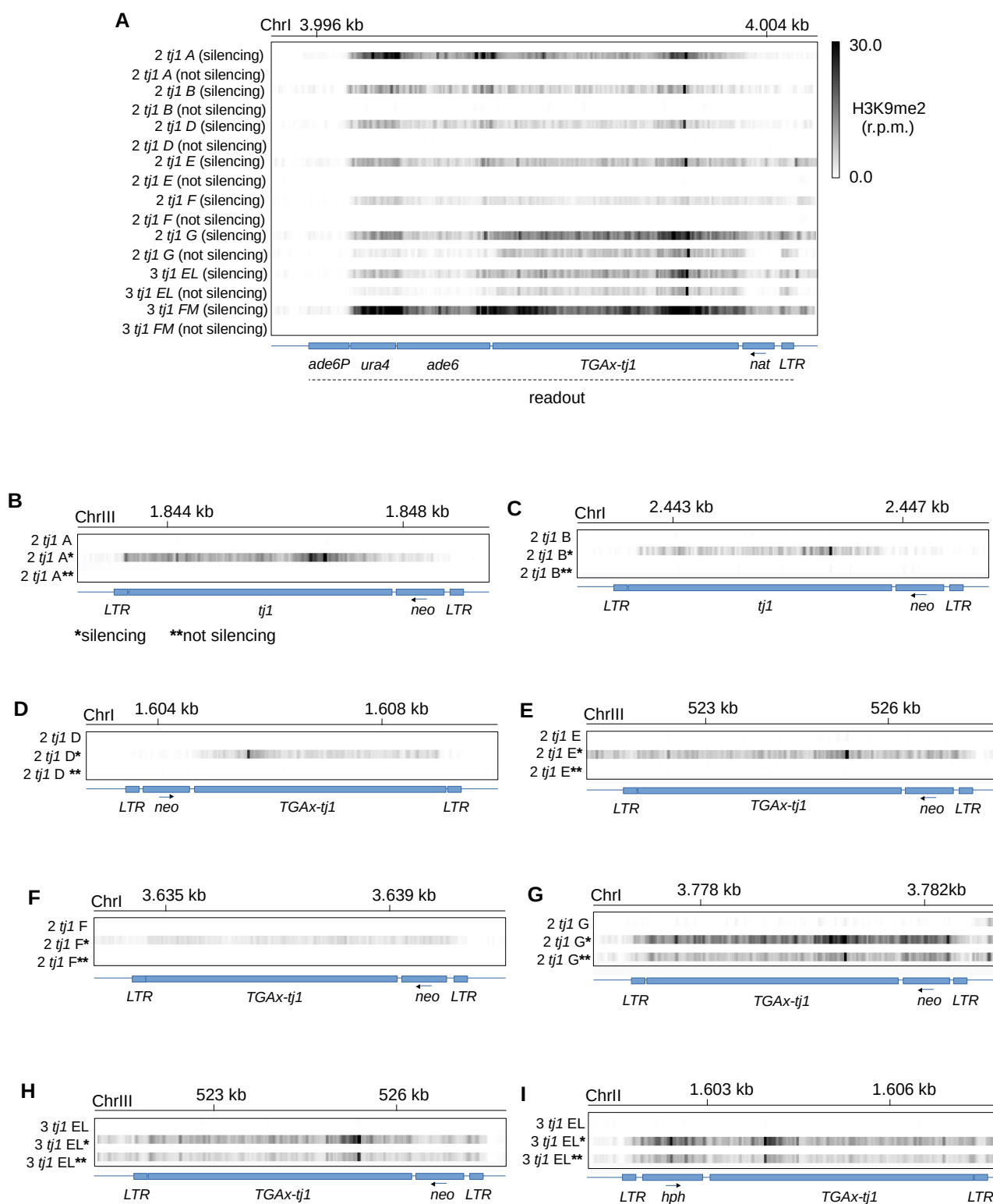
(A) Silencing maintenance through generations assay; starting from stably red colonies, % of red colonies counted on PMG low ade after 10, 30 and 70 generations, in indicated strains. Error bars represent s.e.m of at least 2 independent experiments. **(B)** Silencing maintenance through generations assay averaging euchromatic and heterochromatic *tj1* transposition strains. Error bars represent s.e.m of at least 4 independent experiments. **(C)** H3K9me2 average in cell populations of indicated colony groups. Quantification made by H3K9me2-ChIP sequencing (normalized to background), over strain 0_{nat} . Error bars indicate s.e.m of at least 2 independent experiments. **(D)** With horizontal lines, average silencing establishment in indicated colony groups. Single vertical points represent the single data point used for the average (see Figure 3.7 for more details). Error bars indicate s.e.m. of at least 2 independent experiments. **(E)** Examples of three PMG low ade plating for the maintenance assay. 0_{nat} , euchromatic “2 *tj1* A” and heterochromatic “2 *tj1* G” are shown.

3.12 Locus independent *trans*-silencing of all endogenous *tj1* copies

The observation that on average H3K9 methylation in silencing colonies is present at the readout and *tj1* copies, independently to their euchromatic or pericentromeric transposition loci (Figure 3.11B), suggests that once silencing is established, all the *tj1* elements are silenced independently to their locations, via a *trans*-acting mechanism. If silencing of the *tj1* copy at the readout region is easily detectable by red pigmentation of cells grown on PMG low ade plates, silencing of transposed copies can only be detected through molecular experiments. Therefore, H3K9me2-ChIP and RNA transcription experiments of all “2 *tj1*” and “3 *tj1*” strains, of silencing (red) and not silencing (white from the red), were singularly analyzed. As expected, all silencing colonies present H3K9 methylations at the readout locus, observable at *ura4* and *nat* unique regions (Figure 3.13A). *ade6* at readout doesn't represent a unique sequence, due to the endogenous *ade6M210* which differs from *ade6* only for a single nucleotide mutation and therefore indistinguishable one to another when deep sequencing reads are annealed to the genome. This ends with an assignment of 50% of reads to *ade6* and 50% of reads to *ade6M210*, however, it is expected that the majority of H3K9me2 reads come from the readout *ade6*. Being *ade6* fused to *ura4*, a good estimation of the amount of H3K9me2 at *ade6* is indicated by H3K9me2 present at the neighboring *ura4* sequence (Figure 3.13A). *tj1* is not a unique sequence either, being present at all loci (readout and transposed copies) with sequence differences of maximum one nt, dependently on the presence or absence of the *gag* stop codon (TGA/GGA, see Table 3.1). For this reason, as well as for *ade6/ade6M210*, also *tj1* deep sequencing reads are equally distributed among the *tj1* copies, therefore represented on IGV as an average of all *tj1* copies. The observation of all specific transposition loci, shows that H3K9me2 is deposited in all *tj1* elements (although with different levels, see unique sequences *neo* and *hph*), independently to the insertion environment and the total number of *tj1* copies (Figures 3.13 B-L). As observed before, not only pericentromeric “2 *tj1* G” silencing colony loses silencing specifically at the readout when cells revert to white (not silencing) (Figures 3.11 C,D and 3.11A,G), but also the other pericentromeric *tj1* strain, “3 *tj1* EL” maintains silencing specifically at the transposed copies (Figures 3.11 H,I), losing most of it at the readout (Figure 3.13A). On the other hand, all the other strains, passing from red to white, lose silencing completely in all loci, independently to the number of *tj1* copies, as shown by “3 *tj1* FM” not silencing, that loses completely H3K9me2, identically to all the other euchromatic “2 *tj1*” strains (Figure 3.13). These results indicate, again, that position of transposition in the genome is important, not only for recognition of the TE but also for the stability of its silencing (see H3K9me2 quantification in Figure 3.13L).

Moreover, these results show that all *tj1* elements are silenced, via a *trans*-acting mechanism. Although it is not possible to determine if cells silenced first the transposed copies and afterward, in *trans*, the copy at the readout, it is possible to speculate so, considering that cells establish silencing only when either plasmids are present or *tj1* transposed close to pericentromeric heterochromatin,

suggesting that silencing at the readout is the result of a *trans* silencing mechanism established at other *tj1* elements.



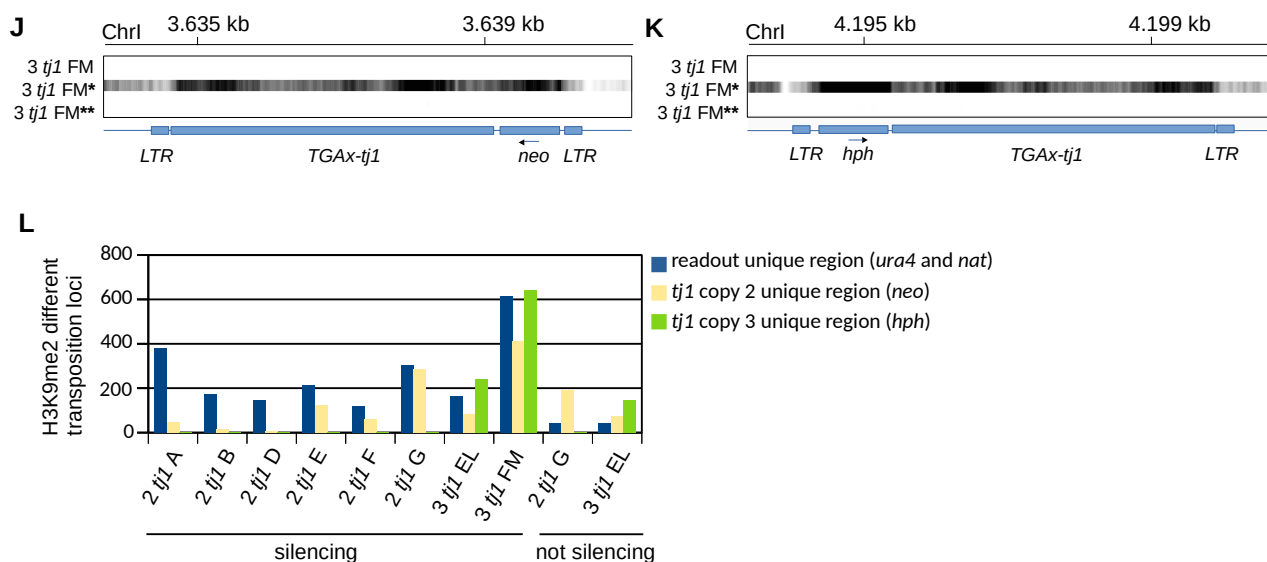
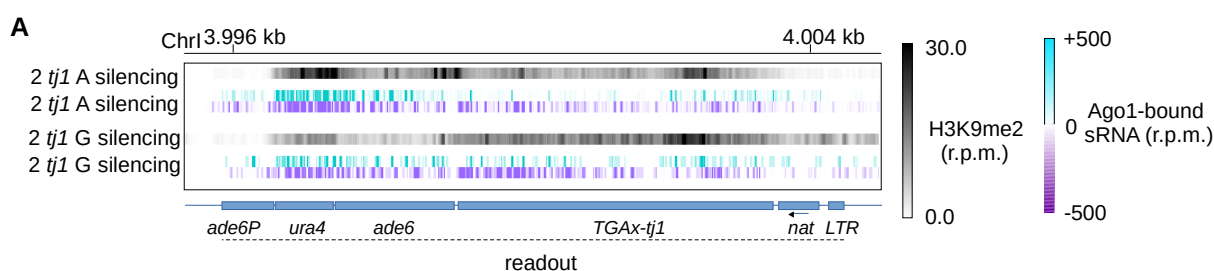


Figure 3.13: In silencing colonies, H3K9me2 is deposited in all *tj1* elements.

(A) H3K9me2 IGV tracks of all silencing (red) and not silencing (white from red) colonies, at readout locus. (B-K) H3K9me2 IGV tracks of indicated colonies, at specific transposition loci (*silencing colony) (**not silencing colony). (A-K) H3K9me2 is represented on black gradation scale, normalized to background and per one million reads (r.p.m.). (L) H3K9me2 quantification at unique regions in indicated colonies (normalized to background).

As shown in section 3.5, sRNAs mediate H3K9me deposition at readout locus in the strain without transpositions 0_{neo} (Figure 3.5A), therefore we wondered whether H3K9 methylation is a process guided by sRNAs also in strains with genomic *tj1* transpositions. Ago1 of “2 *tj1* A” and “2 *tj1* G” was tagged with 3XFLAG epitope and Ago1-bound sRNAs were analyzed in silencing cells. sRNAs are found not only at readout locus (*ura4*, *nat*) but also at the specific *tj1* transposed copy (*neo*) in both strains, indicating that cells repress *tj1* with a *trans* silencing mechanism sRNA-guided (Figures 3.14A-C). Figure 3.14D shows *dh* and *dg* repeats at chrI as Ago1-bound sRNA control for the strain “2 *tj1* A”. Notice the proximity of *tj1* to *dg* and *dh* repeats in the strain “2 *tj1* G” (Figure 3.14C).



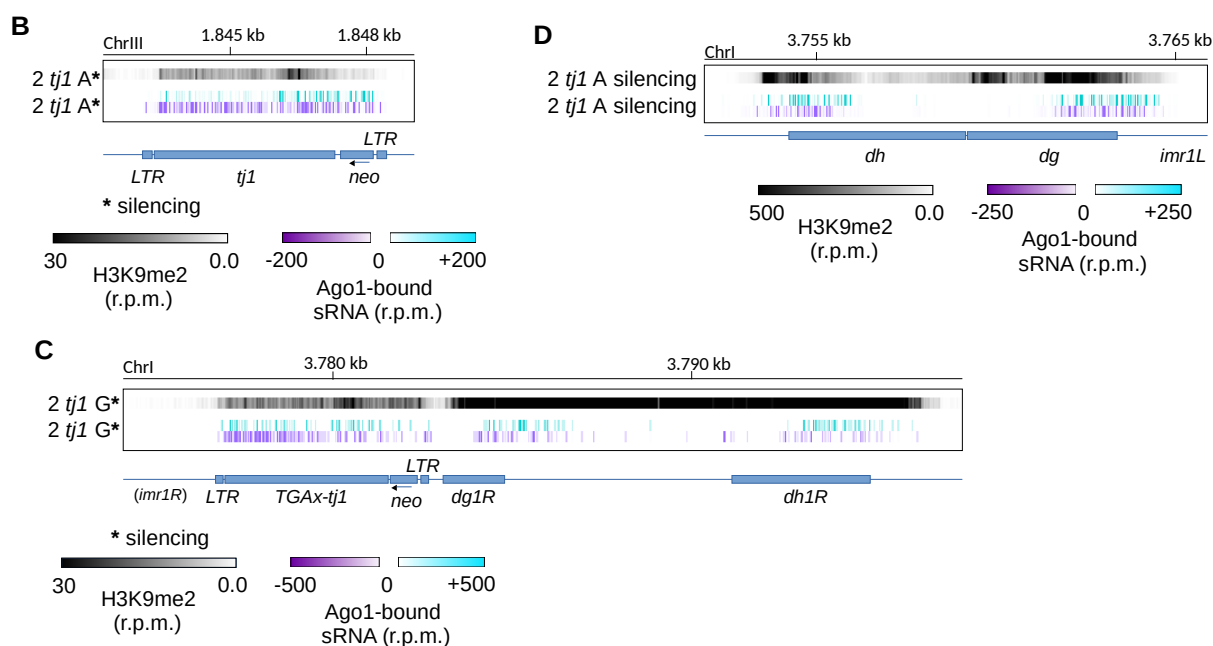


Figure 3.14: Ago1-bound sRNAs guide *trans* silencing of all *tj1* elements.

(A) H3K9me2 and Ago1-bound sRNAs IGV tracks of “2 *tj1* A” and “2 *tj1* G” silencing colonies, at readout locus, (B) at transposed *tj1* copy of “2 *tj1* A” and (C) at *tj1* copy of “2 *tj1* G”. (D) *dh+dg* repeats at chrI in the indicated strain. (A-D) H3K9me2 is represented on black gradation scale, normalized to background and per one million reads (r.p.m.). Positive and negative Ago1-bound sRNAs strands are normalized per one million reads and depicted in light-blue and purple gradations, respectively.

Moreover, in “2 *tj1* A” silencing colony, *trans* acting sRNAs are present also at the endogenous *ade6M210* locus (Figure 3.15A), as indicated by secondary sRNAs at flanking *bub1* gene, similarly to 0_{neo} silencing cells (Figure 3.5C). An analysis of all strains shows that H3K9me2 is deposited at genes flanking *ade6M210* in all silencing colonies, suggesting a common *trans* silencing mechanism at *ade6M210* locus guided by sRNAs generated at *ade6* of readout locus (Figure 3.15B). However, as observed for 0_{neo} silencing cells (Figure 3.5C), on average H3K9me2 at *ade6M210* is not enough to repress transcription of neighboring *bub1* and *vtc4* genes (Figure 3.15C). Figures 3.15D,E show that Ago1-bound sRNAs from “2 *tj1* A” and “2 *tj1* G” silencing colonies have typical U bias at 5' end and a preferred length range of 21-24 nucleotides, comparable to the wild-type *S. pombe*. Altogether, these results show that sRNAs are found at readout, at transposed *tj1* and at the endogenous *ade6M210* loci, where they guide silencing of the regions through *trans* H3K9me2 deposition (Figures 3.14A,B and 3.15A). Interestingly, *trans* silencing of *ade6M210* generates secondary sRNAs at neighboring *bub1* gene, although H3K9me2 is not highly deposited and *bub1* transcription is not affected (Figures 3.4C and 3.15A-C).

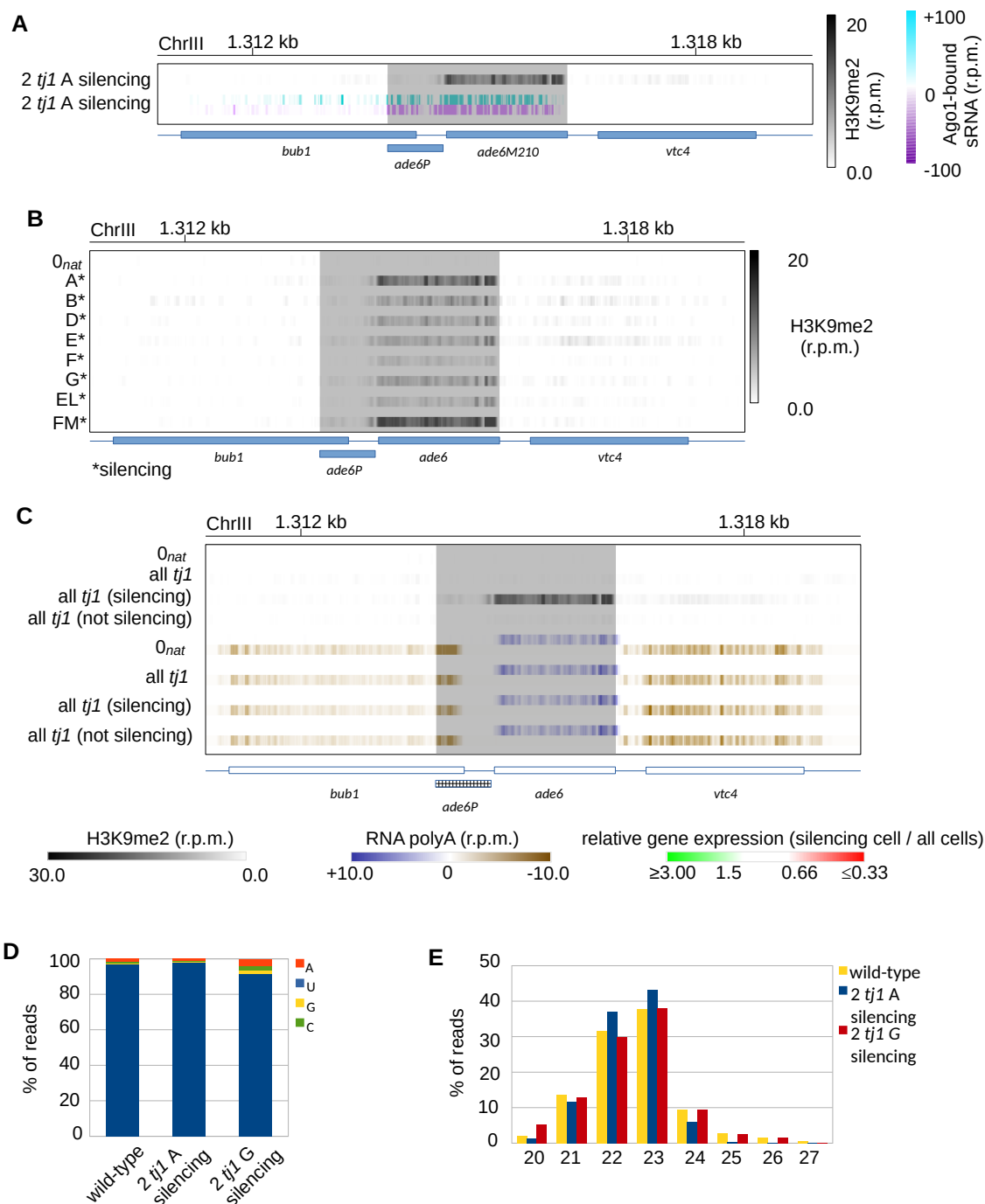


Figure 3.15: Ago1-bound sRNAs guide *trans* H3K9me2 deposition at endogenous *ade6M210*.

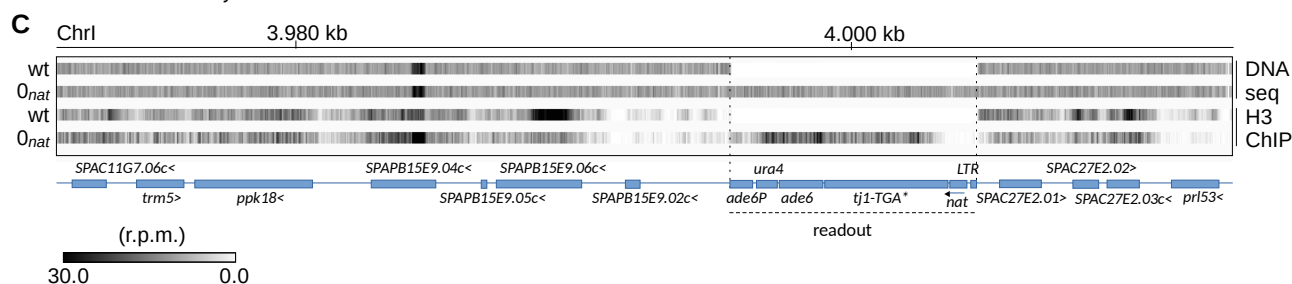
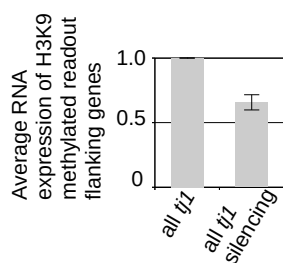
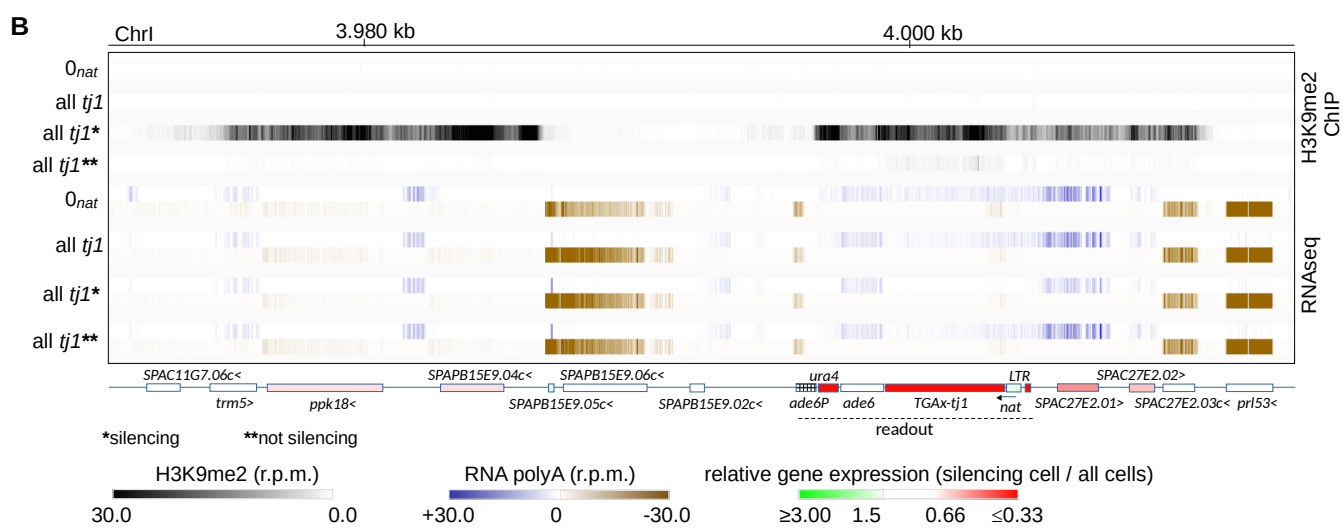
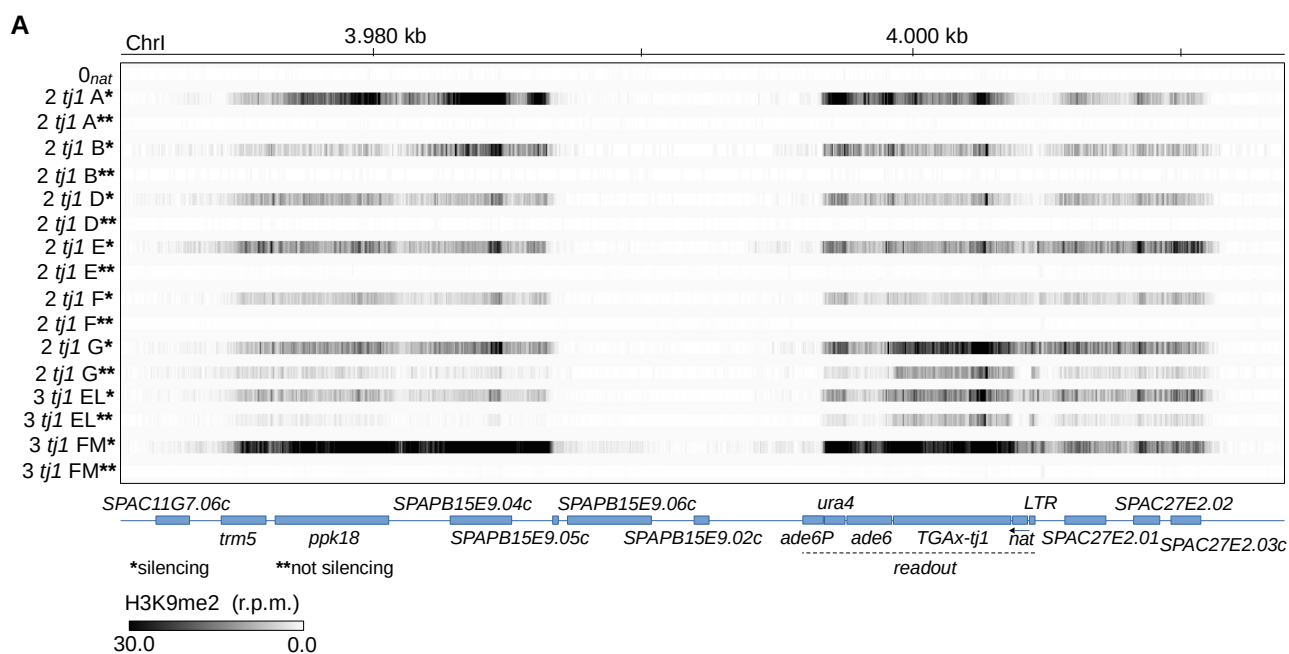
(A) H3K9me2 and Ago1-bound sRNAs IGV tracks of “2 *tj1* A” silencing colony, at *ade6M210* locus. H3K9me2 is represented on black gradation scale, normalized to background and per one million reads (r.p.m.). Positive and negative Ago1-bound sRNAs strands are normalized per one million reads and depicted in light-blue and purple gradations, respectively. (B) H3K9me2 of all strains in silencing colonies, at *ade6M210* locus. Scale and normalization as in A. (C) Average H3K9me2 of all silencing, not silencing and indicated strains at *ade6M210* locus. On black gradation scale H3K9me2 is represented, normalized per one million reads (r.p.m.). RNA-polyA + and – strands are normalized to coding sequences (cds) and represented in dark-blue and brown gradations, respectively. The relative gene expression is indicated with red to green gradation and calculated as ratio between cds normalized RNA-polyA reads of silencing and population cells (all *tj1*). Ade6P is represented as hatched box. (D) 5’ end nucleotide preference of Ago1-bound sRNAs in indicated strains. (E) Length distribution of Ago1-bound sRNAs in indicated cells.

3.13 H3K9me2 spreads to *tj1* neighboring regions

A wider analysis of readout locus in silencing colonies shows that H3K9me2 spreads to neighboring regions, following a profile common to all strains (Figure 3.16A). This result indicates that, at the readout locus, heterochromatin nucleates at *tj1* element and expands to neighboring genes, up to -25kb and -7kb, of 5' and 3' flanking regions, respectively. Interestingly, all not silencing (white from red) colonies lose completely H3K9me2, not only at the readout as observed before (Figure 3.13A) but also at the flanking regions, with the exclusion of pericentromeric transposition strains “2 *tj1* G” and “3 *tj1* EL”, where H3K9me2 at neighboring genes is still present (Figure 3.16A). This suggests again that in pericentromeric strains, not silencing cells lost silencing specifically at the readout as a result of white selection, while regions flanking the readout are maintained H3K9 methylated.

Next, we wondered if transcription of neighboring genes is affected by their H3K9 methylation. Considering that all strains showed a similar H3K9me2 profile at readout flanking regions, it was possible to study RNA transcription as the average of all strains (Figure 3.16B). On average, H3K9 methylated genes are repressed -30% compared to the cell populations (graph in Figure 3.16B). However, some heterochromatic genes are not repressed (i.e. *SPAC11G7.06c*, *trm5* and *SPAC27E2.03c*) (Figure 3.16B). Different hypotheses can explain this outcome; (i) genes that are very highly transcribed, can't be efficiently silenced through this H3K9 methylation level, like *SPAC27E2.03c*. (ii) Contrarily, genes which expression is already very low in cell population, can't be repressed more when H3K9me2 is present, as the case of *SPAC11G7.06c*. For the same reason, the slight increase in transcription of sense *nat* in silencing colonies, compared to cell population, may be an artifact of the low transcription of the gene already observed in the population. *ade6* transcriptional analysis reflects the transcription of both *ade6* at the readout and the endogenous *ade6M210*, therefore it can't be considered as a specific analysis of *ade6* at the readout locus, but as an average of the two genes. Interestingly, H3K9me2 is almost completely absent in all silencing strains between *ade6P* and *SPAPB15E9.05c*, for a total of -8kb long DNA (Figures 3,16A,B). To try to explain this methylation “gap”, we first controlled by DNA sequencing that this region was not eliminated during the readout cloning. As shown in Figure 3.16C, the all DNA region is present, therefore excluding the loss of any DNA part. Then, we performed an H3-ChIP sequencing on 0_{nat} to see if in that DNA region H3 histones were depleted. Our results show that the first -4kb of DNA upstream *ade6P* are scarce in H3 occupancy (Figure 3.16C). However, an H3-ChIP of a wild-type strain, shows a very similar H3 pattern, indicating that the first -4kb of DNA upstream *ade6P* are “naturally” H3 poor and not the consequence of our genome manipulation. This would explain the low H3K9me2 observed in the first -4kb upstream *ade6P*, probably as the result of low H3 density, rather than an actual H3K9me2 depleted region. On the other hand, the rest of the H3K9me2 poor region doesn't show scarce H3 occupancy, indicating that that region is truly methylation depleted (Figure 3.16C). A closer look at RNA transcription of the genes of that region, *SPAPB15E9.05c* and *SPAPB15E9.06c*, shows that these two genes are highly transcribed (Figure 3.16B), suggesting that for this reason they

may be refractory to H3K9 methylation and work as heterochromatin boundaries (Keller et al. 2012b; Rougemaille et al. 2012; Hayashi et al. 2012; Keller et al. 2013a). Similarly, *prl53* at 3' readout flanking region is highly transcribed and poor in H3, therefore it may work as an H3K9me2 border (Figures 3.16B,C). *nat* and LTR regions present low H3 as well, explaining the overall poorer H3K9me2 of these regions, compared to other parts of the readout, like *ura4* (readout unique gene) (Figures 3.13A and 3.16A). H3 analysis of strain "2 *tj1* A" at transposition locus, shows the absence of H3 histones at LTRs, indicating that the LTR sequence of *tj1* is refractory to H3 presence when integrated into the *S. pombe* genome (Figure 3.16D). Furthermore, the nucleosome absence at LTRs of transposed *tj1* doesn't depend on the repression state of the element (Figure 3.16D). Studies on fission yeast showed that *clr4* mutants present Nucleosome-Free Regions (NFRs) at pericentromeric repeats, mating-type and subtelomeric loci, otherwise absent in wild-type cells, suggesting that Clr4 inhibits the formation of NFRs facilitating the H3K9 methylation of those regions (Garcia et al. 2010). On the other hand, at pericentromeric repeats and mating-type locus, some sequences refractory to nucleosome depletion in *clr4* Δ were observed, consisting in a tRNA cluster and an IR repeat respectively, indicating that some regions are resistant to nucleosome occupancy (Garcia et al. 2010). Therefore, LTRs of *tj1* may be refractory to nucleosomes, independently to the chromatin presence of the heterochromatin machinery, similarly to tRNAs and IRs (Figure 3.16C,D). Interestingly, despite the different nucleotide sequence between *tj1* and *tf2* LTRs, *tf2* LTRs show poor H3 presence, suggesting that LTRs of *tj1* and *tf2* possess a conserved feature, sequence-independent, that makes them nucleosome-free (Figure 3.16E). Nucleosome remodelers play a role in positioning nucleosomes at *tf2* LTRs; in response to stress conditions nucleosomes appear less abundant at LTRs, resulting in the full-length *tf2* mRNA transcription, while in normal growth conditions, nucleosome occupancy over LTRs is slightly increased, generating the transcription of a truncated *tf2* mRNA unable to be retrotranscribed (Persson et al. 2016). Solo LTRs dispersed over the genome are H3 poor as well and, interestingly, they work as subtelomeric heterochromatin boundaries (Strålfors et al. 2011; Steglich et al. 2015). There, the recruitment of the chromatin remodeler Fun30 inhibits H3 deposition and the encroachment of euchromatic marks, such as histone acetylations and H2A.Z histone variant deposition, on subtelomeric heterochromatin (Strålfors et al. 2011; Steglich et al. 2015).



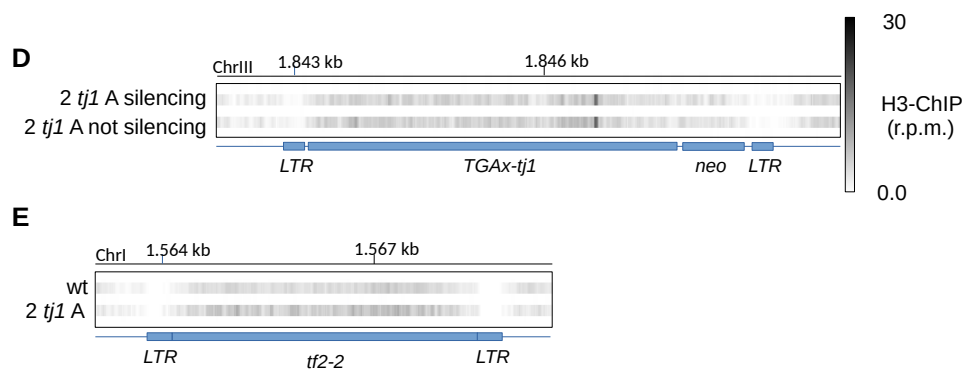
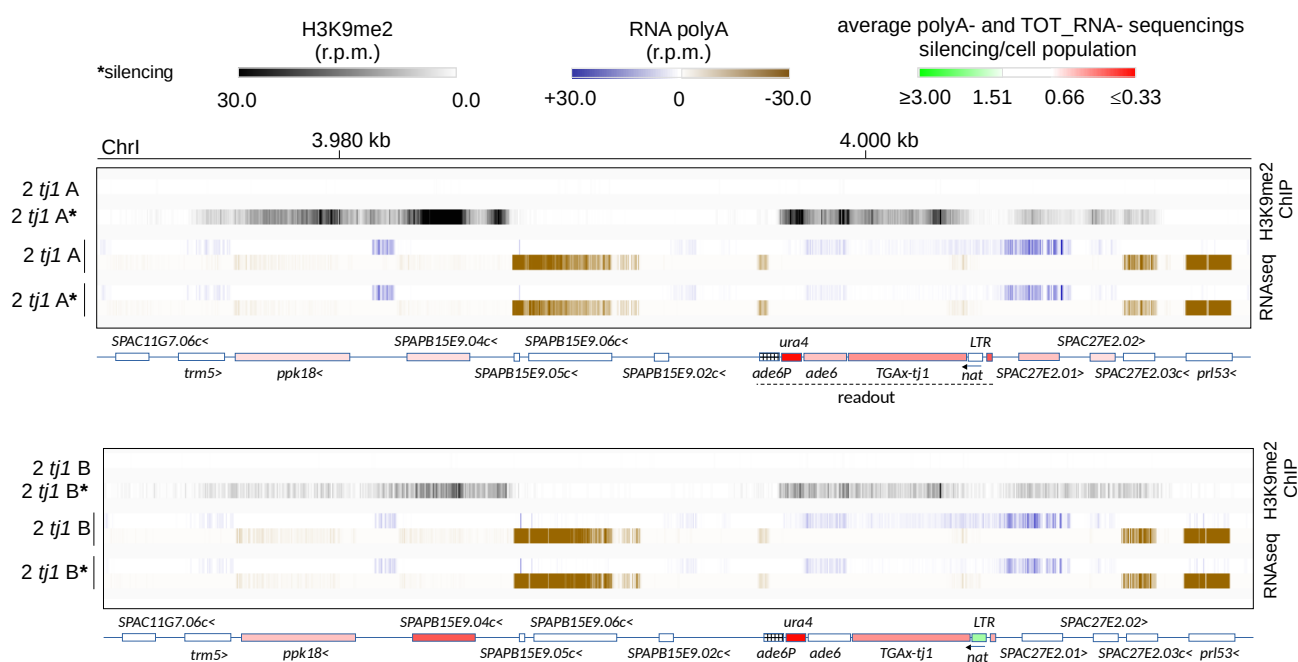
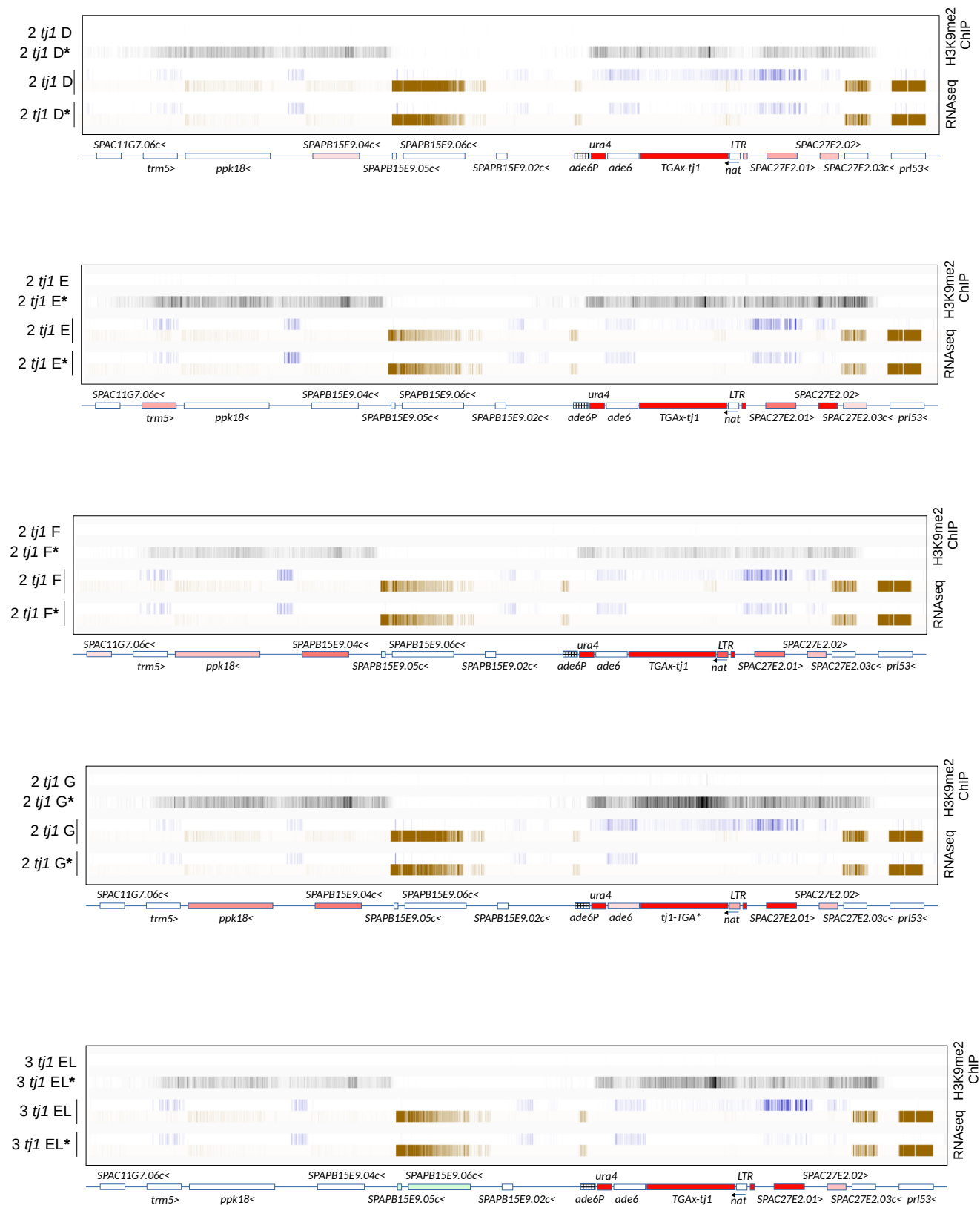


Figure 3.16: H3K9me2 spreads to readout flanking regions.

(A) H3K9me2 IGV tracks of 0_{nat} and all silencing and not silencing colonies, at readout and flanking regions. H3K9me2 is represented on black gradation scale, normalized to background and per one million reads (r.p.m.). **(B)** H3K9me2 and RNA-polyA averages of all strains, as population (all *tj1*), silencing and not silencing colonies. H3K9me2 normalized as in A. RNA-polyA + and – strands are normalized to coding sequences (cds) and represented in dark-blue and brown gradations, respectively. The relative gene expression is indicated with red to green gradation and calculated as ratio between cds normalized RNA-polyA reads of silencing and population cells (all *tj1*). Ade6P is represented as hatched box. **(C)** Average IGV tracks of DNA and H3-ChIP sequencings, in indicated strains. Scale is represented on black gradation (normalized per one million reads, r.p.m.). **(D)** H3-ChIP at transposed *tj1* of indicated colonies. Scale is represented on black gradation (normalized per one million reads, r.p.m.). **(E)** H3-ChIP at *tf2-2* element in indicated strains. Scale and normalization as in D.

H3K9me2, RNA-polyA and transcription ratio at readout flanking regions of each strain are represented in Figure 3.17. In general, a stronger H3K9me2 deposition at readout (see *ura4*), correlates with a stronger methylation of flanking regions, especially at 5' readout side, particularly evident in strains “2 *tj1* A” and “3 *tj1* FM”. In all strains, highly transcribed genes SPAPB15E9.05c, SPAPB15E9.06c and *prl53*, may act as H3K9me2 boundaries.





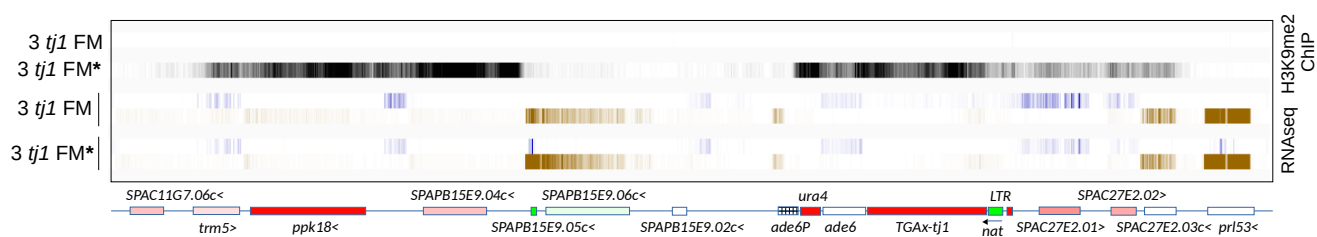
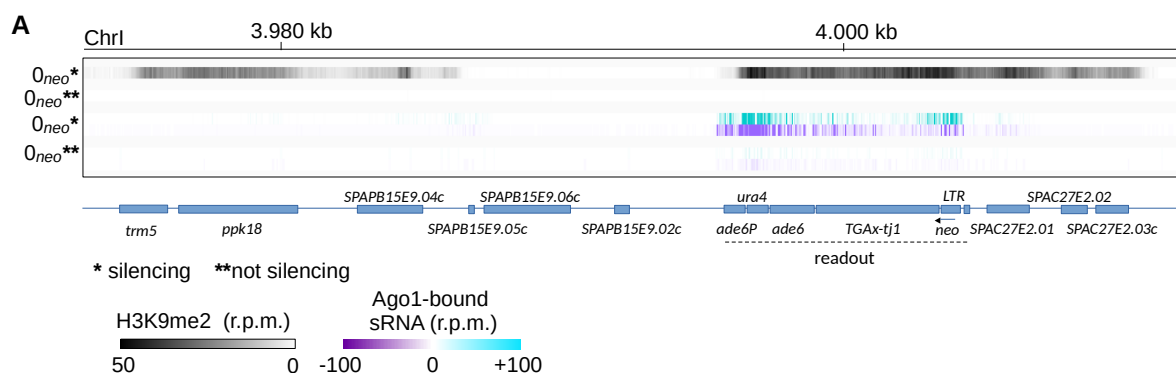


Figure 3.17: H3K9me2 spreading in all silencing colonies at readout flanking regions.

H3K9me2 IGV tracks of all silencing and population strains, at readout and flanking regions. H3K9me2 is represented on black gradation scale, normalized to background and per one million reads (r.p.m.). RNA-polyA + and – strands are normalized to coding sequences (cds) and represented in dark-blue and brown gradations, respectively. The relative gene expression is indicated with red to green gradation and calculated as ratio between cds normalized RNA-polyA reads of silencing and population cells. Ade6P is represented as hatched box.

The H3K9me2 spreading at readout flanking regions, made us wonder whether Ago1-bound sRNAs spread as well to neighboring genes. Ago1-bound sRNA sequencings of silencing 0_{neo} , “2 *tj1 A*” and “2 *tj1 G*” colonies show that sRNAs are weakly present at the readout H3K9 methylated flanking regions (Figure 3.18A,B), suggesting that H3K9 methylation of those regions is not primarily dependent on sRNAs, but rather on spreading of chromatin writers (i.e. Clr4) to those regions from the readout, where heterochromatin nucleates in an sRNA-dependent manner. 0_{neo} not silencing (white colony from a red colony), shows that weak residual Ago1-bound sRNAs are still present at the readout and flanking regions, however, the complete loss of H3K9me2 in these cells, indicates that these sRNAs are not enough to maintain the methylations at readout and consequently their spreading to the flanking regions (Figure 3.18A).



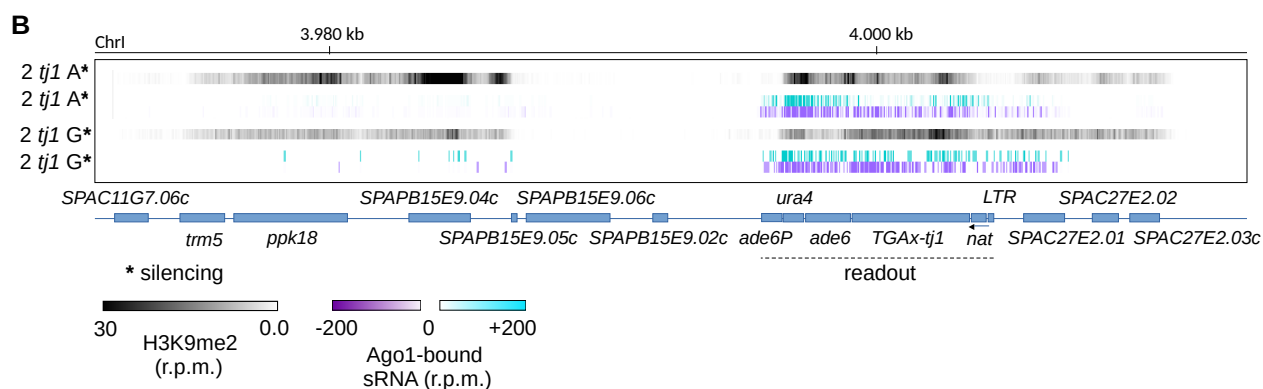


Figure 3.18: H3K9me2 spreading at readout is mostly sRNAs independent.

(A-B) H3K9me2 and Ago1-bound sRNA IGV tracks in indicated strains, at readout locus. H3K9me2 is represented on black gradation scale, normalized to background and per one million reads (r.p.m.). Positive and negative Ago1-bound sRNAs strands are normalized per one million reads and depicted in light-blue and purple gradations, respectively.

Other evidence of not only H3K9 methylation spreading, but also of *trans*-acting silencing mechanisms, were furnished when H3K9me2-ChIP sequencing was performed on silencing colonies carrying plasmids (p1281) (Figure 3.19A). The assay shows H3K9me2 deposition at *tj1* plasmid copy (*hph* plasmid specific sequence) and spreading of heterochromatin to the rest of all the plasmid sequence, in both “2 *tj1* G” and “2 *tj1* D” silencing colonies. The assay shows also that not silencing colonies lose completely H3K9me2 at *tj1*, but not completely at the rest of the plasmid, probability as the result of white selection and therefore of induction of silencing loss at the readout and, in *trans*, at *tj1* in the plasmid. However, as shown previously, white colonies from silencing “2 *tj1* G”, selectively lose silencing at the readout, but not at the transposed *tj1* element (Figures 3.11 and 3.13), while in this assay “2 *tj1* G” (with plasmids) not silencing loses almost completely H3K9me2 at the transposed pericentromeric *tj1* (*neo*) (Figure 3.19B), completely at *tj1* in the plasmid (*hph*) (Figure 3.19A), and not only at readout (*nat*) (Figure 3.19C). A possible explanation is that the silencing of the all plasmid sequence represses transcription of *LEU2* and therefore negatively selects for colonies that silence *tj1*. In fact, cells couldn’t lose the plasmids, due to the experimental growth conditions in this assay, where cells analyzed by H3K9me2-ChIP were grown to see methylation on plasmid copies, therefore, when white colonies (not silencing) were selected, a general loss of H3K9me2, rather than readout specific, was induced, resulting in H3K9me2 depletion at all *tj1* elements. Another experiment supported the idea that the spreading of H3K9me2 in plasmids, specifically at *LEU2*, selects against *tj1* silencing; A red colony of 0_{neo} + plasmids (p1076) was selected, propagated keeping the plasmids (liquid PMG - leu), plated in PMG low ade (-leu) (-1000 cells), a red was selected again, propagated and plated again in PMG low ade, repeating this red selection six times. The % of red colonies in PMG low ade (-leu) plates doesn’t increase along with the red selections, but shows an up and down profile, suggesting that it is not possible to enrich for red colonies if the plasmids are present, due to two events in

opposition: silencing of *tj1* (and *LEU2*) and active transcription of *LEU2* in order to grow in -leu media (Figure 3.19D).

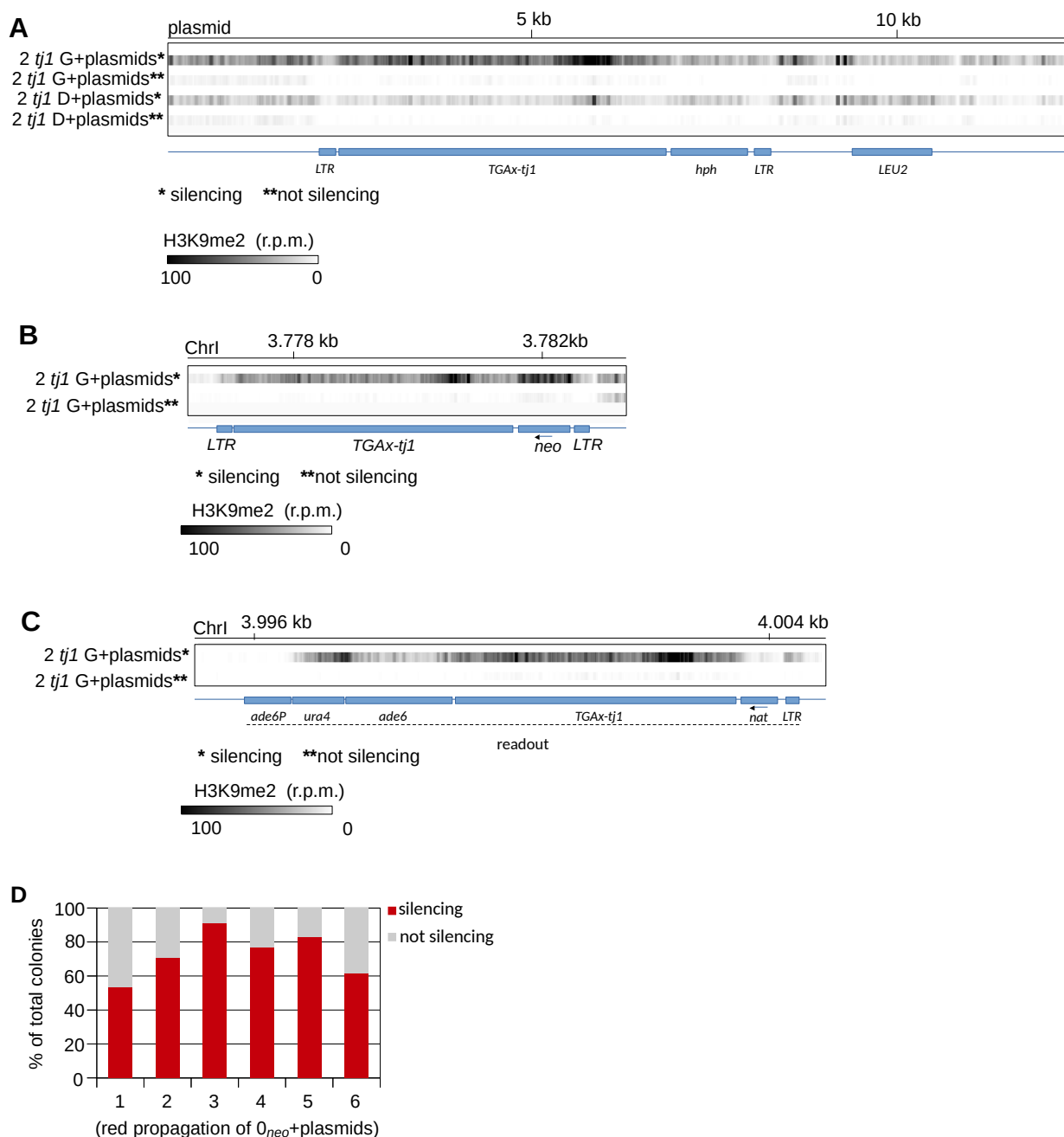


Figure 3.19: Trans H3K9 methylation and heterochromatin spreading in plasmids.

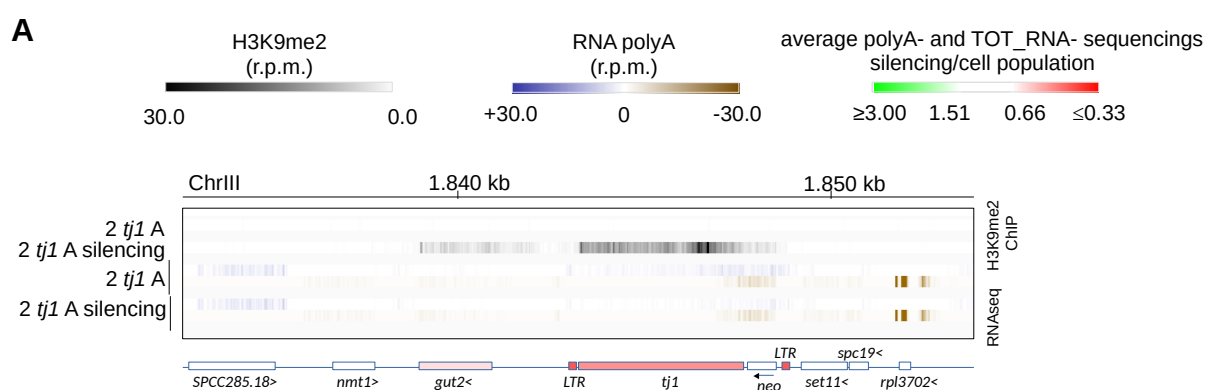
(A-D) H3K9me2 IGV tracks in indicated strains, over plasmids (A), at transposed *tj1* element (B) and at readout locus (C). H3K9me2 is represented on black gradation scale, normalized to background and per one million reads (r.p.m.). (D) Red cells propagation of 0_{neo+} plasmids. A red colony with plasmids was selected, grown and plated in PMG low ade (~1000 cells), a red cell was selected again, grown and plated again (for a total of 6 times). The % of red colonies in each low ade plate was counted.

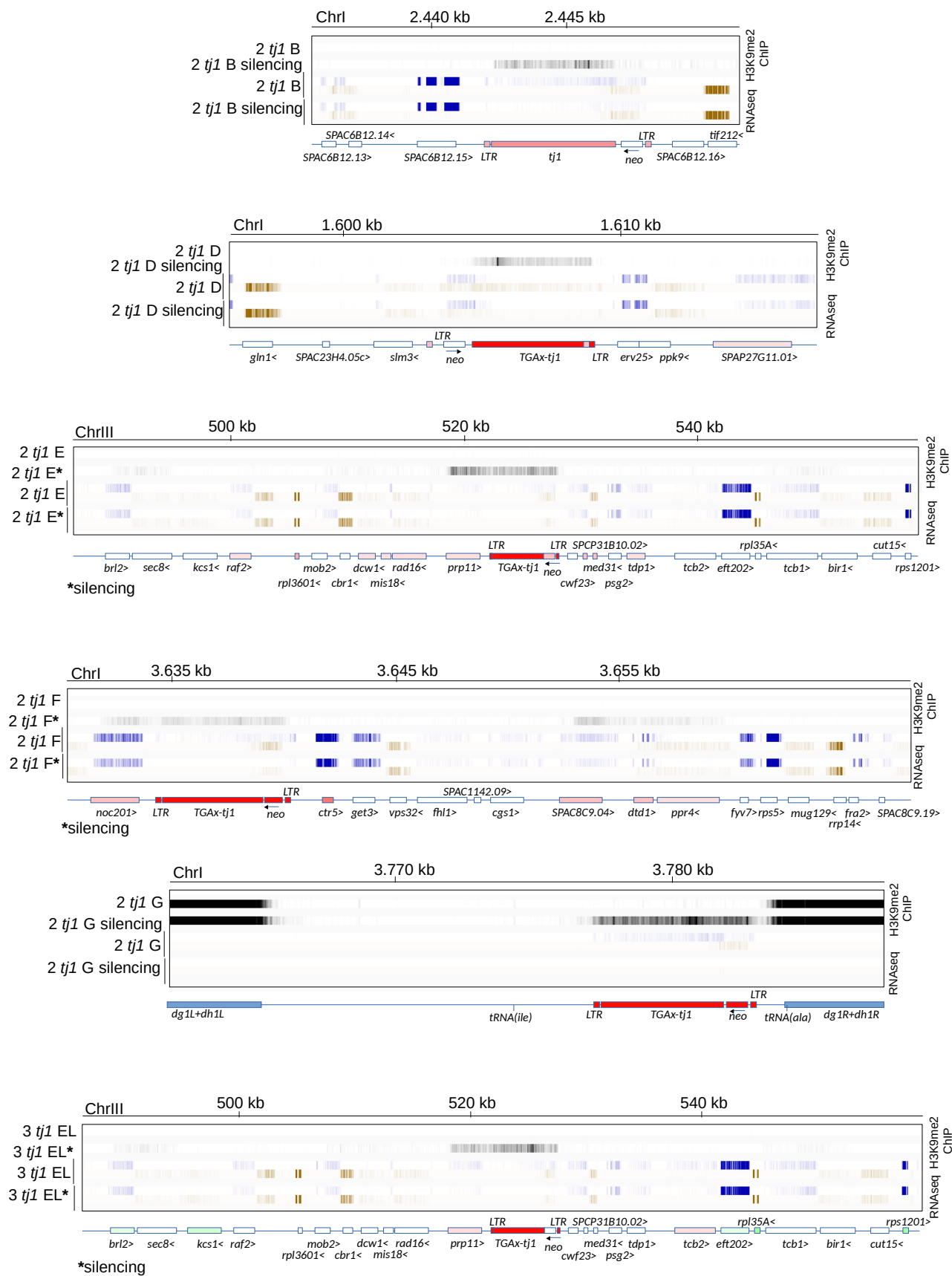
At this point, we wondered if H3K9me2 spreads to the loci where *tj1* transposed. In figure 3.20A, IGV tracks of H3K9me2, RNA-polyA and transcription ratio (between silencing and population cells) of all strains at transposition loci and flanking regions, are represented. Some of the silencing strains show H3K9me2 spreading from the transposed copies to flanking DNA regions (“2 *tj1* A, E, F” and “3 *tj1* EL, FM”). Similar to what was observed at readout locus, H3K9me2 at transposed copies “jumps” from *tj1* to the neighboring genes, leaving H3K9 methylation-free regions (specially evident in strains “2 *tj1* F” and “3 *tj1* FM”). At the readout locus these “gaps” could be explained by the presence of highly transcribed genes and nucleosome poor regions, therefore we first analyzed the H3 occupancy at the flanking regions of all transposition loci. The results showed the absence of H3 poor regions in all the flanking regions (data not shown), indicating that the H3K9 methylation “jumps” at these loci are not due to H3 depletion. Thus, we analyzed the transcription levels of the flanking genes in cell populations (before silencing), grouping the genes according to their positions with respect to the H3K9me2 spread found in the silencing colonies. We obtained three gene groups; “border genes” (first genes immediately downstream or upstream the H3K9me2 borders), “heterochromatic genes” (H3K9 methylated genes) and “gap genes” (genes with no H3K9me2 between border genes). Our analysis shows that on average genes at the heterochromatin borders (and at the gaps) are -2 fold more transcribed than the genes that will be heterochromatic, suggesting that the first may work as a barrier to the H3K9me2 spreading (Figure 3.20B).

To estimate the silencing effects of flanking H3K9 methylated regions in strains “2 *tj1* A, E, F” and “3 *tj1* EL, FM”, all heterochromatic genes were grouped and their RNA transcription was analyzed, compared to cell populations. The results show that, on average, H3K9 methylated genes are -30% down-regulated, compared to cell populations, indicating that heterochromatinization of flanking regions has a substantial function in repressing neighboring genes (Figure 3.20C).

“3 *tj1* EL” silencing maintains some H3K9me spreading at euchromatic locus *tj1* copy, when converts to white (Figure 3.20D), the only case among euchromatic transposed *tj1* copies (data not shown for the other strains).

It is possible to notice the proximity to pericentromeric heterochromatin of *tj1* transposition in strain “2 *tj1* G” and the second transposition (*tj1* with *hph* cassette) in “3 *tj1* EL” (Figure 3.20A).





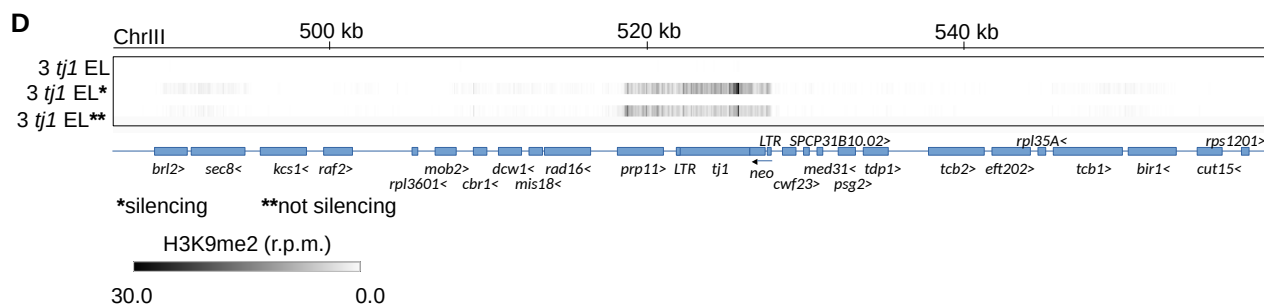
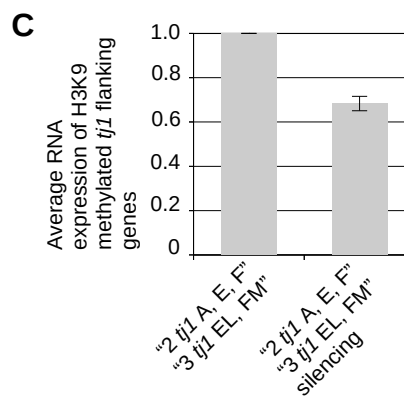
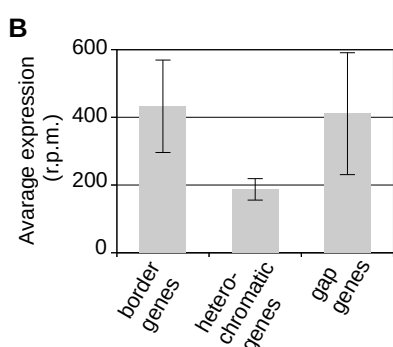
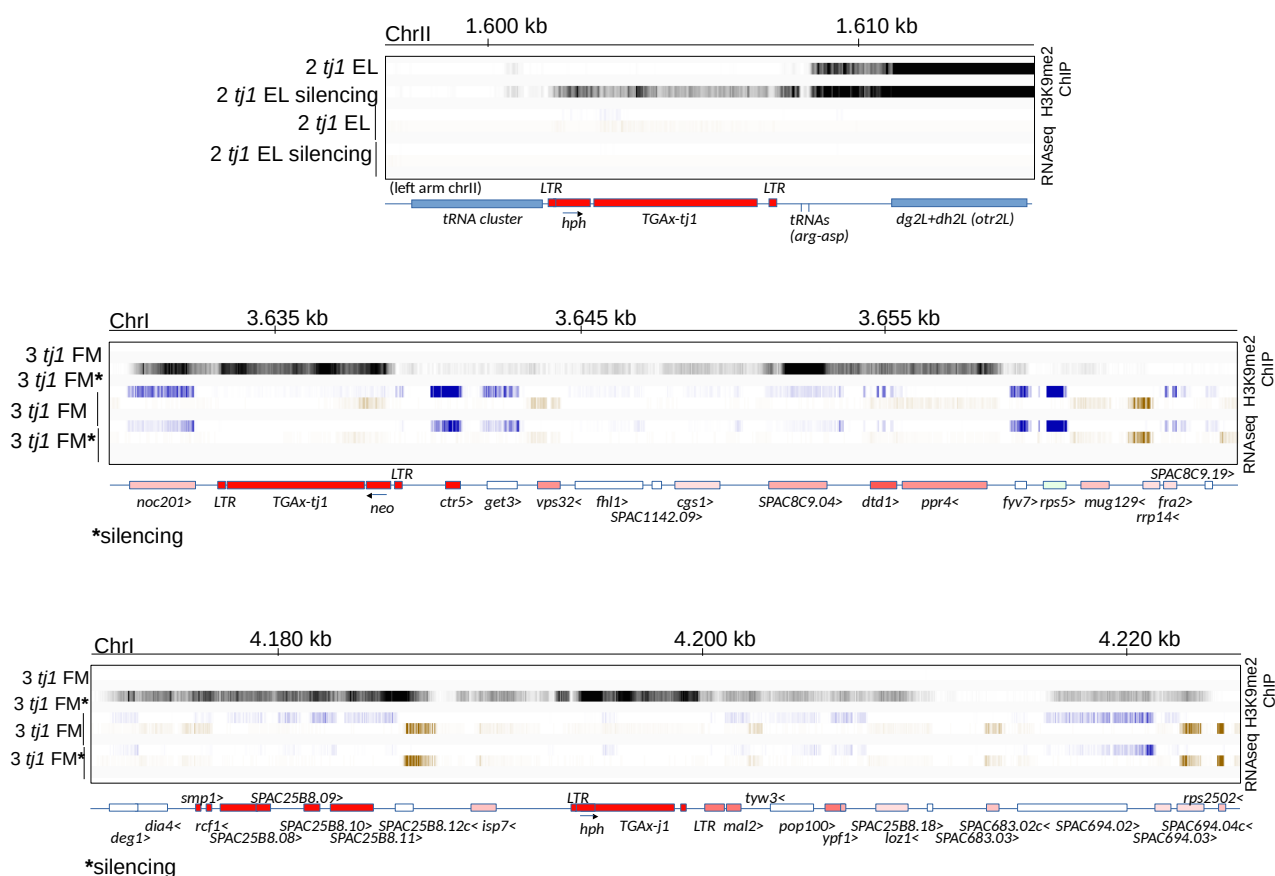
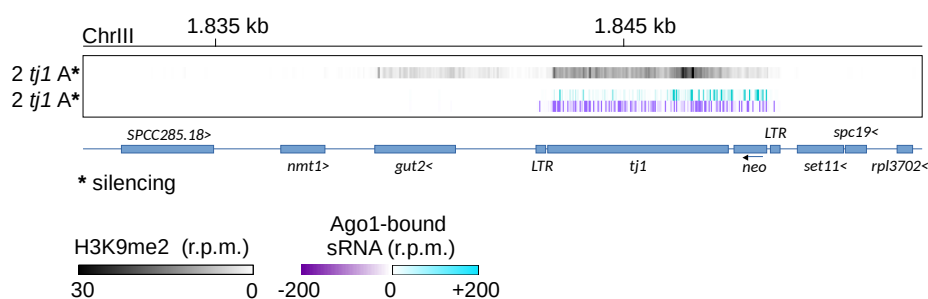


Figure 3.20: H3K9 methylation spreading in flanking regions of transposed *tj1* elements.

(A) H3K9me2 and RNA-polyA IGV tracks of all silencing and population strains, at specific *tj1* transposition loci and flanking regions. H3K9me2 is represented on black gradation scale, normalized to background and per one million reads (r.p.m.). RNA-polyA + and – strands are normalized to coding sequences (cds) and represented in dark-blue and brown gradations, respectively. The relative gene expression is indicated with red to green gradation and calculated as ratio between cds normalized RNA-polyA reads of silencing and population cells. (B) Transcription of flanking genes in the indicated gene groups. Data from polyA and total RNA sequencings, normalized per million reads. Error bars represent s.e.m. of two independent experiments. (C) Average of RNA expression of H3K9 methylated *tj1* flanking genes in indicated silencing strains, compared to cell populations. Quantification from average of RNA-polyA and total RNA sequencings. Error bars indicate s.e.m of 10 independent experiments (normalized to cds). (D) H3K9me2 IGV tracks of EL strain in indicated colonies, at euchromatic *tj1* transposed copy. Scale and normalization as in A.

Finally, we wondered whether heterochromatin spreading at transposed *tj1* copies is a sRNA-mediated process. Ago1-bound sRNAs of silencing strain “2 *tj1* A” show that H3K9 methylated gene *gut2*, doesn’t present sRNAs, therefore suggesting that spreading of heterochromatin from transposed *tj1* to *gut2* is an sRNA-independent process (Figure 3.21), similarly to what observed at readout locus, where sRNAs were only weekly present (Figure 3.18).

**Figure 3.21: H3K9 methylation spreading in flanking region at transposed *tj1* element is sRNA-independent.**

H3K9me2 and Ago1-bound sRNA IGV tracks in indicated strain, at *tj1* transposition locus. H3K9me2 is represented on black gradation scale, normalized to background and per one million reads (r.p.m.). Positive and negative Ago1-bound sRNAs strands are normalized per one million reads and depicted in light-blue and purple gradations, respectively.

3.14 Establishment and maintenance of *tj1* silencing are RNAi-dependent

Our initial analysis indicated that, on average, all “2 *tj1*” and “3 *tj1*” population strains with *tj1* on plasmids could recognize the TE and deposit H3K9me2, leading to a reduction of *tj1* transcription, although not efficiently enough to silence the all cell population (Figure 3.9A,B). Furthermore, we showed that silencing strains strongly repress *tj1* expression via high H3K9 methylation of the TE copies, in a process coupled with Ago1-bound sRNAs enrichment (Figures 3.5, 3.10, 3.13 and 3.15). Altogether these results suggest that *tj1* recognition and initial H3K9me2 deposition in cells establishing silencing might be dependent on the RNA interference (RNAi) pathway, as well as the maintenance of *tj1* repression in colonies silencing the TE copies. In order to determine whether

both the establishment and the maintenance of *tj1* silencing are RNAi-dependent, the two events were studied singularly. For the establishment, *ago1* was deleted in the 0_{nat} strain, generating the strain $0_{nat-ago1\Delta}$. Afterward, $0_{nat-ago1\Delta}$ was transformed with *tj1* plasmids (either p1263 or p1282) and the canonical silencing establishment experiment was performed (as described in section 3.4). The results show that if *ago1* is deleted, no red colonies were found, indicating that cells can't establish silencing of *tj1* in the absence of Ago1 (Figure 3.22A). Moreover, if *tj1* RNA reduction observed in cell population with plasmids (Figure 3.9A,B) depends on low basal H3K9me2 deposition Ago1-mediated, the deletion of *ago1* should lead to de-repression of *tj1* transcription. When *tj1* RNA is analyzed, $0_{nat-ago1\Delta}$ with plasmids shows that each *tj1* copy increases its transcription by -1.5 fold, compared to 0_{nat} (Figure 3.22B). These results suggest that initial recognition of *tj1* elements is a process mediated by Ago1, resulting in basal silencing of the element and eventually in efficient establishment of silencing (generation of red colonies).

To investigate if the maintenance of *tj1* repression, once the element is efficiently silenced, is a process Ago1-dependent, the following experiment was performed; “2 *tj1* A” silencing (without plasmids) was propagated, selecting for a red colony until a stable silencing colony was obtained (as done for the “maintenance” experiment, described on section 3.11). At that point, cells were transformed with *ago1* Δ PCR fragment (carrying *hph* cassette) and plated in hygromycin B plates for selection of *hph*⁺ (*ago1* Δ) mutants. Hygromycin B resistant colonies were finally replica plated in PMG low ade to see the color of *ago1* Δ mutants, an indication of the repression state of *tj1* (Figure 3.22C). To confirm that hygromycin B resistant colonies were actual *ago1* Δ mutants, a genomic PCR was performed, using amplification primers external to the deletion locus, resulting in a shorter PCR product if *ago1* was deleted (Figure 3.22C). All the Hygromycin B resistant colonies, once replica plated in PMG low ade, appeared white. On the other hand, interestingly, several red colonies grew in low ade plate, although absent in Hygromycin B plate. This final observation suggests that those red colonies didn't acquire *hph* cassette (therefore being *ago1*⁺), explaining why they didn't grow in Hygromycin B plate, yet they didn't die either, restarting their growth once replica plated in PMG low ade. Consistently, when some white and red colonies were analyzed by PCR for the *ago1* Δ , all white and red colonies were confirmed to be *ago1* Δ and *ago1*⁺, respectively (Figure 3.22C). This assay indicates that maintenance of *tj1* silencing is Ago1-dependent.

Altogether, these results show that Ago1, and therefore the RNAi pathway, plays a crucial role in both initial recognition of *tj1* and subsequent maintenance of *tj1* silencing (Figure 3.22A-C).

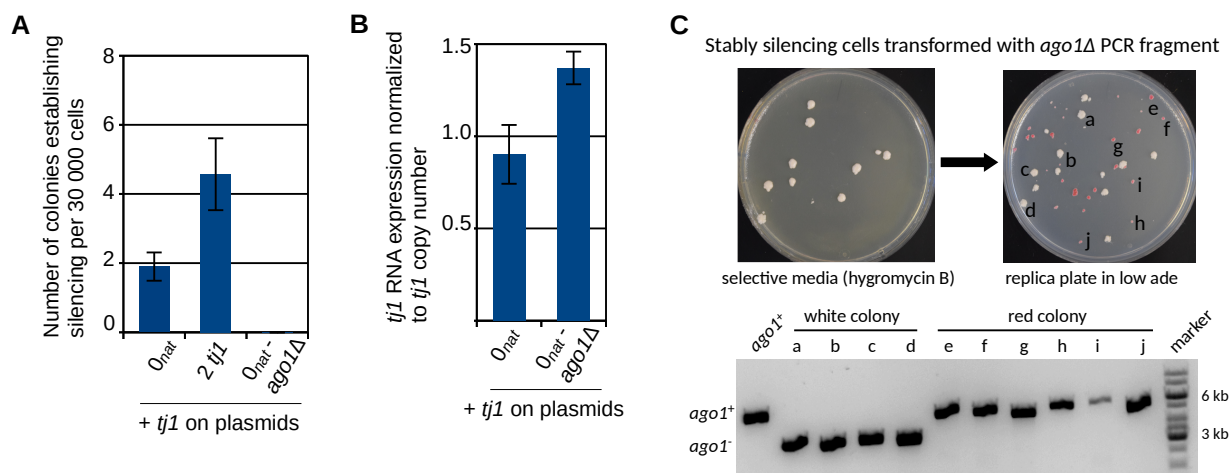


Figure 3.22: Establishment and maintenance of $tj1$ silencing are RNAi-dependent.

(A) Number of silencing establishing colonies per 30000 cells, in indicated strains (+ plasmids). Error bars represent s.e.m. of at least 10 independent plating. **(B)** $tj1$ RNA expression of each $tj1$ copy in indicated strains (+ plasmids). Error bars represent s.e.m. of three technical replicates. **(C)** A culture from a stably red “2 $tj1$ A” colony was transformed with $ago1\Delta$ PCR fragment (hph cassette) and selected in Hygromycin B. Antibiotic resistant cells were replica plated in PMG low ade. 4 white colonies (a-d) and 5 red colonies (e-j) were analyzed by genomic PCR for the presence/absence of $ago1\Delta$. PCR products were run on 1% agarose gel to confirm either the deletion of $ago1$ (~3kb amplicon) or not (~5kb amplicon). A $ago1^+$ control was used. Brighter marker bands indicate 6kb and 3kb DNA sizes.

3.15 $tj1$ silencing is Abp1-independent

In *S. pombe*, the 13 full-length copies of the LTR-retrotransposon $tf2$ are maintained silenced principally through H3-hypoacetylation, in a mechanism involving CENP-B homologous proteins, specially Abp1 (as well named Cbp1), which recruit HDACs Clr3 and Clr6 to $tf2$ elements (Cam et al. 2008; Lorenz et al. 2012). H3K9 methylation and Swi6 are not found at $tf2$ and neither RNAi nor $clr4$ mutants show derepression of $tf2$ transcription, suggesting a marginal role of H3K9 methylation and RNAi in $tf2$ silencing (Cam et al. 2005; Hansen et al. 2005). On the other hand, our results indicate that the exogenous $tj1$ is strongly silenced via H3K9 methylation, in a process RNAi-dependent, suggesting a different mechanism of $tj1$ silencing, compared to the $tf2$ element (Figures 3.13, 3.14, 3.19 and 3.22). However, we couldn't rule out the participation of CENP-B homologous in $tj1$ silencing yet. For this reason, Abp1 was tagged with 3xFLAG and Abp1-ChIP was performed, in O_{nat} cell population, O_{nat} silencing (red colony) and O_{nat} not silencing (white colony from red cells) (Figure 3.23A,B). The results show that Abp1 is not particularly enriched at the readout locus in any strain (Figure 3.23A). A weak Abp1 signal is present right at 5' of the readout though, however, a wider look at the readout locus shows that Abp1 is broadly distributed throughout the genome, indicating an unspecific binding of Abp1 at the region close to the 5' end of the readout. Besides, the presence of that Abp1 signal in all strains supports the idea that the CENP-B homologous is not

involved in *tj1* silencing. As experimental control, Abp1 clearly localizes at *tf2* boundaries (Lorenz et al. 2012) (Figure 3.23B), where, on the contrary, is involved in *tf2* repression.

Our results confirm, as expected, that *tj1* repression is carried out with a distinct silencing mechanism than *tf2*, independent of Abp1 recruitment on chromatin.

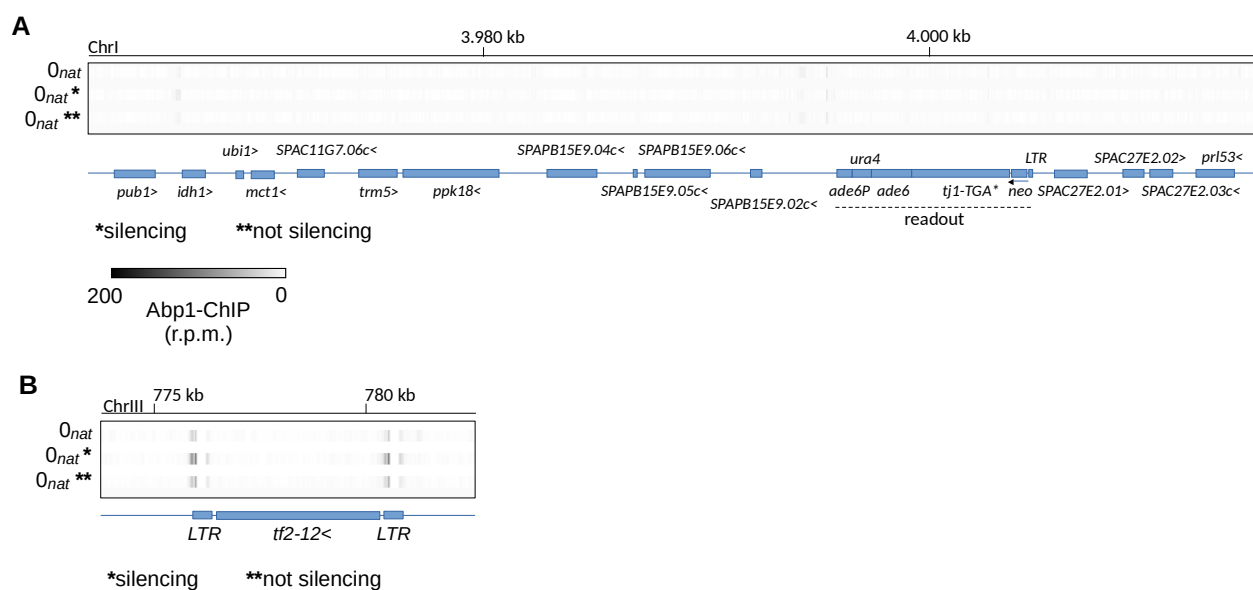


Figure 3.23: *tj1* silencing is Abp1-independent.

(A,B) Abp1-ChIP sequencing IGV tracks in indicated strains, at readout locus (A) and at *tf2-12* element (B), represented on black gradation scale, normalized per one million reads (r.p.m.).

3.16 *tj1* fitness effects

Uncontrolled propagation of TEs may be detrimental for cell viability, hence we wondered whether *tj1* transpositions introduced negative fitness effects on cell populations. A cell competition experiment was performed between *O_{nat}* strain and all the strains with transposition(s); exponentially growing cultures of *O_{nat}* and each of the “2 *tj1*” or “3 *tj1*” were mixed in a 1:1 proportion. Mixed cultures were kept growing exponentially in rich medium (YES) and ~1000 cells were plated in YES at day 0, 4 and 9. Taking advantage of the different antibiotic resistance cassettes present in the strains (*nat* in *O_{nat}*, *nat* + *neo* in “2 *tj1*” and *nat* + *neo* + *hph* in “3 *tj1*”), YES plates of *O_{nat}* mixed with “2 *tj1*” were replica plated in YES + G418 + nourseothricin, while *O_{nat}* mixed with “3 *tj1*” were replica plated in YES + G418 + hygromycin B + nourseothricin. The counting of the colonies grown in YES and in the replica plates at day 0, 4 and 9, furnished the % of *O_{nat}* and cells with transposition(s) in the mixed cultures. On average, “2 *tj1*” and “3 *tj1*” show only a slight decrease (-1.3264%) in culture composition between day 0 and day 9, compared to *O_{nat}* (Figure 3.24A). Considering 10 cell divisions per day, the analysis shows an average -0.0136% ($\pm 0.0103\%$) reduction of cells with transposition(s) in the mixed cultures per cell division. Overall, this result suggests that *tj1* transposition(s) minimally affect the *S. pombe* fitness in the cell populations.

However, a closer analysis at the strain-specific competition experiments, shows that not all the investigated transpositions alter equally the *S. pombe* fitness, with “2 *tj1* A” and “3 *tj1* FM” affecting it negatively the most (Figure 3.24B). This result suggests that *tj1* may affect the *S. pombe* fitness differently, according to the transposition loci.

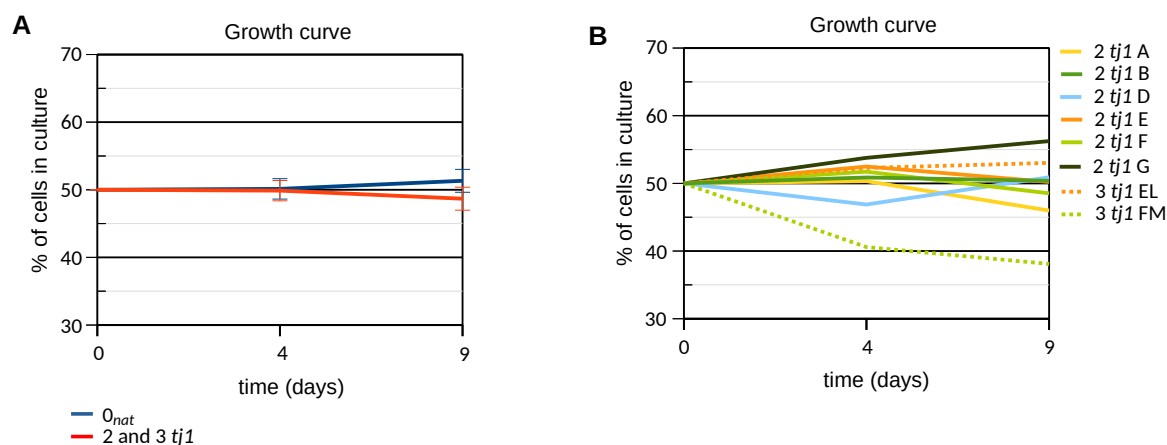


Figure 3.24: Transposition fitness effect.

(A) Average of competition assays between 0_{nat} and “2 and 3 *tj1*” strains. Error bars represent s.e.m. of 8 independent experiments. (B) Specific competition assays between 0_{nat} and the indicated strains.

Finally, we wondered whether cell fitness is affected by *tj1* silencing, considering the H3K9me2 spreading observed at readout flanking regions in all silencing strains (Figures 3.16A,B and 3.17) and at *tj1* transposition loci in some strains (Figure 3.20A), with the relative transcriptional repression of the methylated genes (Figures 3.16B and 3.20B). To answer this question, a series of growth assays were performed; exponentially growing 0_{nat} and stably silencing (and not silencing) cells of all “2 *tj1*” and “3 *tj1*” strains (without plasmids) were each incubated in YES at $OD_{600} = 0.2$ and OD_{600} were measured again after 2, 4 and 6 hours. To exclude from the growth assay the effect of the silenced readout *ade6* and *ura4* genes, which makes all “2 *tj1*” and “3 *tj1*” silencing strains slower than 0_{nat} , a control strain with *ade6* and *ura4* integrated respectively at pericentromeric and subtelomeric heterochromatin, was used (Nimmo et al. 1998). This control, furnished us an evaluation of the less fit strain possible, considering the repression of *ade6* and *ura4*, while 0_{nat} consists of the fittest strain possible, due to the absence of silencing at the readout. Therefore, it is a valid assumption that each “2 *tj1*” and “3 *tj1*” silencing strain that grows slower than the “*ura4* and *ade6* heterochromatic control”, has fitness defects independent of *ura4* and *ade6* silencing at the readout, but directly dependent on other factors, like the observed silencing of neighboring genes. The results show that, on average, “2 *tj1*” and “3 *tj1*” silencing colonies grow slower than the heterochromatic control, while white colonies from red cells (not silencing), recover part of their fitness, growing faster than the heterochromatic control (Figure 3.25A). A closer look at the growth assays of each silencing colony shows that some of them grow particularly slower than the heterochromatic control, like “2 *tj1* G and

B” and “3 *tj1* EL and FM” (Figure 3.25B), suggesting that *tj1* silencing may come with a cost, in terms of negative fitness effects and that this burden depends on each specific transposition scenario.

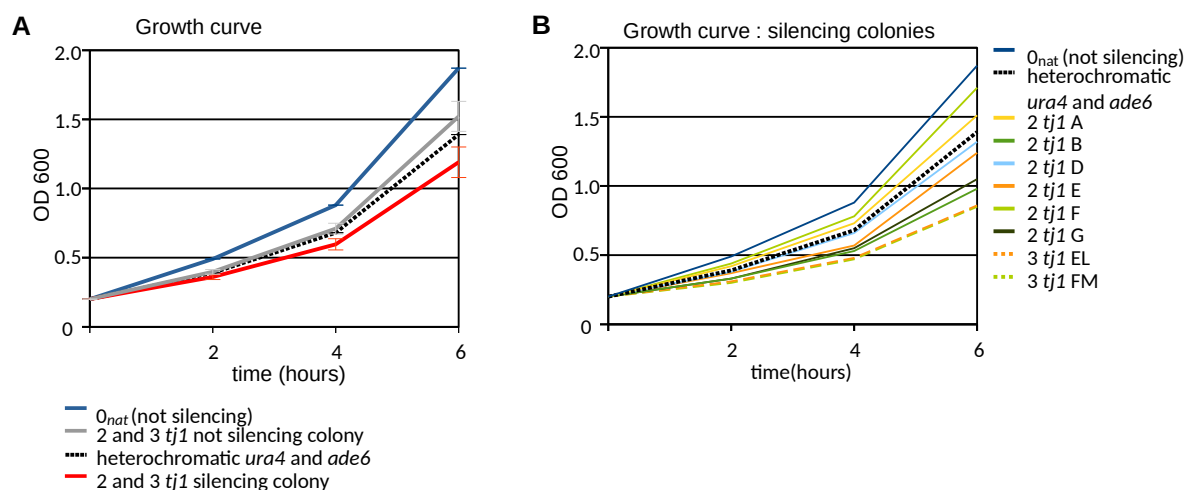


Figure 3.25: *tj1* silencing affects negatively the cellular fitness.

(A) Average growth assays of the indicated colonies. Error bars represent s.e.m. of 8 independent experiments. **(B)** Growth assays of each of the indicated silencing colonies (and 0_{nat} not silencing).

4. DISCUSSION

Uncontrolled propagation of transposable elements is responsible for several human genetic diseases, mostly caused by direct gene disruption or alteration of the splicing process, all resulting in impaired function of the target gene (Payer and Burns 2019). Back in 1988, Kazazian and colleagues showed for the first time the relationship between the human retrotransposon LINE-1 (L1) and haemophilia A (Kazazian et al. 1988). An important percentage of patients presented a *de novo* L1 transposition into the gene for coagulating factor VIII (F8) in chromosome X, resulting in blood clotting disorders (Kazazian et al. 1988). Another example of human disease caused by TEs is Fukuyama congenital muscular dystrophy (FCMD), particularly prevalent in Japan. Here, the SINE-VNTR-Alu (SVA) transposition in the 3'UTR sequence of the *fukutin (FKTN)* gene results in defective mRNA splicing and a mislocation of FKTN protein from the Golgi to the endoplasmic reticulum (Kobayashi et al. 1998; Taniguchi-Ikeda et al. 2011). To date, more than 100 human genetic diseases are associated with transposon activities (Payer and Burns 2019). On the other hand, several examples of co-evolution between TEs and their hosts have been discovered. In this process, described as transposon “domestication”, part of the ancestral transposon functions are conserved to generate proteins with new cellular functions. An example of domestication in humans (and other jawed vertebrates) consists of the RAG recombinase proteins 1 and 2, responsible for the V(D)J recombination and the diverse repertoire of antibodies and T cell receptors. Studies on RAG discovered several analogies with the ancestral RAG transposase, indicating the evolution of RAG recombinase from an ancient RAG transposon (Y. Zhang et al. 2019b).

Although it is clear that, in the long term, transposon activity can lead to beneficial effects in their hosts, it is more evident that uncontrolled transpositions may be detrimental for cell viability and fitness in unicellular organisms, up to significant genetically inherited disorders in the case of *de novo* transpositions in the germline of higher organisms. To limit transposon proliferation, cells have evolved different strategies, from transcriptional and post-transcriptional repression to post-translational silencing.

In budding yeast, Ty1 elements are silenced post-translationally through a fine regulation of the transcription starting point, resulting in a truncated Gag protein (p22) which destabilizes the VLPs and therefore the proper TE cycle (Saha et al. 2015; Pachulska-Wieczorek et al. 2016). Ty1 is silenced post-transcriptionally as well via its bidirectional transcription that leads to the accumulation of a short Ty1 antisense RNA (called Ty1AS) which impairs Ty1 transposition efficiency either directly by targeting Ty1 mRNA (or the RT enzyme) and inhibiting retrotranscription, or indirectly, perturbing the processing of Pol into its active subunits (Matsuda and Garfinkel 2009). Ty5 transposition is guided by the interaction between its integrase and the heterochromatin factor Sir4, therefore Ty5 preferentially targets heterochromatic regions, where it is maintained silenced (Zou et al 1995; Xie et al. 2001).

In *S. pombe* the LTR-retrotransposon Tf2 copies are silenced through hypoacetylation via the recruitment of Clr3 and Clr6, in a process mediated by LTR binding CENP-B homologues (especially Abp1) (Cam et al. 2008). Additionally, the HIRA complex plays a role in silencing Tf2, as well as the H3K4 methyltransferase Set1 (Greenall et al. 2006; Anderson et al. 2009; 2010; Lorenz et al. 2012). Moreover, Tf2 DNA elements are clustered in specific nuclear foci, called Tf bodies, which seem to restrict Tf2 *de novo* recombination and the integration of the extinct Tf1 element (Cam et al. 2008). Despite Tf2 copies not normally being heterochromatic, the perturbation of the exosome machinery (or of the optimal growth conditions) results in sRNA generation and RNAi-dependent heterochromatinization of the elements, suggesting that the RNAi promptly senses and buffers the increased Tf2 activity (Marasovic et al. 2013; Yamanaka et al. 2013).

Schizosaccharomyces japonicus, another member of the fission yeast clade which conserves the RNAi machinery, harbors 10 families of Ty3/gypsy-like retrotransposons (Tj1-10) located predominantly at centromeric and telomeric heterochromatin (Rhind et al. 2011). Therefore, differently to *S. pombe*, the majority of sRNAs (94%) in *S. japonicus* maps to transposable elements, underling the central role of RNAi in maintaining silencing of these TEs (Rhind et al. 2011).

In animals, a relatively new class of small RNAs, called piRNAs, plays a pivotal role in TE suppression, particularly important in germlines. In plants, a sRNA-dependent transposon silencing response is observed as well.

Despite the absence of the RNAi machinery in *S. cerevisiae*, when ago1 and dcr1 are introduced in the genome, cells acquire RNAi and, interestingly, the sRNAs generated target and repress the Ty1 transposon (Drimmenberg et al. 2009b).

Therefore, small RNAs have a central (and conserved) role in silencing TEs in different Kingdoms, from Fungi to Plantae and Animalia (Ugolini and Halic, 2018).

Our study on *S. pombe* shows that fission yeast recognizes the invading retrotransposon *tj1* via a sRNA-dependent mechanism, involving the RNAi machinery and resulting in heterochromatinization of the element(s). We reveal the importance of *tj1* transcription, independently to *tj1* copy number, in the process of recognition and triggering of the silencing, with a crucial role for the antisense transcription. Furthermore, we determined that maintenance of *tj1* silencing is RNAi-dependent, that multiple copies of the element are *trans* silenced and that transposition loci are important for the inheritance of the silenced state. Finally, yet importantly, we show spreading of heterochromatin from the nucleation point (*tj1*) to the flanking regions, resulting in a negative fitness outcome as a side effect of *tj1* silencing.

4.1 H3K9 methylation marks on silenced *tj1* elements

In our experiments, through the color phenotype of colonies grown in low adenine plates, it was possible to identify cells silencing *ade6* at the readout locus, indicated by the accumulation of a red pigmentation (Figures 3.3A,B and 3.4A). With this color screening, we isolated red colonies silencing the readout and, when present, other *tj1* copies either transposed into the genome or on plasmids. By H3K9me2-ChIP we show that the silencing of these elements is due to the heterochromatinization of *tj1*, resulting in dramatic overall repression of *tj1* transcription (Figures 3.5A and 3.10). Our results prove the efficiency of a TGS heterochromatin-mediated mechanism adopted by *S. pombe* to block the propagation of the invading *tj1* element.

The analysis of cell populations of colonies with one and two transpositions, collectively indicated as “2 *tj1*” and “3 *tj1*” respectively, showed a basal H3K9me2 deposition at *tj1* and an RNA decrease further enhanced by the presence of multiple *tj1* copies on plasmids (Figure 3.9A,B). These results indicate that on average all the cells of a population recognize the invading *tj1* element, although not efficiently enough to establish a diffuse strong silencing, achieved only in some colonies among the population, and represented by the red cellular pigmentation.

4.2 sRNA-dependent silencing of *tj1* in *S. pombe*

The study of *tj1* repressing colonies showed that the TE silencing through heterochromatin is coupled with the presence of Ago1-bound sRNAs (Figures 3.5 and 3.14), suggesting a central role for sRNAs and Ago1 in silencing the invading element via an RNAi-mediated H3K9me2 deposition. Accordingly, despite multiple *tj1* copies on plasmids, an *ago1Δ* mutant showed a complete inability to establish *tj1* silencing (Figure 3.22A) and an increase in *tj1* RNA compared to the wild-type strain (Figure 3.22B). These results indicate that at least *tj1* recognition and initial silencing are processes mediated by Ago1, however, this didn't rule out completely the possibility of a sRNA-independent maintenance of silencing, as observed at the mating-type locus and subtelomeric heterochromatin (Hall et al. 2002; Kanoh et al. 2005), or of a redundant pathway involving both Ago1 and a sRNA-independent mechanism. The deletion of *ago1* in a strain stably silencing *tj1*, resulted in the complete loss of silencing in all the analyzed colonies (Figure 3.22C), indicating that maintenance of *tj1* repression through generations is Ago1-dependent. Accordingly, white cells from a silencing colony, show a severe drop of Ago1-bound sRNAs at the readout, accompanied by the complete loss of H3K9me2, underling the relation between *tj1* sRNAs and heterochromatin (Figure 3.5).

Altogether these results show the central role of Ago1 and sRNAs not only in the initial recognition and silencing of *tj1* but also in the subsequent maintenance of repression.

In *S. pombe*, endogenous *tf2* silencing involves CENP-B homologous proteins, in particular Abp1 (Cam et al. 2008). Therefore we wondered whether Abp1 participates in *tj1* silencing. Our results show that Abp1 is not recruited at *tj1* locus in cells silencing the retrotransposon, indicating that Abp1

is not involved in *tj1* repression (Figure 3.23), in line with the central role of Ago1 and sRNAs in *tj1* silencing.

Our observation of the central role of Ago1 and sRNAs in silencing invasive *tj1* through heterochromatin formation, resembles what was observed in *Arabidopsis thaliana* where the *de novo* invasion of the retrotransposon Evadé (EVD) is stably repressed through DNA methylations, in a mechanism guided by Argonaute proteins and TE sRNAs (Marí-Ordóñez et al. 2013).

4.3 The importance of *tj1* transcription for the recognition of the TE

Our experiments on the establishment of silencing in strains with transposed *tj1* copies compared to the strain with the sole readout (0_{nat}), showed that neither one nor two *tj1* transpositions can trigger strong silencing of the transposon (unless transposed close to pericentromeric heterochromatin) (Figure 3.7 E,F), despite the overall basal H3K9me2 deposition and the initial *tj1* RNA decrease in the cell populations (Figure 3.9C,E). On the other hand, the introduction into these strains of multiple *tj1* copies on plasmids, led to the establishment of silencing in the populations (Figure 3.7G,H), indicating that cells respond with more efficient silencing when *tj1* copies increase. Despite the impossibility to determine the precise number of *tj1* copies necessary to lead to an efficient silencing establishment in the cell population (due to the elevated number of antibiotic resistance cassettes necessary to sequentially integrate one *tj1* copy and to the impossibility to control the exact number of *tj1* plasmids), and excluding the strains with transpositions close to pericentromeric heterochromatin (“2 *tj1* G” and “3 *tj1* EL”) (Figure 3.6C,D and Table 3.1), it is possible to estimate that a number between 3 and 6 *tj1* copies (+ the copy at the readout) corresponds to the minimum of transposon copies necessary to trigger efficient silencing in the cell population. In fact, the strain “3 *tj1* FM”, with 2 transpositions (plus *tj1* at the readout) is unable to establish silencing (Figure 3.7F), whereas the strain “2 *tj1* B” carrying 6 *tj1* on plasmids (plus *tj1* at the readout) can establish silencing (Figure 3.7G). However, a comparison among the strains shows that more *tj1* copies don’t necessarily mean more silencing (red) colonies present in the cell population (Figures 3.4B and 3.7G,H) and that into the same population, silencing and not silencing cells contain the same number of *tj1* copies (Figure 3.4C). Therefore, despite multiple copies of *tj1* being necessary for the establishment of efficient silencing, the *tj1* number is not the only determinant for *tj1* recognition and establishment of silencing. Excluding strains with pericentromeric *tj1*, we observed that some of them (“2 *tj1* A” and “2 *tj1* D”) established silencing in the populations more frequently than others (Figure 3.7G,H) and we wondered whether the transcription of *tj1* is important to trigger the strong silencing. We, therefore, grouped the strains in “efficient” and “not efficient” (and “efficient with centromeric insertions”) in establishing silencing and analyzed their average sense and antisense *tj1* transcriptions (Figure 3.8). The results showed that “efficient” strains on average present higher *tj1* antisense RNA than the “not efficient” strains (Figure 3.8B), while sense RNA is comparable (Figure 3.8A), suggesting that higher *tj1* antisense transcription leads to the more frequent establishment of silencing. Finally, we

modulated specifically *tj1* sense transcription by the elimination of the *tj1* 5'LTR (*tj1* promoter) from the plasmid, resulting in a decrease of *tj1* sense RNA accumulation compared to the 0_{nat} strain with a 5'LTR⁺ plasmid (p1263) (Figure 3.8C) and a reduction of cells establishing silencing in the population (Figure 3.8D). The *tj1* sense RNA was still observed in the strain with the 5'LTR deletion, and is likely the result of sense *tj1* transcription from the readout (Figure 3.8C), however, it is not possible to rule out the possibility of the presence of a less efficient internal promoter downstream of 5'LTR, resulting in an additional lower (and likely truncated) sense *tj1* RNA. This experiment proves that not only the antisense transcription of *tj1* is important for its silencing, but also the sense transcription, overall indicating that multiple *tj1* copies are necessary to reach a threshold level of sense and antisense *tj1* RNAs to trigger the efficient establishment of silencing (Figure 3.8).

In the future, it would be interesting to modulate both the sense and antisense transcriptions, in order to simulate *tj1* transposition at different loci, for example, close to a convergent gene, resulting in increased antisense transcription.

4.4 *Trans* silencing of dispersed genomic elements

The genome of *Drosophila melanogaster* was invaded in the mid of 20th century by a DNA transposon called *P* element (Dominique Anxolabéhère et al. 1985; D Anxolabéhère et al. 1988), which was rapidly converted to a repressed state. This rapid response came from *P* elements transposed close to telomeric heterochromatin, causing the repression of other *P* element copies inserted at euchromatic loci (Roche and Rio 1998). This phenomenon was called the *Trans* Silencing Effect (TSE) because of the ability of a *P* element inserted in a location (telomere) to silence other copies, independently to the genomic location of the latter elements (Roche and Rio 1998). Later studies showed a direct correlation between the TSE and the piRNA pathway in the germline, where telomeric piRNA clusters containing *P* elements mediate trans silencing of the dispersed copies (Josse et al. 2007; Brennecke et al. 2008; Todeschini et al. 2010; S. Zhang and Kelleher 2019).

In wild-type *S. pombe*, the existence of a similar *trans* silencing mechanism, involving sRNAs and genomically dispersed homologous DNA elements, has been poorly demonstrated. Bühler and colleagues showed that tethering the RITS complex to a nascent *ura4* transcript induces the heterochromatinization of the target gene, involving the RNAi pathway, Ctr4, Swi6 and the Sir2 histone deacetylase, accompanied by the generation of *ura4* sRNAs (Bühler et al. 2006). However, the sRNAs generated at *ura4* are able to establish *trans* silencing of a second *ura4* copy only when Eri1 double-strand siRNA nuclease gene is deleted, indicating that sRNA action is usually restricted to the generation site (*cis*) by Eri1 function (Bühler et al. 2006; Iida et al. 2006). Iida et al. showed that double-stranded sRNAs generated from an *ura4* hairpin enhance *trans* silencing of *ura4* copies inserted at heterochromatic regions by the reinforcement of RITS-mediated *ura4* mRNA co-transcriptional silencing, with barely detectable effect on euchromatic *ura4* (Iida et al. 2008). Hairpin *ura4* was able to establish *trans* heterochromatinization of euchromatic *ura4* only when Swi6 was

overexpressed, likely due to the interaction between Swi6, Ers1 and the RITS complex at the *ura4* locus, directing the *trans* heterochromatin formation (Iida et al. 2008; Rougemaille et al. 2012). Furthermore, the Swi6-dependent *ura4 trans* silencing was observed only when *ura4* was cloned at the *tp1* locus, with no effect at the endogenous *ura4* locus, therefore indicating a locus effect in the establishment of *trans* silencing (Iida et al. 2008). Interestingly, only at the *tp1* locus antisense *ura4* RNA was detected, while at the endogenous *ura4* antisense transcription wasn't observed, suggesting a role for antisense RNA in directing *trans* silencing of *ura4*. Consistently, when antisense *ura4* transcription was artificially induced, by placing a convergent promoter 3' of *ura4*, *ura4* was efficiently silenced, while it was not when antisense transcription was abolished, suggesting that *trans* silencing depends also on the transcriptional activity/orientation of flanking genes, responsible for the generation (or increase) of target double-strand RNAs (Iida et al. 2008). Accordingly, as discussed already, the initial *tj1* repression efficiency observed in our experiments depends on the *tj1* antisense RNA (Figure 3.8), and strongly silencing colonies maintain their basal *tj1* antisense transcription, despite the dramatic decrease in sense RNA (Figure 3,10C). More recently, Simmer and coworkers proved that hairpin RNAs can induce *trans* heterochromatin formation in wild-type fission yeast, without further genetic manipulations besides the cloning of the hairpin construct (Simmer et al. 2010). Moreover, they observed the Rdp1-dependent generation of secondary sRNAs close to the *ura4* target gene, accompanied by low H3K9 methylation. However, similarly to what was previously reported, Simmer and colleagues showed as well that *trans* silencing is efficient only when the target gene is positioned close to pericentromeric heterochromatin, again underlying a locus effect on *trans* silencing (Iida et al. 2008; Simmer et al. 2010).

In our study we demonstrate that *S. pombe* contains a powerful RNAi-mediated tool for the detection of the invading *tj1* LTR-retrotransposon and the *trans* silencing of all the present elements, without any genetic manipulation at all besides the artificial cloning of the readout construct, incapable per se of inducing silencing (Figures 3.3, 3.4B, 3.7A and 3.9A,G,H). H3K9me2-ChIPs of cell populations show that some basal heterochromatin is deposited at *tj1* elements (particularly in the strains “2 *tj1* E,F,G” and “3 *tj1* EL”), accompanied by a small reduction in *tj1* RNA (observed in all strains, independently to the basal H3K9me2 levels) (Figure 3.9). This result indicates that all cell populations initiate *tj1* silencing post-transcriptionally, supposedly through Ago1 cleavage activity (Sigova et al. 2004), and that in some strain populations weak establishment of heterochromatin is triggered as well (Figure 3.9). In the future, to confirm that *S. pombe* initially recognizes and eliminates *tj1* RNA through the activity of Ago1, it would be interesting to measure *tj1* transcription in the same background strains but with the *clr4* gene deleted. When silencing cells (red) were analyzed, our results show that all *tj1* elements are H3K9 methylated, independently to the loci where transposition occurred (Figure 3.13 A-K), indicating a *trans* silencing mechanism related directly to *tj1*, rather than the genomic transposition contest. Additionally, *trans* heterochromatin is found also in *tj1* elements on plasmids (Figure 3.19A), therefore independently to their insertions into the genome,

further arguing that *tj1* itself guides the silencing of the transposon. The Ago1-bound sRNAs analysis in silencing “2 *tj1* A” and “2 *tj1* G” strains showed that sRNAs are present in all *tj1* elements (Figure 3.14), indicating that the strong *trans* silencing of all dispersed *tj1* copies is mediated by the RNAi machinery. Finally, in silencing cells we observed the generation of secondary sRNAs close to the endogenous *ade6M210* locus (i.e. *bub1* gene), where Ago1-bound sRNAs from the readout are *trans* directed (due to the homology between *ade6* promoter (*ade6P*) and *ade6* of the readout with *ade6M210*), accompanied by weak H3K9me2 deposition (with no transcriptional effects) (Figures 3.5C and 3.15A), similarly to what was previously observed by Simmer et al. (Simmer et al. 2010).

4.5 Maintenance of *tj1* silencing is position-dependent

In this study we isolated several colonies with *de novo* *tj1* transpositions; all insertions occurred in the proximity of an RNA-polymerase III (RPIII) transcribed gene (i.e. tRNA and 5S rRNA genes) and in forward orientation (Table 3.1). Transposition Site Duplications (TSDs) were found in all *tj1* insertions (transposition H excluded, because of bad Nanopore-sequencing reads quality), indicating that these are the results of real retrotransposition events, rather than genetic recombinations (Table 3.1). Therefore, in our hands, *tj1* invasion in fission yeast reproduced the transposition features showed by Guo and colleagues (Guo et al. 2015). The *tj1* transposition bias for RPIII transcribed genes resembles that of Ty3 observed in budding yeast, with the only difference in the orientation with respect to the target gene, only in the forward orientation in the case of *tj1*, while in both forward and reverse orientation in Ty3 (Aye et al. 2001). Among our colonies with *de novo* *tj1* transpositions, eight were deeply investigated (“2 *tj1* A,B,D,E,F,G” and “3 *tj1* EL,FM”) (Figure 3.6C and Table 3.1). All “2 *tj1*” strains contain a transposed copy of *tj1* (plus the copy at the readout), while “3 *tj1* EL” and “3 *tj1* FM” present a second transposed *tj1* element (plus the copy at the readout) and originated from “2 *tj1* E” and “2 *tj1* F” (indicated as “parental to 3 *tj1*”), respectively (Table 3.1). We wondered whether the number of *tj1* elements dispersed within the genome affects the inheritance of the silenced state through cell generations. When stably silencing (red) colonies of the strains 0_{nat} , “2 *tj1*” and “3 *tj1*” (in order carrying only the *tj1* copy at the readout, the copy at the readout plus a transposed element and the copy at the readout plus two transposed copies) were analyzed for their ability to maintain the silencing state through generations, we observed that silencing was clearly more stable when cells acquired one or two transpositions (Figure 3.12A,E). However, no clear change in the stability is present between “2 *tj1*” and “3 *tj1*”, indicating that a third *tj1* transposition doesn’t increase the maintenance of the repressive state through generations (Figure 3.12A). On the other hand, when the transposition loci were analyzed, the silent state was inherited much more stably in strains with *tj1* transpositions close to pericentromeric heterochromatin, than in strains with insertions at euchromatic loci (Figures 3.12B,E, 3.6C,D and Table 3.1). These results indicate that the inheritance of the *tj1* silencing state through generations depends on the chromosome position of the transposon, rather than in the sequentially increasing number of elements at euchromatic loci (Figure

3.12). However, we can't rule out the possibility that increasing further the copies of *tj1* at euchromatic loci, would lead to a more stable maintenance of silencing through generations, resembling what is observed with heterochromatic transpositions. Up to this point, our findings suggest that the presence of constitutive heterochromatin close to the silenced *tj1* somehow stabilizes the inheritance of heterochromatin at *tj1* through cell divisions. The most obvious explanation for that is the proximity to the centromeric *dg* and *dh* repeats, where centromeric heterochromatin nucleates and stably persists after cell divisions, thanks to the RNAi machinery and the heterochromatin proteins Clr4, Chp2, Swi6 and HDACs (Martienssen and Moazed 2015; Zocco et al. 2016; Akoury et al. 2019). There all the members of constitutive heterochromatin are constantly recruited to maintain pericentromeric heterochromatin. It is, therefore, no surprise if *tj1* integrated nearby is stably maintained silenced, where it has in fact become physically part of the centromeric repeats. Moreover, our results showed that *tj1* is bidirectionally transcribed and that Ago1-bound sRNAs are present in silencing colonies, themselves features of heterochromatin nucleation sites. Consequentially, the insertion of *tj1* close to pericentromeric heterochromatin places the element in the proper context for an RNAi-dependent stable heterochromatin maintenance, where it actively mediates its own silencing, alongside the flow of heterochromatin readers and writers from the proximal centromeric repeats.

The analysis of H3K9 methylation and *tj1* transcription in “silencing” (red) colonies and white colonies originated from the re-streaking of the red colonies (indicated as “not silencing” colonies), showed that all *tj1* copies in each silencing strain are on average H3K9 methylated and transcriptionally repressed (Figure 3.10F,G), while the selected white colonies from red colonies maintained heterochromatin and TGS to some extent only in strains with pericentromeric transpositions (Figure 3.10F,G). This result suggests that in “not silencing” colonies of pericentromeric strains heterochromatin was lost specifically at the *ade6* gene of the readout construct in response to our white selection. In other words, this observation points that pericentromeric *tj1* elements retain heterochromatin despite the selective loss of it at the readout locus, while the heterochromatin loss at the readout in strains with *tj1* at euchromatic loci ends with the general impairment of *tj1* silencing. To prove this, we took advantage of the presence of the unique sequences at the readout (*nat*), at the first transposed *tj1* copy (*neo*) and at the second transposed element (*hph*), that permitted us to deeply investigate the specific silencing state of each region in all strains and all phenotypes (Figures 3.11 and 3.13). H3K9me2-ChIPs and RNA sequencings show that silencing colonies repress all *tj1* elements independently to their location (Figure 3.11A,B) and that, as hypothesized, white colonies from red cells only in strains with pericentromeric *tj1* lose specifically heterochromatin at the readout locus, maintaining most of it at the pericentromeric copies (Figures 3.11 and 3.13). Interestingly, the strain “3 *tj1* EL”, that contains one *tj1* transposition at an euchromatin locus and one at the pericentromeric region (characterized by the unique *neo* and *hph*

sequences, respectively), retains heterochromatin at both *tj1* elements when white cells are selected and not only at the pericentromeric copy (Figure 3.13 A,H,I,L).

These results suggest again that strains with pericentromeric transpositions overall maintain *tj1* silencing stronger than strains with the element at euchromatic loci, as showed before with the analysis of the inheritance of the silent state, strongly maintained only in the first group of strains (Figure 3.12B). Moreover, these experiments suggest that cells with pericentromeric *tj1* can selectively modulate the silencing state of the *tj1* element at the euchromatic locus (readout) with minimal alteration of the silencing of the pericentromeric element (and in the case of “3 *tj1* EL”, minimal alteration also of the euchromatic transposition). In the bigger picture, this resembles a transient response to external stimuli, in this case the selection for white colonies and the specific derepression of *ade6*. Consistently, white colonies from red colonies showed the capability to some extent to revert to red phenotypes only in strains with pericentromeric *tj1* (higher than the intrinsic capacity of pericentromeric strains to establish silencing without plasmids (Figure 3.7E,F), data not shown), underling the reversible state of the euchromatic *tj1* at the readout, supposedly mediated by the *trans* acting sRNAs constantly generated at the pericentromeric *tj1* (and at the euchromatic transposon in the strain “3 *tj1* EL”).

4.6 H3K9 methylation spreads from silenced *tj1* elements to flanking regions

Our experiments show that H3K9 methylations in silencing colonies are not restricted to the *tj1* sequences, but they spread to the flanking genes. At the readout locus, despite the different intensity of the methylations, all the strains present a similar spreading profile; -7kb of DNA downstream from the 3' end have methylated H3K9, while at the 5' end methylations are found up to -25kb upstream the *ade6P* (Figure 3.16A). However, the spreading doesn't appear continuous at the 5' side of the readout, where an H3K9me2 gap of -8kb is present. Nucleosome-Free Regions (NFRs) are found at H3K9 methylation borders as a space barrier for H3K9 spreading. In fission yeast, NFRs are naturally present at tRNA genes and IR repeats, well known heterochromatin boundaries at centromeres and MAT loci, respectively (Garcia et al. 2010). Our H3-ChIP showed that the first -4kb upstream of the readout are nucleosome-poor, suggesting that H3K9 methylation can't spread over that region because nucleosomes are not abundant (Figure 3.16B,C). Interestingly the same H3 profile is observed in wild-type cells, indicating that the first -4kb upstream the readout are naturally nucleosome-poor and not the result of the readout cloning (Figure 3.16C). However, the rest of the H3K9 methylation gap (in correspondence of *SPAPB15E9.05c* and *SPAPB15E9.06c* genes) doesn't show H3 depletion at all (Figure 3.16C). A look at the transcription levels of *SPAPB15E9.05c* and *SPAPB15E9.06c* in cell populations indicates that these two genes are highly transcribed (Figure 3.16B, see “all *tj1*” RNA). Previous studies showed that the accumulation of heterochromatic RNA on chromatin, as result of the impairment of the Ccr4-Not mediated RNA degradation pathway or the transcript overexpression, leads to defective heterochromatin assembly (Brönnner et al. 2017). In this

model, accumulating RNAs generate exceptional DNA:RNA hybrids that interfere with the heterochromatin formation. Keller and colleagues showed that at the pericentromeric right boundary of chromosome I, Swi6 binds nascent long non-coding euchromatic RNA (*BORDERLINE* RNA) and directs its processing to sRNAs that are, however, not loaded onto Ago1 like canonical pericentromeric sRNAs, therefore interrupting the RNAi mediated spreading of heterochromatin from centromeres to neighboring euchromatin (Keller et al. 2013b). Interestingly, when the *BORDERLINE* DNA sequence was replaced with a protein-coding sequence (*ura3*), the H3K9 methylation barrier was not only preserved but that barrier activity increased when higher *ura3* transcription was induced (Keller et al. 2013b). Moreover, RNA at heterochromatin competes with H3K9 methylation for the binding with Swi6, resulting in Swi6 eviction from heterochromatin and an HP1 homologue-mediated RNA degradation (Keller et al. 2012b). It is therefore possible that a highly transcribed gene may work as an H3K9 methylation boundary being the result of increased DNA:RNA hybrid formation and Swi6 eviction, altogether working as an heterochromatin barrier. For this reason, the *SPAPB15E9.05c* and *SPAPB15E9.06c* genes at the readout may block heterochromatin spreading, like the highly transcribed gene *prl53* at the 3' boundary might do (Figure 3.16B).

The expression analysis of the heterochromatic genes flanking the readout shows that in silencing cells these genes are on average transcribed -30% less than in cell populations, indicating the silencing function of the spreading H3K9 methylations (Figure 3.16B, lower graph).

When we analyzed the repression of the *tj1* elements in all the silencing strains obtained, we showed that all the *tj1* copies are recognized and heterochromatic, thus, considering the H3K9 methylation spreading observed at the readout, we wondered if heterochromatin spreads to flanking regions also from the transposed *tj1* elements. Our results show that spreading is observed at some of the transposed copies (Figure 3.20A). Similar to the repression effect on heterochromatic flanking genes at the readout locus, H3K9 methylated genes close to the transposed copies present an average reduction in transcription of -30%, compared to cell populations (Figure 3.20C). As well as at the readout locus, gaps in spreading heterochromatin are observed at some of the transposed *tj1* elements (Figure 3.20A). H3-ChIP at these loci didn't show any NFR (data not shown), therefore we investigated whether the transcriptional activity of the *tj1* flanking genes may have a role in controlling heterochromatin spreading, as hypothesized at the readout locus. We divided the flanking genes according to their position with respect to the H3K9me2 spread; thus, we obtained three gene groups: "border genes" (first genes immediately downstream or upstream the H3K9me2 borders), "heterochromatic genes" (H3K9 methylated genes) and "gap genes" (genes with no H3K9me2 between border genes). The transcriptional analysis of these gene groups in cell populations shows that on average genes at the heterochromatin borders (and at the gaps) are -2 folds more transcribed than the genes that will be heterochromatic in silencing colonies, suggesting that the first may work as

a barrier to the H3K9me2 spreading (Figure 3.20B), similarly to what was observed for highly transcribed genes at the readout locus.

Additionally, we wondered whether the DNA sequences immediately flanking the *tj1* elements may have a role in regulating heterochromatin spreading. All the elements transposed close to RPIII transcribed genes in forward orientation with respect to the target genes (some *tj1* targeted tRNA genes, others 5S rRNA genes) (Table 3.1). tRNA genes are found at pericentromeric repeats where they work as efficient heterochromatin barriers (Wood et al. 2002; Scott et al 2006; Keller et al. 2013). On the other hand, in *S. pombe* 5S rRNA genes are dispersed at euchromatic loci within the genome and absent at pericentromeric repeats (Wood et al. 2002). Nothing is known about the 5S rRNA gene activity as an heterochromatin barrier. Historically, tRNA and 5S rRNA genes transcription by RPIII machinery has been described as a conserved process mediated by the transcription factor TFIIB complex, recruited upstream of both the gene types. The TFIIB complex contains the TATA-binding protein (TBP) subunit and is required for the recruitment of the RPIII machinery and subsequent transcription of the tRNA and 5S rRNA genes (Schramm and Hernandez 2002). Despite both tRNA and 5S rRNA genes being transcribed by RPIII recruited through the TFIIB complex, the way by which tRNA and 5S rRNA genes recruit the TFIIB complex upstream of the genes is different (Schramm and Hernandez 2002). In the case of the tRNA genes, another transcriptional factor complex, called TFIIC complex, binds a tRNA DNA internal promoter, consisting of two conserved motifs (A-box and B-box) and subsequently interacts with the TFIIB complex, positioning it upstream the tRNA gene. Differently, the positioning of TFIIB complex upstream of 5S rRNA DNA is mediated by a distinct transcriptional factor, TFIIA, which specifically binds a 5S rRNA gene internal sequence (called IE) and recruits TFIIC, which brings TFIIB upstream the gene (Schramm and Hernandez 2002). The TBP subunit of the TFIIB complex is, therefore, physically brought upstream the RPIII genes by the interaction of the complex with TFIIC, independently to the presence of a TATA box, absent at tRNA and 5S rRNA genes in most eukaryotic organisms (Hamada et al. 2001). However, in *S. pombe* (and similarly in *Arabidopsis thaliana*), TATA elements are found upstream of both tRNA and 5S rRNA genes (-20/30 nucleotides upstream of the transcription starting site) and are essential for their proper transcription (Hamada et al. 2001). Studies on the heterochromatin barrier activity of tRNA found at pericentromeric heterochromatin boundaries, showed that in fission yeast the mutation of the TATA elements decreases, but doesn't destroy completely, the barrier capacity of the tRNA, which is completely impaired when the A-box is mutated (Scott et al. 2006). In *S. pombe*, to contain the spreading of heterochromatin at the mating-type locus, two inverted repeats surround the region, *IR-L* and *IR-R*, and their deletion results in heterochromatin spreading to neighboring regions (Noma et al. 2001). *IR-L* and *IR-R* present repeated copies of the B-box sequences found in the internal promoter of tRNA genes and they recruit the TFIIC complex at the *IR* elements of the mating-type locus, preventing heterochromatin spreading (without recruiting the RPIII machinery) (Noma et al.

2006). These observations suggest that the direct TFIIC binding on DNA sequences mediates the repression of heterochromatin spreading, as shown at tRNA and *IR* repeats (Scott et al. 2006; Noma et al. 2006).

In our study, none of the strains with transpositions upstream of tRNA genes showed spreading of H3K9 methylation at the 3' end of *tj1* (Table 3.1 and Figure 3.20, see strains “2 *tj1* A, B and D”), suggesting that, despite the *tj1* integration between the TATA box and the TSS of the tRNA genes, the recruitment of TFIIC directly on the tRNA DNA restricts heterochromatin from spreading over the 3' side of *tj1*. Furthermore, Scott and colleagues showed that mutations of the TATA element at tRNAs didn't impair completely the barrier activity of the tRNA gene, in accordance with our results (Scott et al. 2006). A look at the strain “2 *tj1* G”, with transpositions close to pericentromeric repeats, shows that silencing cells present a tiny H3K9me2 gap immediately at the 3' end of *tj1* (before pericentromeric heterochromatin), where the target tRNA gene is, further arguing that the tRNA DNA may inhibit heterochromatin formation (Figure 3.20, see strains “2 *tj1* G”). Similarly, the pericentromeric *tj1* copy of the strain “3 *tj1* EL” shows no heterochromatin spreading at its 3' side, where a tRNA cluster is present, and a small methylation gap between the *tj1* 5' end and the pericentromeric heterochromatin where two tRNA genes are found (tRNA-arg/asp) (Figure 3.20, see the pericentromeric *tj1* copy of strain “3 *tj1* EL”). As mentioned, no studies support the role of 5S rRNA genes as heterochromatin barriers and, on the contrary, in *A. thaliana* 5S rRNA copies are repressed through DNA methylations and H3K9me deposition, suggesting that 5S rRNA are not refractory to heterochromatin (Murata et al. 1997; Mathieu et al. 2003; Douet and Tourmente 2007). Therefore, considering the similar 5S rRNA DNA organization between *A. thaliana* and *S. pombe* (Hamada et al. 2001), together with the absence of 5S rRNA genes at heterochromatin boundaries in fission yeast, it is likely that 5S rRNA genes don't work as heterochromatin barriers. Accordingly, our study shows that H3K9 methylation at the 3' side of the *tj1* elements is present only in strains where the transposon inserted at 5S rRNA genes (Table 3.1, strains “2 *tj1* E and F” and “3 *tj1* FM” and Figure 3.20). However, continuous spreading from 3' *tj1* end to neighboring genes is observed only at the two *tj1* copies of the strain “3 *tj1* FM”, while in the strains “2 *tj1* E and F” heterochromatin gaps are present (Figure 3.20).

In *S. pombe* heterochromatin boundaries are also maintained through the recruitment of specific effectors. For example, Epe1, a putative H3K9-demethylase, is recruited to constitutive heterochromatin via Swi6 where it inhibits the spreading of heterochromatin to flanking regions (Ayoub et al. 2003; Zofall and Grewal 2006). Ubiquitination of Epe1 via Cul4-Ddb1^{Cdt2} leads to its degradation (Braun et al. 2011). Interestingly, Epe1 degradation is restricted to proteins found at the central core of constitutive heterochromatin regions, resulting in Epe1 peaks at H3K9 methylation boundaries (Braun et al. 2011). At the IRC boundary elements of chromosome I and III, Epe1 recruits the bromodomain protein Bdf2 which interacts with acetylated H4K16, protecting the nucleosomes from the Sir2 deacetylase activity, therefore inhibiting the deposition of heterochromatic

marks and sub-sequential heterochromatin spreading (J. Wang et al. 2013). The activity of Epe1 is not restricted to pericentromeric heterochromatin, mating-type locus and telomeres, but this protein inhibits spreading of heterochromatin also at ectopic loci, as shown when *epe1* gene deletion resulted in H3K9me spreading from an ectopic *cenH* element to flanking reporter genes *ura4* and *ade6* (Ayoub et al. 2003). Leo1, a component of fission yeast PAF complex (Polymerase-Associated Factor), has been identified as a boundary protein as well (Verrier et al. 2015). The deletion of this protein leads to spreading of heterochromatin at centromeres, telomeres mating-type locus and at an ectopically induced heterochromatin locus, accompanied by H4K16 de-acetylation (Verrier et al. 2015; Sadeghi et al. 2015). Verrier and colleagues suggest a model where Leo1 recruits the H4K16 acetyltransferase Mst1 at H3K9 methylation boundaries, repressing spreading of heterochromatin (Verrier et al. 2015). Moreover, Leo1 deletion shows slower H3 turnover at heterochromatin, suggesting that Leo1 has an additional function in promoting the switch between old and new histones and, therefore, in erasing local heterochromatin marks (Sadeghi et al. 2015). Finally, Leo1 mutation leads to heterochromatin spreading at heterochromatin islands, like *mei4*, and *de novo* heterochromatinization of *tf2* elements, indicating that Leo1 regulates also facultative heterochromatin dynamics (Sadeghi et al. 2015). We cannot exclude that effector proteins like Epe1 and Leo1 might be recruited at *tj1* loci where they regulate heterochromatin boundaries. In the future, it would be interesting to investigate the presence of these effectors at *tj1* silenced loci and the effects of their mutations on H3K9 methylation spreading.

In conclusion, different components may interfere with heterochromatin spreading from silenced *tj1* elements; (i) we suggest that spreading at 3' side of *tj1* may be repressed by targeting a tRNA gene, while it may be more permissive when *tj1* transposes upstream a 5S rRNA gene. (ii) Transcription activity of *tj1* flanking genes may regulate the bidirectional spreading of H3K9 methylation, with boundary genes on average more transcribed, as observed at *tj1* transposed copies and at the readout (Figures 3.20B and 3.16B). (iii) we cannot exclude that heterochromatin spreading over some set of genes would negatively interfere with cell viability, ending with the selection of the heterochromatin patterns obtained in this study, as result of bias from selective pressure or (iv) an active locus-specific heterochromatin spreading control mechanism (involving effector proteins like Epe1 and Leo1).

In order to minimize detrimental effects on the host, transposon mobilization is often restricted to some specific locations. For example, Ty5 in budding yeast transposes preferentially within heterochromatic regions (Zou et al. 1995; Xie et al. 2001). Similarly, Ty3 and Ty1 are preferentially guided close to tRNA and 5S rRNA genes, redundantly present within the genome and therefore transpositions at one of these loci are unlikely to be lethal (Chalker and Sandmeyer 1992; Devine and Boeke 1996). Evidence shows that Ty1 and Ty3 transposition at tRNA genes have a neutral (or stimulatory) effect on tRNA transcription and fitness experiments show no negative selection pressure of some *de novo* Ty1 transpositions (Kinsey and Sandmeyer 1991; Bolton and Boeke 2003; Blanc and Adams 2004). However, considering the different tRNA and 5S rRNA gene organization

between *S. pombe* and *S. cerevisiae*, with the first organism presenting TATA elements upstream of both tRNA and 5S rRNA genes, essential for the proper transcription (Hamada et al. 2001), we wondered whether *tj1* transpositions in our study would affect the overall cellular fitness. Our competition assay, where the strain with the sole readout construct (0_{nat}) was mixed with one of the strains with transposition(s), on averaged showed that transposition(s) may slightly affect the cellular fitness (Figure 3.24A), with an accentuated effect in the strain “3 *tj1* FM” (Figure 3.24B). The fact that “3 *tj1* FM”, but not “3 *tj1* EL”, stands out for its slower growth compared to 0_{nat} , suggests that location, rather than copy number might effect the cellular fitness. While both transposon copies inserted upstream a 5S rRNA gene in “3 *tj1* FM”, in “3 *tj1* EL” the element mobilized upstream both a tRNA and a 5S rRNA gene, indicating that the fitness might be impaired depending on the *tj1* target genes. On the other hand, none of the other strains with *tj1* integrated upstream a 5S rRNA showed fitness defects (“2 *tj1* E” and “3 *tj1* F”), suggesting that cells may tolerate up to one transposition upstream a 5S rRNA gene. These competition experiments represent only some preliminary results and it would be necessary to repeat them, analyzing way more diverse transpositions, before drawing any conclusion.

Finally, yet importantly, we wondered whether the silencing of *tj1* elements leads to fitness defects, likely as a result of the H3K9 methylation spreading observed at the readout of all the strains and the *tj1* transposed copies of some strains. The growth assays of all the silencing strains, the readout strain (0_{nat}) and a heterochromatic control strain (with *ade6* and *ura4* integrated respectively at pericentromeric and subtelomeric heterochromatin), show that silencing colonies grow slower than the heterochromatic control, indicating that silencing of *tj1* elements affects negatively the cellular fitness. Our observation suggests that additional factors, rather than *ade6* and *ura4* silencing at the readout, affect the fitness, with the spreading of heterochromatin to flanking *tj1* elements as a possible explanation. For example, previous experiments in *S. pombe* showed that spreading of heterochromatin from pericentromeric repeats leads to defective meiotic chromosome segregation (Scott et al. 2006), while heterochromatin spreading from the mating-type locus to euchromatic genes leads to growth defects (Garcia et al. 2015). In *D. melanogaster* it has been shown that TEs present at euchromatic loci induce deposition of heterochromatin marks over their sequence and flanking genes, and that the transposons that have higher heterochromatic marks are on average the least frequent TEs in the genome, indirectly suggesting that their epigenetic effects on neighboring genes affect negatively the host fitness (Y. C. G. Lee 2015; Y. C. G. Lee and Karpen 2017; Ninova et al. 2020). Accordingly, in *A. thaliana* strongly heterochromatic TEs are on average less abundant in the genome and more distant from protein-coding genes than not-heterochromatic TEs, suggesting that spreading of heterochromatin from the TEs to neighboring genes has been negatively selected because of its negative effects in the host (Hollister and Gaut 2009). In our study, heterochromatin spreading from *tj1* to flanking regions was observed also in *trans* silenced elements on plasmids, where heterochromatin spans over the *LEU2* gene (Figure 3.19A). The impossibility to obtain stable

red colonies in a strain forced to keep the plasmids (and therefore *LEU2* expression), suggests a balanced action between the transposon repression and the expression of flanking genes, in order to maintain the element “sufficiently” silenced, yet allowing the expression of the neighboring *LEU2* gene (Figure 3.19C). In *S. pombe*, spreading of heterochromatin from subtelomeric regions to flanking euchromatin, promoted by the impairment of heterochromatin boundary elements, causes growth defects (Wang et al 2015). Interestingly, to balance the negative fitness effects of this ectopic heterochromatin spreading, cells deposit H3K9me2 at *clr4* gene, in a negative feedback loop with the aim of repressing the same enzyme responsible for the heterochromatin spreading (Wang et al. 2015). Similarly, when the RNAi machinery triggers ectopic heterochromatin formation at euchromatic genes (as result of defective sRNA decay processes), RNAi genes themselves acquire H3K9 methylations (Pisacane and Halic 2017). In our study, however, none of the *tj1* silencing strains presents H3K9 methylations at genes involved in RNAi-dependent heterochromatin formation (data not shown), suggesting that *tj1* silencing represents an evolutionary priority for the host.

Overall, our experiments show that silencing of *tj1* leads to negative effects on the cell fitness, likely as the result of spreading of heterochromatin over *tj1* flanking genes and their subsequent transcriptional repression. It is intriguing to propose an evolutionary model where *de novo* transposon silencing through heterochromatin represents a double-edged sword, where potentially detrimental transpositions are blocked, yet this activity negatively affects the cell fitness. In other words, the rapid and efficient response to the *tj1* invasion represents a cell “strategy” to avoid further (potentially) lethal transpositions, accepting the (milder) side effects that *tj1* silencing through heterochromatin brings.

4.7 Conclusions and future perspectives

The aim of this study was to simulate an exogenous transposon invasion in *S. pombe* to investigate whether fission yeast carries a mechanism capable to block the potentially detrimental transposon propagation, and, if so, what features the TE has to be identifiable as a non-self DNA. *Tj1*, an LTR-retrotransposon from *S. japonicus* active in *S. pombe*, was utilized. Our results show that fission yeast actively recognizes the retrotransposon already when present on plasmids and, therefore, before its actual genomic integration (Figures 3.4B, 3.7C). Genomic transpositions result in a basal H3K9 methylation deposition and a reduction in *tj1* RNA accumulation (Figure 3,9). The presence of various *tj1* copies on plasmids in strains with transposed copies further enhanced this RNA reduction (Figure 3.9A-F). In any case, for the strong *tj1* silencing observed in some cells among the population, identified by red pigmentation (the result of efficient repression of the readout construct), the presence of multiple *tj1* elements was necessary (Figures 3.10 and 3.11).

However, we also proved that when *tj1* transposed close to constitutive heterochromatin, no additional copies are necessary to induce the efficient silencing observed among the cell population (Figures 3.10, 3.11 and 4.1).

We demonstrate that more important than the copy number, essential for this establishment of efficient silencing among the population is the bidirectional transcription of the *tj1* elements (Figure 3.8).

We showed that transposition location, rather than the copy number itself, is as well important for the maintenance of *tj1* repression through generations, with strains carrying *tj1* elements close to constitutive heterochromatin showing more stable inheritance of the repression state (Figures 3.12, 3.13 and 4.1).

Our epigenetic studies in silencing colonies showed that all the *tj1* copies dispersed over the genome (and on plasmids) are strongly *trans* repressed through deposition of H3K9 methylation, in a process guided by *tj1* sRNAs (Figures 3.5, 3.14, 3.19A and 4.1). This represents the first evidence in fission yeast of a *trans* acting mechanism of gene repression in a completely wild-type genotype, where the only genetic manipulation consisted of the cloning of the readout construct, where *tj1* transpositions within the genome were the result of the natural propagation of the retroelement and where its silencing was the outcome of innate *tj1* properties. Additionally, we observed the generation of secondary sRNAs close to a *trans* silenced region (Figures 3.5C and 3.15A).

We demonstrated that initial recognition and maintenance of the silencing states are processes that require Ago1, suggesting that, together with the sRNA presence in correspondence of heterochromatic *tj1*, silencing of the retrotransposon is mediated by the canonical fission yeast RNAi machinery (Figures 3.22 and 4.1). In support of this, Abp1, a DNA binding protein principally involved in the RNAi-independent repression of the endogenous *tt2* retroelement, is not recruited at *tj1* in silencing cells (Figure 3.23).

Our experiments showed also that heterochromatin spreads from the repressed *tj1* copies to flanking genes (in a process mostly RNAi independent) and that these H3K9 methylated genes are on average repressed (Figures 3.16A,B, 3.17, 3.18, 3.19A, 3.20, 3.21 and 4.1). In this context, on average silencing colonies present fitness disadvantages compared to not silencing colonies, suggesting that epigenetic repression of *tj1* flanking genes represents the negative side effect of the transposon repression (Figure 3.25).

In *S. japonicus*, *tj1* elements are clustered at centromeric and telomeric heterochromatin, where they are kept silenced (Rhind et al. 2011). Interestingly, CENP-B homologous genes appeared in the *S. pombe* genome after its evolutionary divergence with *S. japonicus* (apparently as result of the domestication of a Pogo-like DNA transposase) and, therefore, the latter doesn't present CENP-B homologues (among which Abp1 is found) (Casola et al. 2008; Rhind et al. 2011). This could explain why in *S. japonicus* *tj1* elements are conserved at heterochromatin, in order to maintain their silencing, lacking an alternative RNAi-independent machinery capable of their repression. On the other hand, CENP-B homologue acquisition in *S. pombe* and their direct role in repressing endogenous retrotransposons, permitted the eradication of TEs from the constitutive heterochromatic regions, in fact, absent in nowadays genomes. Our experiments indicate that, in the

absence of *tj1* specific DNA binding proteins capable to trigger the silencing of the exogenous transposon, an ancestral RNAi-mediated mechanism guides the prompt interruption of the transposon propagation, in a sort of retrotransposon survey process. Moreover, our findings showing that the more efficient initiation of silencing and maintenance of *tj1* repression through generations are in strains with pericentromeric *tj1* insertions, suggest that *tj1* might (temporarily) accumulate at centromeres, therefore repopulating constitutive heterochromatin with transposon elements, waiting for the eventual development of *tj1* binding specific proteins to guide *tj1* silencing (like CENP-B homologues with *tf2*), re-permitting the centromeric transposon eradication. In this scenario, the acquisition of an RNAi- and heterochromatin-independent mechanism for *tj1* recognition would as well diminish the negative selective effects caused by the spreading of heterochromatin from *tj1* elements (transposed at euchromatic loci) to the flanking genes.

In this perspective, it would be interesting to see if *S. pombe* (rapidly) develops a more convenient RNAi-independent mechanism to repress *tj1*. In fission yeast, the establishment (but not the maintenance) of heterochromatin at pericentromeric repeats depends on the generation of primal small RNAs (priRNAs), a class of sRNAs derived from the processing of bidirectional centromeric transcripts by the 3'-5' exonuclease Triman protein (Tri1) (Halic and Moazed 2010; Marasovic et al. 2013). In the future, the study of *tj1* recognition in strains with defective Tri1 would help understanding if the silencing of the elements observed in this study, requires the initial activity of the 3'-5' exonuclease, like at pericentromeric heterochromatin, or if, on the contrary, efficient Ago1-bound sRNAs are generated independently of Triman. Additionally, Tri1 mutation in *tj1* silencing background strains would show whether the maintenance of *tj1* repression is priRNAs-dependent or not. We showed that *S. pombe* recognizes and represses *tj1*, an LTR-retrotransposon belonging to the Class I of transportable elements, where transposon moves through an RNA-intermediate. Therefore, it would be interesting to see if fission yeast uses the same molecular tool to recognize Class II Transposable elements (represented by TEs that move via a DNA-intermediate), if it rather uses a different mechanism or if it is instead not capable at all to recognize TEs of this Class.

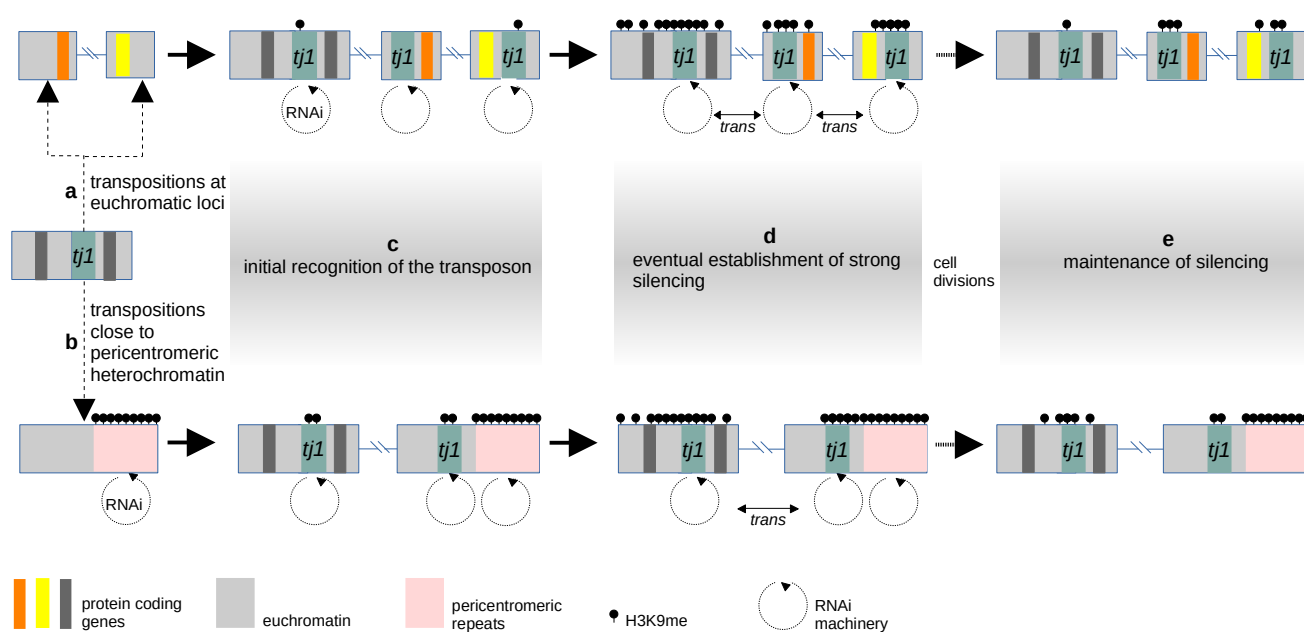


Figure 4.1: Model for *tj1* transposition at euchromatic and heterochromatic targets; initial repression, strong silencing in some cells among the population and differential maintenance of silencing.

Tj1 can transpose either at euchromatic (a) or at constitutive heterochromatic loci (b). Cells initiate a general transposon repression (supposedly) via a co-transcriptional RNAi-mediated silencing and consequent deposition of basal H3K9 methylations (c). Some cells among the population establish strong *tj1* silencing, leading to the efficient *trans* repression of all *tj1* elements through an RNAi-dependent heterochromatinization mechanism (spreading also to *tj1* flanking regions) (d). Cells with transposition(s) at constitutive heterochromatin maintain *tj1* repression more stably through generations (e).

5. MATERIALS AND METHODS

5.1 Materials

5.1.1 Strains used in this study (Table 5.1)

strain	genotype	origin
63	h+ <i>otr1R</i> (SphI):: <i>ura4</i> + <i>ura4-DS/E leu1-32 ade6-M210</i>	SPY137 D.Moazed Lab.
65	h90 <i>otr1R</i> (SphI):: <i>ura4</i> + <i>ura4-DS/E leu1-32 ade6-M210</i> <i>natMX6::3xFLAG-ago1</i>	SPY797 D.Moazed Lab.
78	h- <i>leu1-32 ade6-M210 ura4-D18 his3-Dr</i>	SPY78 D.Moazed Lab.
1267	h- <i>leu1-32 ade6-M210 ura4-D18 his3-Dr Δtf2-5::readout(neo)</i>	
1273	1267 silencing colony	
1276	1273 not silencing colony	
1344	h- <i>leu1-32 ade6-M210 ura4-D18 his3-Dr Δtf2-5::readout(nat)</i>	
1352	h- <i>leu1-32 ade6-M210 ura4-D18 his3-Dr Δtf2-5::readout(nat)</i> <i>SPCTRNAHIS.04::tj1</i>	
1370	1352 silencing colony	
1371	1370 not silencing colony	
1363	h- <i>leu1-32 ade6-M210 ura4-D18 his3-Dr Δtf2-5::readout(nat)</i> <i>SPATRNALYS.03::tj1</i>	
1399	1363 silencing colony	
1409	1399 not silencing colony	
1365	h- <i>leu1-32 ade6-M210 ura4-D18 his3-Dr Δtf2-5::readout(nat)</i> <i>SPATRNAVAL.03::tj1</i>	
1366	h- <i>leu1-32 ade6-M210 ura4-D18 his3-Dr Δtf2-5::readout(nat)</i> <i>SPRRNA.20::TGax-tj1</i>	
1374	h- <i>leu1-32 ade6-M210 ura4-D18 his3-Dr Δtf2-5::readout(nat)</i> <i>SPBTRNAMET.06::tj1</i>	
1375	h- <i>leu1-32 ade6-M210 ura4-D18 his3-Dr Δtf2-5::readout(nat)</i> <i>SPBTRNAGLN.03::tj1</i>	
1376	h- <i>leu1-32 ade6-M210 ura4-D18 his3-Dr Δtf2-5::readout(nat)</i> <i>SPATRNASLU.04::TGax-tj1</i>	
1407	1376 silencing colony	
1412	1407 not silencing colony	
1386	h- <i>leu1-32 ade6-M210 ura4-D18 his3-Dr Δtf2-5::readout(nat)</i> <i>SPATRNASHR.01::TGax-tj1</i>	

1415	1386 silencing colony	
1418	1415 not silencing colony	
1416	h- <i>leu1-32 ade6-M210 ura4-D18 his3-Dr Δtf2-5::readout(nat)</i> <i>SPRRNA.24::TGAx-tj1</i>	
1448	1416 silencing colony	
1453	1448 not silencing colony	
1417	h- <i>leu1-32 ade6-M210 ura4-D18 his3-Dr Δtf2-5::readout(nat)</i> <i>SPRRNA.16::TGAx-tj1</i>	
1442	1417 silencing colony	
1446	1442 not silencing colony	
1419	h- <i>leu1-32 ade6-M210 ura4-D18 his3-Dr Δtf2-5::readout(nat)</i> <i>SPCTRNASER.13::TGAx-tj1</i>	
1427	h- <i>leu1-32 ade6-M210 ura4-D18 his3-Dr Δtf2-5::readout(nat)</i> <i>SPRRNA.16::TGAx-tj1 SPRRNA.19::TGAx-tj1</i>	
1456	1427 silencing colony	
1457	1456 not silencing colony	
1428	h- <i>leu1-32 ade6-M210 ura4-D18 his3-Dr Δtf2-5::readout(nat)</i> <i>SPRRNA.24::TGAx-tj1 SPATRNAGLU.06::TGAx-tj1</i>	
1433	1428 silencing colony	
1439	1433 not silencing colony	
1299	h- <i>leu1-32 ade6-M210 ura4-D18 his3-Dr Δtf2-5::readout(neo)</i> <i>natMX6::3xFLAG-ago1</i> silencing colony	
1301	1299 not silencing colony	
1379	h- <i>leu1-32 ade6-M210 ura4-D18 his3-Dr Δtf2-5::readout(nat)</i> <i>SPCTRNAHIS.04::tj1 hph::3xFLAG-ago1</i>	
1450	h- <i>leu1-32 ade6-M210 ura4-D18 his3-Dr Δtf2-5::readout(nat)</i> <i>SPATRNAGLU.04::TGAx-tj1 hph::3xFLAG-ago1</i>	
1423	h- <i>leu1-32 ade6-M210 ura4-D18 his3-Dr Δtf2-5::readout(nat)</i> <i>hph::cbp1(SPBC1105.04c)-3XFLAG</i>	
1430	1423 silencing colony	
1437	1430 not silencing colony	
1395	h- <i>leu1-32 ade6-M210 ura4-D18 his3-Dr Δtf2-5::readout(nat)</i> <i>SPCTRNAHIS.04::tj1 Δago1::hph</i>	
1354	h- <i>leu1-32 ade6-M210 ura4-D18 his3-Dr Δtf2-5::readout(nat)</i> <i>Δago1::hph</i>	
588	h90 <i>tel(1L)::his3 tel(2L)::ura4 otr1R::ade6</i>	Nimmo et al. 1998

5.1.2 Plasmids used in this study (Table 5.2)

number	description	origin
p1036	TGAX-tj1::neo <i>URA3</i>	Guo et al. 2005
p1076	TGAX-tj1::neo <i>LEU2</i> (donor plasmid_neo)	
p1081	nmt81p::tj1(ORF)::nmt1T <i>his3</i> (expression plasmid)	
p1263	tj1::neo(AI) <i>LEU2</i> (wt plasmid_neo_AI)	
p1265	TGAX-tj1::neo(AI) <i>LEU2</i> (donor plasmid_neo_AI)	
p1282	tj1::hph(AI) <i>LEU2</i> (wt plasmid_hph_AI)	
p1281	TGAX-tj1::hph(AI) <i>LEU2</i> (donor plasmid_hph_AI)	
p1290	Δ 5'LTR::tj1::neo(AI) <i>LEU2</i>	
p1125	232bp_5'OE ::readout(neo)::500bp_3'OE 3'	
p1251	readout(nat)	

5.1.3 Strains + plasmids used in this study (Table 5.3)

strain + plasmid(s)	genotype	number
1267 + p1076	h- <i>leu1-32 ade6-M210 ura4-D18 his3-Dr Δt2-5::readout(neo)</i> + donor plasmid_neo	185
1267 + p1076 + p1081	h- <i>leu1-32 ade6-M210 ura4-D18 his3-Dr Δt2-5::readout(neo)</i> + donor plasmid_neo + expression plasmid	187
1344 + p1265	h- <i>leu1-32 ade6-M210 ura4-D18 his3-Dr Δt2-5::readout(nat)</i> + donor plasmid_neo(AI)	315
1344 + p1263	h- <i>leu1-32 ade6-M210 ura4-D18 his3-Dr Δt2-5::readout(nat)</i> + wt plasmid_neo(AI)	320
1344 + p1265 + p1081	h- <i>leu1-32 ade6-M210 ura4-D18 his3-Dr Δt2-5::readout(nat)</i> + donor plasmid_neo(AI) + expression plasmid	331
1352 + p1282	h- <i>leu1-32 ade6-M210 ura4-D18 his3-Dr Δt2-5::readout(nat)</i> <i>SPCTRNAHIS.04::tj1</i> + wt plasmid_hph(AI)	362
1363 + p1282	h- <i>leu1-32 ade6-M210 ura4-D18 his3-Dr Δt2-5::readout(nat)</i> <i>SPATRNALYS.03::tj1</i> + wt plasmid_hph(AI)	364
1365 + p1282	h- <i>leu1-32 ade6-M210 ura4-D18 his3-Dr Δt2-5::readout(nat)</i> <i>SPATRNAVAL.03::tj1</i> + wt plasmid_hph(AI)	368
1376 + p1281	h- <i>leu1-32 ade6-M210 ura4-D18 his3-Dr Δt2-5::readout(nat)</i> <i>SPATR NAGLU.04::TGAX-tj1</i> + donor plasmid_hph(AI)	376
1386 + p1281	h- <i>leu1-32 ade6-M210 ura4-D18 his3-Dr Δt2-5::readout(nat)</i> <i>SPATR NATHR.01::TGAX-tj1</i> + donor plasmid_hph(AI)	394
1416 + p1281	h- <i>leu1-32 ade6-M210 ura4-D18 his3-Dr Δt2-5::readout(nat)</i> <i>SPRRNA.24::TGAX-tj1</i> + donor plasmid_hph(AI)	418

1417 p1281	+	h- <i>leu1-32 ade6-M210 ura4-D18 his3-Dr Δtf2-5::readout(nat) SPRRNA.16::TGAx-tj1</i> + donor plasmid_hph(AI)	420
1416 p1281 p1081	+	h- <i>leu1-32 ade6-M210 ura4-D18 his3-Dr Δtf2-5::readout(nat) SPRRNA.24::TGAx-tj1</i> + donor plasmid_hph(AI) + expression plasmid	422
1417 p1281 p1081	+	h- <i>leu1-32 ade6-M210 ura4-D18 his3-Dr Δtf2-5::readout(nat) SPRRNA.16::TGAx-tj1</i> + donor plasmid_hph(AI) + expression plasmid	424
1427 p1281	+	h- <i>leu1-32 ade6-M210 ura4-D18 his3-Dr Δtf2-5::readout(nat) SPRRNA.16::TGAx-tj1 SPRRNA.19::TGAx-tj1</i> + donor plasmid_hph(AI)	429
1428 p1281	+	h- <i>leu1-32 ade6-M210 ura4-D18 his3-Dr Δtf2-5::readout(nat) SPRRNA.24::TGAx-tj1 SPATRAGLU.06::TGAx-tj1</i> + donor plasmid_hph(AI)	431
1344 p1290	+	h- <i>leu1-32 ade6-M210 ura4-D18 his3-Dr Δtf2-5::readout(nat)</i> + donor plasmid_neo(AI) + Δ5'LTR::tj1::neo(AI) plasmid	399
1354 p1263	+	h- <i>leu1-32 ade6-M210 ura4-D18 his3-Dr Δtf2-5::readout(nat) Δago1::hph</i> + wt plasmid_neo(AI)	374
1354 p1282	+	h- <i>leu1-32 ade6-M210 ura4-D18 his3-Dr Δtf2-5::readout(nat) Δago1::hph</i> + wt plasmid_hph(AI)	375

5.1.4 Oligonucleotides used in this study (Table 5.4)

number	gene/ construct	sequence	experiment
1152F	<i>LEU2</i>	GGACTAGTATGTCTGCCCTAAGAAGATC	cloning
1152R	<i>LEU2</i>	TTGGCGCGCCTTAAGCAAGGATTTTCTTA	cloning
1153F	<i>LEU2</i>	TTGGCGCGCCAAAAGTATTATAAGTAAATGC	cloning
1153R	<i>LEU2</i>	GGACTAGTGATTTATCTTCGTTTCCTG	cloning
1232F2	readout(neo)	TTAACGATGCATTGCGATTTTGTAG	cloning
1232R	readout(neo)	GAACCATCATTATAGTGAGGTGTTTGG	cloning
1170Fe	readout(nat)	GATACAGACCACAAACAAATGG	cloning
1022F	readout(nat)	CTGCTTCAAACCGCTAACAA	cloning
1158F	nmt81::tj1(ORF)::nmt1T	ATTGGAAGTGGATAACTAAAAGGAATGTCTCCCTTGC	cloning
1158R	nmt81::tj1(ORF)::nmt1T	AATGGATTGGAAGTACCTCGAGGTATGATTTAACAAAGC	cloning
1159F	nmt81::tj1(ORF)::nmt1T	TACTTCCAATCCATTGCAAATGGAATC GGCTTCC	cloning

1159R	nmt81::tj1(ORF)::nmt1T	TTATCCACTTCCAATGTCAAGATTCTT CGGAATCTTC	cloning
1118F	<i>his3</i>	AAAAGCTAGCTAGAATGGTATATCCTT GAA	cloning
1118R	<i>his3</i>	TTCGCCATGGAAAGATTCTCTTTTTTTA TGA	cloning
1119F	<i>his3</i>	AAACCATGGTCATTTTTTTGTATAGTAT TCC	cloning
1119R	<i>his3</i>	AAAGCTAGCATGTTTGATTTGAATACTT G	cloning
1309F	<i>tj1</i> to TGAx- <i>tj1</i>	CAAGAAGGACTGAACGGCCTCATC	iPCR
1309R	<i>tj1</i> to TGAx- <i>tj1</i>	CGGTCTTTGATTGTCGTATTTTGTG	iPCR
1345F	TGAx- <i>tj1</i> to <i>tj1</i>	TGACTGAACGGCCTCATCAATTCGC	iPCR
1345R	TGAx- <i>tj1</i> to <i>tj1</i>	TTCTTGCGGTCTTTGATTGTGCG	iPCR
1337F	Al_into_neo	TCTAAGCTAATCAATAGCGAGCCCATTT ATACCCATATAAATCAGC	iPCR
1337R	Al_into_neo	CTAGTAAATAGCACCTACCGATAATGT CGGGCAATCAGGTGCG	iPCR
1257F	neo to hph	TACTTCCAATCCATTGAACACCCCTTG TATTACTGTTTATG	cloning
1257R	neo to hph	TTATCCACTTCCAATGCAGAATTGGTTA ATTGGTTGTAAC	cloning
1258F	neo to hph	ATTGGAAGTGGATAACTTATTCCTTTG CCCTCGG	cloning
1258R	neo to hph	AATGGATTGGAAGTACATGGGTAAAAA GCCTGAACTCAC	cloning
1346F	Al_into_hph	TCTAAGCTAATCAATAGCGCATATGAAA TCACGCCATG	iPCR
1346R	Al_into_hph	CTAGTAAATAGCACCTACCGATTGCT GATCCCCATGTGTATC	iPCR
219F	<i>act1</i>	GATTCTCATGGAGCGTGGTT	qPCR
219R	<i>act1</i>	CTCATGAATACCGGCGTTTT	RT, qPCR
1170Fb	<i>tj1</i>	CGAAGATTACGAAGAAGTATTTG	qPCR
1190Rb	<i>tj1</i>	CAAAAGGTTTCCTCCTGCTGC	RT, qPCR
1403R1	<i>tj1</i>	GCGCTTCTAGGATTCTCGTAAT	qPCR
1403F1	<i>tj1</i>	ATCACCGAGTGGAAAGACAAAG	RT, qPCR
255	ssRNA 22nt	UGAAAGCUUUAGUUGAUACGUC	marker

1364	ssRNA 26nt	UUUUUUUAUGUUCGAGCUUUGGUACC A	marker
254	ssRNA 30nt	UUGUUCUUUGCCUCGCUCGCUGCGU ACAUG	marker
1170Fh	neo	ACGCTACCTTTGCCATGTTTC	screening
1265R	neo	GAAACGTCTTGTTCGAGGC	screening
1348F	hph	CAGTCCTCGGCCCAAAGC	screening
1348R	hph	CGGGTTCGGCCATTTCG	screening
843F	LEU2	GAACAATACACCGTTCCAGA	screening
843R	LEU2	ATACCATTTAGGTGGGTTGG	screening
1109F	his3	ATGTTTGATTTGAATACTTGTCTTC	screening
1109R	his3	TCATTTTTTTGTATAGTATTCCTGC	screening

RT= Reverse Transcription, qPCR= quantitative PCR, iPCR= inverse PCR, marker= oligonucleotides used as size marker for the Ago1-bound sRNA assay, screening= PCR to screen colonies, underlined sequence= restriction enzyme sites

5.1.5 Media used in this study (Table 5.5)

name	organism	recipe
LB	<i>E.coli</i>	10g/l NaCl, 5g/l Yeast Extract, 10g/l Tryptone
YES	<i>S.pombe</i>	5g/l Yeast Extract, 30g/l glucose, 0.226 g/l leucine, histidine, lysine, adenine,uracil (+ 20g/l agar for solid plates)
YE	<i>S.pombe</i>	5g/l Yeast Extract, 30g/l glucose (+ 20g/l agar for solid plates)
PMG	<i>S.pombe</i>	EMM glutammate (Formedium) 31g/l, 0.226 g/l leucine, histidine, lysine, adenine, uracil (+ 20g/l agar for solid plates)
PMG -leu	<i>S.pombe</i>	Same as PMG, excluding leucine
PMG -his	<i>S.pombe</i>	Same as PMG, excluding histidine
PMG -leu -his	<i>S.pombe</i>	Same as PMG, excluding leucine and histidine
PMG low ade	<i>S.pombe</i>	EMM glutammate (Formedium) 31g/l, 0.226 g/l leucine, histidine, lysine, uracil, 0.004g/l adenine, 20g/l agar
PMG low ade - leu	<i>S.pombe</i>	Same as PMG low ade, excluding leucine
EMMC -ura - ade	<i>S.pombe</i>	12.4 g/l EMM without dextrose (Formedium), 0.226 g/l leucine, histidine, lysine,uracil, 20g/l agar
EMMC -leu	<i>S.pombe</i>	12.4 g/l EMM without dextrose (Formedium),0.226 g/l histidine, lysine, adenine,uracil (+ 20g/l agar for solid plates)
EMMC -his	<i>S.pombe</i>	12.4 g/l EMM without dextrose (Formedium),0.226 g/l leucine, lysine, adenine,uracil (+ 20g/l agar for solid plates)

EMMC +5FOA	<i>S.pombe</i>	12.4 g/l EMM without dextrose (Formedium), 0.226 g/l leucine, histidine, lysine, adenine, uracil, 0.1g/l 5-Fluoroorotic acid (5FOA), 20g/l agar
YES +G418	<i>S.pombe</i>	Same as YES, adding 0.2g/l G418
YES +nourseothricin	<i>S.pombe</i>	Same as YES, adding 0.1g/l nourseothricin
YES +hygromycin B	<i>S.pombe</i>	Same as YES, adding 0.2g/l hygromycin B
YES +G418 +nourseothricin	<i>S.pombe</i>	Same as YES, adding 0.2g/l G418 and 0.1g/l nourseothricin
YES +G418 +nourseothricin +hygromycin B	<i>S.pombe</i>	Same as YES, adding 0.2g/l G418, 0.1g/l nourseothricin and 0.2g/l hygromycin B

5.1.6 Antibodies used in this study (Table 5.6)

name	experiment
FLAG-M2 agarose beads (Sigma-Aldrich, A2220)	Ago1-bound sRNA seq Abp1-ChIP seq
Anti-H3K9me2, Abcam (1220)*	H3K9me2-ChIP seq
Anti-H3 Abcam (176842)*	H3-ChIP seq

*bound to Dynabeads Protein A (Invitrogen)

5.1.7 Sequenced strains (Table 5.7)

strain	experiment					
	total RNA seq	polyA-RNA seq	H3K9me2-Chip seq	H3-Chip seq	Ago1-bound sRNA seq	Abp1-ChIP seq
wild-type (63)				✓ P		
wild-type (65)					✓ P	
O_{neo} (1273, 1276, 1299, 1301)	✓ S,NS	✓ S,NS	✓ S,NS		✓ S,NS	
O_{nat} (1344, 1423, 1430, 1437)	✓ P	✓ P	✓ P	✓ P		✓ P,S,NS

"2 <i>tj1</i> A" (1352, 1370, 1371, 1379)	P, [✓] S,NS	P, [✓] S,NS	P, [✓] S,NS	✓ P	✓ S	
"2 <i>tj1</i> B" (1363, 1399, 1409)	P, [✓] S,NS	P, [✓] S,NS	P, [✓] S,NS	✓ P		
"2 <i>tj1</i> D" (1386, 1415, 1418)	P, [✓] S,NS	P, [✓] S,NS	P, [✓] S,NS	✓ P		
"2 <i>tj1</i> E" (1416, 1448, 1453)	P, [✓] S,NS	P, [✓] S,NS	P, [✓] S,NS	✓ P		
"2 <i>tj1</i> F" (1417, 1442, 1446)	P, [✓] S,NS	P, [✓] S,NS	P, [✓] S,NS	✓ P		
"2 <i>tj1</i> G" (1376, 1407, 1412, 1450)	P, [✓] S,NS	P, [✓] S,NS	P, [✓] S,NS	✓ P	✓ S	
"3 <i>tj1</i> EL" (1428, 1433, 1439)	P, [✓] S,NS	P, [✓] S,NS	P, [✓] S,NS	✓ P		
"3 <i>tj1</i> FM" (1427, 1456, 1457)	P, [✓] S,NS	P, [✓] S,NS	P, [✓] S,NS	✓ P		
"2 <i>tj1</i> G" +plasmids "2 <i>tj1</i> D" +plasmids (376 394)			S, [✓] NS			

P=population, S=silencing colony, NS=not silencing colony (white from red)

5.2 Methods

5.2.1 Strain and plasmid construction

The strains and plasmids generated and used in this study are listed in Tables 5.1 and 5.2. The oligonucleotides used for the cloning procedures are indicated in Table 5.4. To integrate the readout into the genome replacing *tt2-5*, 30-40 ml of *S. pombe* cells were grown in liquid YES, harvested at OD₆₀₀ = 0.3, transformed with ~500ng of a purified readout PCR product (via electroporation, BioRad MicroPulser program ShS) and plated on YES plates. The next day cells were replica plated on YES supplemented with the appropriate antibiotic. Single colonies were isolated and the success of the cloning was verified by PCR and sequencing of the integration loci (Eurofins). Similarly, 3XFLAG tagging of Ago1 and Abp1 was performed, integrating the epitope at N- and C- terminal respectively. Plasmids were generated by inverse PCR, restriction enzyme based cloning and LIC (Ligation Independent Cloning). In all cases, XL1 Blue *E.coli* cells were heat-shock transformed with the plasmids generated, to amplify and store them after positive screening via PCR and sequencing. The LIC protocol was performed as described by Wang and colleagues (T. Wang et al. 2012); briefly, the insert and the vector are amplified by PCR using specific primers with the aim of generating compatible overhangs of ~15bp. The overhangs contain the first nucleotide that is unique in the rest

of the sequence. This design, combined with the exonuclease activity of the T4-DNA polymerase (ThermoFisher), permits the 3' to 5' digestion of the overhangs up to the unique nucleotide, specifically included in the T4-DNA polymerase reaction mix. The insert and vector so generated are mixed at adequate molar ratios to ensure the base pairing between the overhangs of the constructs. The products are transformed into XL1 Blue *E.coli*.

All the PCR reactions for the cloning processes were performed using the High-fidelity PCR Master Mix (Thermo Fischer Scientific). All the PCR product and plasmid purifications were performed using the NucleoSpin Gel and PCR Clean-Up kit (Macherey-Nagel).

5.2.2 Spot and silencing establishment assays

The spot assay was performed using cultures of *S. pombe* at $OD_{600} = 0.7$ grown in the appropriate media; PMG if plasmids were not present, PMG depleted of specific supplement(s) when cells carried plasmids. After washing in autoclaved water, serial dilutions of cells were plated in the needed media, having from ten up to one million cells in each spot.

The silencing establishment assay was performed growing cells over-night in the appropriate PMG media (according to the presence of plasmids). The cultures of exponentially growing cells were refreshed daily to keep them growing exponentially. 30.000 cells were plated in PMG low ade media (using 15mm diameter plates, ThermoFisher) at days 1, 3, 5, 7 and 10 (corresponding to 10, 30, 50, 70 and 100 cell generations). The plates were kept at 32°C for 3 days followed by one over-night incubation at 4°C to highlight the eventual red pigmentation of *tj1* silencing colonies. The number of red colonies in each strain at each day was annotated and the establishment average was calculated.

5.2.3 Transposition induction and isolation of colonies with transposed *tj1*

To induce *tj1* transposition, the strain 0_{nat} was transformed either with p1263 (wt *tj1* plasmid) or with the combination of p1265 and p1081 (donor and expression plasmids, respectively). Both p1263 and p1265 contain the *neo* cassette oriented in opposite direction to *tj1*. *neo* is interrupted by an artificial intron (AI) in frame with *tj1*. This construct permits to have G418-resistant cells only when a complete *tj1* integration cycle is completed (Heidmann, Heidmann, and Nicolas 1988; Levin 1995; Dang et al. 1999). However, this setup doesn't discriminate between *tj1* cDNA integrated into *S. pombe* genome or recombined with *tj1* in the plasmids. Therefore, it was necessary to first induce the cells to lose the plasmids and only afterwards screen for G418-resistant colonies. Cells were grown exponentially for 2-3 consecutive days in PMG w/o the specific supplements (according to the plasmids present) to induce *tj1* transposition. Afterwards, to induce plasmid loss, cells were switched to YES media where they were grown exponentially for 2-3 days. 25×10^6 cells were plated on YES +G418 +nourseothricin and incubated at 32°C until single colonies appeared. The resistant colonies were replica plated on EMMC w/o the specific supplements to identify antibiotic-resistant colonies

that didn't retain the plasmids, indication of a genomic transposition rather than a plasmids recombination. The identified colonies were analyzed by genomic PCR to confirm the transposition. The primers used anneal to *neo* (1170Fh/1265R) and to the plasmids marker genes. The PCR products were run on a TAE 3% agarose gel. A shorter *neo* PCR product indicates that the AI is removed and negative PCRs for the plasmids say that cells don't have plasmids, altogether indicating that *tj1* transposed into the genome. +AI and -AI PCR control were used. To induce a second *tj1* transposition, all the strains with one transposition were re-transformed with the combination of p1281 and p1081 (donor and expression plasmids, respectively). p1281 contains the *hph* cassette with the AI. The same procedure was followed, initially the transposition was induced growing cells in minimal media to keep the plasmids, afterwards cells were switched to YES to lose the plasmids and 100×10^6 cells were plated on YES +G418 +nourseothricin +hygromycin B. The antibiotic-resistant colonies were replica-plated on EMMC -leu and EMMC -his, to select resistant colonies w/o plasmids. These colonies were screened by genomic PCRs using primers for *hph* (1348F/R), *LEU2* and *his3* to confirm the AI-absence and the plasmid loss, as described before for *neo*. Finally, *tj1* transposition(s) were mapped on the genome by Illumina and/or nanopore sequencings (see Section 5.2.8).

5.2.4 Silencing maintenance assay

The assay to investigate the maintenance of silencing in red colonies was performed selecting red colonies which were subsequently grown exponentially for 2 days in YES to induce the loss of the plasmids eventually present. 100 cells were plated in YE and replica printed in the adequate EMMC media to screen for plasmid loss. Red colonies in YE which didn't grow on the EMMC replicas were selected as silencing and plasmid depleted. These colonies were enriched for red pigmentation after plating them in PMG low ade resulted in at least 75% of red colonies among all the colonies. Starting from a stably silencing colony, cells were grown exponentially in YES up to 7 days and ~1000 cells were plated in PMG low ade at days 1, 3 and 7 (corresponding to 10, 30 and 70 cell generations). The number of red colonies in each plate was counted and the % was calculated.

5.2.5 Growth curve and competition assays

To investigate the cellular fitness, the growth curve of the investigated strains was studied. Cells were incubated at 32°C overnight in YES liquid media to have them exponentially growing the morning of the following day. The OD_{600} was measured and all the cultures were diluted to $OD_{600} = 0.2$ and incubated for 30 minutes and the OD_{600} was measured again. This measurement consisted in the initial OD_{600} and it was normalized to 0.2. The OD_{600} was measured again after 2, 4 and 6 hours, leading to the generation of the growth curve.

To investigate the growth competition between the 0_{nat} strain and strains with transpositions in the same culture, each strain was incubated over-night in liquid YES. Exponentially growing cells with the same OD were mixed 1:1 the following day (day 0) and kept growing exponentially up to 9 days (90 generations). ~ 1000 cells were plated in YES at days 0, 4 and 9, incubated 3 days at 32°C and replica plated either in YES +nourseothricin +G418 (in the competition assay between 0_{nat} and “2 *tjI*” strains) or in YES +nourseothricin +G418 +hygromycin B (in the competition assay between 0_{nat} and “3 *tjI*” strains). The number of colonies grown in the antibiotic plates, compared to the correspondent YES plates, furnished the % of 0_{nat} and strains with transpositions in the same culture.

5.2.6 Chromatin Immunoprecipitation and sequencing (ChIP-seq)

50 ml of mid-log phase *S. pombe* cultures were cross-linked using formaldehyde (final concentration 1%) for 15 minutes at room temperature. Afterwards, the cross-linking was quenched with 125mM glycine, incubating 5 minutes. Cells were pelleted and resuspended in lysis buffer (supplemented with 1mM PMSF and Complete EDTA free Protease Inhibitor Cocktail, Roche) keeping a 1:1 ratio with the pellet volume (~ 300 μ l). The lysis buffer used consists in: 250 mM KCl, 1x Triton-X, 0.1% SDS, 0.1% Na-Desoxycholate, 50 mM HEPES pH 7.5, 2 mM EDTA, 2 mM EGTA, 5 mM MgCl₂, 0.1% Nonidet P-40, 20% Glycerol. The cellular lysis was performed adding glass beads to the cells and bead beating them (BioSpec FastPrep-24 bead beater, MP-Biomedicals) for 8 cycles at 6.5 m/s for 30s followed by 3 min on ice. DNA was sheared by sonication (Bioruptor, Diagenode) 35 times for 30s with a 30s break. Cell debris were eliminated taking the supernatant after a centrifugation at 13000g for 15 min. The crude lysate obtained was normalized measuring the RNA concentration (Nanodrop, Thermo Fischer Scientific). 5 μ l of magnetic resin (Dynabeads Protein A, Thermo Scientific) per reaction were coupled with 1.2 μ g of antibody either against H3K9me2 (Abcam 1220) or H3 (Abcam 176842), according to the assay performed, and incubated with the cell lysate over-night at 4°C with gentle rotation. In the case of the Abp1-ChIP, 30 μ l of FLAG-M2 agarose resin (Sigma-Aldrich A2220) were incubated with the crude lysate, followed by over-night incubation at 4°C with gentle rotation. The IP was washed five times with 1ml of lysate buffer and eluted with 150 μ l of elution buffer (50 mM Tris-Cl pH 8.0, 10 mM EDTA, 1% SDS) at 65°C for 15 min. The RNA protein were removed from the IP adding 2 μ l of RNase A (Thermo Fischer Scientific) and Proteinase K (Roche) and incubating at 65°C for at least 5 hours. Finally, the pure DNA was recovered using phenol-chloroform-isoamylalcohol (25:24:1, Roth) followed by ethanol precipitation. For deep illumina sequencing, a ChIP-seq library was prepared using the NEBNext Ultra II DNA Library Prep Kit for Illumina kit (NEB), following the kit instructions. Single end sequencing was performed on an Illumina GAIIIX sequencer at the LAFUGA core facility of the Gene Center, Munich. The Galaxy platform was used to demultiplex the obtained reads.

5.2.7 Ago1-bound sRNA sequencing

The purification and sequencing of Ago1-bound sRNAs were performed as indicated by Pisacane (Pisacane and Halic 2017). Briefly, strains with the endogenous Ago1 3xFLAG tagged were grown in YES and 2.5l of log phase cells were collected. Cells were resuspended in lysis buffer (50 mM HEPES pH 7.5, 1.5 M NaOAc, 5 mM MgCl₂, 2 mM EDTA pH 8, 2 mM EGTA pH 8, 0.1% Nonidet P-40, 20% glycerol) supplemented with 1mM PMSF and Complete EDTA free Protease Inhibitor Cocktail (Roche), keeping a 1:1 ratio between the cell volume and the buffer. Cells were fragmented using glass beads and the bead beater as described for the ChIP protocol. The cell debris was eliminated by centrifugation at 13000g and the crude lysate was incubated with 30µl of FLAG-M2 agarose resin (Sigma-Aldrich A2220) at 4°C for 2h with gentle rotation. The IP was washed five times with the lysis buffer and Ago1 was eluted from the resin mixing 1% SDS with 300 mM NaOAc and phenol-chloroform-isoamylalcohol (25:24:1, Roth). The sRNAs were concentrated by ethanol precipitation, run on an 18% polyacrylamide urea gel together with 22, 26 and 30 nt RNA markers and the bands of sizes between 20 and 30 nt were excised from the gel. A 3' linker was ligated to the sRNAs (5' rAppCTGTAGGCACCATCAAT-NH₂ 3', NEB, reaction concentration 2µM). The 3' ligated products were purified on an 18% acrylamide urea gel with subsequent phenol-chloroform purification and ethanol purification. The 5' adaptor (5'-ACACUCUUUCCCUACACGACGCUC UUCCGAUCU-3', Metabion) ligation was performed, followed by reverse transcription (RT primer: 5'- GTGACTGGAGTTCAGACGTGTGCTCTTCCGATCGATTGATGGTGCCTACAG -3', Metabion). The cDNA was amplified with 12-20 PCR cycles using the Phusion hot start II DNA polymerase kit (ThermoFisher) and the Illumina P5 5' primer (5' -AAT GAT ACG GCG ACC ACC GAG ATC TAC ACT CTT TCC CTA CAC GAC G -3') together with the Illumina P7 3' primer with inserted barcode (5'-CAA GCA GAA GAC GGC ATA CGA GAT XXXXXX GTG ACT GGA GTT CAG ACG TG -3'). The sRNA library was purified from an 8% polyacrylamide gel, ethanol precipitated and sequenced by LAFUGA facility as described for the ChIP sequencing.

5.2.8 Genomic DNA purification

Genomic DNA purification was performed in different ways depending on the subsequent DNA use. For *tj1* copy number quantification via qPCR, 50 ml of mid-log phase cells grown in the adequate liquid media were collected. The pellet was resuspended in 200µl of ChIP lysis buffer, glass beads were added and cells were lysed with 5 cycles of bead beating as described in the ChIP protocol. 50µl of lysate were diluted with 450µl of ddH₂O and treated with RNase A. The DNA was recovered with phenol-chloroform-isoamylalcohol (25:24:1, Roth) and ethanol precipitation. The precipitated DNA was resuspended in 1X TE buffer to 5ng/µl concentration and analyzed by qPCR. Genomic DNA purification for *tj1* transposition mapping via Illumina sequencing was performed similarly to the procedure described above, with the main difference that the cell lysate was sheared by sonication

and the crude lysate was separated to cell debris via centrifugation. The RNA was degraded using Rnase A and the DNA was recovered with phenol-chloroform-isoamylalcohol and ethanol precipitation. The DNA was finally resuspended in 1X TE buffer and used with the NEBNext Ultra II DNA Library Prep Kit for Illumina kit (NEB), following the kit instructions. When *tj1* transposed close to repetitive genomic sequences, like pericentromeric regions, to exactly map the transposition it was necessary to sequence the genomes via Nanopore-seq. This technique needs not fragmented DNA and in order to obtain good quality DNA the protocol described by Tusso and colleagues was followed (Tusso et al. 2019).

5.2.9 Total RNA purification, total RNA and RNA-polyA sequencings

Total RNA purification was performed collecting 2ml of mid-log phase cells grown in the adequate media. Cells were mixed with 500µl of lysis buffer (300 mM NaOAc pH 5.2, 10 mM EDTA, 1% SDS) and 500µl of phenol-chloroform-isoamylalcohol and lysed at 65°C for 10 minutes. The RNA was purified with ethanol precipitation, resuspended in DEPC treated ddH₂O and DNA contamination was eliminated with DNase I (ThermoFisher). 5mM EDTA was added to the reaction and the DNase I was heat inactivated at 75°C for 10 minutes. The total purified RNA obtained was used to make either total RNA or RNA-polyA libraries using the NEBNext Ultra Directional RNA Library Prep Kit for Illumina, following the kit instructions (skipping the polyA-RNA purification step when the total RNA library was made).

When the total purified RNA was used for RT-qPCR experiments, retro transcription was performed instead.

5.2.10 Total RNA reverse transcription (RT)

-300ng of the total RNA were retro transcribed to cDNA using the SuperScript III Reverse Transcriptase kit (ThermoFisher), following the kit instructions and adding to the reaction mix the primer necessary for the RT (Table 5.4). As -RT controls, the same amount of RNA was incubated with water, to later exclude DNA contamination.

5.2.11 Quantitative Real-Time PCR (qPCR)

qPCR was performed either on cDNA from retro transcribed RNA (and -RT controls) (to analyze the differential gene expression among strains) or in purified genomic DNA (to quantify the number of *tj1* copy present). 2X DyNAmo Flash SyBR Green Master Mix qPCR kit (BioZym) was used to prepare a 10µl reaction containing -4ng of template and specific forward and reverse primers (0.4µM) (Table 5.4). Each reaction was assembled in a 96-well plate (4titude) and performed in triplicate. When the *tj1* copy number was quantified, primers for *tj1* and *act1* were used, and *tj1* number was obtained normalizing over the one-copy gene *act1*. When transcription was analyzed, *act1* RNA was

used to normalized the input material. The qPCR cycle consisted in a DNA denaturation step at 95°C for 5 minutes, followed by 46 amplification cycles (95°C denaturation for 10s, 60°C annealing for 20s, 72°C elongation for 15s) and a final melting temperature calculation step ranging from 60°C to 95°C.

5.2.12 Analysis of sequencing data

Demultiplexed illumina reads were mapped to the *S. pombe* genome, allowing 2 nucleotides mismatch to the genome using Novoalign (<http://www.novocraft.com>). The genome sequence and annotation that were available from the *S. pombe* Genome Project were used (Wood et al. 2002). When genomic manipulations were performed and when *tj1* integrated into the genome, the correspond nucleotide sequences were manually added to the reference genome. Reads mapping to multiple locations were randomly assigned. The data were displayed using the Integrative Genomics Viewer (IGV) (Thorvaldsdóttir et al. 2013). Total RNA and RNA-polyA sequencings were normalized to the total protein coding sequence (cds) reads. H3K9me2-ChIP was normalized to the background, consisting of two H3K9me2 absent regions of 200000 bp each (chrI 80000-280000 and chrI 1780000-1980000), with the only exclusion of the H3K9me2-ChIP seq of strains with plasmids (Figure 3.19) where the normalization was done to the number of reads per one million reads (r.p.m). Ago1-bound sRNA, Abp1-ChIP, H3-ChIP and genomic DNA sequencings were normalized to the r.p.m.. The sequenced strains are listed on Table 5.7.

BIBLIOGRAPHY

- Akoury, Elias, Guoli Ma, Segolene Demolin, Cornelia Brönnner, Manuel Zocco, Alexandre Cirilo, Nives Ivic, and Mario Halic. 2019. 'Disordered Region of H3K9 Methyltransferase Clr4 Binds the Nucleosome and Contributes to Its Activity'. *Nucleic Acids Research* 47 (13): 6726–36. <https://doi.org/10.1093/nar/gkz480>.
- Allan, J., G. J. Cowling, N. Harborne, P. Cattini, R. Craigie, and H. Gould. 1981. 'Regulation of the Higher-Order Structure of Chromatin by Histones H1 and H5'. *The Journal of Cell Biology* 90 (2): 279–88. <https://doi.org/10.1083/jcb.90.2.279>.
- Allshire, R. C., E. R. Nimmo, K. Ekwall, J. P. Javerzat, and G. Cranston. 1995. 'Mutations Derepressing Silent Centromeric Domains in Fission Yeast Disrupt Chromosome Segregation'. *Genes & Development* 9 (2): 218–33. <https://doi.org/10.1101/gad.9.2.218>.
- Allshire, Robin C., and Karl Ekwall. 2015. 'Epigenetic Regulation of Chromatin States in *Schizosaccharomyces Pombe*'. *Cold Spring Harbor Perspectives in Biology* 7 (7). <https://doi.org/10.1101/cshperspect.a018770>.
- Allshire, Robin C., Jean-Paul Javerzat, Nicola J. Redhead, and Gwen Cranston. 1994. 'Position Effect Variegation at Fission Yeast Centromeres'. *Cell* 76 (1): 157–69. [https://doi.org/10.1016/0092-8674\(94\)90180-5](https://doi.org/10.1016/0092-8674(94)90180-5).
- Allshire, Robin C., and Hiten D. Madhani. 2018. 'Ten Principles of Heterochromatin Formation and Function'. *Nature Reviews Molecular Cell Biology* 19 (4): 229–44. <https://doi.org/10.1038/nrm.2017.119>.
- Andersen, Peter Refsing, Laszlo Tirian, Milica Vunjak, and Julius Brennecke. 2017. 'A Heterochromatin-Dependent Transcription Machinery Drives PiRNA Expression'. *Nature* 549 (7670): 54–59. <https://doi.org/10.1038/nature23482>.
- Anderson, Holly E., Alexander Kagansky, Josephine Wardle, Juri Rappsilber, Robin C. Allshire, and Simon K. Whitehall. 2010. 'Silencing Mediated by the *Schizosaccharomyces Pombe* HIRA Complex Is Dependent upon the Hpc2-like Protein, Hip4'. *PloS One* 5 (10): e13488. <https://doi.org/10.1371/journal.pone.0013488>.
- Anderson, Holly E., Josephine Wardle, Senay Vural Korkut, Heather E. Murton, Luis López-Maury, Jürg Bähler, and Simon K. Whitehall. 2009. 'The Fission Yeast HIRA Histone Chaperone Is Required for Promoter Silencing and the Suppression of Cryptic Antisense Transcripts'. *Molecular and Cellular Biology* 29 (18): 5158–67. <https://doi.org/10.1128/MCB.00698-09>.
- Anxolabéhère, D, M G Kidwell, and G Periquet. 1988. 'Molecular Characteristics of Diverse Populations Are Consistent with the Hypothesis of a Recent Invasion of *Drosophila Melanogaster* by Mobile P Elements.' *Molecular Biology and Evolution* 5 (3): 252–69. <https://doi.org/10.1093/oxfordjournals.molbev.a040491>.
- Anxolabéhère, Dominique, Danielle Nouaud, Georges Périquet, and Paul Tchen. 1985. 'P-Element Distribution in Eurasian Populations of *Drosophila Melanogaster*: A Genetic and Molecular Analysis'. *Proceedings of the National Academy of Sciences* 82 (16): 5418–22. <https://doi.org/10.1073/pnas.82.16.5418>.
- Aravin, Alexei A., Ravi Sachidanandam, Deborah Bourc'his, Christopher Schaefer, Dubravka Pezic, Katalin Fejes Toth, Timothy Bestor, and Gregory J. Hannon. 2008. 'A PiRNA Pathway Primed by Individual Transposons Is Linked to de Novo DNA Methylation in Mice'. *Molecular Cell* 31 (6): 785–99. <https://doi.org/10.1016/j.molcel.2008.09.003>.
- Aravin, Alexei A., Ravi Sachidanandam, Angelique Girard, Katalin Fejes-Toth, and Gregory J. Hannon. 2007. 'Developmentally Regulated PiRNA Clusters Implicate MILI in Transposon Control'. *Science (New York, N.Y.)* 316 (5825): 744–47. <https://doi.org/10.1126/science.1142612>.
- Arcangioli, B., and A. J. Klar. 1991. 'A Novel Switch-Activating Site (SAS1) and Its Cognate Binding Factor (SAP1) Required for Efficient Mat1 Switching in *Schizosaccharomyces Pombe*'. *The EMBO Journal* 10 (10): 3025–32.

- Ashe, Alyson, Alexandra Sapetschnig, Eva-Maria Weick, Jacinth Mitchell, Marloes P. Bagijn, Amy C. Cording, Anna-Lisa Doebley, et al. 2012. 'PiRNAs Can Trigger a Multigenerational Epigenetic Memory in the Germline of *C. Elegans*'. *Cell* 150 (1): 88–99. <https://doi.org/10.1016/j.cell.2012.06.018>.
- Atwood, A., J. H. Lin, and H. L. Levin. 1996. 'The Retrotransposon Tf1 Assembles Virus-like Particles That Contain Excess Gag Relative to Integrase Because of a Regulated Degradation Process'. *Molecular and Cellular Biology* 16 (1): 338–46. <https://doi.org/10.1128/mcb.16.1.338>.
- Aye, Michael, Sandra L. Dildine, Jonathan A. Claypool, Sabine Jourdain, and Suzanne B. Sandmeyer. 2001. 'A Truncation Mutant of the 95-Kilodalton Subunit of Transcription Factor III C Reveals Asymmetry in Ty3 Integration'. *Molecular and Cellular Biology* 21 (22): 7839–51. <https://doi.org/10.1128/MCB.21.22.7839-7851.2001>.
- Ayoub, Nabieh, Ken-ichi Noma, Sara Isaac, Tamar Kahan, Shiv I. S. Grewal, and Amikam Cohen. 2003. 'A Novel JmjC Domain Protein Modulates Heterochromatization in Fission Yeast'. *Molecular and Cellular Biology* 23 (12): 4356–70. <https://doi.org/10.1128/MCB.23.12.4356-4370.2003>.
- Baldi, S., Korber, P. & Becker, P.B. Beads on a string—nucleosome array arrangements and folding of the chromatin fiber. *Nat Struct Mol Biol* 27, 109–118 (2020). <https://doi.org/10.1038/s41594-019-0368-x>
- Banères, Jean-Louis, Aimée Martin, and Joseph Parello. 1997. 'The N Tails of Histones H3 and H4 Adopt a Highly Structured Conformation in the Nucleosome'. Edited by T. Richmond'. *Journal of Molecular Biology* 273 (3): 503–8. <https://doi.org/10.1006/jmbi.1997.1297>.
- Baum, M, V K Ngan, and L Clarke. 1994. 'The Centromeric K-Type Repeat and the Central Core Are Together Sufficient to Establish a Functional *Schizosaccharomyces Pombe* Centromere.' *Molecular Biology of the Cell* 5 (7): 747–61. <https://doi.org/10.1091/mbc.5.7.747>.
- Bayne, Elizabeth H., Sharon A. White, Alexander Kagansky, Dominika A. Bijos, Luis Sanchez-Pulido, Kwang-Lae Hoe, Dong-Uk Kim, et al. 2010. 'Stc1: A Critical Link between RNAi and Chromatin Modification Required for Heterochromatin Integrity'. *Cell* 140 (5): 666–77. <https://doi.org/10.1016/j.cell.2010.01.038>.
- Begniss, Martina, Manasi S. Apte, Hirohisa Masuda, Devanshi Jain, David Lee Wheeler, and Julia Promisel Cooper. 2018. 'RNAi Drives Nonreciprocal Translocations at Eroding Chromosome Ends to Establish Telomere-Free Linear Chromosomes'. *Genes & Development* 32 (7–8): 537–54. <https://doi.org/10.1101/gad.311712.118>.
- Behrens, Ralf, Jacky Hayles, and Paul Nurse. 2000. 'Fission Yeast Retrotransposon Tf1 Integration Is Targeted to 5' Ends of Open Reading Frames'. *Nucleic Acids Research* 28 (23): 4709–16.
- Bendandi, Artemi, Alessandro S. Patelli, Alberto Diaspro, and Walter Rocchia. 2020. 'The Role of Histone Tails in Nucleosome Stability: An Electrostatic Perspective'. *Computational and Structural Biotechnology Journal* 18 (January): 2799–2809. <https://doi.org/10.1016/j.csbj.2020.09.034>.
- Bernstein, E., A. A. Caudy, S. M. Hammond, and G. J. Hannon. 2001. 'Role for a Bidentate Ribonuclease in the Initiation Step of RNA Interference'. *Nature* 409 (6818): 363–66. <https://doi.org/10.1038/35053110>.
- Berretta, Julia, Marina Pinskaya, and Antonin Morillon. 2008. 'A Cryptic Unstable Transcript Mediates Transcriptional Trans-Silencing of the Ty1 Retrotransposon in *S. Cerevisiae*'. *Genes & Development* 22 (5): 615–26. <https://doi.org/10.1101/gad.458008>.
- Bilanchone, V. W., J. A. Claypool, P. T. Kinsey, and S. B. Sandmeyer. 1993. 'Positive and Negative Regulatory Elements Control Expression of the Yeast Retrotransposon Ty3'. *Genetics* 134 (3): 685–700.
- Bisht, Kamlesh Kumar, Sumit Arora, Shakil Ahmed, and Jagmohan Singh. 2008. 'Role of Heterochromatin in Suppressing Subtelomeric Recombination in Fission Yeast'. *Yeast* 25 (8): 537–48. <https://doi.org/10.1002/yea.1603>.
- Blanc, Victoria M., and Julian Adams. 2004. 'Ty1 Insertions in Intergenic Regions of the Genome of *Saccharomyces Cerevisiae* Transcribed by RNA Polymerase III Have No Detectable Selective Effect'. *FEMS Yeast Research* 4 (4–5): 487–91. [https://doi.org/10.1016/S1567-1356\(03\)00199-5](https://doi.org/10.1016/S1567-1356(03)00199-5).

- Bolton, Eric C., and Jef D. Boeke. 2003. 'Transcriptional Interactions between Yeast TRNA Genes, Flanking Genes and Ty Elements: A Genomic Point of View'. *Genome Research* 13 (2): 254-63. <https://doi.org/10.1101/gr.612203>.
- Bowen, Nathan J., I. King Jordan, Jonathan A. Epstein, Valerie Wood, and Henry L. Levin. 2003. 'Retrotransposons and Their Recognition of Pol II Promoters: A Comprehensive Survey of the Transposable Elements From the Complete Genome Sequence of Schizosaccharomyces Pombe'. *Genome Research* 13 (9): 1984-97. <https://doi.org/10.1101/gr.1191603>.
- Braun, Sigurd, Jennifer F. Garcia, Margot Rowley, Mathieu Rougemaille, Smita Shankar, and Hiten D. Madhani. 2011. 'The Cul4-Ddb1Cdt2 Ubiquitin Ligase Inhibits Invasion of a Boundary-Associated Antisilencing Factor into Heterochromatin'. *Cell* 144 (1): 41-54. <https://doi.org/10.1016/j.cell.2010.11.051>.
- Brennecke, Julius, Alexei A. Aravin, Alexander Stark, Monica Dus, Manolis Kellis, Ravi Sachidanandam, and Gregory J. Hannon. 2007. 'Discrete Small RNA-Generating Loci as Master Regulators of Transposon Activity in Drosophila'. *Cell* 128 (6): 1089-1103. <https://doi.org/10.1016/j.cell.2007.01.043>.
- Brennecke, Julius, Colin D. Malone, Alexei A. Aravin, Ravi Sachidanandam, Alexander Stark, and Gregory J. Hannon. 2008. 'An Epigenetic Role for Maternally Inherited PiRNAs in Transposon Silencing'. *Science (New York, N.Y.)* 322 (5906): 1387-92. <https://doi.org/10.1126/science.1165171>.
- Brierley, C., and A. J. Flavell. 1990. 'The Retrotransposon Copia Controls the Relative Levels of Its Gene Products Post-Transcriptionally by Differential Expression from Its Two Major MRNAs'. *Nucleic Acids Research* 18 (10): 2947-51. <https://doi.org/10.1093/nar/18.10.2947>.
- Brönner, Cornelia, Luca Salvi, Manuel Zocco, Ilaria Ugolini, and Mario Halic. 2017. 'Accumulation of RNA on Chromatin Disrupts Heterochromatic Silencing'. *Genome Research* 27 (7): 1174-83. <https://doi.org/10.1101/gr.216986.116>.
- Bühler, Marc, André Verdel, and Danesh Moazed. 2006. 'Tethering RITS to a Nascent Transcript Initiates RNAi- and Heterochromatin-Dependent Gene Silencing'. *Cell* 125 (5): 873-86. <https://doi.org/10.1016/j.cell.2006.04.025>.
- Buker, Shane M., Tetsushi Iida, Marc Bühler, Judit Villén, Steven P. Gygi, Jun-Ichi Nakayama, and Danesh Moazed. 2007. 'Two Different Argonaute Complexes Are Required for siRNA Generation and Heterochromatin Assembly in Fission Yeast'. *Nature Structural & Molecular Biology* 14 (3): 200-207. <https://doi.org/10.1038/nsmb1211>.
- C. elegans Sequencing Consortium. 1998. 'Genome Sequence of the Nematode C. Elegans: A Platform for Investigating Biology'. *Science (New York, N.Y.)* 282 (5396): 2012-18. <https://doi.org/10.1126/science.282.5396.2012>.
- Cam, Hugh P., Ken-ichi Noma, Hirotaka Ebina, Henry L. Levin, and Shiv I. S. Grewal. 2008. 'Host Genome Surveillance for Retrotransposons by Transposon-Derived Proteins'. *Nature* 451 (7177): 431-36. <https://doi.org/10.1038/nature06499>.
- Cam, Hugh P., Tomoyasu Sugiyama, Ee Sin Chen, Xi Chen, Peter C. FitzGerald, and Shiv I. S. Grewal. 2005. 'Comprehensive Analysis of Heterochromatin- and RNAi-Mediated Epigenetic Control of the Fission Yeast Genome'. *Nature Genetics* 37 (8): 809-19. <https://doi.org/10.1038/ng1602>.
- Canzio, Daniele, Maofu Liao, Nariman Naber, Ed Pate, Adam Larson, Shenping Wu, Diana B. Marina, et al. 2013. 'A Conformational Switch in HP1 Releases Auto-Inhibition to Drive Heterochromatin Assembly'. *Nature* 496 (7445): 377-81. <https://doi.org/10.1038/nature12032>.
- Cao, Xiaofeng, and Steven E. Jacobsen. 2002. 'Role of the Arabidopsis DRM Methyltransferases in de Novo DNA Methylation and Gene Silencing'. *Current Biology: CB* 12 (13): 1138-44. [https://doi.org/10.1016/s0960-9822\(02\)00925-9](https://doi.org/10.1016/s0960-9822(02)00925-9).
- Carmell, Michelle A., Angélique Girard, Henk J. G. van de Kant, Deborah Bourc'his, Timothy H. Bestor, Dirk G. de Rooij, and Gregory J. Hannon. 2007. 'MIWI2 Is Essential for Spermatogenesis and Repression of Transposons in the Mouse Male Germline'. *Developmental Cell* 12 (4): 503-14. <https://doi.org/10.1016/j.devcel.2007.03.001>.

- Carr, Martin, Douda Bensasson, and Casey M. Bergman. 2012. 'Evolutionary Genomics of Transposable Elements in *Saccharomyces Cerevisiae*'. *PLoS One* 7 (11): e50978. <https://doi.org/10.1371/journal.pone.0050978>.
- Casola, Claudio, Donald Hucks, and Cédric Feschotte. 2008. 'Convergent Domestication of Pogo-like Transposases into Centromere-Binding Proteins in Fission Yeast and Mammals'. *Molecular Biology and Evolution* 25 (1): 29–41. <https://doi.org/10.1093/molbev/msm221>.
- Chalker, D. L., and S. B. Sandmeyer. 1992. 'Ty3 Integrates within the Region of RNA Polymerase III Transcription Initiation'. *Genes & Development* 6 (1): 117–28. <https://doi.org/10.1101/gad.6.1.117>.
- Chatterjee, Atreyi Ghatak, Caroline Esnault, Yabin Guo, Stephen Hung, Philip G. McQueen, and Henry L. Levin. 2014. 'Serial Number Tagging Reveals a Prominent Sequence Preference of Retrotransposon Integration'. *Nucleic Acids Research* 42 (13): 8449–60. <https://doi.org/10.1093/nar/gku534>.
- Chen, Xiaoying, Jennica Zaro, and Wei-Chiang Shen. 2013. 'Fusion Protein Linkers: Property, Design and Functionality'. *Advanced Drug Delivery Reviews* 65 (10): 1357–69. <https://doi.org/10.1016/j.addr.2012.09.039>.
- Clayton J, Dennis C. 2016. *50 Years of DNA*. Palgrave Macmillan.
- Coelho, Teresa, David Adams, Ana Silva, Pierre Lozeron, Philip N. Hawkins, Timothy Mant, Javier Perez, et al. 2013. 'Safety and Efficacy of RNAi Therapy for Transthyretin Amyloidosis'. *New England Journal of Medicine* 369 (9): 819–29. <https://doi.org/10.1056/NEJMoa1208760>.
- Colmenares, Serafin U., Shane M. Buker, Marc Buhler, Mensur Dlakić, and Danesh Moazed. 2007. 'Coupling of Double-Stranded RNA Synthesis and siRNA Generation in Fission Yeast RNAi'. *Molecular Cell* 27 (3): 449–61. <https://doi.org/10.1016/j.molcel.2007.07.007>.
- Cox, D. N., A. Chao, and H. Lin. 2000. 'Piwi Encodes a Nucleoplasmic Factor Whose Activity Modulates the Number and Division Rate of Germline Stem Cells'. *Development (Cambridge, England)* 127 (3): 503–14.
- Creasey, Kate M., Jixian Zhai, Filipe Borges, Frederic Van Ex, Michael Regulski, Blake C. Meyers, and Robert A. Martienssen. 2014. 'miRNAs Trigger Widespread Epigenetically Activated siRNAs from Transposons in Arabidopsis'. *Nature* 508 (7496): 411–15. <https://doi.org/10.1038/nature13069>.
- Dai, Jumbiao, Weiwu Xie, Troy L. Brady, Jiquan Gao, and Daniel F. Voytas. 2007. 'Phosphorylation Regulates Integration of the Yeast Ty5 Retrotransposon into Heterochromatin'. *Molecular Cell* 27 (2): 289–99. <https://doi.org/10.1016/j.molcel.2007.06.010>.
- Dang, Van Dinh, Michael J. Benedik, Karl Ekwall, Jeannie Choi, Robin C. Allshire, and Henry L. Levin. 1999. 'A New Member of the Sin3 Family of Corepressors Is Essential for Cell Viability and Required for Retroelement Propagation in Fission Yeast'. *Molecular and Cellular Biology* 19 (3): 2351–65.
- Darricarrère, Nicole, Na Liu, Toshiaki Watanabe, and Haifan Lin. 2013. 'Function of Piwi, a Nuclear Piwi/Argonaute Protein, Is Independent of Its Slicer Activity'. *Proceedings of the National Academy of Sciences* 110 (4): 1297–1302. <https://doi.org/10.1073/pnas.1213283110>.
- Das, Partha P., Marloes P. Bagijn, Leonard D. Goldstein, Julie R. Woolford, Nicolas J. Lehrbach, Alexandra Sapetschnig, Heeran R. Buhecha, et al. 2008. 'Piwi and PiRNAs Act Upstream of an Endogenous siRNA Pathway to Suppress Tc3 Transposon Mobility in the *Caenorhabditis Elegans* Germline'. *Molecular Cell* 31 (1): 79–90. <https://doi.org/10.1016/j.molcel.2008.06.003>.
- De Fazio, Serena, Nenad Bartonicek, Monica Di Giacomo, Cei Abreu-Goodger, Aditya Sankar, Charlotta Funaya, Claude Antony, Pedro N. Moreira, Anton J. Enright, and Dónal O'Carroll. 2011. 'The Endonuclease Activity of Mili Fuels PiRNA Amplification That Silences LINE1 Elements'. *Nature* 480 (7376): 259–63. <https://doi.org/10.1038/nature10547>.
- Deng, Wei, and Haifan Lin. 2002. 'Miwi, a Murine Homolog of Piwi, Encodes a Cytoplasmic Protein Essential for Spermatogenesis'. *Developmental Cell* 2 (6): 819–30. [https://doi.org/10.1016/S1534-5807\(02\)00165-X](https://doi.org/10.1016/S1534-5807(02)00165-X).
- Devine, S. E., and J. D. Boeke. 1996. 'Integration of the Yeast Retrotransposon Ty1 Is Targeted to Regions Upstream of Genes Transcribed by RNA Polymerase III'. *Genes & Development* 10 (5): 620–33. <https://doi.org/10.1101/gad.10.5.620>.

- Ding, Shou-Wei, Qingxia Han, Jinyan Wang, and Wan-Xiang Li. 2018. 'Antiviral RNA Interference in Mammals'. *Current Opinion in Immunology* 54 (October): 109-14. <https://doi.org/10.1016/j.coi.2018.06.010>.
- Ding, Shou-Wei, Hongwei Li, Rui Lu, Feng Li, and Wan-Xiang Li. 2004. 'RNA Silencing: A Conserved Antiviral Immunity of Plants and Animals'. *Virus Research, Viral Gene Silencing by RNA Interference*, 102 (1): 109-15. <https://doi.org/10.1016/j.virusres.2004.01.021>.
- Djupedal, Ingela, Manuela Portoso, Henrik Spåhr, Carolina Bonilla, Claes M. Gustafsson, Robin C. Allshire, and Karl Ekwall. 2005. 'RNA Pol II Subunit Rpb7 Promotes Centromeric Transcription and RNAi-Directed Chromatin Silencing'. *Genes & Development* 19 (19): 2301-6. <https://doi.org/10.1101/gad.344205>.
- Douet, J., and S. Tourmente. 2007. 'Transcription of the 5S RRNA Heterochromatic Genes Is Epigenetically Controlled in Arabidopsis Thaliana and Xenopus Laevis'. *Heredity* 99 (1): 5-13. <https://doi.org/10.1038/sj.hdy.6800964>.
- Drimmenberg, Ines A., David E. Weinberg, Kathleen T. Xie, Jeffrey P. Mower, Kenneth H. Wolfe, Gerald R. Fink, and David P. Bartel. 2009a. 'RNAi in Budding Yeast'. *Science (New York, N.Y.)* 326 (5952): 544-50. <https://doi.org/10.1126/science.1176945>.
- . 2009b. 'RNAi in Budding Yeast'. *Science (New York, N.Y.)* 326 (5952): 544-50. <https://doi.org/10.1126/science.1176945>.
- Ecco, Gabriela, Marco Cassano, Annamaria Kauzlaric, Julien Duc, Andrea Coluccio, Sandra Offner, Michaël Imbeault, Helen M. Rowe, Priscilla Turelli, and Didier Trono. 2016. 'Transposable Elements and Their KRAB-ZFP Controllers Regulate Gene Expression in Adult Tissues'. *Developmental Cell* 36 (6): 611-23. <https://doi.org/10.1016/j.devcel.2016.02.024>.
- Egel, R, D H Beach, and A J Klar. 1984. 'Genes Required for Initiation and Resolution Steps of Mating-Type Switching in Fission Yeast.' *Proceedings of the National Academy of Sciences of the United States of America* 81 (11): 3481-85.
- Ekwall, K., J. P. Javerzat, A. Lorentz, H. Schmidt, G. Cranston, and R. Allshire. 1995. 'The Chromodomain Protein Swi6: A Key Component at Fission Yeast Centromeres'. *Science (New York, N.Y.)* 269 (5229): 1429-31. <https://doi.org/10.1126/science.7660126>.
- Elder, R. T., T. P. St John, D. T. Stinchcomb, R. W. Davis, S. Scherer, and R. W. Davis. 1981. 'Studies on the Transposable Element Ty1 of Yeast. I. RNA Homologous to Ty1. II. Recombination and Expression of Ty1 and Adjacent Sequences'. *Cold Spring Harbor Symposia on Quantitative Biology* 45 Pt 2: 581-91. <https://doi.org/10.1101/sqb.1981.045.01.075>.
- Ellermeier, Chad, Emily C. Higuchi, Naina Phadnis, Laerke Holm, Jennifer L. Geelhood, Genevieve Thon, and Gerald R. Smith. 2010. 'RNAi and Heterochromatin Repress Centromeric Meiotic Recombination'. *Proceedings of the National Academy of Sciences of the United States of America* 107 (19): 8701-5. <https://doi.org/10.1073/pnas.0914160107>.
- Engel, Stacia R, Fred S Dietrich, Dianna G Fisk, Gail Binkley, Rama Balakrishnan, Maria C Costanzo, Selina S Dwight, et al. 2014. 'The Reference Genome Sequence of Saccharomyces Cerevisiae: Then and Now'. *G3 Genes/Genomes/Genetics* 4 (3): 389-98. <https://doi.org/10.1534/g3.113.008995>.
- Esnault, Caroline, Michael Lee, Chloe Ham, and Henry L. Levin. 2019. 'Transposable Element Insertions in Fission Yeast Drive Adaptation to Environmental Stress'. *Genome Research* 29 (1): 85-95. <https://doi.org/10.1101/gr.239699.118>.
- Feng, Gang, Young-Eun Leem, and Henry L. Levin. 2013. 'Transposon Integration Enhances Expression of Stress Response Genes'. *Nucleic Acids Research* 41 (2): 775-89. <https://doi.org/10.1093/nar/gks1185>.
- Fenley, Andrew T., David A. Adams, and Alexey V. Onufriev. 2010. 'Charge State of the Globular Histone Core Controls Stability of the Nucleosome'. *Biophysical Journal* 99 (5): 1577-85. <https://doi.org/10.1016/j.bpj.2010.06.046>.
- Feschotte, Cédric, and Ellen J. Pritham. 2007. 'DNA Transposons and the Evolution of Eukaryotic Genomes'. *Annual Review of Genetics* 41: 331-68. <https://doi.org/10.1146/annurev.genet.40.110405.090448>.

- Fire, Andrew, SiQun Xu, Mary K. Montgomery, Steven A. Kostas, Samuel E. Driver, and Craig C. Mello. 1998. 'Potent and Specific Genetic Interference by Double-Stranded RNA in *Caenorhabditis Elegans*'. *Nature* 391 (6669): 806–11. <https://doi.org/10.1038/35888>.
- Fischer, Tamás, Bowen Cui, Jothy Dhakshnamoorthy, Ming Zhou, Chanan Rubin, Martin Zofall, Timothy D. Veenstra, and Shiv I. S. Grewal. 2009. 'Diverse Roles of HP1 Proteins in Heterochromatin Assembly and Functions in Fission Yeast'. *Proceedings of the National Academy of Sciences* 106 (22): 8998–9003. <https://doi.org/10.1073/pnas.0813063106>.
- Flemming, W. 1879. 'Ueber Das Verhalten Des Kerns Bei Der Zellteilung Und Über Die Bedeutung Mehrkerniger Zellen.' *Arch. Pathol. Anat.*, 1–28.
- Fultz, Dalen, Sarah G Choudury, and R Keith Slotkin. 2015. 'Silencing of Active Transposable Elements in Plants'. *Current Opinion in Plant Biology*, Cell signalling and gene regulation, 27 (October): 67–76. <https://doi.org/10.1016/j.pbi.2015.05.027>.
- Gan, Haiyun, Xiwen Lin, Zhuqiang Zhang, Wei Zhang, Shangying Liao, Lixian Wang, and Chunsheng Han. 2011. 'PiRNA Profiling during Specific Stages of Mouse Spermatogenesis'. *RNA* 17 (7): 1191–1203. <https://doi.org/10.1261/rna.2648411>.
- Garcia, Jennifer F, Bassem Al-Sady, and Hiten D Madhani. 2015. 'Intrinsic Toxicity of Unchecked Heterochromatin Spread Is Suppressed by Redundant Chromatin Boundary Functions in *Schizosaccharomyces Pombe*'. *G3 Genes/Genomes/Genetics* 5 (7): 1453–61. <https://doi.org/10.1534/g3.115.018663>.
- Garcia, Jennifer F., Phillip A. Dumesic, Paul D. Hartley, Hana El-Samad, and Hiten D. Madhani. 2010. 'Combinatorial, Site-Specific Requirement for Heterochromatic Silencing Factors in the Elimination of Nucleosome-Free Regions'. *Genes & Development* 24 (16): 1758–71. <https://doi.org/10.1101/gad.1946410>.
- Gimeno, C. J., P. O. Ljungdahl, C. A. Styles, and G. R. Fink. 1992. 'Unipolar Cell Divisions in the Yeast *S. Cerevisiae* Lead to Filamentous Growth: Regulation by Starvation and RAS'. *Cell* 68 (6): 1077–90. [https://doi.org/10.1016/0092-8674\(92\)90079-r](https://doi.org/10.1016/0092-8674(92)90079-r).
- Girard, Angélique, Ravi Sachidanandam, Gregory J. Hannon, and Michelle A. Carmell. 2006. 'A Germline-Specific Class of Small RNAs Binds Mammalian Piwi Proteins'. *Nature* 442 (7099): 199–202. <https://doi.org/10.1038/nature04917>.
- Goriaux, Coline, Sophie Desset, Yoan Renaud, Chantal Vaury, and Emilie Brasset. 2014. 'Transcriptional Properties and Splicing of the Flamenco PiRNA Cluster'. *EMBO Reports* 15 (4): 411–18. <https://doi.org/10.1002/embr.201337898>.
- Gou, Lan-Tao, Peng Dai, Jian-Hua Yang, Yuanchao Xue, Yun-Ping Hu, Yu Zhou, Jun-Yan Kang, et al. 2014. 'Pachytene PiRNAs Instruct Massive mRNA Elimination during Late Spermiogenesis'. *Cell Research* 24 (6): 680–700. <https://doi.org/10.1038/cr.2014.41>.
- Greenall, Amanda, Emma S. Williams, Katherine A. Martin, Jeremy M. Palmer, Joe Gray, Cong Liu, and Simon K. Whitehall. 2006. 'Hip3 Interacts with the HIRA Proteins Hip1 and Slm9 and Is Required for Transcriptional Silencing and Accurate Chromosome Segregation'. *The Journal of Biological Chemistry* 281 (13): 8732–39. <https://doi.org/10.1074/jbc.M512170200>.
- Grewal, SIS., and AJS. Klar. 1997. 'A Recombinationally Repressed Region between Mat2 and Mat3 Loci Shares Homology to Centromeric Repeats and Regulates Directionality of Mating-Type Switching in Fission Yeast'. *Genetics* 146 (4): 1221–38.
- Grimm, C., J. Kohli, J. Murray, and K. Maundrell. 1988. 'Genetic Engineering of *Schizosaccharomyces Pombe*: A System for Gene Disruption and Replacement Using the Ura4 Gene as a Selectable Marker'. *Molecular & General Genetics: MGG* 215 (1): 81–86. <https://doi.org/10.1007/BF00331307>.
- Grunstein, Michael, and Susan M. Gasser. 2013. 'Epigenetics in *Saccharomyces Cerevisiae*'. *Cold Spring Harbor Perspectives in Biology* 5 (7). <https://doi.org/10.1101/cshperspect.a017491>.
- Gunawardane, Lalith S., Kuniaki Saito, Kazumichi M. Nishida, Keita Miyoshi, Yoshinori Kawamura, Tomoko Nagami, Haruhiko Siomi, and Mikiko C. Siomi. 2007. 'A Slicer-Mediated Mechanism for Repeat-Associated siRNA 5' End Formation in *Drosophila*'. *Science* 315 (5818): 1587–90. <https://doi.org/10.1126/science.1140494>.
- Guo, Yabin, and Henry L. Levin. 2010. 'High-Throughput Sequencing of Retrotransposon Integration Provides a Saturated Profile of Target Activity in *Schizosaccharomyces Pombe*'. *Genome Research* 20 (2): 239–48. <https://doi.org/10.1101/gr.099648.109>.

- Guo, Yabin, Parmit Kumar Singh, and Henry L. Levin. 2015. 'A Long Terminal Repeat Retrotransposon of *Schizosaccharomyces Japonicus* Integrates Upstream of RNA Pol III Transcribed Genes'. *Mobile DNA* 6 (October). <https://doi.org/10.1186/s13100-015-0048-2>.
- Halic, Mario, and Danesh Moazed. 2010. 'Dicer-Independent Primal RNAs Trigger RNAi and Heterochromatin Formation'. *Cell* 140 (4): 504-16. <https://doi.org/10.1016/j.cell.2010.01.019>.
- Hall, Ira M., Gurumurthy D. Shankaranarayana, Ken-ichi Noma, Nabieh Ayoub, Amikam Cohen, and Shiv I. S. Grewal. 2002. 'Establishment and Maintenance of a Heterochromatin Domain'. *Science* 297 (5590): 2232-37. <https://doi.org/10.1126/science.1076466>.
- Hamada, M., Y. Huang, T. M. Lowe, and R. J. Maraia. 2001. 'Widespread Use of TATA Elements in the Core Promoters for RNA Polymerases III, II, and I in Fission Yeast'. *Molecular and Cellular Biology* 21 (20): 6870-81. <https://doi.org/10.1128/MCB.21.20.6870-6881.2001>.
- Hamilton, Andrew J., and David C. Baulcombe. 1999. 'A Species of Small Antisense RNA in Posttranscriptional Gene Silencing in Plants'. *Science* 286 (5441): 950-52. <https://doi.org/10.1126/science.286.5441.950>.
- Hansen, Klavs R., Gavin Burns, Juan Mata, Thomas A. Volpe, Robert A. Martienssen, Jürg Bähler, and Geneviève Thon. 2005. 'Global Effects on Gene Expression in Fission Yeast by Silencing and RNA Interference Machineries'. *Molecular and Cellular Biology* 25 (2): 590-601. <https://doi.org/10.1128/MCB.25.2.590-601.2005>.
- Hansen, Klavs R., Pablo Tejero Ibarra, and Geneviève Thon. 2006. 'Evolutionary-Conserved Telomere-Linked Helicase Genes of Fission Yeast Are Repressed by Silencing Factors, RNAi Components and the Telomere-Binding Protein Taz1'. *Nucleic Acids Research* 34 (1): 78-88. <https://doi.org/10.1093/nar/gkj415>.
- Harigaya, Yuriko, Hirotsugu Tanaka, Soichiro Yamanaka, Kayoko Tanaka, Yoshinori Watanabe, Chihiro Tsutsumi, Yuji Chikashige, Yasushi Hiraoka, Akira Yamashita, and Masayuki Yamamoto. 2006. 'Selective Elimination of Messenger RNA Prevents an Incidence of Untimely Meiosis'. *Nature* 442 (7098): 45-50. <https://doi.org/10.1038/nature04881>.
- Harris, Adam N., and Paul M. Macdonald. 2001. 'Aubergine Encodes a *Drosophila* Polar Granule Component Required for Pole Cell Formation and Related to EIF2C'. *Development* 128 (14): 2823-32. <https://doi.org/10.1242/dev.128.14.2823>.
- Hayashi, Aki, Mayumi Ishida, Rika Kawaguchi, Takeshi Urano, Yota Murakami, and Jun-ichi Nakayama. 2012. 'Heterochromatin Protein 1 Homologue Swi6 Acts in Concert with Ers1 to Regulate RNAi-Directed Heterochromatin Assembly'. *Proceedings of the National Academy of Sciences* 109 (16): 6159-64. <https://doi.org/10.1073/pnas.1116972109>.
- He, Chao, Sreerexha S. Pillai, Francesca Tagliani, Fudong Li, Ke Ruan, Jiahai Zhang, Jihui Wu, Yunyu Shi, and Elizabeth H. Bayne. 2013. 'Structural Analysis of Stc1 Provides Insights into the Coupling of RNAi and Chromatin Modification'. *Proceedings of the National Academy of Sciences* 110 (21): E1879-88. <https://doi.org/10.1073/pnas.1212155110>.
- Heidmann, T, O Heidmann, and J F Nicolas. 1988. 'An Indicator Gene to Demonstrate Intracellular Transposition of Defective Retroviruses.' *Proceedings of the National Academy of Sciences of the United States of America* 85 (7): 2219-23.
- Heitz, E. 1928. 'Das Heterochromatin Der Moose. I.' *Jahrb. Wiss. Bot.*
- Hickey, Anthony, Caroline Esnault, Anasuya Majumdar, Atreyi Ghatak Chatterjee, James R. Iben, Philip G. McQueen, Andrew X. Yang, Takeshi Mizuguchi, Shiv I. S. Grewal, and Henry L. Levin. 2015. 'Single-Nucleotide-Specific Targeting of the Tf1 Retrotransposon Promoted by the DNA-Binding Protein Sap1 of *Schizosaccharomyces Pombe*'. *Genetics* 201 (3): 905-24. <https://doi.org/10.1534/genetics.115.181602>.
- Hizi, Amnon. 2008. 'The Reverse Transcriptase of the Tf1 Retrotransposon Has a Specific Novel Activity for Generating the RNA Self-Primer That Is Functional in cDNA Synthesis'. *Journal of Virology* 82 (21): 10906-10. <https://doi.org/10.1128/JVI.01370-08>.
- Hoffman, Charles S., Valerie Wood, and Peter A. Fantes. 2015. 'An Ancient Yeast for Young Geneticists: A Primer on the *Schizosaccharomyces Pombe* Model System'. *Genetics* 201 (2): 403-23. <https://doi.org/10.1534/genetics.115.181503>.

- Hollister, Jesse D., and Brandon S. Gaut. 2009. 'Epigenetic Silencing of Transposable Elements: A Trade-off between Reduced Transposition and Deleterious Effects on Neighboring Gene Expression'. *Genome Research* 19 (8): 1419–28. <https://doi.org/10.1101/gr.091678.109>.
- Horwich, Michael D., Chengjian Li, Christian Matrangola, Vasily Vagin, Gwen Farley, Peng Wang, and Phillip D. Zamore. 2007. 'The Drosophila RNA Methyltransferase, DmHen1, Modifies Germline PiRNAs and Single-Stranded siRNAs in RISC'. *Current Biology: CB* 17 (14): 1265–72. <https://doi.org/10.1016/j.cub.2007.06.030>.
- Hoy, Sheridan M. 2018. 'Patisiran: First Global Approval'. *Drugs* 78 (15): 1625–31. <https://doi.org/10.1007/s40265-018-0983-6>.
- Iida, Tetsushi, Rika Kawaguchi, and Jun-ichi Nakayama. 2006. 'Conserved Ribonuclease, Eri1, Negatively Regulates Heterochromatin Assembly in Fission Yeast'. *Current Biology: CB* 16 (14): 1459–64. <https://doi.org/10.1016/j.cub.2006.05.061>.
- Iida, Tetsushi, Jun-ichi Nakayama, and Danesh Moazed. 2008. 'siRNA-Mediated Heterochromatin Establishment Requires HP1 and Is Associated with Antisense Transcription'. *Molecular Cell* 31 (2): 178–89. <https://doi.org/10.1016/j.molcel.2008.07.003>.
- Imbeault, Michaël, Pierre-Yves Helleboid, and Didier Trono. 2017. 'KRAB Zinc-Finger Proteins Contribute to the Evolution of Gene Regulatory Networks'. *Nature* 543 (7646): 550–54. <https://doi.org/10.1038/nature21683>.
- Ipsaro, Jonathan J., Astrid D. Haase, Simon R. Knott, Leemor Joshua-Tor, and Gregory J. Hannon. 2012. 'The Structural Biochemistry of Zucchini Implicates It as a Nuclease in PiRNA Biogenesis'. *Nature* 491 (7423): 279–83. <https://doi.org/10.1038/nature11502>.
- Iwasaki, Wakana, Yuta Miya, Naoki Horikoshi, Akihisa Osakabe, Hiroyuki Taguchi, Hiroaki Tachiwana, Takehiko Shibata, Wataru Kagawa, and Hitoshi Kurumizaka. 2013. 'Contribution of Histone N-Terminal Tails to the Structure and Stability of Nucleosomes'. *FEBS Open Bio* 3 (January): 363–69. <https://doi.org/10.1016/j.fob.2013.08.007>.
- Iwasaki, Yuka W., Mikiko C. Siomi, and Haruhiko Siomi. 2015. 'PIWI-Interacting RNA: Its Biogenesis and Functions'. *Annual Review of Biochemistry* 84 (1): 405–33. <https://doi.org/10.1146/annurev-biochem-060614-034258>.
- Jacks, T., M. D. Power, F. R. Masiarz, P. A. Luciw, P. J. Barr, and H. E. Varmus. 1988. 'Characterization of Ribosomal Frameshifting in HIV-1 Gag-Pol Expression'. *Nature* 331 (6153): 280–83. <https://doi.org/10.1038/331280a0>.
- Jain, Devanshi, Anna K. Hebden, Toru M. Nakamura, Kyle M. Miller, and Julia Promisel Cooper. 2010. 'HAATI Survivors Replace Canonical Telomeres with Blocks of Generic Heterochromatin'. *Nature* 467 (7312): 223–27. <https://doi.org/10.1038/nature09374>.
- Jain, Ruchi, Nahid Iglesias, and Danesh Moazed. 2016. 'Distinct Functions of Argonaute Slicer in siRNA Maturation and Heterochromatin Formation'. *Molecular Cell* 63 (2): 191–205. <https://doi.org/10.1016/j.molcel.2016.05.039>.
- Jansen, An, and Kevin Verstrepen. 2011. 'Nucleosome Positioning in *Saccharomyces Cerevisiae*'. *Microbiology and Molecular Biology Reviews: MMBR* 75 (June): 301–20. <https://doi.org/10.1128/MMBR.00046-10>.
- Jia, Songtao, Ryuji Kobayashi, and Shiv I. S. Grewal. 2005. 'Ubiquitin Ligase Component Cul4 Associates with Clr4 Histone Methyltransferase to Assemble Heterochromatin'. *Nature Cell Biology* 7 (10): 1007–13. <https://doi.org/10.1038/ncb1300>.
- Jia, Songtao, Ken-ichi Noma, and Shiv I. S. Grewal. 2004. 'RNAi-Independent Heterochromatin Nucleation by the Stress-Activated ATF/CREB Family Proteins'. *Science* 304 (5679): 1971–76. <https://doi.org/10.1126/science.1099035>.
- Johnson, Lianna M., Magnolia Bostick, Xiaoyu Zhang, Edward Kraft, Ian Henderson, Judy Callis, and Steven E. Jacobsen. 2007. 'The SRA Methyl-Cytosine-Binding Domain Links DNA and Histone Methylation'. *Current Biology: CB* 17 (4): 379–84. <https://doi.org/10.1016/j.cub.2007.01.009>.
- Johnson, Lianna M., Jiamu Du, Christopher J. Hale, Sylvain Bischof, Suhua Feng, Ramakrishna K. Chodavarapu, Xuehua Zhong, et al. 2014. 'SRA- and SET-Domain-Containing Proteins Link RNA Polymerase V Occupancy to DNA Methylation'. *Nature* 507 (7490): 124–28. <https://doi.org/10.1038/nature12931>.

- Josse, Thibaut, Laure Teyssset, Anne-Laure Todeschini, Clara M Sidor, Dominique Anxolabéhère, and Stéphane Ronsseray. 2007. 'Telomeric Trans-Silencing: An Epigenetic Repression Combining RNA Silencing and Heterochromatin Formation'. *PLoS Genetics* 3 (9). <https://doi.org/10.1371/journal.pgen.0030158>.
- Kaji, Takuto, Yusuke Oizumi, Sanki Tashiro, Yumiko Takeshita, and Junko Kanoh. 2020. 'Complete Sequences of Schizosaccharomyces Pombe Subtelomeres Reveal Multiple Patterns of Genome Variation'. *BioRxiv*, March, 2020.03.09.983726. <https://doi.org/10.1101/2020.03.09.983726>.
- Kalmykova, Alla I., Mikhail S. Klenov, and Vladimir A. Gvozdev. 2005. 'Argonaute Protein PIWI Controls Mobilization of Retrotransposons in the Drosophila Male Germline'. *Nucleic Acids Research* 33 (6): 2052-59. <https://doi.org/10.1093/nar/gki323>.
- Kanoh, Junko, Mahito Sadaie, Takeshi Urano, and Fuyuki Ishikawa. 2005. 'Telomere Binding Protein Taz1 Establishes Swi6 Heterochromatin Independently of RNAi at Telomeres'. *Current Biology: CB* 15 (20): 1808-19. <https://doi.org/10.1016/j.cub.2005.09.041>.
- Kato, Hiroaki, Derek B. Goto, Robert A. Martienssen, Takeshi Urano, Koichi Furukawa, and Yota Murakami. 2005. 'RNA Polymerase II Is Required for RNAi-Dependent Heterochromatin Assembly'. *Science* 309 (5733): 467-69. <https://doi.org/10.1126/science.1114955>.
- Kazazian, H. H., C. Wong, H. Youssoufian, A. F. Scott, D. G. Phillips, and S. E. Antonarakis. 1988. 'Haemophilia A Resulting from de Novo Insertion of L1 Sequences Represents a Novel Mechanism for Mutation in Man'. *Nature* 332 (6160): 164-66. <https://doi.org/10.1038/332164a0>.
- Ke, N., P. A. Irwin, and D. F. Voytas. 1997. 'The Pheromone Response Pathway Activates Transcription of Ty5 Retrotransposons Located within Silent Chromatin of Saccharomyces Cerevisiae'. *The EMBO Journal* 16 (20): 6272-80. <https://doi.org/10.1093/emboj/16.20.6272>.
- Keller, Claudia, Ricardo Adaixo, Rieka Stunnenberg, Katrina J. Woolcock, Sebastian Hiller, and Marc Bühler. 2012a. 'HP1(Swi6) Mediates the Recognition and Destruction of Heterochromatic RNA Transcripts'. *Molecular Cell* 47 (2): 215-27. <https://doi.org/10.1016/j.molcel.2012.05.009>.
- . 2012b. 'HP1Swi6 Mediates the Recognition and Destruction of Heterochromatic RNA Transcripts'. *Molecular Cell* 47 (2): 215-27. <https://doi.org/10.1016/j.molcel.2012.05.009>.
- Keller, Claudia, Raghavendran Kulasegaran-Shylini, Yukiko Shimada, Hans-Rudolf Hotz, and Marc Bühler. 2013a. 'Noncoding RNAs Prevent Spreading of a Repressive Histone Mark'. *Nature Structural & Molecular Biology* 20 (8): 994-1000. <https://doi.org/10.1038/nsmb.2619>.
- . 2013b. 'Noncoding RNAs Prevent Spreading of a Repressive Histone Mark'. *Nature Structural & Molecular Biology* 20 (8): 994-1000. <https://doi.org/10.1038/nsmb.2619>.
- Kim, J. M., S. Vanguri, J. D. Boeke, A. Gabriel, and D. F. Voytas. 1998. 'Transposable Elements and Genome Organization: A Comprehensive Survey of Retrotransposons Revealed by the Complete Saccharomyces Cerevisiae Genome Sequence'. *Genome Research* 8 (5): 464-78. <https://doi.org/10.1101/gr.8.5.464>.
- Kinsey, P T, and S B Sandmeyer. 1991. 'Adjacent Pol II and Pol III Promoters: Transcription of the Yeast Retrotransposon Ty3 and a Target TRNA Gene.' *Nucleic Acids Research* 19 (6): 1317-24.
- Klattenhoff, Carla, Hualin Xi, Chengjian Li, Soohyun Lee, Jia Xu, Jaspreet S. Khurana, Fan Zhang, et al. 2009. 'The Drosophila HP1 Homolog Rhino Is Required for Transposon Silencing and PiRNA Production by Dual-Strand Clusters'. *Cell* 138 (6): 1137-49. <https://doi.org/10.1016/j.cell.2009.07.014>.
- Kobayashi, K., Y. Nakahori, M. Miyake, K. Matsumura, E. Kondo-Iida, Y. Nomura, M. Segawa, et al. 1998. 'An Ancient Retrotranspositional Insertion Causes Fukuyama-Type Congenital Muscular Dystrophy'. *Nature* 394 (6691): 388-92. <https://doi.org/10.1038/28653>.
- Kornberg, R. D. 1974. 'Chromatin Structure: A Repeating Unit of Histones and DNA'. *Science (New York, N.Y.)* 184 (4139): 868-71. <https://doi.org/10.1126/science.184.4139.868>.
- Kouzarides, Tony. 2007. 'Chromatin Modifications and Their Function'. *Cell* 128 (4): 693-705. <https://doi.org/10.1016/j.cell.2007.02.005>.
- Kovalchuk, Andriy. 2005. 'Molecular Analysis of the LTR Retrotransposon Ylt1 from the Genome of Dimorphic Fungus Yarrowia Lipolytica'.

- Krupovic, Mart, Pierre Béguin, and Eugene V. Koonin. 2017. 'Casposons: Mobile Genetic Elements That Gave Rise to the CRISPR-Cas Adaptation Machinery'. *Current Opinion in Microbiology* 38 (August): 36-43. <https://doi.org/10.1016/j.mib.2017.04.004>.
- Kuramochi-Miyagawa, S., T. Kimura, K. Yomogida, A. Kuroiwa, Y. Tadokoro, Y. Fujita, M. Sato, Y. Matsuda, and T. Nakano. 2001. 'Two Mouse Piwi-Related Genes: Miwi and Mili'. *Mechanisms of Development* 108 (1-2): 121-33. [https://doi.org/10.1016/s0925-4773\(01\)00499-3](https://doi.org/10.1016/s0925-4773(01)00499-3).
- Kuramochi-Miyagawa, Satomi, Toshiaki Watanabe, Kengo Gotoh, Yasushi Totoki, Atsushi Toyoda, Masahito Ikawa, Noriko Asada, et al. 2008. 'DNA Methylation of Retrotransposon Genes Is Regulated by Piwi Family Members MILI and MIWI2 in Murine Fetal Testes'. *Genes & Development* 22 (7): 908-17. <https://doi.org/10.1101/gad.1640708>.
- Kusevic, Denis, Srikanth Kudithipudi, Nahid Iglesias, Danesh Moazed, and Albert Jeltsch. 2017. 'Clr4 Specificity and Catalytic Activity beyond H3K9 Methylation'. *Biochimie* 135 (April): 83-88. <https://doi.org/10.1016/j.biochi.2017.01.013>.
- Lander, E. S., L. M. Linton, B. Birren, C. Nusbaum, M. C. Zody, J. Baldwin, K. Devon, et al. 2001. 'Initial Sequencing and Analysis of the Human Genome'. *Nature* 409 (6822): 860-921. <https://doi.org/10.1038/35057062>.
- Law, Julie A., Jiamu Du, Christopher J. Hale, Suhua Feng, Krzysztof Krajewski, Ana Marie S. Palanca, Brian D. Strahl, Dinshaw J. Patel, and Steven E. Jacobsen. 2013. 'Polymerase-IV Occupancy at RNA-Directed DNA Methylation Sites Requires SHH1'. *Nature* 498 (7454): 385-89. <https://doi.org/10.1038/nature12178>.
- Le Thomas, Adrien, Alicia K. Rogers, Alexandre Webster, Georgi K. Marinov, Susan E. Liao, Edward M. Perkins, Junho K. Hur, Alexei A. Aravin, and Katalin Fejes Tóth. 2013. 'Piwi Induces PiRNA-Guided Transcriptional Silencing and Establishment of a Repressive Chromatin State'. *Genes & Development* 27 (4): 390-99. <https://doi.org/10.1101/gad.209841.112>.
- Lee, Heng-Chi, Weifeng Gu, Masaki Shirayama, Elaine Youngman, Darryl Conte, and Craig C. Mello. 2012. 'C. Elegans PiRNAs Mediate the Genome-Wide Surveillance of Germline Transcripts'. *Cell* 150 (1): 78-87. <https://doi.org/10.1016/j.cell.2012.06.016>.
- Lee, Nathan N., Venkata R. Chalamcharla, Francisca Reyes-Turcu, Sameet Mehta, Martin Zofall, Vanivilasini Balachandran, Jothy Dhakshnamoorthy, et al. 2013. 'Mtr4-like Protein Coordinates Nuclear RNA Processing for Heterochromatin Assembly and for Telomere Maintenance'. *Cell* 155 (5): 1061-74. <https://doi.org/10.1016/j.cell.2013.10.027>.
- Lee, Yuh Chwen G. 2015. 'The Role of PiRNA-Mediated Epigenetic Silencing in the Population Dynamics of Transposable Elements in *Drosophila Melanogaster*'. *PLOS Genetics* 11 (6): e1005269. <https://doi.org/10.1371/journal.pgen.1005269>.
- Lee, Yuh Chwen G, and Gary H Karpén. 2017. 'Pervasive Epigenetic Effects of *Drosophila* Euchromatic Transposable Elements Impact Their Evolution'. *ELife* 6. <https://doi.org/10.7554/eLife.25762>.
- Leem, Young-Eun, Tracy Ripmaster, Felice Kelly, Hirotaka Ebina, Marc Heincelman, Ke Zhang, Shiv I. S. Grewal, Charles S. Hoffman, and Henry L. Levin. 2008. 'Retrotransposon Tf1 Is Targeted to Pol II Promoters by Transcription Activators'. *Molecular Cell* 30 (1): 98-107. <https://doi.org/10.1016/j.molcel.2008.02.016>.
- Lejeune, Erwan, and Robin C Allshire. 2011. 'Common Ground: Small RNA Programming and Chromatin Modifications'. *Current Opinion in Cell Biology*, Nucleus and gene expression, 23 (3): 258-65. <https://doi.org/10.1016/j.ceb.2011.03.005>.
- Lepesant, Julie M J, Carole Iampietro, Eugenia Galeota, Benoit Augé, Marion Aguirrenbengoa, Clémentine Mercé, Camille Chaubet, et al. 2020. 'A Dual Role of DLsd1 in Oogenesis: Regulating Developmental Genes and Repressing Transposons'. *Nucleic Acids Research* 48 (3): 1206-24. <https://doi.org/10.1093/nar/gkz1142>.
- Levin, H L. 1995. 'A Novel Mechanism of Self-Primed Reverse Transcription Defines a New Family of Retroelements.' *Molecular and Cellular Biology* 15 (6): 3310-17. <https://doi.org/10.1128/MCB.15.6.3310>.

- Levin, H. L. 1996. 'An Unusual Mechanism of Self-Primed Reverse Transcription Requires the RNase H Domain of Reverse Transcriptase to Cleave an RNA Duplex'. *Molecular and Cellular Biology* 16 (10): 5645-54. <https://doi.org/10.1128/mcb.16.10.5645>.
- Levin, H L, D C Weaver, and J D Boeke. 1990. 'Two Related Families of Retrotransposons from *Schizosaccharomyces Pombe*.' *Molecular and Cellular Biology* 10 (12): 6791-98.
- Li, Chengjian, Vasily V. Vagin, Soohyun Lee, Jia Xu, Shengmei Ma, Hualin Xi, Hervé Seitz, et al. 2009. 'Collapse of Germline PiRNAs in the Absence of Argonaute3 Reveals Somatic PiRNAs in Flies'. *Cell* 137 (3): 509-21. <https://doi.org/10.1016/j.cell.2009.04.027>.
- Li, Qing, Hui Zhou, Hugo Wurtele, Brian Davies, Bruce Horazdovsky, Alain Verreault, and Zhiguo Zhang. 2008. 'Acetylation of Histone H3 Lysine 56 Regulates Replication-Coupled Nucleosome Assembly'. *Cell* 134 (2): 244-55. <https://doi.org/10.1016/j.cell.2008.06.018>.
- Li, Yang, Megha Basavappa, Jinfeng Lu, Shuwei Dong, D. Alexander Cronkite, John T. Prior, Hans-Christian Reinecker, et al. 2016. 'Induction and Suppression of Antiviral RNA Interference by Influenza A Virus in Mammalian Cells'. *Nature Microbiology* 2 (December): 16250. <https://doi.org/10.1038/nmicrobiol.2016.250>.
- Lin, H., and A. C. Spradling. 1997. 'A Novel Group of Pumilio Mutations Affects the Asymmetric Division of Germline Stem Cells in the *Drosophila* Ovary'. *Development (Cambridge, England)* 124 (12): 2463-76.
- Lin, J. H., and H. L. Levin. 1997. 'A Complex Structure in the MRNA of Tfl Is Recognized and Cleaved to Generate the Primer of Reverse Transcription.' *Genes & Development* 11 (2): 270-85. <https://doi.org/10.1101/gad.11.2.270>.
- Locke, Sarahjane, and Robert Martienssen. 2009. 'Epigenetic Silencing of Pericentromeric Heterochromatin by RNA Interference in *Schizosaccharomyces Pombe*'. In *Epigenomics*, edited by Anne C. Ferguson-Smith, John M. Gready, and Robert A. Martienssen, 149-62. Dordrecht: Springer Netherlands. https://doi.org/10.1007/978-1-4020-9187-2_9.
- Lorenz, David R., Irina V. Mikheyeva, Peter Johansen, Lauren Meyer, Anastasia Berg, Shiv I. S. Grewal, and Hugh P. Cam. 2012. 'CENP-B Cooperates with Set1 in Bidirectional Transcriptional Silencing and Genome Organization of Retrotransposons'. *Molecular and Cellular Biology* 32 (20): 4215-25. <https://doi.org/10.1128/MCB.00395-12>.
- Luger, Karolin, Armin W. Mäder, Robin K. Richmond, David F. Sargent, and Timothy J. Richmond. 1997. 'Crystal Structure of the Nucleosome Core Particle at 2.8 Å Resolution'. *Nature* 389 (6648): 251-60. <https://doi.org/10.1038/38444>.
- Luteijn, Maartje J, Petra van Bergeijk, Lucas J T Kaaij, Miguel Vasconcelos Almeida, Elke F Roovers, Eugene Berezikov, and René F Ketting. 2012. 'Extremely Stable Piwi-Induced Gene Silencing in *Caenorhabditis Elegans*'. *The EMBO Journal* 31 (16): 3422-30. <https://doi.org/10.1038/emboj.2012.213>.
- Malone, Colin D, Ruth Lehmann, and Felipe Karam Teixeira. 2015. 'The Cellular Basis of Hybrid Dysgenesis and Stellate Regulation in *Drosophila*'. *Current Opinion in Genetics & Development*, Cell reprogramming, regeneration and repair, 34 (October): 88-94. <https://doi.org/10.1016/j.gde.2015.09.003>.
- Manakov, Sergei A., Dubravka Pezic, Georgi K. Marinov, William A. Pastor, Ravi Sachidanandam, and Alexei A. Aravin. 2015. 'MIWI2 and MILI Have Differential Effects on PiRNA Biogenesis and DNA Methylation'. *Cell Reports* 12 (8): 1234-43. <https://doi.org/10.1016/j.celrep.2015.07.036>.
- Marasovic, Mirela, Manuel Zocco, and Mario Halic. 2013. 'Argonaute and Triman Generate Dicer-Independent PriRNAs and Mature SiRNAs to Initiate Heterochromatin Formation'. *Molecular Cell* 52 (2): 173-83. <https://doi.org/10.1016/j.molcel.2013.08.046>.
- Marí-Ordóñez, Arturo, Antonin Marchais, Mathilde Etcheverry, Antoine Martin, Vincent Colot, and Olivier Voinnet. 2013. 'Reconstructing de Novo Silencing of an Active Plant Retrotransposon'. *Nature Genetics* 45 (9): 1029-39. <https://doi.org/10.1038/ng.2703>.
- Martienssen, Robert, and Danesh Moazed. 2015. 'RNAi and Heterochromatin Assembly'. *Cold Spring Harbor Perspectives in Biology* 7 (8). <https://doi.org/10.1101/cshperspect.a019323>.
- Martinez, Javier, Agnieszka Patkaniowska, Henning Urlaub, Reinhard Lührmann, and Thomas Tuschl. 2002. 'Single-Stranded Antisense SiRNAs Guide Target RNA Cleavage in RNAi'. *Cell* 110 (5): 563-74. [https://doi.org/10.1016/S0092-8674\(02\)00908-X](https://doi.org/10.1016/S0092-8674(02)00908-X).

- Mason, James M., Radmila Capkova Frydrychova, and Harald Biessmann. 2008. 'Drosophila Telomeres: An Exception Providing New Insights'. *BioEssays: News and Reviews in Molecular, Cellular and Developmental Biology* 30 (1): 25–37. <https://doi.org/10.1002/bies.20688>.
- Mathieu, Olivier, Zuzana Jasencakova, Isabelle Vaillant, Anne-Valerie Gendrel, Vincent Colot, Ingo Schubert, and Sylvette Tourmente. 2003. 'Changes in 5S RDNA Chromatin Organization and Transcription during Heterochromatin Establishment in Arabidopsis'. *The Plant Cell* 15 (12): 2929–39. <https://doi.org/10.1105/tpc.017467>.
- Matsuda, Emiko, and David J. Garfinkel. 2009. 'Posttranslational Interference of Ty1 Retrotransposition by Antisense RNAs'. *Proceedings of the National Academy of Sciences of the United States of America* 106 (37): 15657–62. <https://doi.org/10.1073/pnas.0908305106>.
- McClintock, Barbara. 1950. 'The Origin and Behavior of Mutable Loci in Maize'. *Proceedings of the National Academy of Sciences* 36 (6): 344–55. <https://doi.org/10.1073/pnas.36.6.344>.
- McCue, Andrea D, Kaushik Panda, Saivageethi Nuthikattu, Sarah G Choudury, Erica N Thomas, and R Keith Slotkin. 2015. 'ARGONAUTE 6 Bridges Transposable Element MRNA-Derived siRNAs to the Establishment of DNA Methylation'. *The EMBO Journal* 34 (1): 20–35. <https://doi.org/10.15252/embj.201489499>.
- McGinty, Robert K., and Song Tan. 2015. 'Nucleosome Structure and Function'. *Chemical Reviews* 115 (6): 2255–73. <https://doi.org/10.1021/cr500373h>.
- Meyer, G. F., O. Hess, and W. Beermann. 1961. 'Phasenspezifische Funktionsstrukturen in Spermatozytenkernen von Drosophila melanogaster und Ihre Abhängigkeit vom Y-Chromosom'. *Chromosoma* 12 (1): 676–716. <https://doi.org/10.1007/BF00328946>.
- Mohn, Fabio, Grzegorz Sienski, Dominik Handler, and Julius Brennecke. 2014. 'The Rhino-Deadlock-Cutoff Complex Licenses Noncanonical Transcription of Dual-Strand piRNA Clusters in Drosophila'. *Cell* 157 (6): 1364–79. <https://doi.org/10.1016/j.cell.2014.04.031>.
- Morillon, Antonin, Mathias Springer, and Pascale Lesage. 2000. 'Activation of the Kss1 Invasive-Filamentous Growth Pathway Induces Ty1 Transcription and Retrotransposition in Saccharomyces Cerevisiae'. *Molecular and Cellular Biology* 20 (15): 5766–76.
- Motamedi, Mohammad R., Eun-Jin Erica Hong, Xue Li, Scott Gerber, Carilee Denison, Steven Gygi, and Danesh Moazed. 2008. 'HP1 Proteins Form Distinct Complexes and Mediate Heterochromatic Gene Silencing by Non-Overlapping Mechanisms'. *Molecular Cell* 32 (6): 778–90. <https://doi.org/10.1016/j.molcel.2008.10.026>.
- Motamedi, Mohammad R., André Verdel, Serafin U. Colmenares, Scott A. Gerber, Steven P. Gygi, and Danesh Moazed. 2004. 'Two RNAi Complexes, RITS and RDRC, Physically Interact and Localize to Noncoding Centromeric RNAs'. *Cell* 119 (6): 789–802. <https://doi.org/10.1016/j.cell.2004.11.034>.
- Muller, H. J. 1930. 'Types of Visible Variations Induced by X-Rays InDrosophila'. *Journal of Genetics* 22 (3): 299–334. <https://doi.org/10.1007/BF02984195>.
- Murata, M., J. S. Heslop-Harrison, and F. Motoyoshi. 1997. 'Physical Mapping of the 5S Ribosomal RNA Genes in Arabidopsis Thaliana by Multi-Color Fluorescence in Situ Hybridization with Cosmid Clones'. *The Plant Journal: For Cell and Molecular Biology* 12 (1): 31–37. <https://doi.org/10.1046/j.1365-313x.1997.12010031.x>.
- Murton, Heather E., Patrick J. R. Grady, Tsun Ho Chan, Hugh P. Cam, and Simon K. Whitehall. 2016. 'Restriction of Retrotransposon Mobilization in Schizosaccharomyces Pombe by Transcriptional Silencing and Higher-Order Chromatin Organization'. *Genetics* 203 (4): 1669–78. <https://doi.org/10.1534/genetics.116.189118>.
- Musselman, Catherine A., Marie-Eve Lalonde, Jacques Côté, and Tatiana G. Kutateladze. 2012. 'Perceiving the Epigenetic Landscape through Histone Readers'. *Nature Structural & Molecular Biology* 19 (12): 1218–27. <https://doi.org/10.1038/nsmb.2436>.
- Nakagawa, Hiromi, Joon-Kyu Lee, Jerard Hurwitz, Robin C. Allshire, Jun-ichi Nakayama, Shiv I. S. Grewal, Katsunori Tanaka, and Yota Murakami. 2002. 'Fission Yeast CENP-B Homologs Nucleate Centromeric Heterochromatin by Promoting Heterochromatin-Specific Histone Tail Modifications'. *Genes & Development* 16 (14): 1766–78. <https://doi.org/10.1101/gad.997702>.

- Nakayama, Jun-ichi, Judd C. Rice, Brian D. Strahl, C. David Allis, and Shiv I. S. Grewal. 2001. 'Role of Histone H3 Lysine 9 Methylation in Epigenetic Control of Heterochromatin Assembly'. *Science* 292 (5514): 110–13. <https://doi.org/10.1126/science.1060118>.
- Nambiar, Mridula, and Gerald R. Smith. 2018. 'Pericentromere-Specific Cohesin Complex Prevents Meiotic Pericentric DNA Double-Strand Breaks and Lethal Crossovers'. *Molecular Cell* 71 (4): 540–553.e4. <https://doi.org/10.1016/j.molcel.2018.06.035>.
- Napoli, C., C. Lemieux, and R. Jorgensen. 1990. 'Introduction of a Chimeric Chalcone Synthase Gene into Petunia Results in Reversible Co-Suppression of Homologous Genes in Trans.' *The Plant Cell* 2 (4): 279–89. <https://doi.org/10.1105/tpc.2.4.279>.
- Ng, Huck Hui, Qin Feng, Hengbin Wang, Hediye Erdjument-Bromage, Paul Tempst, Yi Zhang, and Kevin Struhl. 2002. 'Lysine Methylation within the Globular Domain of Histone H3 by Dot1 Is Important for Telomeric Silencing and Sir Protein Association'. *Genes & Development* 16 (12): 1518–27. <https://doi.org/10.1101/gad.1001502>.
- Nimmo, Elaine R., Alison L. Pidoux, Paul E. Perry, and Robin C. Allshire. 1998. 'Defective Meiosis in Telomere-Silencing Mutants of *Schizosaccharomyces Pombe*'. *Nature* 392 (6678): 825–28. <https://doi.org/10.1038/33941>.
- Ninova, Maria, Baira Godneeva, Yung-Chia Ariel Chen, Yicheng Luo, Sharan J. Prakash, Ferenc Jankovics, Miklós Erdélyi, Alexei A. Aravin, and Katalin Fejes Tóth. 2020. 'The SUMO Ligase Su(Var)2-10 Controls Eu- and Heterochromatic Gene Expression via Establishment of H3K9 Trimethylation and Negative Feedback Regulation'. *Molecular Cell* 77 (3): 571–585.e4. <https://doi.org/10.1016/j.molcel.2019.09.033>.
- Nishimasu, Hiroshi, Hirotsugu Ishizu, Kuniaki Saito, Satoshi Fukuhara, Miharuru K. Kamatani, Luc Bonnefond, Naoki Matsumoto, et al. 2012. 'Structure and Function of Zucchini Endoribonuclease in PiRNA Biogenesis'. *Nature* 491 (7423): 284–87. <https://doi.org/10.1038/nature11509>.
- Noma K, null, C. D. Allis, and S. I. Grewal. 2001. 'Transitions in Distinct Histone H3 Methylation Patterns at the Heterochromatin Domain Boundaries'. *Science (New York, N.Y.)* 293 (5532): 1150–55. <https://doi.org/10.1126/science.1064150>.
- Noma, Ken-ichi, C. David Allis, and Shiv I. S. Grewal. 2001. 'Transitions in Distinct Histone H3 Methylation Patterns at the Heterochromatin Domain Boundaries'. *Science* 293 (5532): 1150–55. <https://doi.org/10.1126/science.1064150>.
- Noma, Ken-ichi, Hugh P. Cam, Richard J. Maraia, and Shiv I. S. Grewal. 2006. 'A Role for TFIIC Transcription Factor Complex in Genome Organization'. *Cell* 125 (5): 859–72. <https://doi.org/10.1016/j.cell.2006.04.028>.
- Nuthikattu, Saivageethi, Andrea D. McCue, Kaushik Panda, Dalen Fultz, Christopher DeFraia, Erica N. Thomas, and R. Keith Slotkin. 2013. 'The Initiation of Epigenetic Silencing of Active Transposable Elements Is Triggered by RDR6 and 21-22 Nucleotide Small Interfering RNAs'. *Plant Physiology* 162 (1): 116–31. <https://doi.org/10.1104/pp.113.216481>.
- Ohno, S. 1972. 'So Much "Junk" DNA in Our Genome'. *Brookhaven Symposia in Biology* 23: 366–70.
- Ohtani, Hitoshi, Yuka W. Iwasaki, Aoi Shibuya, Haruhiko Siomi, Mikiko C. Siomi, and Kuniaki Saito. 2013. 'DmGTSF1 Is Necessary for Piwi-PiRISC-Mediated Transcriptional Transposon Silencing in the *Drosophila* Ovary'. *Genes & Development* 27 (15): 1656–61. <https://doi.org/10.1101/gad.221515.113>.
- Okada, Teruaki, Jun-ichirou Ohzeki, Megumi Nakano, Kinya Yoda, William R. Brinkley, Vladimir Larionov, and Hiroshi Masumoto. 2007. 'CENP-B Controls Centromere Formation Depending on the Chromatin Context'. *Cell* 131 (7): 1287–1300. <https://doi.org/10.1016/j.cell.2007.10.045>.
- Okita, Akiko K., Faria Zafar, Jie Su, Dayalini Weerasekera, Takuya Kajitani, Tatsuro S. Takahashi, Hiroshi Kimura, Yota Murakami, Hisao Masukata, and Takuro Nakagawa. 2019. 'Heterochromatin Suppresses Gross Chromosomal Rearrangements at Centromeres by Repressing Tfs1/TFIIS-Dependent Transcription'. *Communications Biology* 2 (1): 1–13. <https://doi.org/10.1038/s42003-018-0251-z>.
- Olins, A. L., and D. E. Olins. 1974. 'Spheroid Chromatin Units (v Bodies)'. *Science (New York, N.Y.)* 183 (4122): 330–32. <https://doi.org/10.1126/science.183.4122.330>.

- Olins, Donald E., and Ada L. Olins. 2003. 'Chromatin History: Our View from the Bridge'. *Nature Reviews Molecular Cell Biology* 4 (10): 809–14. <https://doi.org/10.1038/nrm1225>.
- Oya, Eriko, Reiko Nakagawa, Yuriko Yoshimura, Mayo Tanaka, Gohei Nishibuchi, Shinichi Machida, Atsuko Shirai, et al. 2019. 'H3K14 Ubiquitylation Promotes H3K9 Methylation for Heterochromatin Assembly'. *EMBO Reports* 20 (10): e48111. <https://doi.org/10.15252/embr.201948111>.
- Ozata, Deniz M., Ildar Gainetdinov, Ansgar Zoch, Dónal O'Carroll, and Phillip D. Zamore. 2019. 'PIWI-Interacting RNAs: Small RNAs with Big Functions'. *Nature Reviews. Genetics* 20 (2): 89–108. <https://doi.org/10.1038/s41576-018-0073-3>.
- Pachulska-Wieczorek, Katarzyna, Leszek Błaszczuk, Julita Gumna, Yuri Nishida, Agniva Saha, Marcin Biesiada, David J. Garfinkel, and Katarzyna J. Purzycka. 2016. 'Characterizing the Functions of Ty1 Gag and the Gag-Derived Restriction Factor P22/P18'. *Mobile Genetic Elements* 6 (2): e1154637. <https://doi.org/10.1080/2159256X.2016.1154637>.
- Palumbo, G., S. Bonaccorsi, L. G. Robbins, and S. Pimpinelli. 1994. 'Genetic Analysis of Stellate Elements of *Drosophila Melanogaster*'. *Genetics* 138 (4): 1181–97.
- Partridge, Janet F, Kristin S. C Scott, Andrew J Bannister, Tony Kouzarides, and Robin C Allshire. 2002. 'Cis-Acting DNA from Fission Yeast Centromeres Mediates Histone H3 Methylation and Recruitment of Silencing Factors and Cohesin to an Ectopic Site'. *Current Biology* 12 (19): 1652–60. [https://doi.org/10.1016/S0960-9822\(02\)01177-6](https://doi.org/10.1016/S0960-9822(02)01177-6).
- Pastor, William A., Hume Stroud, Kevin Nee, Wanlu Liu, Dubravka Pezic, Sergei Manakov, Serena A. Lee, et al. 2014. 'MORC1 Represses Transposable Elements in the Mouse Male Germline'. *Nature Communications* 5 (1): 5795. <https://doi.org/10.1038/ncomms6795>.
- Payer, Lindsay M., and Kathleen H. Burns. 2019. 'Transposable Elements in Human Genetic Disease'. *Nature Reviews Genetics* 20 (12): 760–72. <https://doi.org/10.1038/s41576-019-0165-8>.
- Persson, Jenna, Babett Steglich, Agata Smialowska, Mette Boyd, Jette Bornholdt, Robin Andersson, Catherine Schurra, et al. 2016. 'Regulating Retrotransposon Activity through the Use of Alternative Transcription Start Sites'. *EMBO Reports* 17 (5): 753–68. <https://doi.org/10.15252/embr.201541866>.
- Peters, Lasse, and Gunter Meister. 2007. 'Argonaute Proteins: Mediators of RNA Silencing'. *Molecular Cell* 26 (5): 611–23. <https://doi.org/10.1016/j.molcel.2007.05.001>.
- Pezic, Dubravka, Sergei A. Manakov, Ravi Sachidanandam, and Alexei A. Aravin. 2014. 'PiRNA Pathway Targets Active LINE1 Elements to Establish the Repressive H3K9me3 Mark in Germ Cells'. *Genes & Development* 28 (13): 1410–28. <https://doi.org/10.1101/gad.240895.114>.
- Piovesan, Allison, Maria Chiara Pelleri, Francesca Antonaros, Pierluigi Strippoli, Maria Caracausi, and Lorenza Vitale. 2019. 'On the Length, Weight and GC Content of the Human Genome'. *BMC Research Notes* 12 (February). <https://doi.org/10.1186/s13104-019-4137-z>.
- Pisacane, Paola, and Mario Halic. 2017. 'Tailing and Degradation of Argonaute-Bound Small RNAs Protect the Genome from Uncontrolled RNAi'. *Nature Communications* 8 (May). <https://doi.org/10.1038/ncomms15332>.
- Preez, Louis L. du, and Hugh-G. Patterton. 2013. 'Secondary Structures of the Core Histone N-Terminal Tails: Their Role in Regulating Chromatin Structure'. *Sub-Cellular Biochemistry* 61: 37–55. https://doi.org/10.1007/978-94-007-4525-4_2.
- Quenneville, Simon, Priscilla Turelli, Karolina Bojkowska, Charlène Raclot, Sandra Offner, Adamandia Kapopoulou, and Didier Trono. 2012. 'The KRAB-ZFP/KAP1 System Contributes to the Early Embryonic Establishment of Site-Specific DNA Methylation Patterns Maintained during Development'. *Cell Reports* 2 (4): 766–73. <https://doi.org/10.1016/j.celrep.2012.08.043>.
- Rangan, Prashanth, Colin D. Malone, Caryn Navarro, Sam P. Newbold, Patrick S. Hayes, Ravi Sachidanandam, Gregory J. Hannon, and Ruth Lehmann. 2011. 'PiRNA Production Requires Heterochromatin Formation in *Drosophila*'. *Current Biology: CB* 21 (16): 1373–79. <https://doi.org/10.1016/j.cub.2011.06.057>.

- Rath, Devashish, Lina Amlinger, Archana Rath, and Magnus Lundgren. 2015. 'The CRISPR-Cas Immune System: Biology, Mechanisms and Applications'. *Biochimie*, Special Issue: Regulatory RNAs, 117 (October): 119–28. <https://doi.org/10.1016/j.biochi.2015.03.025>.
- Rea, Stephen, Frank Eisenhaber, Dónal O'Carroll, Brian D. Strahl, Zu-Wen Sun, Manfred Schmid, Susanne Opravil, et al. 2000. 'Regulation of Chromatin Structure by Site-Specific Histone H3 Methyltransferases'. *Nature* 406 (6796): 593–99. <https://doi.org/10.1038/35020506>.
- Reuter, Michael, Philipp Berninger, Shinichiro Chuma, Hardik Shah, Mihoko Hosokawa, Charlotta Funaya, Claude Antony, Ravi Sachidanandam, and Ramesh S. Pillai. 2011. 'Miwi Catalysis Is Required for PiRNA Amplification-Independent LINE1 Transposon Silencing'. *Nature* 480 (7376): 264–67. <https://doi.org/10.1038/nature10672>.
- Rhind, Nicholas, Zehua Chen, Moran Yassour, Dawn A Thompson, Brian J Haas, Naomi Habib, Ilan Wapinski, et al. 2011. 'Comparative Functional Genomics of the Fission Yeasts'. *Science (New York, N.Y.)* 332 (6032): 930–36. <https://doi.org/10.1126/science.1203357>.
- Robine, Nicolas, Nelson C. Lau, Sudha Balla, Zhigang Jin, Katsutomo Okamura, Satomi Kuramochi-Miyagawa, Michael D. Blower, and Eric C. Lai. 2009. 'A Broadly Conserved Pathway Generates 3'UTR-Directed Primary PiRNAs'. *Current Biology: CB* 19 (24): 2066–76. <https://doi.org/10.1016/j.cub.2009.11.064>.
- Roche, S E, and D C Rio. 1998. 'Trans-Silencing by P Elements Inserted in Subtelomeric Heterochromatin Involves the Drosophila Polycomb Group Gene, Enhancer of Zeste.' *Genetics* 149 (4): 1839–55.
- Romano, N., and G. Macino. 1992. 'Quelling: Transient Inactivation of Gene Expression in Neurospora Crassa by Transformation with Homologous Sequences'. *Molecular Microbiology* 6 (22): 3343–53. <https://doi.org/10.1111/j.1365-2958.1992.tb02202.x>.
- Rougemaille, Mathieu, Sigurd Braun, Scott Coyle, Phillip A. Dumesic, Jennifer F. Garcia, Richard Stefan Isaac, Domenico Libri, Geeta J. Narlikar, and Hiten D. Madhani. 2012. 'Ers1 Links HP1 to RNAi'. *Proceedings of the National Academy of Sciences* 109 (28): 11258–63. <https://doi.org/10.1073/pnas.1204947109>.
- Rowe, Helen M., Marc Friedli, Sandra Offner, Sonia Verp, Daniel Mesnard, Julien Marquis, Tugce Aktas, and Didier Trono. 2013. 'De Novo DNA Methylation of Endogenous Retroviruses Is Shaped by KRAB-ZFPs/KAP1 and ESET'. *Development (Cambridge, England)* 140 (3): 519–29. <https://doi.org/10.1242/dev.087585>.
- Roy, Babhrubahan, Neha Varshney, Vikas Yadav, and Kaustuv Sanyal. 2013. 'The Process of Kinetochore Assembly in Yeasts'. *FEMS Microbiology Letters* 338 (2): 107–17. <https://doi.org/10.1111/1574-6968.12019>.
- Ruby, J. Graham, Calvin Jan, Christopher Player, Michael J. Axtell, William Lee, Chad Nusbaum, Hui Ge, and David P. Bartel. 2006. 'Large-Scale Sequencing Reveals 21U-RNAs and Additional MicroRNAs and Endogenous siRNAs in C. Elegans'. *Cell* 127 (6): 1193–1207. <https://doi.org/10.1016/j.cell.2006.10.040>.
- Sadeghi, Laia, Punit Prasad, Karl Ekwall, Amikam Cohen, and J Peter Svensson. 2015. 'The Paf1 Complex Factors Leo1 and Paf1 Promote Local Histone Turnover to Modulate Chromatin States in Fission Yeast'. *EMBO Reports* 16 (12): 1673–87. <https://doi.org/10.15252/embr.201541214>.
- Saha, Agniva, Jessica A. Mitchell, Yuri Nishida, Jonathan E. Hildreth, Joshua A. Ariberre, Wendy V. Gilbert, and David J. Garfinkel. 2015. 'A Trans-Dominant Form of Gag Restricts Ty1 Retrotransposition and Mediates Copy Number Control'. *Journal of Virology* 89 (7): 3922–38. <https://doi.org/10.1128/JVI.03060-14>.
- Saito, Kuniaki, Sachi Inagaki, Toutai Mituyama, Yoshinori Kawamura, Yukiteru Ono, Eri Sakota, Hazuki Kotani, Kiyoshi Asai, Haruhiko Siomi, and Mikiko C. Siomi. 2009. 'A Regulatory Circuit for Piwi by the Large Maf Gene Traffic Jam in Drosophila'. *Nature* 461 (7268): 1296–99. <https://doi.org/10.1038/nature08501>.
- Saito, Kuniaki, Kazumichi M. Nishida, Tomoko Mori, Yoshinori Kawamura, Keita Miyoshi, Tomoko Nagami, Haruhiko Siomi, and Mikiko C. Siomi. 2006. 'Specific Association of Piwi with RasiRNAs Derived from Retrotransposon and Heterochromatic Regions in the Drosophila Genome'. *Genes & Development* 20 (16): 2214–22. <https://doi.org/10.1101/gad.1454806>.

- Saito, Kuniaki, Yuriko Sakaguchi, Takeo Suzuki, Tsutomu Suzuki, Haruhiko Siomi, and Mikiko C. Siomi. 2007. 'Pimet, the Drosophila Homolog of HEN1, Mediates 2'-O-Methylation of Piwi-Interacting RNAs at Their 3' Ends'. *Genes & Development* 21 (13): 1603-8. <https://doi.org/10.1101/gad.1563607>.
- Salinero, Alicia C., Elisabeth R. Knoll, Z. Iris Zhu, David Landsman, M. Joan Curcio, and Randall H. Morse. 2018. 'The Mediator Co-Activator Complex Regulates Ty1 Retromobility by Controlling the Balance between Ty1i and Ty1 Promoters'. *PLOS Genetics* 14 (2): e1007232. <https://doi.org/10.1371/journal.pgen.1007232>.
- SanMiguel, P., A. Tikhonov, Y. K. Jin, N. Motchoulskaia, D. Zakharov, A. Melake-Berhan, P. S. Springer, et al. 1996. 'Nested Retrotransposons in the Intergenic Regions of the Maize Genome'. *Science (New York, N.Y.)* 274 (5288): 765-68. <https://doi.org/10.1126/science.274.5288.765>.
- Sarot, Emeline, Geneviève Payen-Groschêne, Alain Bucheton, and Alain Pélisson. 2004. 'Evidence for a Piwi-Dependent RNA Silencing of the Gypsy Endogenous Retrovirus by the Drosophila *Melanogaster* Flamenco Gene'. *Genetics* 166 (3): 1313-21. <https://doi.org/10.1534/genetics.166.3.1313>.
- Savitsky, Mikhail, Dmitry Kwon, Pavel Georgiev, Alla Kalmykova, and Vladimir Gvozdev. 2006. 'Telomere Elongation Is under the Control of the RNAi-Based Mechanism in the Drosophila Germline'. *Genes & Development* 20 (3): 345-54. <https://doi.org/10.1101/gad.370206>.
- Schramm, Laura, and Nouria Hernandez. 2002. 'Recruitment of RNA Polymerase III to Its Target Promoters'. *Genes & Development* 16 (20): 2593-2620. <https://doi.org/10.1101/gad.1018902>.
- Schreiner, Patrick, and Peter W. Atkinson. 2017. 'PiClusterBuster: Software for Automated Classification and Characterization of PiRNA Cluster Loci'. Preprint. Bioinformatics. <https://doi.org/10.1101/133009>.
- Scott, Kristin C., Stephanie L. Merrett, and Huntington F. Willard. 2006. 'A Heterochromatin Barrier Partitions the Fission Yeast Centromere into Discrete Chromatin Domains'. *Current Biology: CB* 16 (2): 119-29. <https://doi.org/10.1016/j.cub.2005.11.065>.
- Seth, Meetu, Masaki Shirayama, Weifeng Gu, Takao Ishidate, Darryl Conte, and Craig C. Mello. 2013. 'The C. Elegans CSR-1 Argonaute Pathway Counteracts Epigenetic Silencing to Promote Germline Gene Expression'. *Developmental Cell* 27 (6): 656-63. <https://doi.org/10.1016/j.devcel.2013.11.014>.
- Shah, Sneha, Sina Wittmann, Cornelia Kilchert, and Lidia Vasiljeva. 2014. 'LncRNA Recruits RNAi and the Exosome to Dynamically Regulate Pho1 Expression in Response to Phosphate Levels in Fission Yeast'. *Genes & Development* 28 (3): 231-44. <https://doi.org/10.1101/gad.230177.113>.
- Shukla, Manu, Pin Tong, Sharon A. White, Puneet P. Singh, Angus M. Reid, Sandra Catania, Alison L. Pidoux, and Robin C. Allshire. 2018. 'Centromere DNA Destabilizes H3 Nucleosomes to Promote CENP-A Deposition during the Cell Cycle'. *Current Biology* 28 (24): 3924-3936.e4. <https://doi.org/10.1016/j.cub.2018.10.049>.
- Sigman, Meredith J., and R. Keith Slotkin. 2016. 'The First Rule of Plant Transposable Element Silencing: Location, Location, Location'. *The Plant Cell* 28 (2): 304-13. <https://doi.org/10.1105/tpc.15.00869>.
- Sigova, Alla, Nicholas Rhind, and Phillip D. Zamore. 2004. 'A Single Argonaute Protein Mediates Both Transcriptional and Posttranscriptional Silencing in *Schizosaccharomyces Pombe*'. *Genes & Development* 18 (19): 2359-67. <https://doi.org/10.1101/gad.1218004>.
- Simmer, Femke, Alessia Buscaino, Isabelle C Kos-Braun, Alexander Kagansky, Abdelhalim Boukaba, Takeshi Urano, Alastair R W Kerr, and Robin C Allshire. 2010. 'Hairpin RNA Induces Secondary Small Interfering RNA Synthesis and Silencing in Trans in Fission Yeast'. *EMBO Reports* 11 (2): 112-18. <https://doi.org/10.1038/embor.2009.273>.
- Singleton, Teresa L., and Henry L. Levin. 2002. 'A Long Terminal Repeat Retrotransposon of Fission Yeast Has Strong Preferences for Specific Sites of Insertion'. *Eukaryotic Cell* 1 (1): 44-55. <https://doi.org/10.1128/ec.01.1.44-55.2002>.
- Siomi, Mikiko C., Kaoru Sato, Dubravka Pezic, and Alexei A. Aravin. 2011. 'PIWI-Interacting Small RNAs: The Vanguard of Genome Defence'. *Nature Reviews. Molecular Cell Biology* 12 (4): 246-58. <https://doi.org/10.1038/nrm3089>.

- Smirnov, M. N., V. N. Smirnov, E. I. Budowsky, S. G. Inge-Vechtomov, and N. G. Serebrjakov. 1967. 'Red Pigment of Adenine-Deficient Yeast *Saccharomyces Cerevisiae*'. *Biochemical and Biophysical Research Communications* 27 (3): 299–304. [https://doi.org/10.1016/S0006-291X\(67\)80096-2](https://doi.org/10.1016/S0006-291X(67)80096-2).
- Steglich, Babet, Annelie Strålfors, Olga Khorosjutina, Jenna Persson, Agata Smialowska, Jean-Paul Javerzat, and Karl Ekwall. 2015. 'The Fun30 Chromatin Remodeler Fft3 Controls Nuclear Organization and Chromatin Structure of Insulators and Subtelomeres in Fission Yeast'. *PLoS Genetics* 11 (3): e1005101. <https://doi.org/10.1371/journal.pgen.1005101>.
- Strålfors, Annelie, Julian Walfridsson, Hasanuzzaman Bhuiyan, and Karl Ekwall. 2011. 'The FUN30 Chromatin Remodeler, Fft3, Protects Centromeric and Subtelomeric Domains from Euchromatin Formation'. *PLoS Genetics* 7 (3). <https://doi.org/10.1371/journal.pgen.1001334>.
- Sugawara, Neal Francis. 1988. *DNA Sequences at the Telomeres of the Fission Yeast S. Pombe*. Harvard University.
- Sugiyama, Tomoyasu, Hugh P. Cam, Rie Sugiyama, Ken-ichi Noma, Martin Zofall, Ryuji Kobayashi, and Shiv I. S. Grewal. 2007. 'SHREC, an Effector Complex for Heterochromatic Transcriptional Silencing'. *Cell* 128 (3): 491–504. <https://doi.org/10.1016/j.cell.2006.12.035>.
- Sugiyama, Tomoyasu, and Rie Sugioka-Sugiyama. 2011. 'Red1 Promotes the Elimination of Meiosis-Specific MRNAs in Vegetatively Growing Fission Yeast'. *The EMBO Journal* 30 (6): 1027–39. <https://doi.org/10.1038/emboj.2011.32>.
- Sun, Hui Bin, Jin Shen, and Hiroki Yokota. 2000. 'Size-Dependent Positioning of Human Chromosomes in Interphase Nuclei'. *Biophysical Journal* 79 (1): 184–90. [https://doi.org/10.1016/S0006-3495\(00\)76282-5](https://doi.org/10.1016/S0006-3495(00)76282-5).
- Tabara, H., M. Sarkissian, W. G. Kelly, J. Fleenor, A. Grishok, L. Timmons, A. Fire, and C. C. Mello. 1999. 'The Rde-1 Gene, RNA Interference, and Transposon Silencing in *C. Elegans*'. *Cell* 99 (2): 123–32. [https://doi.org/10.1016/s0092-8674\(00\)81644-x](https://doi.org/10.1016/s0092-8674(00)81644-x).
- Takahashi, K., E. S. Chen, and M. Yanagida. 2000. 'Requirement of Mis6 Centromere Connector for Localizing a CENP-A-like Protein in Fission Yeast'. *Science (New York, N.Y.)* 288 (5474): 2215–19. <https://doi.org/10.1126/science.288.5474.2215>.
- Taniguchi-Ikeda, Mariko, Kazuhiro Kobayashi, Motoi Kanagawa, Chih-chieh Yu, Kouhei Mori, Tetsuya Oda, Atsushi Kuga, et al. 2011. 'Pathogenic Exon-Trapping by SVA Retrotransposon and Rescue in Fukuyama Muscular Dystrophy'. *Nature* 478 (7367): 127–31. <https://doi.org/10.1038/nature10456>.
- Tashiro, Sanki, Tomohiro Asano, Junko Kanoh, and Fuyuki Ishikawa. 2013. 'Transcription-Induced Chromatin Association of RNA Surveillance Factors Mediates Facultative Heterochromatin Formation in Fission Yeast'. *Genes to Cells: Devoted to Molecular & Cellular Mechanisms* 18 (4): 327–39. <https://doi.org/10.1111/gtc.12038>.
- Thorvaldsdóttir, Helga, James T. Robinson, and Jill P. Mesirov. 2013. 'Integrative Genomics Viewer (IGV): High-Performance Genomics Data Visualization and Exploration'. *Briefings in Bioinformatics* 14 (2): 178–92. <https://doi.org/10.1093/bib/bbs017>.
- Todeschini, Anne-Laure, Laure Teyssset, Valérie Delmarre, and Stéphane Ronsseray. 2010. 'The Epigenetic Trans-Silencing Effect in *Drosophila* Involves Maternally-Transmitted Small RNAs Whose Production Depends on the PiRNA Pathway and HP1'. *PLoS ONE* 5 (6). <https://doi.org/10.1371/journal.pone.0011032>.
- Tusso, Sergio, Bart P S Nieuwenhuis, Fritz J Sedlazeck, John W Davey, Daniel C Jeffares, and Jochen B W Wolf. 2019. 'Ancestral Admixture Is the Main Determinant of Global Biodiversity in Fission Yeast'. *Molecular Biology and Evolution* 36 (9): 1975–89. <https://doi.org/10.1093/molbev/msz126>.
- Ugolini, Ilaria, and Mario Halic. 2018. 'Fidelity in RNA-Based Recognition of Transposable Elements'. *Philosophical Transactions of the Royal Society B: Biological Sciences* 373 (1762): 20180168. <https://doi.org/10.1098/rstb.2018.0168>.
- Vagin, Vasily V., Mikhail S. Klenov, Alla I. Kalmykova, Anastasia D. Stolyarenko, Roman N. Kotelnikov, and Vladimir A. Gvozdev. 2004. 'The RNA Interference Proteins and Vasa Locus Are Involved in the Silencing of Retrotransposons in the Female Germline of *Drosophila Melanogaster*'. *RNA Biology* 1 (1): 54–58.

- Vagin, Vasily V., Alla Sigova, Chengjian Li, Hervé Seitz, Vladimir Gvozdev, and Phillip D. Zamore. 2006. 'A Distinct Small RNA Pathway Silences Selfish Genetic Elements in the Germline'. *Science (New York, N.Y.)* 313 (5785): 320–24. <https://doi.org/10.1126/science.1129333>.
- Verdel, André, Songtao Jia, Scott Gerber, Tomoyasu Sugiyama, Steven Gygi, Shiv I. S. Grewal, and Danesh Moazed. 2004. 'RNAi-Mediated Targeting of Heterochromatin by the RITS Complex'. *Science (New York, N.Y.)* 303 (5658): 672–76. <https://doi.org/10.1126/science.1093686>.
- Verrier, Laure, Francesca Tagliani, Ramon R. Barrales, Shaun Webb, Takeshi Urano, Sigurd Braun, and Elizabeth H. Bayne. 2015. 'Global Regulation of Heterochromatin Spreading by Leo1'. *Open Biology* 5 (5): 150045. <https://doi.org/10.1098/rsob.150045>.
- Volpe, Thomas A., Catherine Kidner, Ira M. Hall, Grace Teng, Shiv I. S. Grewal, and Robert A. Martienssen. 2002. 'Regulation of Heterochromatic Silencing and Histone H3 Lysine-9 Methylation by RNAi'. *Science (New York, N.Y.)* 297 (5588): 1833–37. <https://doi.org/10.1126/science.1074973>.
- Waldeyer, H.W. 1888. 'Über Karyokinese Und Ihre Beziehungen Zu Den Befruchtungsvorgängen.' *Arch. Mikrosk. Anat.*, 1–22.
- Wang, Jiyong, Bharat D. Reddy, and Songtao Jia. 2015. 'Rapid Epigenetic Adaptation to Uncontrolled Heterochromatin Spreading'. *ELife* 4 (March). <https://doi.org/10.7554/eLife.06179>.
- Wang, Jiyong, Xavier Tadeo, Haitong Hou, Patricia G. Tu, James Thompson, John R. Yates, and Songtao Jia. 2013. 'Epe1 Recruits BET Family Bromodomain Protein Bdf2 to Establish Heterochromatin Boundaries'. *Genes & Development* 27 (17): 1886–1902. <https://doi.org/10.1101/gad.221010.113>.
- Wang, Sidney H., and Sarah C. R. Elgin. 2011. 'Drosophila Piwi Functions Downstream of PiRNA Production Mediating a Chromatin-Based Transposon Silencing Mechanism in Female Germ Line'. *Proceedings of the National Academy of Sciences* 108 (52): 21164–69. <https://doi.org/10.1073/pnas.1107892109>.
- Wang, Tianwen, Xingyuan Ma, Hu Zhu, Aitao Li, Guocheng Du, and Jian Chen. 2012. 'Available Methods for Assembling Expression Cassettes for Synthetic Biology'. *Applied Microbiology and Biotechnology* 93 (5): 1853–63. <https://doi.org/10.1007/s00253-012-3920-8>.
- Wang, Xiaoying, Susan C. Moore, Mario Laszckzak, and Juan Ausiós. 2000. 'Acetylation Increases the α -Helical Content of the Histone Tails of the Nucleosome'. *Journal of Biological Chemistry* 275 (45): 35013–20. <https://doi.org/10.1074/jbc.M004998200>.
- Watts, Beth R, Sina Wittmann, Maxime Wery, Camille Gautier, Krzysztof Kus, Adrien Birot, Dong-Hyuk Heo, Cornelia Kilchert, Antonin Morillon, and Lidia Vasiljeva. 2018. 'Histone Deacetylation Promotes Transcriptional Silencing at Facultative Heterochromatin'. *Nucleic Acids Research* 46 (11): 5426–40. <https://doi.org/10.1093/nar/gky232>.
- Weaver, Daniel C, George V Shpakovski, Emerita Caputo, Henry L Levin, and J. D Bocke. 1993. 'Sequence Analysis of Closely Related Retrotransposon Families from Fission Yeast'. *Gene* 131 (1): 135–39. [https://doi.org/10.1016/0378-1119\(93\)90682-S](https://doi.org/10.1016/0378-1119(93)90682-S).
- Wicker, Thomas, François Sabot, Aurélie Hua-Van, Jeffrey L. Bennetzen, Pierre Capy, Boulos Chalhouh, Andrew Flavell, et al. 2007. 'A Unified Classification System for Eukaryotic Transposable Elements'. *Nature Reviews Genetics* 8 (12): 973–82. <https://doi.org/10.1038/nrg2165>.
- Wood, V., R. Gwilliam, M.-A. Rajandream, M. Lyne, R. Lyne, A. Stewart, J. Sgouros, et al. 2002. 'The Genome Sequence of Schizosaccharomyces Pombe'. *Nature* 415 (6874): 871–80. <https://doi.org/10.1038/nature724>.
- Woodcock, C. L., J. P. Safer, and J. E. Stanchfield. 1976. 'Structural Repeating Units in Chromatin. I. Evidence for Their General Occurrence'. *Experimental Cell Research* 97 (January): 101–10. [https://doi.org/10.1016/0014-4827\(76\)90659-5](https://doi.org/10.1016/0014-4827(76)90659-5).
- Woolcock, Katrina J., Dimos Gaidatzis, Tanel Punga, and Marc Bühler. 2011. 'Dicer Associates with Chromatin to Repress Genome Activity in Schizosaccharomyces Pombe'. *Nature Structural & Molecular Biology* 18 (1): 94–99. <https://doi.org/10.1038/nsmb.1935>.
- Xie, Weiwu, Xiaowu Gai, Yunxia Zhu, David C. Zappulla, Rolf Sternglanz, and Daniel F. Voytas. 2001. 'Targeting of the Yeast Ty5 Retrotransposon to Silent Chromatin Is Mediated by

- Interactions between Integrase and Sir4p'. *Molecular and Cellular Biology* 21 (19): 6606–14. <https://doi.org/10.1128/MCB.21.19.6606-6614.2001>.
- Xu, Feng, Kangling Zhang, and Michael Grunstein. 2005. 'Acetylation in Histone H3 Globular Domain Regulates Gene Expression in Yeast'. *Cell* 121 (3): 375–85. <https://doi.org/10.1016/j.cell.2005.03.011>.
- Xu, H., and J. D. Boeke. 1991. 'Inhibition of Ty1 Transposition by Mating Pheromones in *Saccharomyces Cerevisiae*'. *Molecular and Cellular Biology* 11 (5): 2736–43. <https://doi.org/10.1128/mcb.11.5.2736>.
- Xue, Jing, Hongwen Chen, Jian Wu, Miho Takeuchi, Haruna Inoue, Yanmei Liu, Hong Sun, Yong Chen, Junko Kanoh, and Ming Lei. 2017. 'Structure of the Fission Yeast *S. Pombe* Telomeric Tpz1-Poz1-Rap1 Complex'. *Cell Research* 27 (12): 1503–20. <https://doi.org/10.1038/cr.2017.145>.
- Yamada, Takatomi, Wolfgang Fischle, Tomoyasu Sugiyama, C. David Allis, and Shiv I. S. Grewal. 2005. 'The Nucleation and Maintenance of Heterochromatin by a Histone Deacetylase in Fission Yeast'. *Molecular Cell* 20 (2): 173–85. <https://doi.org/10.1016/j.molcel.2005.10.002>.
- Yamada-Inagawa, Tomoko, Amar J. S. Klar, and Jacob Z. Dalgaard. 2007. 'Schizosaccharomyces Pombe Switches Mating Type by the Synthesis-Dependent Strand-Annealing Mechanism'. *Genetics* 177 (1): 255–65. <https://doi.org/10.1534/genetics.107.076315>.
- Yamanaka, Soichiro, Sameet Mehta, Francisca E. Reyes-Turcu, Fanglei Zhuang, Ryan T. Fuchs, Yikang Rong, Gregory B. Robb, and Shiv I. S. Grewal. 2013. 'RNAi Triggered by Specialized Machinery Silences Developmental Genes and Retrotransposons'. *Nature* 493 (7433): 557–60. <https://doi.org/10.1038/nature11716>.
- Yamanaka, Soichiro, Akira Yamashita, Yuriko Harigaya, Ryo Iwata, and Masayuki Yamamoto. 2010. 'Importance of Polyadenylation in the Selective Elimination of Meiotic MRNAs in Growing *S. Pombe* Cells'. *The EMBO Journal* 29 (13): 2173–81. <https://doi.org/10.1038/emboj.2010.108>.
- Yieh, L., G. Kassavetis, E. P. Geiduschek, and S. B. Sandmeyer. 2000. 'The Brf and TATA-Binding Protein Subunits of the RNA Polymerase III Transcription Factor IIIB Mediate Position-Specific Integration of the Gypsy-like Element, Ty3'. *The Journal of Biological Chemistry* 275 (38): 29800–807. <https://doi.org/10.1074/jbc.M003149200>.
- Yieh, Lynn, Heather Hatzis, George Kassavetis, and Suzanne B. Sandmeyer. 2002. 'Mutational Analysis of the Transcription Factor IIIB-DNA Target of Ty3 Retroelement Integration'. *The Journal of Biological Chemistry* 277 (29): 25920–28. <https://doi.org/10.1074/jbc.M202729200>.
- Yu, Yang, Jiaqi Gu, Ying Jin, Yicheng Luo, Jonathan B. Preall, Jinbiao Ma, Benjamin Czech, and Gregory J. Hannon. 2015. 'Panoramix Enforces PiRNA-Dependent Cotranscriptional Silencing'. *Science (New York, N.Y.)* 350 (6258): 339–42. <https://doi.org/10.1126/science.aab0700>.
- Zanni, Vanessa, Angéline Eymery, Michael Coiffet, Matthias Zytnicki, Isabelle Luyten, Hadi Quesneville, Chantal Vaury, and Silke Jensen. 2013. 'Distribution, Evolution, and Diversity of Retrotransposons at the Flamenco Locus Reflect the Regulatory Properties of PiRNA Clusters'. *Proceedings of the National Academy of Sciences* 110 (49): 19842–47. <https://doi.org/10.1073/pnas.1313677110>.
- Zaratiegui, Mikel, Matthew W. Vaughn, Danielle V. Irvine, Derek Goto, Stephen Watt, Jürg Bähler, Benoit Arcangioli, and Robert A. Martienssen. 2011. 'CENP-B Preserves Genome Integrity at Replication Forks Paused by Retrotransposon LTR'. *Nature* 469 (7328): 112–15. <https://doi.org/10.1038/nature09608>.
- Zhang, Ke, Tamas Fischer, Rebecca L. Porter, Jothy Dhakshnamoorthy, Martin Zofall, Ming Zhou, Timothy Veenstra, and Shiv I. S. Grewal. 2011. 'Clr4/Suv39 and RNA Quality Control Factors Cooperate to Trigger RNAi and Suppress Antisense RNA'. *Science* 331 (6024): 1624–27. <https://doi.org/10.1126/science.1198712>.
- Zhang, Ke, Kerstin Mosch, Wolfgang Fischle, and Shiv I. S. Grewal. 2008. 'Roles of the Clr4 Methyltransferase Complex in Nucleation, Spreading and Maintenance of Heterochromatin'. *Nature Structural & Molecular Biology* 15 (4): 381–88. <https://doi.org/10.1038/nsmb.1406>.

- Zhang, Lulu, Lan Yan, Jingchen Jiang, Yan Wang, Yuanying Jiang, Tianhua Yan, and Yongbing Cao. 2014. 'The Structure and Retrotransposition Mechanism of LTR-Retrotransposons in the Asexual Yeast *Candida Albicans*'. *Virulence* 5 (6): 655-64. <https://doi.org/10.4161/viru.32180>.
- Zhang, Shuo, and Erin S. Kelleher. 2019. 'PiRNA-Mediated Silencing of an Invading Transposable Element Evolves Rapidly through Abundant Beneficial de Novo Mutations'. *BioRxiv*, April, 611350. <https://doi.org/10.1101/611350>.
- Zhang, Yuhang, Tat Cheung Cheng, Guangrui Huang, Qingyi Lu, Marius D. Surleac, Jeffrey D. Mandell, Pierre Pontarotti, et al. 2019a. 'Transposon Molecular Domestication and the Evolution of the RAG Recombinase'. *Nature* 569 (7754): 79-84. <https://doi.org/10.1038/s41586-019-1093-7>.
- . 2019b. 'Transposon Molecular Domestication and the Evolution of the RAG Recombinase'. *Nature* 569 (7754): 79-84. <https://doi.org/10.1038/s41586-019-1093-7>.
- Zhang, Zhao, Jie Wang, Nadine Schultz, Fan Zhang, Swapnil S. Parhad, Shikui Tu, Thom Vreven, Phillip D. Zamore, Zhiping Weng, and William E. Theurkauf. 2014. 'The HP1 Homolog Rhino Anchors a Nuclear Complex That Suppresses PiRNA Precursor Splicing'. *Cell* 157 (6): 1353-63. <https://doi.org/10.1016/j.cell.2014.04.030>.
- Zocco, Manuel, Mirela Marasovic, Paola Pisacane, Silvija Bilokapic, and Mario Halic. 2016. 'The Chp1 Chromodomain Binds the H3K9me Tail and the Nucleosome Core to Assemble Heterochromatin'. *Cell Discovery* 2 (April): 16004. <https://doi.org/10.1038/celldisc.2016.4>.
- Zofall, Martin, and Shiv I. S. Grewal. 2006. 'Swi6/HP1 Recruits a JmjC Domain Protein to Facilitate Transcription of Heterochromatic Repeats'. *Molecular Cell* 22 (5): 681-92. <https://doi.org/10.1016/j.molcel.2006.05.010>.
- Zofall, Martin, Soichiro Yamanaka, Francisca E. Reyes-Turcu, Ke Zhang, Chanan Rubin, and Shiv I. S. Grewal. 2012. 'RNA Elimination Machinery Targeting Meiotic MRNAs Promotes Facultative Heterochromatin Formation'. *Science (New York, N.Y.)* 335 (6064): 96-100. <https://doi.org/10.1126/science.1211651>.
- Zou, S., D. A. Wright, and D. F. Voytas. 1995. 'The *Saccharomyces Ty5* Retrotransposon Family Is Associated with Origins of DNA Replication at the Telomeres and the Silent Mating Locus HMR'. *Proceedings of the National Academy of Sciences of the United States of America* 92 (3): 920-24. <https://doi.org/10.1073/pnas.92.3.920>.

ACKNOWLEDGMENTS

Questo periodo della mia vita é stato una montagna russa di emozioni, dove le picchiate sono sembrate piú numerose e lunghe dei momenti dolci e di calma. La voglia di scendere dalla carrozza é stata tanta, ma invece ho terminato la corsa, ce l'ho fatta e lo devo soprattutto a te, Paula. Grazie per il supporto, per avermi ascoltato, sopportato, incoraggiato e soprattutto amato. E allora posso dire che ce l'abbiamo fatta, insieme. Te amo linda, mucho.

Grazie Giacomo per l'esempio di determinazione, sei forte, puoi fare tutto, fallo.

Grazie Claudio per esserti preso anche la mia parte di responsabilitá quando ero lontano da casa.

Grazie babbo e mamma per essere persone speciali, vi voglio bene, mi siete mancati tanto, spero di vedervi molto, ma molto di piú e presto.

Grazie nonna, sei una ventata di felicitá ogni volta che ti sento.

Grazie Fabio e Lorenzo per esserci sempre stati, anche da lontano. Sono fortunatissimo ad avervi come amici, vi voglio bene e vi voglio per sempre al mio fianco.

Grazie anche ai ragazzi del laboratorio: Ilaria, per la compagnia e i consigli sul lavoro. Paola, per essere una persona di rara disponibilitá, ma soprattutto un'amica. Nives, you are a great person, it was a pleasure to meet you. Thanks to Sigrun, extremely professional and kind. Thanks Silvija for the professional help and the suggestions you gave me. I also thank Guoli, Petr, Manuel and Saed, you are all fantastic people, it was fun to work with you, thanks!

I thank Joe, for helping with english and for being a great and beautiful person. Thank you, really.

I thank Thomas for the kindness and help you gave me, it was so important.

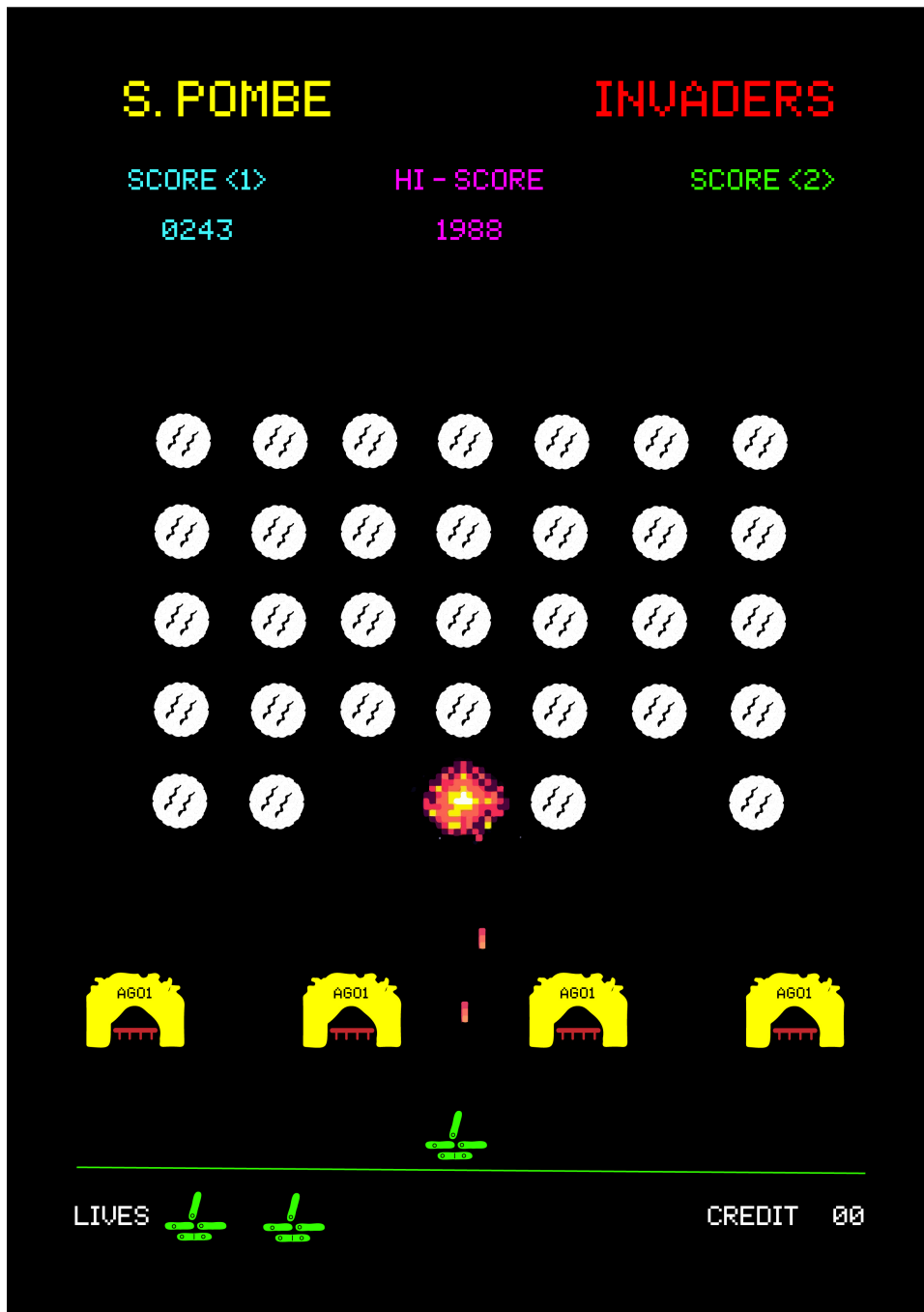
I thank Louiza and Stephanie, two extremely friendly and helpful persons at the Gene Center, you are great!

I would like to thank Dr. Mario Halic for the possibility to do research in such a prestigious University and for the support to achieve the results showed in this Thesis.

I thank Prof. Dr. Klaus Förstemann for being my Gutachter and for the help in organizing my Defence.

I thank all the other Committee members for making my Defence possible.

I thank Prof. Dr. Karl-Peter Hopfner, for being always available to discuss and for taking care of me at the Gene Center.



S. pombe Invaders (Paula Camila Niño Rodriguez, 2021. Adapted from “Space Invaders”).